Microscopic modelling of walking behaviour

Campanella, Mario

DOI
10.4233/uuid:b65e6e12-a85e-4846-9122-0bb9be47a762

Publication date
2016

Document Version
Final published version

Citation (APA)
Campanella, M. (2016). *Microscopic modelling of walking behaviour*. [Dissertation (TU Delft), Delft University of Technology]. TRAIL Research School. https://doi.org/10.4233/uuid:b65e6e12-a85e-4846-9122-0bb9be47a762

Microscopic Modelling of Walking Behaviour

Mario Carlos Campanella

Delft University of Technology, 2016

Cover illustration: Mario Campanella

Microscopic Modelling of Walking Behaviour

Proefschrift

ter verkrijging van de graad van doctor
aan de Technische Universiteit Delft,
op gezag van de Rector Magnificus prof.ir. K.C.A.M. Luyben,
voorzitter van het College voor Promoties,
in het openbaar te verdedigen op maandag 21 november 2016 om 12:30 uur

door

Mario Carlos CAMPANELLA
Master of Science in Computer Science
Instituto Militar de Engenharia, Brazilië
geboren te Rio de Janeiro, Brazilië.

Dit proefschrift is goedgekeurd door de:
promotor: Prof. dr. S.P. Hoogendoorn
copromotor: Dr. ir. W. Daamen

Samenstelling promotiecommissie:

Rector Magnificus	voorzitter
Prof. dr. ir. S.P. Hoogendoorn	promotor
Dr. ir. W. Daamen	copromotor

Onafhankelijke leden:

Prof. dr. ir. J.W.C. van Lint	Faculteit Civiele Techniek en Geowetenschappen, TU Delft
Prof. ir. R.J. Dijkstra	Faculteit Bouwkunde, TU Delft
Prof. dr. S. Bandini	Universita di Milano - Bicocca
Prof. dr. H.J.P. Timmermans	Technische Universiteit Eindhoven
Dr. ir. P. Goatin	Centre Inria Sophia Antipolis

TRAIL Thesis Series T2016/20, the Netherlands Research School TRAIL

TRAIL
P.O. Box 5017
2600 GA Delft
the Netherlands
E-mail: info@rsTRAIL.nl

ISBN 978-90-5584-214-8

Printed in the Netherlands

"Brian, the eponymous hero of the Monty Python film, furious at having been proclaimed Messiah and being followed wherever he went by a horde of worshippers, tried hard but in vain to convince his pursuers to stop behaving like a flock of sheep and to disperse. 'You are all individuals!' he shouted. 'We are all individuals!' duly responded, in unison, the chorus of devotees. Only a small lonely voice objected: 'I am not...' Brian tried another argument. 'You have to be different!' he cried. 'Yes, we are all different! the chorus rapturously agreed. Again, just one voice objected: 'I am not...' Hearing that, the crowd looked around angrily, eager to lynch the dissenter if only he could be found in the mass of lookalikes."

Zygmunt Bauman 2005 Liquid Life, Cambridge

Preface

Anyone attentive while walking in the business centre of a large metropolis in the midday or in a busy train station in the peak hour, can only wonder how come so many people are able to walk that fast without bumping into each other? For a researcher this puzzle is a source of inspiration since understanding dense crowds is a difficult task. Studying pedestrians is a fascinating mixture between human psychology, crowd sociology and engineering rationality. This interdisciplinary aspect and ethical dimension is exactly what kept my interest through these rich and intense years.

What brought a sense of accomplishment was the opportunity to apply the knowledge acquired in this dissertation in my native country Brazil. From the perspective of daily commuters, the conditions of the public transport network in Brazil's big cities are very unsatisfying. The metro, regional trains and bus systems are frequently run with far too insufficient capacity creating extreme discomfort and very often real danger.

During a period of almost two years I had the opportunity to work closely with the metro companies of Rio de Janeiro and São Paulo trying to address the numerous problems facing their stations and carriages. The application of the simulation model developed in this dissertation to assess a new metro station in Rio de Janeiro was a personal confirmation of the usefulness and the value of what is known as the 'Pedestrian and Evacuation Dynamics' research field.

The Nomad pedestrian simulation model implemented and applied during this dissertation was a significant achievement for me, given that it had the double role of being a research platform and an application tool. The large effort to make it accurate, capable to simulate complex pedestrian facilities with good computational efficiency and user friendliness gave me a unique working experience. Furthermore, the extensive calibration and validation procedures developed in this dissertation produced the confidence that allowed the free distribution of Nomad. It was with great satisfaction that I saw during these years, many professionals applying Nomad for their research and their commercial projects.

I want to start thanking my supervisors professor Serge Hoogendoorn and dr. Winnie Daamen for accepting me in their group and giving me the opportunity to dedicate so intensively in these studies. This PhD was certainly not an easy process but their strong support and commitment kept me afloat and pointing to the right direction even in less calm moments.

Also I want to thank all my colleagues through out these years for their nice camaraderie, friendship and knowledge. My long stay had the positive effect of introducing me to many colleagues and it would be beyond the purpose of this preface to mention all of them. However, some colleagues became friends and these I want to mention for the great moments we shared: Giselle, Femke, Tamara, Francesco(s), Andrea, Frank, Chris, Adam, Yufei, Daniel, Pavle, Bernat, Niharika and Goof.

This dissertation profited from a very inspiring conversation on statistical testing with professor Geurt Jongbloed from the Faculty of Electrical Engineering, Mathematics and Computer Science (EWI). Also thanks for Anders Johansson and Dietmar Bauer for the generous offer of pedestrian trajectories.

My partner deserves the largest gratitude that I can express. Wendelien kept me steady and comforted always! Her love was a sure place where I could retreat to find the fundamental support that one needs for such a project.

This dissertation was a long journey, so long that my little daughter Lina blossomed and became an incredible individual that makes me proud like nothing else. I want to dedicate this dissertation to Lina that grew seeing me working for long hours behind (many) screens.

At the end of this process, Suely Rolnik played a vital role of helping me staying in the path to reach the end and I want to thank her for her wisdom and understanding.

Mario Campanella, November 2016

Contents

Summary

In the first part of this dissertation we performed a state-of-the art of walker models, distinguishing models by characteristics relevant from a model developer point of view (chapter 2). We introduced an agent-based model representation for walker models using a 'humanised' description of model components. The descriptions are unique by equating the model components to pedestrian behavioural and physical aspects. The agent representation results in a logical and meaningful way to compare the different types of models resulting in model families that differ according to the type of 'reasoning' that pedestrians undertake to predict their next moves.

We applied the agent representation to create a scoring system to evaluate the types of models. The aim of the scoring system was to determine which type was most suited to be further developed to simulate large pedestrian facilities and what components should be improved or introduced. We identified that Nomad originally proposed by Hoogendoorn and Bovy (2002) ranked amongst the best walker models, had some important features such as being originated from a pedestrian theory that should facilitate the further development.

Nomad was changed from a pure reactive model to a reactive/anticipative model (chapter 3). A level of anticipation is provided by a zero acceleration assumption that enforces Nomad pedestrians to consider future positions of nearby pedestrians to derive their interaction reactions. Furthermore, the reactive interaction component was modified to intensify the lateral avoiding manoeuvres in frontal collision paths eliminating the unrealistic interactions occurring with the original formulation of Nomad and with the original Social Force models.

New behaviours that are common in pedestrian facilities such as waiting, passing turnstiles, queuing choice behaviour, and changing levels using stairs and escalators are modelled and implemented in Nomad. All these new activities are implemented according to the normative principles proposed in the Nomad pedestrian theory allowing for a complete integration between the different behavioural levels.

Microscopic models are notoriously slower when compared with macroscopic models (Duives et al. (2013)). Therefore, we proposed new numerical methods in chapter 3 to improve the computation efficiency without significant loss of accuracy. The numerical method is composed by a variable time step numerical scheme based on the principle

that pedestrians that do not have much traffic in their vicinity, can walk with less regard to the neighbouring pedestrians.

The variable time step resulted in significant performance gains. A very large simulation area of more than 80,000 m^2 containing more than 3,000 pedestrians was accelerated almost 5 times without loss of accuracy and numerical stability. This unique method can be easily adapted to most walker models with the exception of CA models.

Walker models are not reliable if not presented with validations indicating their overall accuracy. An obstacle for the popularisation of walker models, is the impractical effort to calibrate and validate models for each specific situation that they are applied. Therefore, models and their parameters must present good validations in a significant array of different situations that will (hopefully) account for the situations encountered by real pedestrians in complex pedestrian facilities.

The first step in preparing models like Nomad for their prediction tasks was to investigate what are the conditions that the calibration and validation process must possess to increase the probability that Nomad (and other walker models) are predicting pedestrian behaviours accurately.

For that we first introduced methodologies in chapter 4 that describe and logically organise the processes of calibration and validation of walker models. The most important component of the methodology is the scenario, that contains all items necessary to obtain a measure of accuracy. Its core is a function that maps the reference and simulated data into an indicator that is used to quantify the accuracy of the model.

The methodology is based on the principle that walker models that will be of general use need to be calibrated and validated using several flows and performance indicators that account for different walking situations (multi-scenarios). Furthermore, the calibration methodology requires a final significance test to confirm that the calibrated parameters (or the component of the model) are significant (influences the outcomes).

In chapter 5 we realised a series of calibrations using synthetic trajectories generated by Nomad. The parameters that created the data became the 'ground truth' values allowing for comparisons of calibration results with the original parameter values. This allowed for a detailed assessment of factors affecting calibration and resulted in conclusions about the accuracy of the calibration processes.

Chapter 6 presents extensive calibrations of Nomad with empirical data obtained from several experiments. The calibrations in this chapter were performed for the individuals resulting in parameter sets optimised for their particular trajectories. These individual results allowed for detailed analysis of pedestrian behaviours that are not easily measurable by analysing the parameter values defining the components of the Nomad model. Calibrated parameters were compared over population heterogeneity, level of urgency, types of flow and local conditions.

We performed detailed validations of eight parameter sets in chapter 7 using quantitive indicators that included average travel times, $u \times k$ relations and bottleneck capacity.

The accuracy from the different parameter sets were compared using empirical data from four different flows. We found that the accuracy of single scenario sets to predict flows other than those used in their calibrations is much lower than the accuracy of multi-scenario sets. We also found that adding a second performance indicator in the calibration of multi-scenario sets improved significantly the accuracy of predictions in flows other than those used in the calibrations.

The investigations ended in chapter 8 with examples of novel applications of walker models that go beyond the assessments of safety regulations. Nomad was used for determination of bottlenecks and circulation problems, applied to an optimisation problem, and for the determination of the maximum demand that would fulfil comfort criteria. To accomplish the case studies in large pedestrian facilities, new features of Nomad namely waiting behaviours, escalators and stairs, queuing and server activities were face validated and applied. The application of Nomad showed the feasibility to apply walker models to reveal insights about pedestrian behaviour in large pedestrian facilities.

Samenvatting

In het eerste deel van deze dissertatie bestuderen we de state-of-the-art in loopmodellen waarbij we modelkarakteristieken in kaart brengen die relevant zijn voor modelontwikkeling (hoofdstuk 2). We introduceren een microscopisch atomaire (zogenoemde agent-based) representatie voor loopmodellen gebruik makend van een 'menselijke' beschrijving van model componenten. Deze beschrijvingen zijn uniek in de wijze waarop de model componenten direct gekoppeld zijn aan gedragsmatige en fysieke aspecten van voetgangers. De atomaire agent representatie resulteert in een logische en begrijpbare manier om verschillende modeltypen te vergelijken en hier families van modellen uit af te leiden die onderling verschillen in het denkproces van voetgangers om hun volgende stappen te voorspellen.

Met behulp van de agent representatie hebben we een scoringssysteem ontwikkeld om de verschillende typen modellen te evalueren. Het doel van dit scoringssysteem is om vast te stellen welk modeltype het best geschikt is als startpunt voor verdere ontwikkeling met het oog op het simuleren van grootschalige voetgangersfaciliteiten en welke modelcomponenten dienen te worden verbeterd of ontwikkeld. We identificeren Nomad, oorspronkelijk gepresenteerd door Hoogendoorn and Bovy (2002), als een van de beste loopmodellen dankzij enkele belangrijke karakteristieken waaronder het feit dat er een voetgangerstheorie aan ten grondslag ligt wat verdere modelontwikkeling faciliteert.

Nomad is aangepast van puur reactief model naar reactief-anticiperend model (hoofdstuk 3). Een mate van anticipatie is toegevoegd waarbij Nomad-voetgangers rekening houden met verwachtte interacties met nabije voetgangers onder de aanname van geen acceleratie. Verder is het modelcomponent voor reactieve interacties aangepast om laterale uitwijkmanoeuvres bij kans op frontale botsing te versterken. Dit voorkomt onrealistische interacties die zichtbaar zijn bij de oorspronkelijke formuleringen van Nomad en andere Social Force modellen.

Nieuwe vormen van gedrag zijn geïmplementeerd in Nomad die te zien zijn in veel voetgangersfaciliteiten, zoals wachten, het passeren van toegangspoortjes, (keuze)gedrag rondom wachtrijen en het loopgedrag bij vaste trappen en roltrappen. Al deze nieuwe activiteiten zijn geïmplementeerd volgens normatieve principes in de Nomad voetgangerstheorie wat zorgt voor een complete integratie in alle niveaus van gedrag.

Microscopische modellen zijn notoir langzamer in vergelijking tot macroscopische

modellen (Duives et al. (2013)). Daarom introduceren we nieuwe numerieke methodes in hoofdstuk 3 om de rekenefficiëntie te verbeteren zonder significante afbreuk in nauwkeurigheid. De numerieke methodes maken gebruik van een numeriek schema met variabele tijdstap en nemen daarbij in acht dat voetgangers met weinig ander verkeer in hun nabijheid kunnen lopen zonder rekening te houden met naburige voetgangers.

De variabele tijdstap zorgt voor een significante vooruitgang. Een zeer grote simulatieomgeving van 80.000 m2 met meer dan 3.000 voetgangers is tot vrijwel 5 maal sneller door te rekenen zonder in te leveren op nauwkeurigheid of numerieke stabiliteit. Deze unieke methode kan eenvoudig geïntroduceerd worden in de meeste loopmodellen met uitzondering van Cellulair Automata modellen.

Loopmodellen zijn onbetrouwbaar zolang hun nauwkeurigheid niet is gevalideerd. Een obstakel in het populariseren van loopmodellen is de omvangrijke moeite ten aanzien van het kalibreren en valideren van deze modellen voor elke specifieke situatie waarvoor de modellen worden toegepast. Modellen en modelparameters dienen daarom gevalideerd te worden in een significante set aan situaties wat (hopelijk) representatief is voor de situaties ervaren door echte voetgangers in complexe voetgangersfaciliteiten.

De eerste, voorbereidende stap in het toepassen van modellen zoals Nomad voor het maken van voorspellingen is het bestuderen van de omstandigheden waarvoor kalibratie en validatie uitgevoerd moet worden. Dit om zeker te stellen dat het voorspelde voetgangersgedrag voldoende nauwkeurig is.

Hiertoe introduceren we in hoofdstuk 4 methodes die de kalibratie- en validatieprocessen beschrijven en op logische wijze structureren. Het belangrijkste onderdeel van deze methodes is het scenario, welk alle vereiste aspecten dient te bevatten zodat de mate van modelnauwkeurigheid betrouwbaar kan worden vastgesteld. De kern is een functie wat de referentiedata en simulatiedata combineert tot een indicator die het mogelijk maakt om de modelnauwkeurigheid te kwantificeren.

De methodologie is gebaseerd op het principe dat loopmodellen welk voor generieke toepassingen gebruikt worden, dienen te worden gekalibreerd en gevalideerd gebruik makend van meerdere verkeersstroom- en functioneringsindicatoren en op basis van verschillende loopsituaties (multi-scenario). Verder dient de kalibratiemethode ook een uiteindelijke significantietest te bevatten om vast te stellen dat alle gekalibreerde parameters (of de modelcomponenten) daadwerkelijk significant zijn (en dus de modeluitkomsten beïnvloeden).

In hoofdstuk 5 voeren we een serie kalibraties uit op basis van synthetische trajectoriën gegenereerd in Nomad. Door de parameters die ten grondslag liggen aan de synthetische trajectoriën te positioneren als werkelijkheid kunnen we de kalibratie uitkomsten vergelijken en beoordelen. Dit stelt ons in staat om te bestuderen welke factoren de kalibratie beïnvloeden en om conclusies te trekken over de nauwkeurigheid van de kalibratie alsmede de gevolgen van het gebruik van verschillende parametersets.

Hoofdstuk 6 presenteert uitgebreide kalibraties in Nomad met empirische data uit verschillende experimenten. De kalibraties in dit hoofdstuk zijn uitgevoerd op individu niveau wat leidt tot geoptimaliseerde parametersets voor hun specifieke trajectoriën. Deze individuele resultaten maken gedetailleerde analyses van voetgangersgedrag mogelijk wat doorgaans moeilijk meetbaar is wanneer men de geaggregeerde parameterwaarden van deze modelcomponenten beschouwd. Zo zijn gekalibreerde parameters vergeleken ten aanzien van populatie heterogeniteit, mate van urgentie, typen van verkeersstromen en lokale omstandigheden.

In hoofdstuk 7 voeren we gedetailleerde validatie uit op acht parametersets waarbij we gebruik maken van kwantitatieve indicatoren waaronder gemiddelde reistijden, snelheid-dichtheid relaties en knelpuntcapaciteiten. We vergelijken de nauwkeurigheid van de verschillende parametersets op basis van empirische data van vier verschillende stromen. We laten zien dat de nauwkeurigheid van enkel-scenario sets voor het voorspellen van andere stromen dan waarop is gekalibreerd veel lager ligt dan de nauwkeurigheid van multi-scenario sets. Tevens laten we zien dat het toevoegen van een tweede functioneringsindicator in de multi-scenario kalibratie de nauwkeurigheid van de voorspellingen significant verbetert.

Tot slot in hoofdstuk 8 besluiten we deze studie met voorbeelden van innovatieve toepassingen van loopmodellen die verder gaan dan het beoordelen van veiligheidsregels. Nomad is toegepast voor het vaststellen van knelpunt- en circulatieproblemen, voor een optimalisatieprobleem en voor het bepalen van de maximale vraag wat nog voldoet aan comfort criteria. Voor het doorrekenen van deze casussen in grote voetgangersfaciliteiten zijn de nieuwe modelkarakteristieken van Nomad – betreffende wachtgedrag, trappen en roltrappen, wachtrijen en service activiteiten – geverifieerd en toegepast. Deze toepassingen van Nomad tonen de haalbaarheid om op basis van loopmodellen inzichten te verkrijgen over voetgangersgedrag in grote voetgangersfaciliteiten.

List of Figures

List of Tables

Notation

Overview of pedestrian state variables

Symbol	Explanation
$\vec{r}$	position: location of the pedestrian from the origin (m,m,m).
$\vec{v}$	velocity: vector with the speeds. in each reference axis $(m/s,m/s,m/s)$.
$\vec{a}$	acceleration: vector with the acceleration values. in each reference axis $(m/s^2,m/s^2,m/s^2)$.
$\vec{z}$	dynamic state: the three dynamic components ($\vec{r}$,$\vec{v}$,$\vec{a}$).
X_p	trajectory: the set of all states of a pedestrian p.

Overview of pedestrian traffic variables

Symbol	Explanation
u	speed.
$\hat{u}$	average speed.
k	density.
q	flow.
$u \times k$	speed density relation.
$u \times q$	speed flow relation.
$q \times k$	flow density relation.
q_c	capacity.
TT	travel time.
ξ	traffic state (for the Nomad model are the velocities and positions from pedestrians).

Overview of Nomad parameters. The double lines separate the parameters according to the pedestrian characteristics and the three model components: path following, pedestrian interactions and obstacle interactions. The single lines separate the four parts of the pedestrian interaction component: pedestrian avoidance, physical interaction, influence area, lateral avoidance and anticipation.

Symbol	Explanation
rad	pedestrian radius (m).
v_0	free-speed (m/s), speed at which pedestrians would walk when unhindered.
τ	acceleration time (s), the time required to accelerate towards the free-speed v_0 in the direction of the desired path. Small values of τ will force pedestrians to walk very close to their desired path and to their free-speeds. Any deviation from the path will generate large path following accelerations.
a_0	interaction strength (m/s^2), controls the intensity in which pedestrians are avoiding each other. Larger values of a_0 indicate an increase of the avoidance accelerations due to other pedestrians.
r_0	interaction distance (m), controls how sensitive the avoidance accelerations are to the distance between pedestrians. Small values of r_0 ($\sim 0.0m$) signify that only small distances between pedestrian cause avoidance accelerations.
k_0	controls the intensity of the longitudinal physical forces between pedestrians.
k_1	controls the intensity of the tangential physical forces between pedestrians.
c_0^-	transforms the shape of the influence area behind pedestrians from circular (value = 1) to an ellipsoid. For values smaller than one the main axis of the ellipsoid is in the walking direction otherwise; in the perpendicular direction.
c_0^+	transforms the shape of the influence area in front of pedestrians from circular to an elongated ellipsoid similar to c_0^-.
ie_f	influence area extension at the front (m), the largest distance at the front at which a pedestrian will provoke avoiding behaviours.
ie_b	influence area extension at the back (m), the largest distance at the front at which a pedestrian will provoke avoiding behaviours.
a_1	lateral interaction strength for pedestrians (m/s^2), controls the intensity of the extra lateral component of the avoidance accelerations when pedestrians are walking towards each other.
r_1	lateral interaction distance for pedestrians (m), controls how responsive the extra lateral avoidance accelerations are to the lateral distances of pedestrians walking towards each other.
t_A	anticipation time (s), the time in the future that pedestrians project the current locations of neighbouring pedestrians.
a_W	obstacle interaction strength (m/s^2), controls the intensity in which pedestrians are avoiding obstacles. Larger values of a_W indicate an increase of importance of the obstacle avoidance accelerations.

Overview of pedestrian simulation variables

Symbol	Explanation
WF	the walking facility in which the pedestrians are walking. It comprises of all walking areas and infrastructures (obstacles).
c	the cells in which the walking area is divided into.
T	the period of time in which a pedestrian traffic occurs.
ΔT	the discrete interval of time in which the simulation state is updated.
P	the set of all pedestrians that walk in WF during T.
A	all areas accessible to pedestrians in WF.
I	the set of all infrastructures present in WF.
θ	the set of parameters that are used in walker models.
β	all the information necessary to run a simulation with a walker model apart of the value of the parameters.

Chapter 1

Introduction

Most metropoles face pedestrian congestion on a daily basis. The movement of commuters in cities such as Rio de Janeiro, São Paulo, London, New York, Tokyo and Shanghai creates large demands on their public transport systems, routinely exposing pedestrians to crowded stations and public transport vehicles. The large demand of daily movements is not diminishing; on the contrary more commuters will use public transportation.

According to the United Nations, approximately 53% of the world population was urban in 2015 and 70% will be in 2050 (UN (2007)). The trend shows both an increase in the absolute number of large cities and cities reaching unprecedented sizes. However, most of this growth will not occur in the largest cities, but in smaller and secondary cities (Cohen (2004)).

This means that many more cities will have their CBD (Central Business Districts), their primary transportation nodes (especially in the peak hours) and other heavily used pedestrian areas crowded with high intensity pedestrian flows. Furthermore, there is a global consensus about the necessity to mitigate carbon emissions and to improve the sustainability and liveability of cities (UN (2010)). This consensus is putting pressures to city managers to discourage car travel favouring alternative modes of transport and simultaneously to support pedestrianism (Gehl (2010)). Cities will need to prepare for these concentrations of pedestrians.

The costs and difficulties in managing large and dense crowds on a daily basis lead to the anticipation of the effects of large crowds in the design phase of heavily used walking areas. Creating good circulation, reserving buffer areas, avoiding extreme densities and providing short travel times should be an integral part of the design of pedestrian facilities (TRB (2000)).

1.1 Background

The movements that pedestrians perform are complex and pedestrian flows show a wide range of phenomena from individual to collective patterns. Pedestrians are capable to perform very high accelerations when initiating movement or when stopping (Goffman (1972)). They can walk in directions including backwards and sidestepping (Wolff (1973)). Self-organised collective patterns such as lanes that are formed in bi-directional flows or stripes in 90°crossing flows appear without coordination, makes operations highly efficient and influence the traffic characteristics of pedestrian flows (Helbing et al. (2005), Hoogendoorn and Bovy (2006)). Behaviours vary among other things according to the composition of the population and their cultural backgrounds (Chattaraj et al. (2009)), time of the day (Weidmann (1993)) and demographics (Daamen and Hoogendoorn (2009a)).

When assessing pedestrian flows for evacuation regulations or for normal conditions, especially during peak hours it is necessary to determine precisely where are the areas with high levels of density and flows. However, the complexities of pedestrian behaviour can create uneven distributions of pedestrians (heterogeneous distribution) and flow interactions that can very often not be predicted by simple calculations.

1.1.1 Designing pedestrian facilities

A common practice is to consider the maximum flow of pedestrians per unity of time (capacity q_c) and apply it to determine corridor widths and size of exits. However, capacity conditions cause the development of queues and congestion and as Fruin (1971) recognises on page 71: *"capacity design is planned congestion"*. Therefore, this is not a good practice since good pedestrian facility should provide safety, efficiency and attractiveness to pedestrians (Gehl (2010)).

Intense pedestrian flows need to be kept safe by avoiding unhealthy or dangerous situations, efficient by not causing unnecessary delays and attractive encouraging people to walk. This is not an easy task since pedestrian facilities usually include several functions in the same area such as transportation, recreation, shopping and business. This mix of functions creates many opportunities for different behaviours to coexist.

To design pedestrian facilities it is necessary to predict pedestrian behaviours quantitatively and accurately to assess different layouts and plans. The problem can be summarised as: *to find the balance between the cost of construction and future expansion of pedestrian facilities and the different planning objectives*.

To operationalise this, studies and guidelines were proposed and have been applied for more than 40 years. (Fruin (1971), Predtechenskii and Milinskii (1978), TRB (2010)).

What these guidelines have in common is that they rely on simple calculations and graphs to estimate widths of sidewalks, corridors, stairways or quantity of escalators.

These methods divide pedestrian facilities into uni- or bi-dimensional components, apply the expected demand and by varying the components parameters reach desired level-of-service (LOS)[1] or travel times.

Although practical and popular, these guidelines suffer from the inherent problem of not considering heterogeneity in the pedestrian population, the fact that different populations may occur at different times and the heterogeneity in distribution over the network, caused by the distribution of origins and destinations, but also by the demand compared to local capacity.

Many pedestrian facilities cannot be easily translated into a network of components. Atriums or transfer station halls are often large two or even three dimensional areas that cannot be represented by unidimensional components. Furthermore, real areas include localised obstacles such as boards, ticket machines and seats. Therefore, more advanced tooling is needed to support the design process and assess the movements and distributions of pedestrians over time.

Simulations are being used for different purposes in natural and social sciences (Hartmann (1996)). They are applied when problems get too complex to be described in its entirety by analytic equations. This is the type of problems that arise when we need to determine pedestrian traffic in large pedestrian facilities submitted to large flows and with complex pedestrian behaviours (Still (2000)). It is just natural that accurate pedestrian flow models are needed and are being promoted for traffic engineers, architects, urban planners and fire engineers (Kuligowski and Gwynne (2005)).

Pedestrian models are able to simulate the dynamics of walking in practically all configurations (Schadschneider et al. (2009)). Furthermore, they allow to quantitatively and objectively compare the performance of different designs. Pedestrian models are developed to cope with complexity of situations and generate visual evidence of the dynamics of situations by means of renderings of the flows.

1.1.2 Need for the development of accurate pedestrian models

Shmueli (2010) argues that models that have a good predictive capacity and simultaneously provide a platform for exploration of human behaviours are more valuable to science (fidelity of behaviours). We take the view that this is also valid for the science of pedestrian modelling.

To be useful for practical applications, pedestrian models have to fulfil some requirements: Kuligowski and Gwynne (2005) mention model characteristics (representation and approach), accuracy of the outcomes (verification and validation) and commercial aspects of models. Daamen (2004) enumerates the refinement of the input, the type of performance indicators available in the output, functionality of the model (which

[1] Level Of Service associates levels of comfort with density intervals (Fruin (1971)). It is an effective tool to relate individual well being to traffic characteristics.

behaviours the model is capable to reproduce) and user-friendliness of the graphical user interface.

Fidelity to human behaviour, *accuracy* of the outcomes and the *functionality* available are requirements to both scientific research and practical applications and will become the focus of this dissertation.

Behavioural fidelity

The large and complex range of pedestrian behaviours, reflected by their individual movements and collective patterns must be correctly represented by pedestrian models. Pedestrian models must be able to predict correctly self-organised patters that naturally occur in different types of flows: lane formation, diagonal stripes and zipper effect (Hoogendoorn and Daamen (2005b)).

If models are able to simulate individuals (microscopic models) then their movement should resemble what is observed on average from real pedestrians: smooth movements, large accelerations, no restriction in the walking direction, good collision avoidance and (occasional) sidestepping.

This requirement of high fidelity is not easy to be accomplished and no model predicts individual behaviours and collective patterns perfectly and probably will never do so.

Quantitative accuracy

Models must be thoroughly tested and made adequate for the tasks of prediction (Galea (1998)). Models reproducing walking behaviour will very likely present errors when compared to reality. However, this does not deter the use of models if their predictions are validated against empirical data.

Most practical applications assess situations with large flows that usually result in congestion and high densities. Therefore, models must be shown to be accurate in the whole range of traffic variables, especially in high densities (Campanella et al. (2012)). Therefore, models should present quantitive evidence of the predictions of these phenomena (Campanella et al. (2008)).

Microscopic pedestrian models suffer from the problem of having too many parameters (Bellomo et al. (2011)). The principle of parsimony that states that models should be as simple as possible should be considered when developing models to keep them as generic as possible and reducing the complexity of the calibration task.

Model functionality

The majority of the pedestrian models is developed to predict situations where pedestrians are only walking. Moreover, their application in large facilities requires other

activities such as waiting, queuing, shopping and should thus be covered by the model.[2]

1.1.3 Pedestrian models development cycle

Obtaining a pedestrian model that is of scientific and practical use requires several important steps. In this dissertation we will focus in developing walker models following development cycle for a model based on empirics and theory, proposed in Daamen (2004) and presented in figure 1.1.

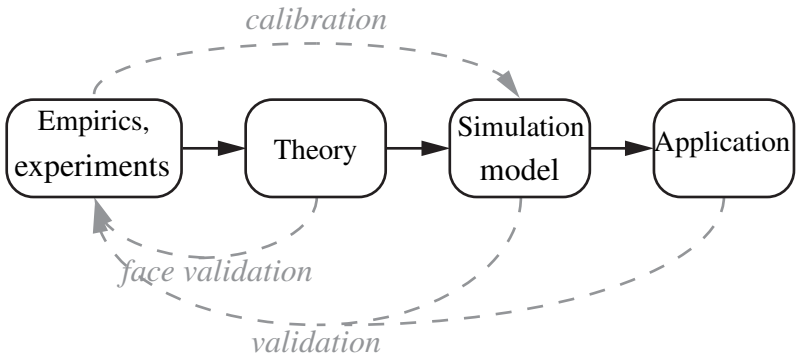

Figure 1.1: The cycle for the development of pedestrian models (adapted from Daamen (2004)).

The first step is to collect data and evidence on pedestrian behaviours. Since modelling of pedestrian flows is an inductive science, this is achieved by observation in real situations (Shi et al. (2007)) and in laboratory experiments (Daamen and Hoogendoorn (2003)). Data collection can be performed using field observations and questionnaires (Hill (1982)) or via sensors: video recordings and video tracking tools (Hoogendoorn et al. (2003)), infrared (Kerridge et al. (2005)), laser scanning (Bauer and Kitazawa (2010)), bluetooth and wifi sensors (Millonig and Gartner (2008)); and gps for route choices (Van Der Spek et al. (2009)).

The knowledge gathered in observations is used to derive and test walking principles and behavioural assumptions. These principles are mostly qualitative synthesis of empirical evidence such as the fact that pedestrians interact more intensively with pedestrians nearby and in their front. These are used to justify modelling decisions (Moussaïd et al. (2011)) or to develop a walking theory (Hoogendoorn (2001)). The development of a theory is more powerful because it can be tested against empirical evidence and allows for deduction of new walking principles.

[2]User oriented aspects are important for the regular use of walker models. These are discussed extensively in Daamen (2004) and Kuligowski and Gwynne (2005). Given that this is not the topic of this dissertation we will not discuss these aspects. However, we point that it is desired that the model presents good computational performance to be of practical use, especially for simulations involving many pedestrians (>1,000 peds).

The third step is to create a model based on the theory. Sometimes a mathematical model is developed and subsequently a simulation model that can be implemented in a computer is derived from it. Here we simplify and consider these as one step.

The last step is the application of the simulation model in cases that will be used to calibrate the model parameters (Schadschneider et al. (2010)) and more importantly validate its predictions (Ronchi et al. (2014)).

1.2 Research scope

Figure 1.1 showed the four steps necessary to develop pedestrian models for application and study of behaviours. One dissertation cannot cover all steps in depth. Therefore, we limit the scope of this research. We will concentrate on the last two steps: the development of the simulation model and the steps necessary to successfully apply it (the two last boxes and the arrows connecting them).

According to Hoogendoorn (2007) amongst the most important characteristics of traffic models are the level-of-detail in traffic representation and in behaviour modelling. Section 1.2.1 will discuss level-of-detail of pedestrian models and the choice made in this dissertation.

The other important research scope of this dissertation refers to the 'tasks' pedestrians perform. Pedestrians do not only walk but also perform activities during their trips. Furthermore, pedestrians make choices regarding the trip and pedestrian models need to incorporate all these behaviours. Section 1.2.2 presents these tasks on different behaviour levels and the choice of focusing on the walking behaviour.

1.2.1 Level-of-detail of models

Level-of-detail in traffic representation refers to the size of the smallest parts of the traffic. Microscopic representation describes each pedestrian as an individual, while macroscopic representation incorporates pedestrians as continuum groups distributed over certain areas (Bellomo et al. (2012)). The level-of-detail in behavioural representation indicates if the model describes the movement of each pedestrian (microscopic) or the movement of the entire population by means of the three traffic characteristics speed, density and flow.

Most types of models are either microscopic (Cellular Automata and Social Force) or macroscopic (Continuum). However, some models that describe the walking area as a system of interconnected links are of referred to as mesoscopic models (Bellomo et al. (2012)). Løvås (1994) and Daamen (2004) are examples of such models. At each link the walking speeds are set according to their occupation (density). Such models are able to predict important features of pedestrian traffic such as spill-back upstream of

congestions. Although theoretically possible, such models must be calibrated with a large amount of specific data to simulate detailed features of the walking areas such as columns and crossing flows in wide areas. This makes them not practical to be used in complex pedestrian areas.

In general, macroscopic modelling allows for faster simulations, big pedestrian facilities and large population size (Duives et al. (2013)). These models are being promoted for real-time applications when models are deployed for crowd-management purposes (Hoogendoorn et al. (2014)). Encouraging developments such as by Hoogendoorn et al. (2014) are showing that self-organised phenomena can be predicted by macroscopic models. However, these are preliminary results that still need further development. Furthermore, the continuum nature macroscopic models is not appropriate to study individual behaviour (Hughes (2002)).

Microscopic models offer the possibility of detailed descriptions of the environment and of the pedestrians (Bellomo et al. (2012)). They are suitable for simulations of diverse types of pedestrian facilities (Kuligowski et al. (2010)). Microscopic models are per definition predicting movements of individuals and this allows for heterogeneous populations that are important for the realistic description of pedestrian flows (Moussaïd et al. (2012)). For all these reasons, we choose microscopic models as the focus of this dissertation.

*This thesis deals with a **microscopic model** with individual pedestrian behaviours.*

1.2.2 Modelling paradigm and pedestrian behavioural levels

By definition, a trip starts at an origin and ends at a destination and this also holds for pedestrians. Between the origin and destination the trip may include many activities. Walking can be regarded as the movement to connect the activity locations. A typical trip starts with a plan of what the pedestrian is going to do during the trip, the start time and the (initial) routes he or she will take. The initial decisions can be re-evaluated during the trip due to (un)foreseen conditions until the final destination is reached. This general description applies to the most common trip purposes like commuting between an origin and destination. Leisure walking in a park, shopping in a commercial area and evacuating from a building do may not follow a plan and present walking and re-evaluations according to a specific goals or desires.

To simulate such a trip many different aspects of pedestrian behaviours need to be modelled. Hoogendoorn and Bovy (2004) describes the pedestrian behaviours using a three level modelling approach. The three level concept originated in traffic modelling and is being adopted by many pedestrian modellers (Schadschneider et al. (2009), Papadimitriou et al. (2009), Antonini et al. (2006), Sahaleh et al. (2012), Johansson (2013)).

The *strategic* level contains all planning done before the trip initiates. This plan includes the choice of activities that will be performed during the trip, the order that they will be performed and the route that will be taken. The *tactical* level deals with all changes of the plan and all choices that are made during the trip. The *operational* level describes how pedestrians move in space and the behavioural actions such as walking, waiting. Models that implement the operational level are also referred to as *walker models* and are the base of any pedestrian simulation model. Details of the three level pedestrian model are presented in chapter 3.

The importance of the operational level and the fact that it is not yet fully developed and thoroughly tested motivated us to concentrate only in this level. This allowed for an in-depth investigation of the operational level including developments of new behaviours and validation of the walking behaviour in several situations.

All pedestrian levels described in this dissertation are implemented, but only the ***operational level*** *is studied in depth.*

1.3 Research objectives

We mentioned before that we are interested in walker models that are predictive (accurate) and explanatory (based on a theoretical framework). After inspecting the literature we can see that there is a discrepancy between the relatively wide use of models (Galea and Galparsoro (1994), Klüpfel and Meyer-Konig (2003), Daamen et al. (2008), Kuligowski et al. (2010)) and the non existence of good calibration and validation approaches. Developers validate their models in different ways making it difficult to assess them.

Furthermore, there are no studies comparing the outcomes of calibrations regarding the different situations pedestrians are walking in. What is the accuracy of parameters obtained with certain flows such as unidirectional flows that do not display frontal avoidance interactions when predicting bidirectional or crossing flows?

These fundamental issues regarding the accuracy and general use of walker models did not get much attention, not even for commercial models, thus motivating the development of methodologies and using them to investigate the processes of calibration and validation.

The main objective of this thesis is to develop ***calibration and validation methods*** *that result in parameter sets of general use that are accurate in many walking situations, including situations not used in the calibration.*

By comparing several characteristics of different types of models we chose the Nomad model proposed by Hoogendoorn and Bovy (2003) to be implemented, improved and be used in the investigations of this thesis.

Nomad not only has been proven to deliver good results (Hoogendoorn et al. (2004)) but it is also derived from a normative theory that pretends to explain pedestrian behaviours by the principle of utility maximisation (Hoogendoorn (2001)). The maximisation principle is a basis for all the developments proposed in this dissertation.

The original Nomad model only modelled the walking and its original version had a limited application due to a lack of other behaviours such as waiting and level changes. Furthermore, the Nomad model also needed improvements in accuracy and computational efficiency to simulate large facilities.

The second and final objective of this thesis is to investigate, develop, implement, calibrate and validate a walker model that is accurate and able to simulate large pedestrian facilities. This objective is achieved with a new version of the ***Nomad model*** *that is modified to include behaviours that occur in large pedestrian facilities.*

1.4 Research approach

Research objectives result in research questions that are answered using the approaches described below.

How to compare walker models based in model characteristics that are necessary to accurately simulate large pedestrian facilities? (chapter 2)

We undertake a literature research that identifies how the existing types of walker models describe pedestrian behaviour in the individual level. We use an agent based description of walker models to describe the characteristics of models based in the 'PAGE' components - Perception, Action, Goals and Environment from Russell and Norvig (1995). These components result in a 'humanised' description of the characteristics needed to simulate large pedestrian facilities.

The question is answered by assigning scores to the desired characteristics of the four 'Page' components. Each walker model receives a total score that is the sum of all characteristics scores. The total score and the scores obtained in the four 'PAGE' components are used to objectively compare different walker model types.

How to model and implement walking behaviour and pedestrian activities found in large pedestrian facilities? (chapter 3)

We use the normative principle of utility maximisation put forward in the Nomad pedestrian theory (Hoogendoorn and Bovy (2002)) to modify the original Nomad model. All new features are developed by defining indicators described as utilities to be gained or as a cost to be minimised.

What are the requirements for calibration and validation that result in parameter sets that are accurate in predictions of complex situations occurring in large pedestrian facilities? (chapter 4)

We use the hypothesis that states that: parameter sets calibrated with several indicators will likely perform better in many situations than specialised parameter sets. We use this hypothesis to propose methodologies to calibrate and validate walker models that combine different flows and performance indicators in what we called *multi-scenario* calibrations.

How to determine the accuracy of calibration procedures and how to improve their quality? (chapter 5)

In this question we are interested in assessing the quality of the calibrations. For that, we adapt the trajectory based calibration (Hoogendoorn and Daamen (2010)) that estimates optimal parameters for individual pedestrians to the multi-scenario methodology from chapter 4.

The procedure keeps all pedestrians in their video tracked positions at each time step. For each individual, the procedure determines via an optimisation algorithm the parameter set that results in the maximum log-likelihood estimate of the predicted accelerations for this individual along his or her trajectory.

We apply the trajectory based calibration to synthetic trajectories (trajectories created by Nomad simulations that provide known parameters). By comparing the resulting calibration to the 'correct' parameter values we are able to assess the calibration procedure and determine the factors that affect its accuracy and assess the beneficial effects of using multi-scenario calibrations.

What is the influence of type of flows, population composition, urgency and local conditions to walking behaviour? (chapter 6)

To answer this question we use calibration results to discuss the influence of some walking variables in the individual walking characteristics. The trajectory based calibration gives an opportunity to investigate in the individual level how pedestrians behave.

The most important parameters of Nomad are calibrated from trajectories originated from 11 different experiments resulting in 11 sets of parameter samples.

The parameter samples are composed by statistically significant parameters that are analysed according to different variables of interest: type of flows, population composition, urgency and local conditions.

To what degree multi-scenario calibrations improve the accuracy of parameters? (chapter 7)

To answer this question, we use three parameters sets obtained in chapter 6 and five new parameter sets calibrated using the methodology proposed in chapter 5. The calibration procedure uses errors from macroscopic performance indicators resulting in one parameter set representing the average behaviour of the whole population.

The parameter sets are divided between the so called *specialised* and *multi-scenario* sets. The specialised sets are obtained with travel times errors from one of three different experiments that create unidirectional, bidirectional and narrow bottleneck flows. The calibrations result in 3 sets of specialised parameters.

The multi-scenarios sets are obtained using the combined error of the three flows. One multi set uses only the travel time errors and the other uses the combined error of travel times and $u \times k$ relations.

The accuracy of the calibrated sets is assessed using a validation procedure derived from the methodology presented in chapter 5. The procedure uses average relative errors to obtain assessments in percentages varying from 'Good'(0-5% error), 'Medium'(5-10%) and 'Bad' (>10%).

The parameter set accuracy is measured on the three flows used in the calibrations and on a crossing flow. These measurements allow to compare the accuracy of the specialised and multi-scenario parameter sets over a wide range of flows that includes novel situations to investigate the occurrence of overfitting (Van Lint (2009)).

How a walker model can be used to reveal insights about pedestrian operations in transport nodes? (chapter 8)

The case studies represent real problems proposed by operators of large pedestrian facilities comprising an airport, train platforms and a complete metro station. We detect the development of congestion, assess LOS values and its durations, and we measure queuing and walking times.

For these case studies we use the full version of Nomad that includes the strategic level with activity and route choice behaviours and tactical level with activity area and queue choices.

1.5 Thesis contributions

This thesis deals with improving the accuracy of the Nomad model for application and behaviour investigation. It also deals with methods to improve the quality of calibrations and validations of walker models. Within this research several scientific and practical contributions have been achieved.

1.5.1 Scientific contributions

The main scientific contribution of this thesis is the development and extensive analysis of the calibration and validation processes. All investigations were performed with newly developed methods, comparing different objective functions with emphasis on multi-objectives. The investigations also covered heterogeneity in pedestrian populations and used several flow situations. These investigations resulted in important contributions that are presented below.

Calibration and validation methodology

A novel methodology that describes the components of calibration and validation of pedestrian models is proposed. The methodology is generic and can be used to calibrate any walker model with any aspect of pedestrian traffic. This methodology is based on separate scenarios that are paired using multi-objective functions.

Use of synthetic trajectories for analysis of calibration procedures

The approach of calibrating the Nomad model using synthetic trajectories is novel in pedestrian research. Using trajectories obtained in simulations allowed to evaluate the performance of the calibration procedure and to find factors that affected calibrations.

Multi-scenario quantitative validation

We proposed and applied a multi-objective function to be used in validations by model developers to perform quantitative validations. This approach uses a multi-objective that averages the indicator errors in a final error that is translated into ordinal scores such as ‘Bad’, ‘Medium’ and ‘Good’. The average error and the associated score allows for cross comparisons between different parameters in the same model and comparisons between different models.

Investigation of pedestrian characteristics with individual calibrations

Another contribution was the use of calibrations based on individual trajectories. This method allows for findings on pedestrian behaviour that are not obtained with direct analysis of the movements.

Agent-based model representation

The agent-based representation of walker models is divided over four ‘human-like’ elements that describe pedestrians: their Perception of the environment, the Actions they

can perform, their Goals and the Environment that they are walking in. The representation is a novel type of analyses of modelling strategies from different types of models. The representation enables an objective assessment of models using quantitative scores that measured the model elements against empirical evidence.

Introducing anticipation in the walking behaviour

An interaction behaviour of pedestrians introduces anticipation in walker models. Instead of reacting only at the current distances to opposing pedestrians, the new behaviour uses the expected distance in a nearby future. This behaviour gives significantly better results for frontal collisions and reflects how humans anticipate (Olivier et al. (2013)).

Modelling of non-walking behaviours

Waiting behaviours are used in simulations of areas in which pedestrians do not walk. The waiting behaviours cover small areas to be occupied by single or cover large areas such as train platforms and arrival halls with many pedestrians interacting. If the location is very dense, waiting pedestrians move slightly, letting others pass by in a step-and-sliding movement as observed by Wolff (1973).

Another contribution are new ordered queues behind servers that represent turnstiles or security checks. The modelled queues allow for traffic to pass very close or even cross them if the queues are blocking the traffic while not disturbing the queuing process.

Efficient numerical methods

The computational performance of microscopic models is directly dependent on the size of the discretised time-step. We developed a variable time-step scheme that only uses the smallest time-step for pedestrians walking in situations so dense that they face imminent collision.

1.5.2 Practical contributions

The practical contributions of this dissertation are related to the implementation of the Nomad model in a simulation tool. This tool that is available without costs in (www.pedestrians.tudelft.nl).

The simulation tool implements the three behavioural levels and was developed with modular and scalable architecture for future developments. The tool has several forms of inputs, a graphical user interface (gui) and can be used in different types of optimisation problems.

The Nomad model was applied in three test cases using novel methods to obtain insights in assessing transport nodes. The contribution was the setup and realisation of investigations that used the results of simulations to solve optimisation problems.

1.6 Outline of the thesis

Figure 1.2 presents the scheme of how the chapters follow logically from each other.

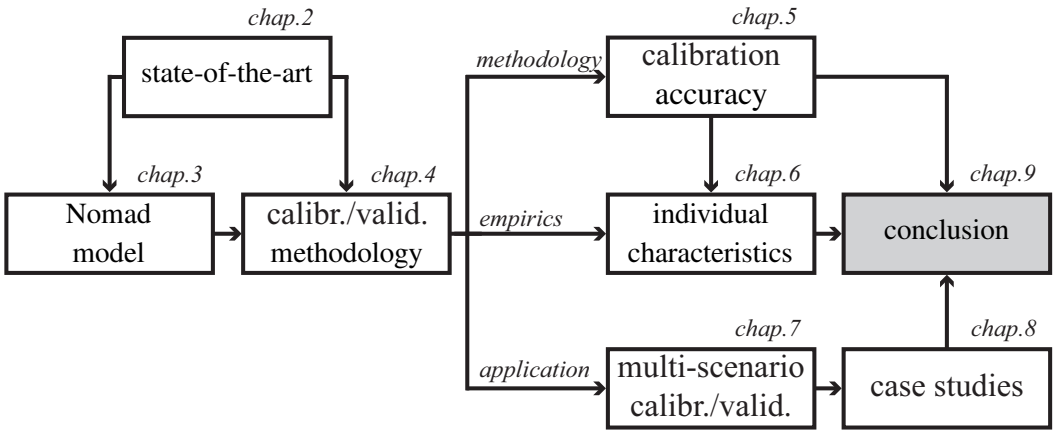

Figure 1.2: The structure of the thesis.

Chapter 2 gives an overview of pedestrian models by selecting the most important characteristics models must present to perform detailed assessments. The overview follows an agent-based framework to compare the characteristics of different types of models and their developments. The conclusion of the chapter indicates the reasons for choosing the Nomad model for improvement, extension, calibration, validation and application.

Chapter 3 presents the Nomad pedestrian theory and the equivalent model. The chapter discusses and presents modifications of the Nomad model aiming at modelling new behaviours, improving its accuracy and increasing the computational performance. This model is used in the following chapters.

Chapter 4 provides an overview of calibration and validation procedures including their shortcomings. These lead to the development of a generic calibration and validation methodology. The methodology is based on different simulation scenarios forming multi-objective functions.

Chapter 5 shows how synthetic trajectories are used to calibrate parameters of Nomad that represent individual behaviours. The calibrations follow the methodology presented in chapter 4 and the distributions of calibrated parameters are used to investigate factors affecting the accuracy of calibrations.

Chapter 6 uses the trajectory based calibration presented in chapter 5 on trajectories obtained from walking experiments. The results of the diverse calibrations are used

to determine distributions of parameters that are used to study individual behaviour. The distribution of parameters over the population represents the large heterogeneity encountered in pedestrian behaviours.

Chapter 7 investigates the improvement in prediction accuracy when using multi-scenarios in calibrations with macroscopic performance indicators. The calibrations and validations follow the methodology from chapter 4 providing quantitative measures of accuracy using experimental data.

Chapter 8 presents three applications of the improved Nomad model using the most accurate parameter set obtained in chapter 7. The cases studies illustrate novel uses of walker models to answer questions regarding pedestrians comfort in large pedestrian facilities. The cases also shows uses of the new behaviours of Nomad introduced in chapter 3.

The conclusion in chapter 9 presents a synthesis of the main contributions of the thesis. These are related to the current field of pedestrian modelling and simulation by highlighting the implications to the application of models. Furthermore, the findings of thesis are reflected upon indicating future directions of research.

Chapter 2

An agent-based perspective on walker models

Planning for pedestrian traffic started in the decade of 1970. This was much later than planning for car traffic (Helbing (1997)). The late start of pedestrian planning occurred even though there was plenty of evidence of the dangers due to overcrowding (Still (2000), Helbing et al. (2002)).

According to Van Wageningen-Kessels (2013) the first microscopic car traffic model was proposed in 1953, the field rapidly developed and soon car traffic models were applied by practitioners. However, pedestrian planners had to wait for another 20 years for the first walker models and even longer for their regular use.

Batty (2001) gives a historical account of the development of the pedestrian models of the 60's and 70's. He hypothesises that the static nature of the models and the lack of detailed and accurate predictions explain why decision makers did not apply these early models. Johansson (2013) mentions the much larger complexity of pedestrian behaviours when compared to car traffic as an inhibitor for their development.

Even though some microscopic models from the 70's as described in Hirai and Tarui (1975) and Okazaki (1979) are comparable to models appearing later in the 90's they had not much impact on the development of the field after their publication. Both models were developed in Japan and did not catch the attention of traffic planners, fire engineers or scientists in Europe or in the US, which had experience with car models.

It is considered that pedestrian modelling begins in the mid 80's as an independent research field and really got popular in the 90's (Batty (2001), Helbing et al. (2002)). Since then, the tools to study, collect data and to model pedestrians advanced fast.

In this thesis we take the view exposed in chapter 1 that models must accurately predict the individual walking and activity movements encountered in large pedestrian facilities. None of previous overviews such as Duives et al. (2013), Bellomo and Dogbe (2011), Kuligowski et al. (2010), Schadschneider et al. (2009), Gwynne et al. (1999)

discuss models according to these two requirements. Thus we need a different approach to assess walker models.

Here, we will review the existing walker model paradigms according to empirics of walking behaviour and assess their suitability to simulate large pedestrian facilities. It is not our aim to present an exhaustive list of walker models.

A second aim of the state-of-the-art is to choose a model to be further developed in this thesis. We show that the Nomad model meets all the requirements and allows for the implementation of behaviours occurring in large pedestrian facilities, thus being generic in its applicability. The model assessments in this chapter are done using a novel agent-based representation that relates model characteristics to behavioural aspects of pedestrians.

In the 80's the field of Artificial Intelligence introduced agent-based modelling approaches to solve problems of complex systems with large amounts of interacting parts (Russell and Norvig (1995)). The advantage is that highly nonlinear situations can be studied by the outcomes of the collective behaviour of the constituent parts.

There is not a universal definition of what makes a model agent-based. We adopt a generic definition by Russell and Norvig (1995) on page 33: *For each possible percept sequence, an ideal rational agent should do whatever action is expected to maximise its performance measure, on the basis of the evidence provided by the percept sequence and whatever built-in knowledge the agent has*.

Microscopic models (or individual-based models according to Hoogendoorn (1999)) are always described by a separation between the individuals and the environment (Duives et al. (2013), Bandini et al. (2014), Gwynne et al. (1999), Papadimitriou et al. (2009), Kuligowski et al. (2010), Bellomo and Dogbe (2011)). Therefore, they naturally fit in an agent-based representation.

Characterising pedestrian models in the agent paradigm is not new but it was never formalised for pedestrians (Batty (2001), Nagel and Marchal (2005), Helbing and Johansson (2009), Klügl (2008)). We do not consider agent-based a special type of model even when authors did name their models as such: Kukla et al. (2003), Bansal et al. (2008), Teknomo and Gerilla (2005), Toyama et al. (2006), Pelechano et al. (2007), Doniec et al. (2008)). All walker models that we encountered in our overview are successfully classified into four distinct agent types: rule, force, goal and utility-based models. These categories will be explained in the following sections.

In this chapter we propose the agent representation of walker models in section 2.1. Section 2.2 presents walker models according to the agent representation. We proceed in section 2.3 to present characteristics of walker models that represent pedestrian behaviours and model characteristics necessary to simulate large pedestrian facilities.

The rule, force, goal and utility-based models are assessed according to the agent representation and discussed in section 2.4. Section 2.5 presents the conclusions from the review of walker models, requirements for application in large pedestrian facilities and with arguments why we decided to further develop the Nomad model.

2.1 Agent representation of walker models

This section proposes an agent representation for walker models that is based on the PAGE concept of Percepts, Action, Goals and Environment described in Russell and Norvig (1995). These four elements represent the tasks (walking, waiting ...) and elements of the walking behaviour and are used to characterise the walker models.

Figure 2.1 proposes the representation of pedestrian behavioural levels as explained in sections 1.2 and 3.1. The figure shows how pedestrians walking on a dynamic environment may need to make choices (tactical level) based in what they are perceiving from the environment. These choices must be in accordance to their strategic goals directing the current actions (operational level).

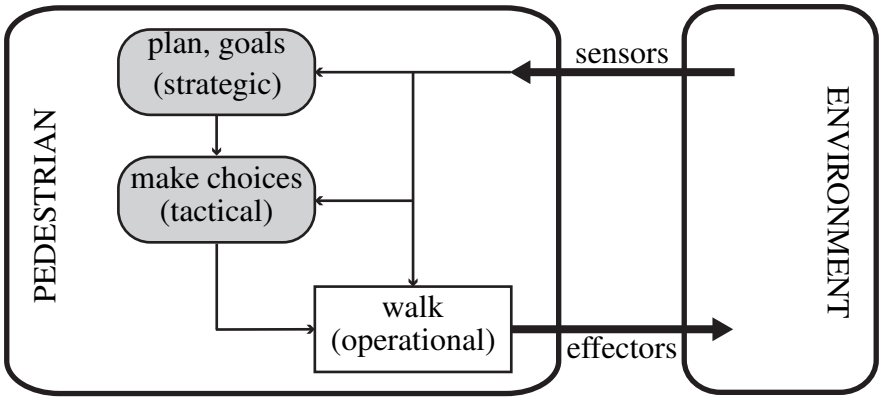

Figure 2.1: An agent-based adaptation of the three pedestrian behavioural levels by Hoogendoorn and Bovy (2004). The representation is inspired by Russell and Norvig (1995).

Given the focus of this thesis on the operational level (walker model), the strategic and tactical levels will not be further elaborated in this overview. A walker agent is a representation of the walking behaviour of a pedestrian using the 'humanised' PAGE elements.

*The walker agent perceives its surroundings for pedestrians and infrastructures; based on the interpretation of its **percepts** and its **goals** it will decide on an **action** and perform it, thus affecting the **environment**.*

Perception is all the information that agents get from the environment and from other pedestrians. They will perceive the pedestrian traffic, the infrastructures and information via signs or communication. We use the more general name of infrastructures instead of obstacles to include all possible objects that pedestrians interact with. Perception is not only the result of sensing, but also the interpretation thereof (thus including observation and interpretation errors).

Actions are everything that they can do in the walking facility, such as walking, accelerating, stopping, waiting and taking elevators.

Goals involve the aims of agents when walking such as spending the minimum amount of walking effort (Zipf (1949)), maximising utilities (Hoogendoorn and Bovy (2002)) or avoiding collisions (Moussaïd et al. (2011)). Note that the goals do not necessarily have to be represented explicitly by the agent. The goals describe the performance measure by which the agent is designed.

For each individual the **environment** comprehends the available walking and non-walking areas, infrastructure and the environmental conditions such as the presence of smoke or light.

An important aspect of agents is their **state**. The state of pedestrians ξ are their dynamic state $\vec{z}$ (position $\vec{r}$, velocity $\vec{v}$ and acceleration $\vec{a}$) and other properties that may be used in models such as urgency (Daamen and Hoogendoorn (2009a)) and fatigue (Shields et al. (2009)). Table 2.1 shows examples of agent states and PAGE elements.

Table 2.1: A walker agent representation with examples of the four PAGE agent elements (derived from Russell and Norvig (1995)).

state	percepts	actions	goals	environment
position, velocity, urgency, fatigue	vision, signs, communication	accelerate, stop, wait, steer, interact, climb stairs	avoid collisions, maximise utilities, minimise effort	walking areas, ramps, stairs, escalators, obstacles

The following section will present the four types of agents: rule, force, goal and utility-based. The types of walker agents differ according to the process of applying the percepts to perform the actions.[1]

The most simple walker agent has actions defined by rules, selected as reactions to the perceived traffic and infrastructures. The force-based agents do not have explicit actions, the actions 'emerge' from reactions to the percepts. Goal oriented models also have actions emerging but the reactions have an explicit intention of collision avoidance. The last type is utility-based that assigns utilities to different intentions and to reactions that also result in emergent actions.

2.2 Walker modelling paradigms

This section classifies walker models as they are known in the pedestrian modelling literature according to the four agent categories: rule, force, goal and utility models.

[1]Other types of agent are suggested by Russell and Norvig (1995) but they involve higher level of reasoning usually associated with the strategic and tactical levels.

2.2.1 Rule-based reactive agents

The most simple process to apply the percepts is using rules that directly describe the actions to be performed without using any state variable. An example is the first rule for a CA model proposed by Blue and Adler (1999): If two pedestrians need to sidestep to the same lateral cell then assign it to one of them with a probability of 50%.

Rule-based selection of actions represents a reactive behaviour and consequently, such models create **rule-based reactive** agents. The rules are in general of the if-then type. Most rule-based models do not use the dynamic state to apply the rules, therefore not needing to keep the agent state.

The limitation of such models is the necessity of predicting all situations pedestrians can encounter and encoding the actions to overcome them. The more complex the situations, the more exceptions must be described by the rules (Schadschneider et al. (2009)) turning them less intuitive and less naturalistic. Figure 2.2 shows a representation of a **rule-based reactive** agent.

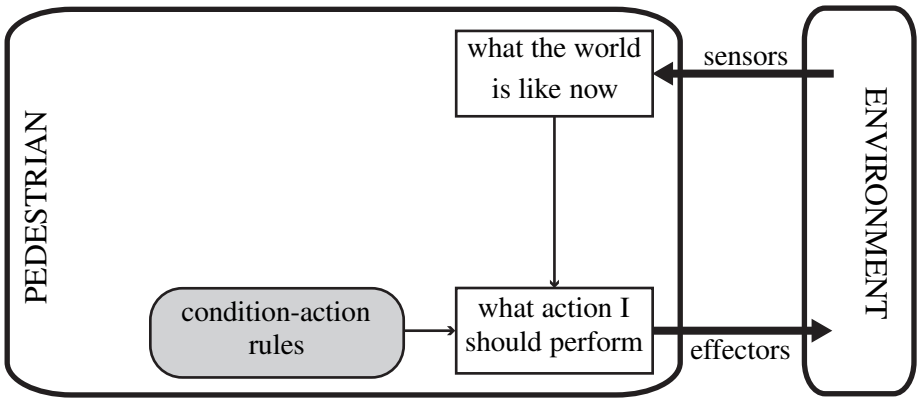

Figure 2.2: An agent representation of a rule-based reactive walker model.

Cellular Automata (CA)

Particle Hopping models are spatially and temporally discrete models. The walking area is divided into cells that (usually) accommodate only one pedestrian (figure 2.3). At each time-step of the simulation a pedestrian can stay in its current cell or 'hop' to a neighbouring cell. The typical cell size is $40-50cm$ that approximately represents the private space of a standing pedestrian.

If only one pedestrian is allowed in a cell and the movement of all pedestrians is updated simultaneously, the particle hopping model is named Cellular Automata (Wolfram (2002)). However, after decades of development this distinction is not relevant for walker models and we will use the popular term CA for all particle hopping models (Schadschneider et al. (2009)).

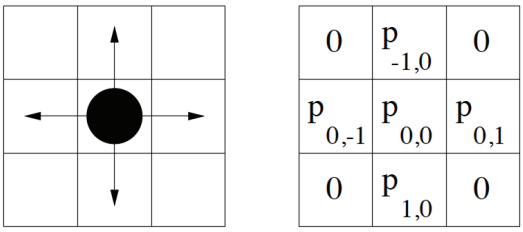

Figure 2.3: A particle, its possible directions of motion and the corresponding transition probabilities p_{ij} for the case of a von Neumann neighbourhood (from Schadschneider et al. (2009)).

Some models do not allow hopping in diagonals in what is called the Neumann neighbourhood (figure 2.3). Other models make use of a Moore neighbourhood that allow the access of eight neighbouring cells to increase the possible walking directions (Gipps and Marksjo (1985), Burstedde et al. (2001)). Blue and Adler (1999) proposed a model that creates pedestrians with different speeds by hopping up to three cells at one time step extending the cell neighbourhood.

Figure 2.3 shows a case of a CA model defining the probability rules for the neighbouring cells. This shows the distinctive characteristic of rule based models: rules can be deterministic or probabilistic. Usually this distinction appears in the rules that deal with solving conflicts that arise when more than one pedestrian is assigned to the same cell (see figure 2.13).

Deterministic rules require the model to have a rule for all conflicts, creating very large number of rules. The model proposed by Kukla et al. (2001) has up to 80 rules. The majority of the models have probabilistic assignments to solve conflicts. These can be in the form of a random draw (Burstedde et al. (2001)), the introduction of friction effects (Kirchner et al. (2003)) or to non-parallel update schemes (Keßel et al. (2002)).

Some CA models present a 'dynamic floor field' that acts similarly as a pheromone type of behaviour in which a 'chemical' attractive trail is left by walking pedestrians that creates a lane behaviour significantly reducing conflicts (Burstedde et al. (2001)). This floor field also is used to create different groups of pedestrians that walk after each other in different directions.

Suma et al. (2012) introduces anticipation in a CA model to mitigate conflicts likely to occur. They propose an anticipation floor field that recognises the cells likely to be occupied by walking pedestrians. The probability rules for these cells are modified taking into account the likelihood that they will be occupied.

Schadschneider et al. (2009) discuss the different solutions for conflicts and their consequences for the accuracy and realistic depiction of human behaviours. The authors mention that creating very complex solutions for conflict resolution generally has a negative impact in the computational efficiency of CA models.

CA models are shown to present good results for aggregate indicators, such as fundamental relations and egress times (Schadschneider and Seyfried (2009a)) and some

form of self-organising phenomena (Blue and Adler (1999), Burstedde et al. (2001)). Furthermore, due to their simplicity, CA models usually present the best computation efficiency under the walker models.

The literature shows us that much effort was put into improving the prediction of CA models. These efforts require many artefacts complicating CA models without making them a good predictor of individual behaviours (Schadschneider and Seyfried (2009b)).

Space Syntax model

Another type of rule based models is derived from Space Syntax principles (Hillier and Hanson (1984)). The Space Syntax model was proposed by Penn and Turner (2001) and further developed in Turner and Penn (2002). Their basic hypothesis is derived from empirical studies by the psychologist James Gibson (Gibson (1979)). They describe the main movement hypothesis in Turner and Penn (2002) on page 480 as: *When engaging in natural movement, a human will simply guide him or herself by moving towards further available walkable surface. The existence of walkable surface will be determined via the most easily accessed sense, typically his or her visual field.*

This hypothesis is implemented by means of a two-dimensional grid with cells of arbitrary size over the walking area (figure 2.4).

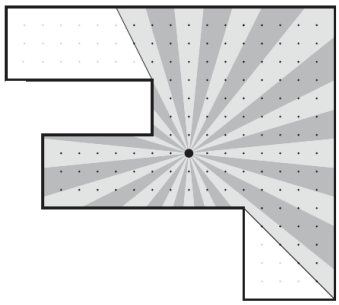

Figure 2.4: The 32 angular bins containing the centre of the visibility cells (small dots) for the pedestrian (large dot), from Penn and Turner (2001).

Each pair of cells that is able to be connected by a line not passing through an obstacle are put in a visibility graph prior to the simulation. At each position a pedestrian will have a field of view that contains a set of angular bins with their visible vertices. The walking behaviour is resulting from simple rules:

1. Choose randomly a vertex that is visible and inside your field of view.
2. Take on average, n steps towards that vertex, based on a Poisson distribution.
3. Repeat 1.

Bins with more vertices have a larger probability to be chosen creating the tendency of walking towards further available space as intended by the hypothesis. Therefore, pedestrians will tend to follow corridors but areas with doors and obstacles disrupt this tendency creating movements that somewhat resemble an explorative behaviour. These simple rules were expanded including side-stepping to address conflicts.

Simulations of an art gallery showed good agreement between observed and simulated occupancy of rooms. However, they point that pedestrians have small probabilities to exit corridors and simulations of large open spaces results in random walk.

Space syntax models show the power of simple rules to create a kind of leisure behaviour. However, they certainly need to be further developed to predict realistic pedestrian flows and self-organised phenomena.

2.2.2 Force-based reactive models

Force models are also reactive agents where the percepts are directly input into a movement equation, usually describing the acceleration. What distinguishes them from the rule-based models is the fact that the actions are not explicitly determined, but are the consequence of the different forces acting. These models are therefore more realistic because they combine forces for the *emergence* of the actions.

Force based models consider pedestrians as particles that attract or repel each other according to particular behaviours. The collision avoidance behaviours usually involve repulsion forces and grouping behaviours usually involve attractive behaviours.

Force models usually use the dynamic state variables such as position and speed from themselves and other pedestrians to obtain the accelerations. Therefore, they need to keep their state in memory becoming **force-based reactive** agents with state (Figure 2.5).

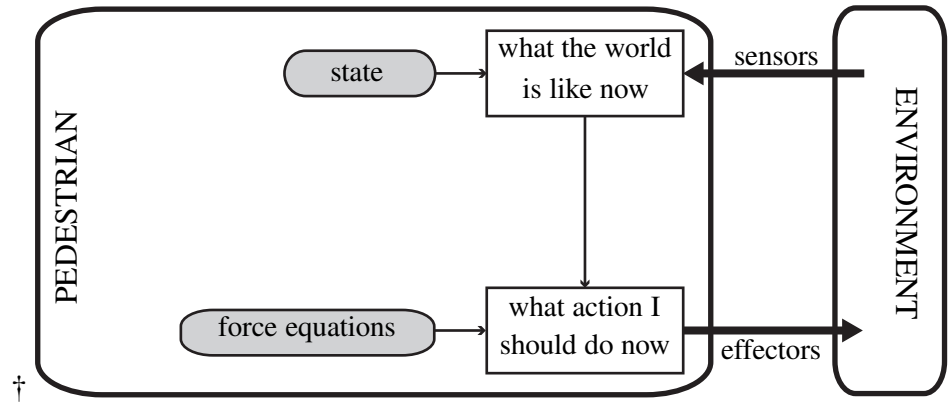

Figure 2.5: An agent representation of a force-based reactive walker model with state.

Social Force

The most popular force model is the so called Social Force model that has been developed in many different variations since its original proposal by Helbing and Molnar (1995) as a purely reactive model.

The social force model associates the behaviours of pedestrians to 'forces' that guide their behaviours. From the perspective of a reference pedestrian α all other pedestrians and infrastructures exert a force that are added to calculate the total effect to the velocity of pedestrian α. These forces are: to follow a certain path (that will eventually lead to a destination), to keep distances to other pedestrians and infrastructures (preventing collisions) and to be close to pedestrians that are part of an interest group such as a family or street artists. These are formulated according to the following equation by Helbing and Molnar (1995):

$$\vec{F}_\alpha(t) = \vec{F}^0_\alpha(\vec{v}_\alpha, v^0_\alpha \vec{e}_\alpha) + \sum_\beta \vec{F}_{\alpha\beta}(\vec{e}_\alpha, \vec{r}_\alpha - \vec{r}_\beta) + \sum_B \vec{F}_{\alpha B}(\vec{e}_\alpha, \vec{r}_\alpha - \vec{r}^\alpha_B) + \sum_i \vec{F}_{\alpha i}(\vec{e}_\alpha, \vec{r}_\alpha - \vec{r}_i, t) \tag{2.1}$$

where:
$\vec{F}_\alpha(t)$ is the total social force exerted into pedestrian α at the location $\vec{r}_\alpha$.
$\vec{F}^0_\alpha$ is the force towards the desired direction $\vec{e}_\alpha$.
$\vec{F}_{\alpha\beta}$ is the repulsive force of other pedestrians β at the locations $\vec{r}_\beta$.
$\vec{F}_{\alpha B}$ is the repulsive force of infrastructures B at their closest locations $\vec{r}^\alpha_B$ to α.
$\vec{F}_{\alpha i}$ is the attractive force of other pedestrians i at the locations $\vec{r}_i$.

Equation (2.1) shows the purely reactive nature of the social force model indicating that collisions are not anticipated and therefore they can occur depending on the traffic conditions.

The social force model assumes that pedestrians will always try to follow a trajectory with a desired direction $\vec{e}_\alpha(t)$ at a constant desired speed v^0_α (free-speed). In case pedestrians need to change their velocity, they will do so with an acceleration that is linearly dependent on the difference between the desired velocity $v^0_\alpha \vec{e}_\alpha$ and the current velocity $\vec{v}_\alpha$:

$$\vec{F}^0_\alpha(\vec{v}_\alpha, v^0_\alpha \vec{e}_\alpha) = \frac{1}{\tau_\alpha}\left(v^0_\alpha \vec{e}_\alpha - \vec{v}_\alpha\right) \tag{2.2}$$

where
τ_α is the relaxation time. The smaller its value the less a pedestrian will give way to others and the closer he or she will stay to his or her desired velocity. Extreme small

values of τ result in uncooperative behaviour.

The perception of the pedestrian is anisotropic in the shape of an ellipse with semi-axis b. This causes a stronger repulsion from pedestrians closer to the walking direction than to those in lateral positions. The repulsion force is governed by an exponential equation:

$$\vec{F}_{\alpha\beta}(\vec{e}_\alpha, \vec{r}_\alpha - \vec{r}_\beta) = -V^0_{\alpha\beta} e^{-b/\sigma} \cdot \vec{e}_{\alpha\beta} \tag{2.3}$$

where:
$V^0_{\alpha\beta}$ is the repulsion strength.
σ is the repulsion distance factor. The smaller this factor the closer pedestrians must be to repel each other.

The acceleration $\vec{F}_{\alpha B}$ is similarly described by an exponential equation. The authors did not implement attraction forces, but mentioned the dependence to time t accounting for the attenuation of the attraction force with the passage of time.

This first formulation of the social force model already exhibited good results with the authors mentioning the formation of lanes in bidirectional flows and oscillations in bidirectional bottlenecks. Since its proposal, the social force model has been further developed and validated to include other features and to improve some of the problems identified (Steffen and Seyfried (2008)).

Aube and Shield (2004) used the social force model to implement leader-follower and grouping behaviour that would occur in evacuations.

In Helbing et al. (2002) the social force model is extended with pressure forces due to collisions. Helbing et al. (2005) introduces the notion of impatience that increases the free-speed v^0_α if the walking time is longer than expected by the pedestrian.

Steffen and Seyfried (2008) point out that the interaction forces as formulated originally cause abrupt reactions and sharp turns that are not realistic. They propose a simple type of anticipation to smooth the reactions. They report that the behaviours were improved in single lane situations but not for other situations.

Chraibi and Seyfried (2008) also modify the repulsion force in a unidimensional single lane social force model to avoid oscillations that occur when pedestrians are constantly reacting with pedestrians in the front and in the back. Their model introduces an event driven interaction component that will adapt the velocities keeping a minimum distance to the pedestrian in front. They report improvements to prediction of the fundamental diagrams for densities until $1.0 peds/m^2$ but their model seems unable to reach densities higher than $1.6 peds/s$.

Zanlungo et al. (2011) introduced anticipation into a social force model by using anticipated positions in a similar way as described in section 2.2.3. The authors report better results than by an original social force model.

Johansson (2013) introduced three waiting behaviours in a social force model. All of them have the pedestrian fixing his gaze to a point accounting for situations such as looking at information boards. The first and most simple waiting behaviour does not fix the waiting location but sets $v_\alpha^0 = 0$. The pedestrian however is still submitted to the interaction forces, thus drifting accordingly. The second waiting behaviour fixes a preferred waiting position that pedestrians will always try to return to if they had to give way for passing pedestrians. The third allows the waiting position to wander relaxing the condition of always walking back to a previously chosen waiting position.

Force based CA model

Gipps and Marksjo (1985) proposed the first CA walker model. Differently from what was later more popular it had repulsion and attraction forces instead of rules. In this model each cell gets a repulsive score that is calculated due to the proximity of pedestrians. Simultaneously, the location of a cell in relation to the destination provides a benefit. The next cell is chosen not by a set of rules but by the one that gives the best gain between the repulsion score and the benefit of the distance to the destination.

Magnetic force

Okazaki (1979) proposed a force model based on the magnetic force equation (2.4). Pedestrians and obstacles are of the same positive pole and therefore repulsive. The destinations are negative and therefore attractive to pedestrians. The maximum velocity of pedestrians is limited and is an individual parameter.

$$\vec{F} = \left[\frac{k_{q_1,q_2}}{|r|^3}\right]\vec{r} \tag{2.4}$$

where:
$\vec{F}$ is the magnetic force.
k is a constant value.
q_1 is the intensity of magnetic load of a pedestrian.
q_2 is the intensity of a magnetic pole.
$\vec{r}$: is the vector from a pedestrian to a magnetic pole.

Although it is probably the oldest walker model, it already presented several interesting features such as three different walking strategies: following the shortest route, following a previously set route and a seeking strategy without known route. The model also presents queuing and waiting behaviours. Unfortunately, no modelling details for these special features were presented and also no validation evidence.

2.2.3 Goal-based models

Pure force models have the disadvantage of not being explicit in the goals that pedestrians want to achieve whilst walking. Force models propose minimising walking time as the main pedestrian strategy, but they mostly provide a 'drive' towards the destination. Goal based-models make the minimisation of walking time explicit. Furthermore, they usually combine it with a second goal of collision avoidance. The collision avoidance is different from the reaction force from the force models in that it explicitly searches for locations that do not result in collisions. The search for paths without collision results from an intention that is not equal to the purely reactive repulsion forces that just create a tendency to avoidance of collisions.

Goal-based walker models present optimisation strategies that will govern pedestrian actions. To realise that, they need to anticipate the consequences of their actions, compare alternatives and choose the action that best fulfils their goals. At the moment of this review the only goal based models are collision avoidance models and this section will concentrate on them. Collision avoidance models constitute the newest type of walker models and were originated in the computer graphic community (Pettré et al. (2014)). Figure 2.6 shows the representation of goal oriented models.

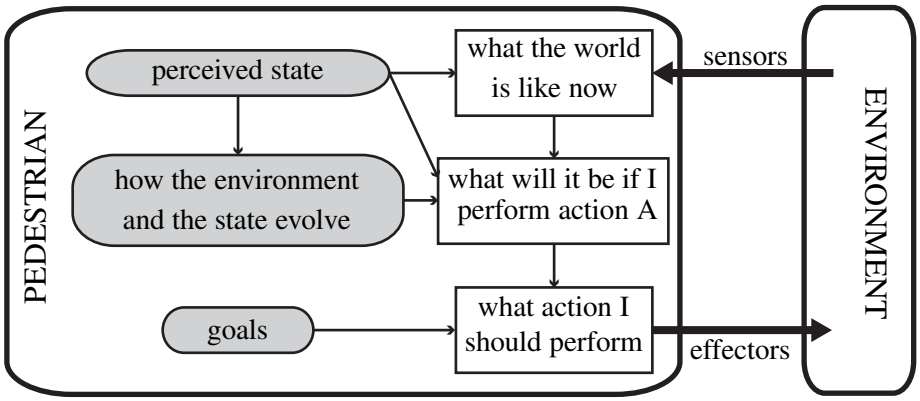

Figure 2.6: An agent representation of a goal-based walker model (based on Russell and Norvig (1995)).

Collision avoidance models are purely anticipatory models. Usually, these models determine the imminence of collisions and according to some logic they produce velocity changes to prevent these collisions to occur. Paris et al. (2007) propose the notion of admissible velocities as the set of velocities that pedestrians can maintain without risking a collision. Therefore, if a pedestrian is currently walking with an inadmissible velocity, he or she (probably) changes it.

Models differ in the way they calculate the probability of collisions and in the way they modify the inadmissible velocities. Given the complex dynamics of the pedestrian traffic, anticipatory models need to make simplifying assumptions of the future progress of the traffic. The most common is the zero acceleration asumption that states that: *Pedestrians keep the same velocity in the nearby future*.

Figure 2.7(a) taken from Paris et al. (2007) shows the most general case of collision prediction between a reference pedestrian and an opponent. It uses the zero acceleration assumption to create the cone with the time x position search space for 360° walking directions for the reference pedestrian. The opponent is assumed to maintain the same velocity, thus his or her search space is a cylinder with the radius equal to the sum of both pedestrian radii (assuming circular pedestrians). The intersection of both geometric figures is the possible collisions boundary (black polygon). Figure 2.7(b), also taken from Paris et al. (2007), shows the various collision polygons for different speeds of the reference pedestrian.

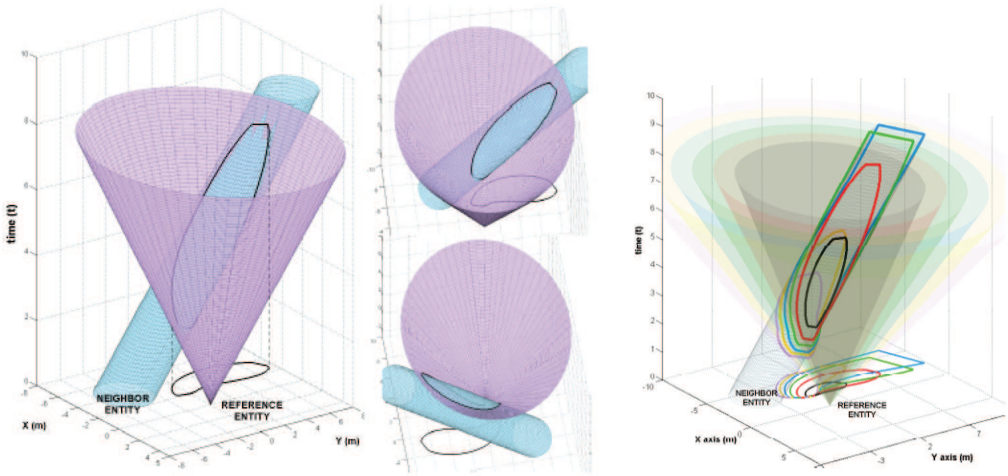

(a) (b)

Figure 2.7: (a) The position x time space representation of two pedestrians. The purple cone is the space with possible locations of the reference pedestrian walking on a constant speed for all directions. The blue cylinder is the space of the other pedestrian walking on constant velocity. The black polygon is the intersection boundary of possible collisions. (b) The same representation for different speeds of the reference pedestrian (from Paris et al. (2007)).

The zero acceleration assumption allows the calculation of some important variables concerning collision avoidance behaviour: the time-to-collision (TTC), time-to-interaction (TTI), distance-to-interaction (DTI) and minimum pedestrian distance (MPD). If a collision will occur, the TTC is the time it takes for the pedestrians to collide (Daamen and Hoogendoorn (2006)). If no collision occurs, TTI and DTI are the time it would take and the distance to reach the minimum distance (MPD) between the two pedestrians (Degond et al. (2013)). TTI and DTI are positive for a pedestrian if the interaction location will be reached in the future and negative otherwise.

Anticipation models can be divided into two categories: models that determine the behaviour according to the admissible velocities space (Pettré et al. (2009), Asano et al. (2010), Karamouzas and Overmars (2010) and Moussaïd et al. (2011)) and models that use perception clues to predict the avoiding behaviour (Ondřej et al. (2010)). Degond et al. (2013) and Pettré et al. (2014) present reviews of collision avoidance models.

Admissible velocity models

Figure 2.7 shows that the space of admissible velocities is too large for simulations with many pedestrians, requiring simplifying assumptions to restrict the space. The most common assumption is to limit the field-of-view with an arc ϕ and a maximum anticipation time (Pettré et al. (2009), Karamouzas and Overmars (2010), Asano et al. (2010)) or maximum interaction distance (Moussaïd et al. (2011)).

Paris et al. (2007) proposed the first of collision avoidance model by calculating the admissible speeds and proposing a cost function to choose one of them. The model determines the minimum speed (and correspondent orientation) the reference pedestrian needs to pass in front of the opponent and the maximum speed that he or she can have to pass behind the opponent (with MPD as a safety factor) for four different anticipation times. These velocities form the boundaries of the admissible velocities for the anticipation time for the interaction with a pedestrian or an obstacle. With the set of admissible velocities for the entire interaction population the model applies a score system based on several assumptions, such as the desire to stay close to a direction leading to the destination. The velocity with the lowest score is chosen.

The authors reported that the model was able to reproduce the interaction behaviour accurately and that the calibrated model managed to reproduce some self organised phenomena such as lane formation. However, they only obtained good validations results for models calibrated in the same experimental setup indicating a strong specialisation of the model. They also reported that the computational time was somewhat high even considering the relatively low flows simulated.

Moussaïd et al. (2011) simplifies the admissible velocity models by not trying to guarantee a collision free model (this model includes a collision model for situations with high densities). The authors describe the walking behaviour into simple equations that calculate the pedestrian velocities without searching the whole space of admissible velocities. Instead, they limit the area of perception into a field of view with a radius that they called “horizon distance”. If pedestrians and obstacles are inside the field-of-view, their anticipated positions are used to determine the DTI of each of them and input in the equations that calculate the new direction and the speed.

The authors report some qualitative and quantitative validation results. Their model was able to reproduce turbulent flows in very dense situations and fit a speed x occupation fundamental relation. However, these were preliminary results and the model used different set of parameters in the validations and there is no evidence that a single set would perform well in all conditions. Furthermore, no evidence of important self-organised behaviour such as lane formation was presented.

The synthetic vision model

Ondřej et al. (2010) also proposes a model that does not guarantee a collision free solution. The model is based on the empirical evidence that pedestrians are able to

predict collisions based on the variation of the bearing to the other object and that they are able to predict the TTC based on the rate of the size change of the other object.

Figure 2.8(a) shows the relationship between the bearing angle derivative $\dot{\alpha}$ and the three possible situations in crossing trajectories (the reference pedestrian is walking up): if the reference pedestrian passes over the interaction point after the other pedestrian then $\dot{\alpha} < 0$, if they collide then $\dot{\alpha} = 0$ and $\dot{\alpha} > 0$ otherwise.

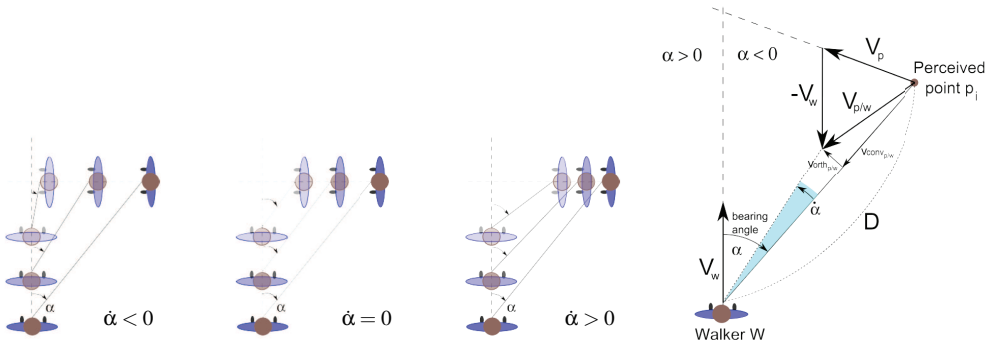

(a) (b)

Figure 2.8: (a) The relationship between the bearing angle derivative $\dot{\alpha}$ and the three possible situations in crossing trajectories. (b) The model inputs are deduced from the relative position and velocity between the reference pedestrian W and the perceived pedestrian (from Ondřej et al. (2010)).

Figure 2.8(b) shows the graphic representation of the three input values for the reference pedestrian W given the perceived pedestrian i: $(\alpha_i, \dot{\alpha}_i, \mathrm{TTI}_i)$. The model first determines the set P_{col} of the perceived pedestrians that risk colliding with W by satisfying the following conditions:

$$p_i \in P_{col} \text{ if } \mathrm{TTI}_i > 0 \text{ and } \mid \dot{\alpha}_i \mid < \tau_1(\mathrm{TTI}_i) \tag{2.5}$$

The condition states that pedestrian W must be walking towards the interaction location and that the absolute value of the rate of bearing change is smaller than a threshold value τ_1. The value of τ_1 increases exponentially when $\mathrm{TTI}_i \to 0$.

The model is called 'synthetic-vision' because it uses a 3D visual field to determine the points of interest in the pedestrians and obstacles. The synthetic-vision model has the merits of being simpler than models that enforce only admissible velocities and the authors report realistic results, particularly self-organised behaviour such as lane formation and diagonal stripes in 90° crossing flows. However, there is no evidence that the model can handle complex and dense situations.

2.2.4 Utility-based models

Frequently, walking behaviour involves a combination of factors. Whilst pedestrians may want to reach their destinations as quickly as possible, they may also want to min-

imise the effort required to avoid other pedestrians. These different goals may conflict if the traffic ahead is intense. Utility models make use of the idea that pedestrians show some degree of rationality by finding trade-offs. These trade-offs are achieved by assigning relative weights on the different utilities ('the quality of being useful') gained or lost when walking.

Utilities are functions that map a pedestrian state onto a real number, which describes the associated degree of usefulness. Another way to understand utility is to think on its inverse: the cost. A pedestrian walks by simultaneously minimising the cost of time to achieve a destination and the cost of accelerating (as a proxy for effort) to avoid traffic and obstacles.

Utility-based models for human behaviour were introduced in economics to model market dynamics based on the idea that people are always trying to maximise their benefits. Humans do not always appear to behave rationally when making decisions (Ariely (2008)). However, for modelling walking behaviour utility models offer a powerful and practical framework to combine different goals.

Earlier utility-based models for pedestrians were developed for pedestrian route choices in business areas (Seneviratne and Morrall (1985)) and choices between stairs and escalators in metro stations (Cheung and Lam (1998)). Both are respectively for the strategic and tactical levels. Only later, utility-based walker models were proposed: Nomad by Hoogendoorn et al. (2003) and discrete choice models (Antonini et al. (2004)). Recently, a fuzzy logic model by Nasir et al. (2012) was proposed combining an inference model with social forces.

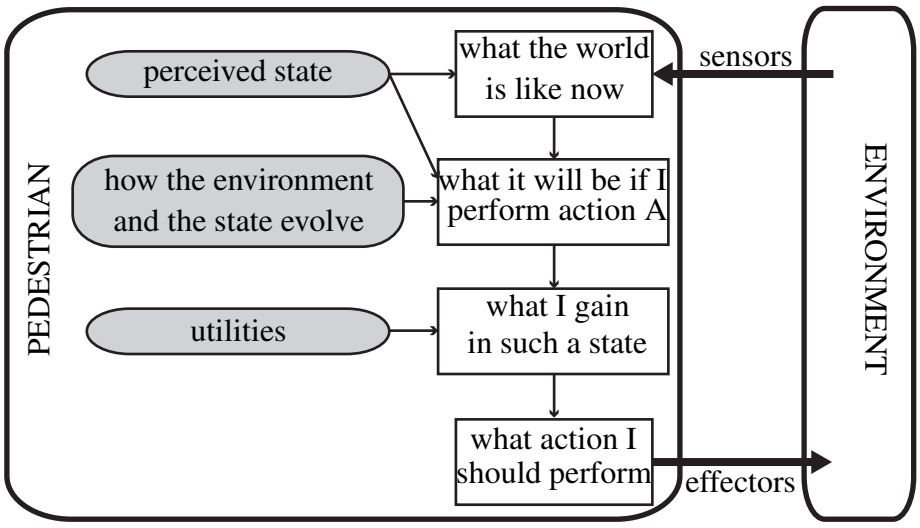

Figure 2.9: An agent representation of a utility-based walker model (based on Russell and Norvig (1995)).

Nomad

What distinguishes the Nomad model from all other models is that it is derived from a normative pedestrian walking theory (Hoogendoorn (2001)). The theory applies the principle of least effort by Zipf (1949) to walking and to activities performed between walking. In the Nomad theory, the idea of minimising effort is not directly related to physical effort, but to the more general concepts of utility and cost.

The Nomad model is a complete pedestrian model in which all three levels: strategic, tactical and operational are derived from the same normative theory. Furthermore, Nomad is the only explicit activity based model. Activities such as buying tickets, waiting in platforms are an integral part of its formulation. This makes Nomad a complete platform for modelling behaviours in complex pedestrian facilities. Below, we will introduce the Nomad walker model that is the focus of this dissertation (for details of the activity and route choice models refer to Hoogendoorn and Bovy (2004)).

In the theory, every action of pedestrians during walking, such as overtaking, accelerating and slowing down creates costs. These costs are associated with the physical effort that they require. Therefore, pedestrians will walk minimising them. The Nomad model assign cost functions to these manoeuvres and to interactions with other pedestrians and obstacles. The total cost function is minimised resulting in the acceleration model. The resulting mathematical formulation of the original Nomad model given certain assumptions is similar to the original Social Force model presented in section 2.2.2. The complete formulation of the Nomad walker model is presented in chapter 3.

The Nomad model was later expanded in Hoogendoorn (2004) with an impatience factor that depends on the difference between the current speed and the free-speed of the pedestrians. The idea is that if pedestrians are much slower (or much faster) than their free-speed, they will more forcefully accelerate towards it and will take less avoiding manoeuvres inside the traffic. This would represent an 'aggressive' behaviour due to urgency as explained in section 2.3.6.

The original Nomad model was successfully applied (Hoogendoorn et al. (2004)) and shown to reproduce many important flow properties such as self-organised phenomena (Hoogendoorn and Bovy (2003)). However, the same problems of non realistic walking behaviours in certain situations existing in social force models appointed by Steffen and Seyfried (2008) occur with the original formulation of the Nomad model.

Discrete Choice models

Discrete choice walker models were proposed by Antonini et al. (2004) and further developed by Robin et al. (2009). The basic idea is that pedestrians choose the next location from 33 possible cells in a discretised target area in their front (figure 2.10).

There are two overlapping sections that create the 33 cells. First, 11 different sized angular sections divide a 170°arc. Secondly, there are three arched zones that represent

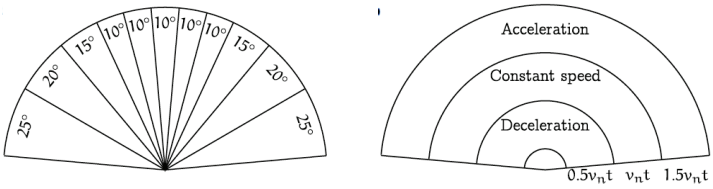

Figure 2.10: The space discretisation of the target area of the discrete choice models (from Antonini et al. (2004)).

the position pedestrians could reach if they decelerate, remain in the same speed or accelerate.

The original model has 8 attributes that account for the intentions of pedestrians such as reaching a destination and the interaction with other pedestrians. The original model implements a utility function V_j with five variables responsible for the choice of the next target area cell. The variables account for the occupation attribute of the cell, the location of the cell regarding the movement direction (expressing the preference to keep the current walking direction), the location of the cell regarding the direction of the destination, the cost of accelerating and decelerating.

$$V_j = \beta_{occupation} \cdot occupation_j + \beta_{direction} \cdot direction_j + \beta_{destination} \cdot destination_j + \beta_{acc} \cdot v_{norm}^{\lambda_{acc}} + \beta_{dec} \cdot v_{norm}^{\lambda_{dec}} \quad (2.6)$$

where:
β are the alternative-specific coefficients.
v_{norm} represents the normalised speed module of the decision maker.

Later, Robin et al. (2009) expanded the basic choice model by introducing two more components in the utility functions: one accounting for leader-follower behaviour (assuming that the decision maker is attracted by a leader that is walking in a similar direction and not too far ahead) and the other for explicit collision avoidance behaviours (captures the effects of possible collisions on the decision maker's trajectory).

Robin et al. (2009) uses one set of empirical trajectory data to calibrate the model and two different sets to validate the model. The authors report that the trained model delivered good results including lane formation, but there is no evidence of the general application of the calibrated parameters.

Fuzzy logic force models

The proposed fuzzy logic model by Nasir et al. (2012) combines the characteristically reactive nature of force models with the inferential power of utility models. The environmental stimulus are represented by the interaction forces of a Social Force Model

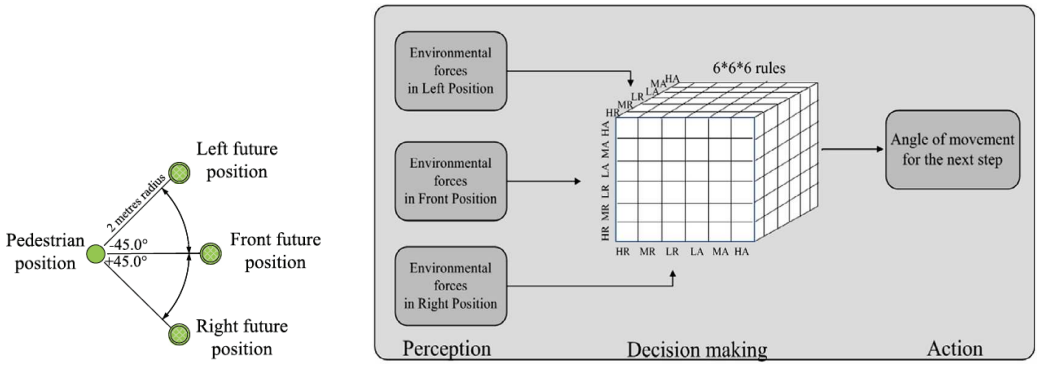

Figure 2.11: The three positions ahead and the architecture of the steering fuzzy model (from Nasir et al. (2014)).

(section 2.2.2) and the action is chosen by a fuzzy logic steering model presented in figure 2.11.

The model discretises radially three positions in front of the pedestrian and for each position it calculates the environmental forces based in attraction and repulsion forces from social force equations (equation (2.1)). These forces are fuzzified into six membership functions (MF's): High Attractive (HA), Medium Attractive (MA), Low Attractive (LA), Low Repulsive (LR), Medium Repulsive (MR), High Repulsive (HR). These three positions and the six MF's create $6^3 = 216$ fuzzy rules that transfer the inputs of the system to the output that is the walking direction. These rules guide pedestrians towards attractive areas and avoid the repulsive interactions.

Nasir et al. (2014) calibrated the fuzzy variables using a genetic algorithm and reported good agreement for single trajectories. Pedestrians are repelled by the obstacles and attracted by the desired route.

The fuzzy part of the model creates a decision layer that is more powerful (and more complex) than the simple addition of the social forces. One could imagine that other decision parameters could be incorporated in the walker model approaching it to the other utility models. By the time of this literature research the model was still very basic and no pedestrian interactions were included. Until this type of model shows good performance in dense situations and in several types of flow we cannot consider it for more complex walking situations.

2.3 Agent characteristics for model assessment

We saw in the previous section that the agent representation helps to understand what type of 'reasoning' is implemented in walker models. In this section we use the PAGE concept to relate agent characteristics to walking processes found in large pedestrian facilities and to a realistic depiction of individual pedestrian behaviour.

The characteristics will be used to create scoring indicators. The indicator will receive a value 1 if the criteria is met. The value of the scores is not important. What is important is the fact that models with non 0 score in the Perception and Goal characteristics can be considered more 'realistic' (as 'human like') and more 'general' in the Actions and Environment.

Parameters reflect modelling decisions or results from calibrations that focused on particular performance indicators. It is not our intention to assess the types of models according to the closeness of the reported parameter values to empirical data. Model characteristics will receive a good score if they are similar to empirical evidence and the parameter values can assume realistic values. Figure 2.12 shows the characteristics that are included in the assessments.

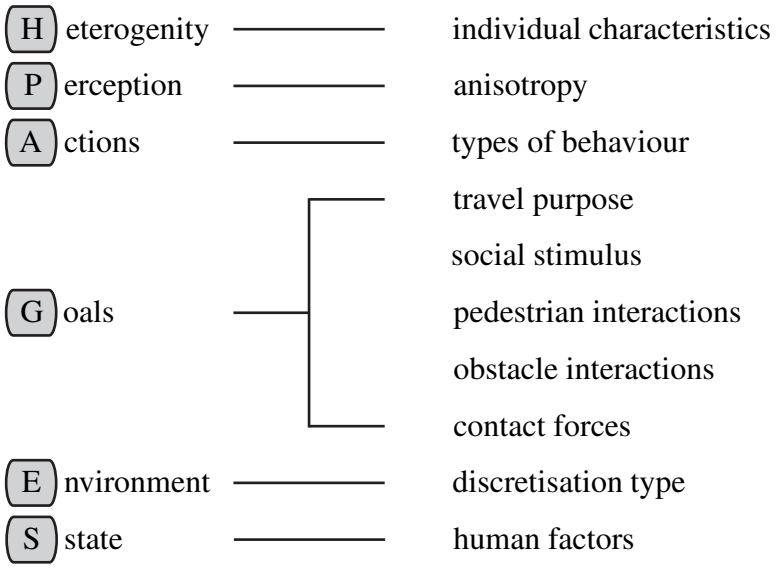

Figure 2.12: The model characteristics that will be assessed in this overview organised according to the PAGE concept.

Figure 2.12 also shows heterogeneity as an assessment criteria. Studies showed that the amount of *heterogeneity* (variation of the individual characteristics) in the population affects the traffic characteristics. Including heterogeneity as an extra score for the other agent characteristics would increase significantly weight of heterogeneity in the final score. Therefore, it is presented as a separate assessment criteria in section 2.3.1.

The *perception* is discussed in section 2.3.2. We assess in section 2.3.3 if the models implement other types of behaviours besides normal walkings such as waiting, taking escalators, passing turnstiles and if they implement level changes.

Agents may have several *goals* that are explicit, such as in goal and utility-based models or implicit by having been used to derive the model. Section 2.3.4 presents goals that create a wide range of factors influencing walking behaviour.

The discretisation type of the *environment* has a large influence on the outcomes of the model and is discussed and, assessed in section 2.3.5. The type of infrastructures such

as stairs and turnstiles is directly connected with the available actions and will not be assessed in the environment.

Section 2.3.6 present the agent *state* variables representing human factors that are relevant for modelling non normal behaviours.

All sections will end with a list of the criteria that the agent characteristics are assessed. The first item of the list is the absence or the most basic case of the characteristic and receives a 0 score. Every other possible criterion in the list add 1 to the model score, thus is represented by a +1.

2.3.1 Heterogeneity

The variability of an individual is called *intra-pedestrian* heterogeneity. Usually, models are not developed to describe the behaviour of a specific individual. Therefore, we will not consider intra-pedestrian heterogeneity as a comparison characteristic.

Variations among individuals also known as *inter-pedestrian* heterogeneity, are much more important. Campanella et al. (2009a), Moussaïd et al. (2012) and Yang et al. (2014) showed that increasing levels of heterogeneity increased the probability of gridlocks in bidirectional flows.

Several characteristics of walking behaviour vary between pedestrians. Pedestrians walk faster when they are young (Buchmueller and Weidmann (2006)), may display more or less cooperative behaviour (Wolff (1973)), walk differently due to cultural characteristics (Chattaraj et al. (2009)) and are less manoeuvrable when they are old (Luchies et al. (2002)). This shows that walker models must allow for variation in the population. Therefore, we will put a larger importance to models that implement heterogeneous populations.

The most important characteristic that is an input to all walker models is the free-speed. This is the speed at which pedestrians would walk when no pedestrians or obstacles are in the vicinity. The free-speed has been measured for several different factors, such as gender, culture, age group and time of the day (Weidmann (1993), Daamen and Hoogendoorn (2006)).

Other pedestrian characteristics may be present in models and their variability may describe heterogeneous populations. Given the significant differences between the types of models, we will not include the amount or the kind of parameters that are varied. Only if the model allows variability of behaviour.

The heterogeneity criteria are:

0 if population is homogeneous.

+1 if the free-speed varies.

+1 if other pedestrian characteristics are varied.

2.3.2 Perception characteristics

Modelled pedestrians perceive the state of other pedestrians and of the infrastructures. Real pedestrians mostly rely on vision to perceive other pedestrians (Goffman (1972), Patla and Vickers (2003)). Furthermore, pedestrians put their attention on a limited region of the vision field concentrated around their walking axis (Johansson et al. (2007), Moussaïd et al. (2009), Kitazawa and Fujiyama (2010)). This means that their interaction behaviour is dependent on the relative direction of movements and is more intense for pedestrians on a collision route (Goffman (1972)) and for those that are closer (Johansson et al. (2007), Moussaïd et al. (2009)). This characterises an anisotropy regarding the area around a walking pedestrian and a spatial limit (bounded area). Areas in front and close to the walking directions are perceived and interpreted more intensively than areas laterally and backwards.

In the remainder we will name the perception area as the *influence area* (see section 3.2.7). Therefore, models that limit the perception of pedestrians (bounded) for interaction purposes and put more importance to pedestrians in their walking direction reflect a more natural behaviour.

The perception criteria are:

0 if the perception is isotropic.

+1 if the perception varies with distances.

+1 if the perception is anisotropic.

Kitazawa and Fujiyama (2010) performed eye tracking experiments and determined that pedestrians perceive static obstacles already at $4.6m$ and rarely in angles larger than 45° from the walking direction. However, there is very little other empirical evidence on the perception of infrastructures and given that the interactions with static infrastructures are much simpler than between pedestrians (see the description of the shy-away distance behaviour in section 2.3.4) we will not assess the perception of obstacles specifically.

2.3.3 Action characteristics

All walker models implement explicitly or implicitly the basic actions required for walking: accelerating longitudinally and laterally, and interacting with other pedestrians. Models that are more basic than that are not considered in this review. [2]

[2] Wolff (1973) describes the so-called step-and-slide movement that plays an important role in collision avoidance in dense situations. The step-and-slide is a the combination of side-stepping (an almost instantaneous change of 90°walking direction). Side-stepping is important and is possible in all models presented in this review.

Other more complex behaviours such as waiting, taking escalators, passing turnstiles are less frequently modelled. However, these are needed for the application of the models in large pedestrian facilities. We create three criteria based in requirements for pedestrian models (Daamen (2004) and Kuligowski et al. (2010)): waiting behaviours, queues and server behaviours and level changing such as stairs and escalators.

The waiting actions criteria are:

0 if only *normal walking* is modelled.

+1 waiting behaviours.

+1 queuing behaviours.

+1 changing level behaviours.

2.3.4 Goal characteristics

Pedestrians may have several goals that influence their behaviours. We will enumerate the goals that are present in walker models from a higher to a lower behavioural level.

The highest level goal defines the intentions of the pedestrians, their *travel-purpose*. The behaviours occurring on different travel-purpose such as commuting to known destinations, evacuation from dangerous situations or shopping are very different.

The next level of goal to be pursued by pedestrians is *social stimulus*. Independent of their travel-purpose, pedestrians may aim to walk in groups or follow a leader (Connell (2001), Still (2000)).

The lowest and most common level of goals is the interaction with other pedestrians and obstacles. On any travel-purpose pedestrians will always try to avoid a collision. Therefore, some sort of pedestrian and obstacle interaction component must be present.

However, collisions do happen and are important for the realistic outcomes of models (Helbing et al. (2000a)). Some studies show the positive effects of adding friction effects to models (Kirchner et al. (2003), Henein and White (2007)). Therefore, the existence of contact forces components are included in the assessment characteristics.

In the following, we describe each goal in more detail.

Travel purpose

Weidmann (1993) distinguishes four travel purposes: business district patrons, commuters, shoppers and leisure walkers. The walking speeds measured in these areas are in descending order from business districts to leisure reflecting the different behaviours. These are similar to those proposed in TRB (2010).

Commuters and business district patrons are purposeful walkers. They know where they are going and walk directly to their destination. Shoppers display a more exploratory behaviour. According to empirical observations by Borgers and Timmermans (2014) only 50% of the pedestrians in a shopping area walk along shortest distances. Leisure walking would be encountered in parks, museums, open-air concerts or public squares. These behaviours are arguably difficult to define and are rarely mentioned in the pedestrian modelling context.

Most locations with high pedestrian flows such as train stations, airports and central business districts that need the application of walker models present mostly commuters. This explains why most models available represent commuter walking behaviours.

However, there is interest in applications of pedestrian modelling for evacuation and for shopping areas (Haklay et al. (2001)). Although most model developers consider evacuation behaviours similar to commuters aiming to exits (Kuligowski et al. (2010)), there is empirical evidence that not all pedestrians behave similarly (Leach (1994)) requiring modification to the model. Shopping behaviour is different from commuting and most models would need different approaches (Borgers et al. (2009)).

We consider it a positive development if models are able to be applied for more travel purposes.

The travel-purpose criteria are:

+1 if commuters are modelled.

+1 if the shopping or an exploratory behaviour is modelled.

+1 if evacuation is modelled.

Social stimulus (group, leader-follower)

Empirical results show that the presence of groups has a great influence on the movement of crowds (Duives et al. (2014b), Costa (2010), Moussaïd et al. (2010), Zanlungo et al. (2014)). In general, larger groups are slower and the size of groups tends to influence the group geometries.

Similarly, the tendency of delegating decisions to other pedestrians in extreme situations plays an important role in evacuations by creating groups that start evacuating together (Helbing et al. (2005), Isobe et al. (2004), Saloma et al. (2003)). The most common consequence is the unequal use of emergency exits delaying evacuations. [3]

[3]The term 'herding' is not well defined in the context of pedestrian behaviours. Schadschneider et al. (2009) suggests that these terms should be avoided because they imply a loss individuality. Instead he affirms that these terms should be replaced by a social attachment theory (the typical response to a variety of threats and disasters is not to flee but to seek the proximity of familiar persons and places).

Arguably, we see less group formation and leader-follower dynamics in areas visited regularly by commuters such as train stations and central business districts than in public events, commercial streets and concerts. Therefore, it is understandable that very few models implement them. However, they are important for other types of travel purpose and especially to evacuation behaviour analysis. Therefore we consider that it is a positive to model them.

The social stimulus criteria are:

0 if only *individual walking* is modelled.

+1 if walking in groups is also implemented.

+1 if leader-follower is also implemented.

Pedestrian interaction

We showed that **reactive** force models predict behaviours by quantifying a direct effect (usually a repulsive acceleration) of nearby pedestrians. Usually the interaction behaviour is than the simple addition of all interaction effects. These models are reported to work well in intense flows predicting several self-organised phenomena (Helbing et al. (2001)). However, purely reactive models tend to rely too much in speed reduction for interactions instead of lateral avoidance manoeuvres, creating non realistic frontal collisions (Steffen (2010)).

Goal based models, usually involve pre-computation of collisions to determine collision free paths that result in **anticipation**. These models are reported to predict good behaviours in low and mid density flows (Sparnaaij (2015)). In high intensity flows when the number of possible collisions increases dramatically they may not find viable solutions or take too long to find them.

In the literature we observe that purely reactive models such as social force models were modified receiving anticipation components to improve their predictions. Sparnaaij (2015) shows that in the majority of the situations that he tested a social force model modified with anticipation by Moussaïd et al. (2009) performed better than a purely anticipatory model by Karamouzas (2012).

These results are in agreement with empirical studies that suggest that pedestrians apply a mixed strategy of reactive and anticipatory behaviour when interacting with other pedestrians and obstacles (Duives et al. (2014a)). In situations where pedestrians are far, anticipation strategies improve the interactions by reducing the conflicts (Olivier et al. (2013), Duives et al. (2014a)) or unexpected behaviours (Johansson (2009)). In short distances pedestrians do not have opportunities to anticipate and become more reactive to neighbouring pedestrians (Wolff (1973)).

These findings suggest that these different 'strategies' should be modelled: the *anticipation* of other pedestrian movements into the future and *reactive* change of the path due to the proximity of another pedestrian or infrastructure. Therefore, we consider that combining anticipatory with reactive behaviours is more realistic and accurate:

The collisions avoidance criterion is:

0 if pure reactive behaviour is modelled.

+1 if anticipation is combined with reactive behaviours.

Interaction with infrastructures

Pedestrians keep a safe distance (shy-away distance) to different types of infrastructures (Weidmann (1993)). It varies according to the type of the infrastructures ($1.0m$ for shop windows and about half of this for concrete walls) and the roughness of the walls (shy-away distance for metal walls is about half the distance for concrete walls). Daamen (2004) presents a table with shy-away distance according to the types of the infrastructures. Therefore, we assess if the models implement the shy-away distance behaviour.

The shy-away distance criterion is:

0 if no shy-away distance is modelled.

+1 if the shy-away distance is modelled to a fixed distance.

+1 if the shy-away distance varies with type of infrastructures and materials.

Contact forces

The ultimate cause of injury and deaths in crowd disaster are the crushing forces in the bodies (Helbing and Mukerji (2012), Still (2014)). Very few studies managed to determine quantitatively the pressure inside real crowds (Fruin (1993)) and relate them with densities. This lack of data makes it impossible to a quantitative assessment of the pressure calculation models. However, several important crowd phenomena are related or resulting from the forces generated by physical contact.

Helbing et al. (2000b) shows that pedestrian flows with large fluctuations have a tendency to gridlock. They called this phenomena 'freezing by heating' caused by friction forces when pedestrians rub their shoulders. Helbing et al. (2000a) show that these phenomena can reduce the capacities of exits.

Johansson et al. (2008) and Helbing et al. (2007) show how turbulence and stop-and-go waves with very high body pressures form in extremely dense situations. In such

situations pedestrians loose almost all control of their walking and the physical forces predominantly determine their movement.

Therefore, models that predict the pressure forces in collisions are more realistic and more useful than models without collision.

The contact force criteria are:

0 if no contact force is modelled.

+1 if friction is modelled.

+1 if pressure is modelled.

2.3.5 Environmental characteristics

The most important aspect of the environment is the discretisation of the walking area. It is very determinant for the outcomes if pedestrians are free to walk in any location (continuous models) or are restricted (discrete models) [4].

Discrete walking areas limit the locations of pedestrians to the centre of the cells. The most common discretisation are square grids with sides representing the human width around $0.5m$. This is possible because according to Fruin (1971) the private space of standing pedestrians is almost square ($0.5mx0.4m$). However, newer empirical evidence points out that in very narrow corridors pedestrians displace laterally in 'zipper like' patterns and not in parallel lanes (Hoogendoorn and Daamen (2005b)). Figure C.1 in appendix C shows these patterns in a narrow corridor.

These zipper patterns cannot be reproduced in squared grids walking areas with pedestrians occupying single cells. Schadschneider et al. (2009) mention that motion in directions not parallel to the main axis of the lattice are difficult to realise and can only be approximated by a sequence of steps parallel to the main directions.

For discrete environments with single occupied cells, everything must be conform to the dimensions of the lattices. For square grids of $0.5m$ doors with $0.8m$ cannot be correctly represented. Furthermore, densities are limited by the size of the cells:

$$k_{max} = \frac{1}{(\text{cell size})^2} \tag{2.7}$$

Because of these limitations models with smaller grid cells have been proposed (Fang et al. (2012)), where pedestrians occupy multiple cells. However, Kirchner et al. (2004) point that conflicts due to pedestrians trying to move to the same cells increase significantly (figure 2.13).

[4] We do not include the environmental models that describe the development of weather, temperature, fire and smoke because their influence to walking behaviour is not the focus of this dissertation.

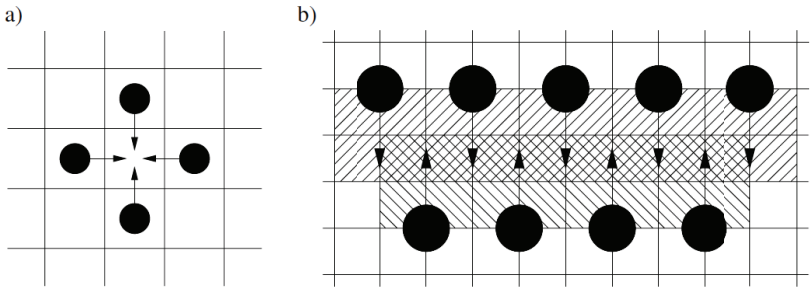

Figure 2.13: a) Typical local conflict in a 40 cm cell grid. b) In the 20 cm cell grid pedestrians can be part of more than one conflict. Hatched cells contribute to the non-local conflict (from Kirchner et al. (2004)).

Other types of lattices were also proposed. Maniccam (2003) compared a hexagonal lattice with a square grid CA model for a bidirectional corridor (figure 2.14). Marconi and Chopard (2002) also proposed a hexagonal lattice model with friction equations. The hexagonal lattice does provide more walking directions, but only allows for 90° crossing paths to be reproduced via jagged paths.

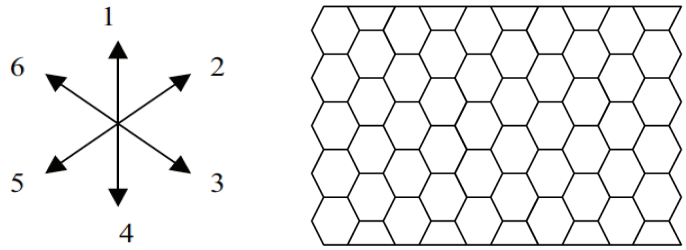

Figure 2.14: A hexagonal lattice and the six walking directions (from Maniccam (2003)).

All the mentioned problems with discrete environment result in models with continuous representation of space being more realistic.

The type of walking area environmental characteristic criterion is:

0 if the walking area is discrete.

+1 if the walking area is continuous.

2.3.6 State (human factors)

The necessity to include the dynamic properties such as position and velocity in the state is dependent on the type of the model and we do not consider this a positive feature of models. However, human factors that affect walking behaviours are important modelling decisions and are discussed in this section.

Empirical studies show that evacuation behaviour is strongly influenced by human factors. Evacuations in extreme situations have different effects on the behaviour of pedestrians (Leach (2004)). Depending on the level of urgency or hazard conditions pedestrians may walk faster and become more 'pushy' (Helbing et al. (2000a)). Some people in extreme situations simply do not react and stay paralysed often dying from inaction (Leach (2004)). This thesis is not focusing on evacuations in extreme situations that are still not completely understood and results in non normal behaviours (Leach (1994), Kobes et al. (2010), Galea et al. (2010)).

Instead we will concentrate on two human factors that affect normal walking: urgency and fatigue (Kuligowski (2009), Choi et al. (2011)).

It is safe to assume that almost everyone in an evacuation situation during extreme circumstances will have a sense of **urgency**. That is kind of an 'instinct': the urge to leave a dangerous situation due to time pressure (Kuligowski (2009)). It is a common answer to the cognitive process of perceiving and assessing the situation of danger (Sime (1986)). Daamen and Hoogendoorn (2012) applied slow whoops and stroboscope lights to create an aggressive environment in evacuation experiments. They found out that these conditions increased walking speeds and to a lesser degree door capacities. This shows that behaviour associated to an increased sense of urgency has an influence on evacuation behaviour and could be important in models.

Shields et al. (2009) pointout that evacuees from the World Trade Center presented mental and physical **fatigue** that significantly slowed their pace after descending several floors. Galea et al. (2010) analysed the consequences of fatigue in the evacuation of the World Trade Center and obtained through a survey that 10% of the stoppages where due to fatigue. Choi et al. (2011) made experiments in tall buildings obtaining similar conclusions. Daamen and Hoogendoorn (2009a) mention that during evacuation experiments fatigue could explain the decrease of capacity for experiments with similar populations performed at the end of the day.

We will consider that if a model presents any of them it is more realistic.

The human factors criteria are:

0 if no human factor is modelled.

+1 if urgency is modelled.

+1 if fatigue is modelled.

2.4 Results of model assessment

We chose the most representative models and those that present the latest developments from each type to be assessed. All walker models that we discuss in this review were

subjected to at least one quantitative validation report to justify their inclusion in this review.

The models are evaluated using the scores presented in section 2.3. Each model characteristic score is the sum of the different criteria. Table 2.2 shows the range for each characteristic in brackets and the total scores for all models calculated by adding the scores of all characteristics.

We did not use weights to increase the importance of the subcategories of the characteristics. Table 2.2 shows that only goal characteristics change significantly the ranking of models.

The scores of the other 5 characteristics are more influenced by the agent type. The force, goal and utility models receive larger scores for the other 5 characteristics than the rule models. A sensitivity analysis showed that weighting the other characteristics did not change the rankings significantly.

Furthermore, by having nine subcategories, the goal characteristics already have a larger influence in the outcomes and we consider that it is subjective to decide which goal characteristics are more important to other goal characteristics.

The first observation is that the best model (Nomad) achieved 12 points from a total possible of 19 showing that all models can be further improved.

Social force, collision avoidance, Nomad and discrete choice models perform reasonably well. The Nomad model also scored well in four of the five assessment categories.

The discrete nature of CA models makes them score badly. The biggest problem being the difficulties to introduce heterogeneity, to simulate collision avoidance and to model other actions. Results have shown that CA models are able to estimate accurately aggregated indicators such as exit capacities and fundamental diagram relations. The wide use of CA models indicates that accuracy in estimating aggregate indicators may be enough for several applications. However, for the questions being asked in this dissertation a CA model is not able to estimate individual behaviour with high detail and accuracy.

The large amount of social force model modifications and the good scores from some of them shows the potential of these models to be applied for individual walking behaviour. However, there is no publicly applied (non-commercial) of the social force model that can be implemented for complex situations.

Collision avoidance models are a promising new type of model that seem to be accurate in reproducing individual behaviours, but there is not enough evidence of their accuracy and computational performance in very high densities. Furthermore, it is not shown yet that such models are generic enough to be able to simulate significantly different situations with the same set of parameters and still be accurate.

From the utility models Nomad is the most promising for further development and adaptation for the simulation of complex situations. Furthermore, the pedestrian theory

Table 2.2: Overview of walker models.

agent type	Reference	model type	H	Perception	Actions	Goals					Environment	S	Total
			Heterogeneity	bounded, anisotropic	waiting, stairs	travel purpose	social stimulus	reactive x anticipatory	contact forces	shy-away	continuous x discrete	**State** (human factors)	
	Range		(2)	(2)	(3)	(3)	(2)	(1)	(1)	(2)	(1)	(2)	**(19)**
Rule	Blue and Adler (1999)	CA	1	2	0	1	0	0	0	0	0	0	**4**
	Burstedde et al. (2001)	CA	0	1	0	1	1	0	0	0	0	1	**4**
	Kirchner et al. (2003)	CA	0	1	0	1	0	0	0	0	0	0	**2**
	Suma et al. (2012)	CA	0	1	0	1	0	1	0	0	0	0	**3**
	Turner and Penn (2002)	SS	0	1	0	1	0	0	0	0	0	0	**2**
Force	Gipps and Marksjo (1985)	CA	1	1	0	1	0	0	0	0	0	0	**3**
	Okazaki (1979)	MF	1	0	1	2	0	0	0	1	2	0	**7**
	Helbing and Molnar (1995)	SF	1	2	0	1	0	0	0	1	2	0	**7**
	Aube and Shield (2004)	SF	1	2	0	1	2	0	0	1	2	0	**9**
	Helbing et al. (2005)	SF	1	2	0	1	0	0	2	1	2	1	**10**
	Zanlungo et al. (2011)	SF	1	2	0	1	0	1	2	1	2	0	**10**
	Johansson (2013)	SF	1	2	1	1	0	0	0	1	2	0	**8**
Goal	Paris et al. (2007)	CO	1	2	0	1	0	0	0	1	2	0	**8**
	Ondřej et al. (2010)	CO	1	2	0	1	0	0	0	0	2	0	**7**
	Moussaïd et al. (2011)	CO	1	2	0	1	0	0	2	0	2	0	**9**
Utility	Hoogendoorn and Bovy (2002)	NO	2	2	0	1	0	0	2	2	2	0	**11**
	Hoogendoorn (2004)	NO	2	2	0	1	0	0	2	2	2	1	**12**
	Antonini et al. (2004)	DC	1	2	0	1	0	0	0	0	2	0	**6**
	Robin et al. (2009)	DC	1	2	0	1	1	0	0	0	2	0	**7**
	Nasir et al. (2014)	FL	0	2	0	1	0	0	0	1	2	0	**6**

Where: CA - Cellular Automata, MF - Magnetic Force, SF - Social Force, SS - Space Syntax,
CO - Collision Avoidance, NO - Nomad, DC - Discrete Choice, FL - Fuzzy Logic

that is the foundation of Nomad is a powerful explanatory tool to interpret the outcomes and to orient the developments. The discrete choice models are also promising. Their direct derivation from empirical data makes them very useful for investigation of pedestrian movements. However, these models will get more complex when other actions such as waiting behaviours and other travel purposes are implemented.

In the following, we will discuss the assessment of the five agent characteristics and the heterogeneity for the type of models.

2.4.1 Heterogeneity

Only the Nomad model explicitly proposes heterogeneity to other parameters than the free-speeds. However, there is no impediment for Social force and discrete choice models to be used in the same way. The same cannot be said for collision avoidance models. Their strict enforcement of avoidance manoeuvres make it difficult to vary walking behaviours among the population. Even though one CA model proposed three different free-speeds, heterogeneity is not easily enforced in spatially discrete models. The restriction of hopping fixed distances strongly limits variation in behaviour. This is shown by the low amount of heterogeneous CA models.

2.4.2 Perception

An anisotropic perception corresponding to real pedestrian perception appears in all spatially continuous models apart from the magnetic and the fuzzy logic models. The fine description of continuous environments is clearly benefitting these models with more realistic description of pedestrians perception.

There are differences in the perception area between the types of models. CA models are clearly in disadvantage here because of the grids. CA models can only define a limited geometry of neighbouring cells for the perception area. Social force and the Nomad models apply perception areas that are elliptical with the reference pedestrian in one of the focal points. This perception area also considers the influence of pedestrians very close, but behind the reference pedestrian. This is justified by the use of other senses such as hearing or the use of the short term memory of a passing pedestrian for perception outside the field-of-view. The collision avoidance and discrete choice models use more a strict ‘vision’ based perception. They define a visual field-of-view with a fixed angle spreading from the walking direction. It is still disputed which of the two perception areas is more realistic, but the elliptical perception area is certainly more general by including the area behind the pedestrian.

2.4.3 Actions

No model presented changing level behaviours indicating an important blank spot in their development. Furthermore, not many different actions were proposed. Two spatially continuous force models implemented waiting behaviours indicating that it is possible to implement them in the Nomad model (as we show in section 3.3). To implement different actions in collision avoidance and discrete choice models will considerably increase their complexity. For collision avoidance models, the movements that would occur in dense situations such as train platforms would probably need to be attenuated due to non realistic accelerations and trajectory changes.

2.4.4 Goals

From the maximum of 9 goal points possible to be achieved, Nomad was the best performing with 5. If we combine all the goal attributes from the different Social force models we achieve 8 points. Other types of models score worse. These observations indicate the complexity of implementing all these sometimes conflicting goals in a single model.

Travel purpose

Apart from the space syntax model all models have a 'drive' to reach a destination corresponding to commuter behaviour. Only the magnetic model mentions an explorative behaviour but without any description of how it was implemented. It seems that it is not impossible for any other type of model to simulate different behaviours exchanging the drive to the destination for a different walking strategy. However, the discussion on the difficulty to implement different actions in collision avoidance and discrete choice models probably applies for the implementation of other travel purposes.

Social stimulus

Only CA and Social force models presented implementations of group behaviour. In reality, the 'dynamic floor field' for CA models creates lane behaviour and recent studies showed that they do not reproduce realistic group behaviour.

There is nothing preventing the other model types to implement grouping and leader following behaviour. A simple solution would be to adapt the boids model introduced by Reynolds (1987). However, it could be significantly more complex to realise them with collision avoidance models due to the inevitable difficulties arising from conflicting stimuli such as avoidance and attractive behaviours.

Similarly to the group behaviour it would be possible for the other types of models to implement leader-follower using attractive accelerations.

Pedestrian interaction

The survey showed that the models in general are divided into reactive (almost all models) and anticipatory (collision avoidance). One implementation of the Social force model and one of the CA included foresight by accounting for anticipated positions of pedestrians effectively combining both strategies. The superior results reported by the authors support the claim that models should combine the strategies.

Obstacle interaction

Only spatially continuous models can implement shy-away distances that vary according to the situation and this is reflected by the low scores of CA models. It appears that all types of models are able to enforce a shy-away distance, but only the Nomad model explicitly mentions it and it also allows for the dependency to the type of obstacle.

Contact forces

The mechanism of calculating the pressure during collisions is similar in all types of models (see section 3.2.11 for details). Pedestrians are considered non-rigid bodies and the deformation is the overlapping distance of the colliding pedestrians. All implementations consider circular pedestrians for simplicity, although this is not obligatory. Only CA models do not offer a possibility to easily calculate pressure forces. Some authors introduce a friction force to solve some conflict situations, but these are not comparable to real physical forces.

2.4.5 Environment

Here, the models divide themselves very clearly between CA models and the rest. CA models are discrete by definition and the rest spatially continuous. However, discrete choice and fuzzy logic models make a discretisation in the perception areas to reduce the search complexity. It is not clear how this discretisation affects pedestrian freedom to reach all locations, therefore we did not take any points from these models.

2.4.6 State (human factors)

The CA model with a human factor presented an abstract concept of ‘happiness’ for two different states of pedestrians. The other two human factors implementations by a Social force model and the Nomad were similar and basically increased the speed of pedestrians given some conditions of urgency. This same principle could be easily introduced to any model apart from CA models that are not able to easily apply different speeds for pedestrians.

2.5 Conclusions

This state-of-the art assessed the different types of walker models with the objective to choose the most promising for further research on walking behaviour as well as to gain insight into pedestrian behaviours. The discussion of the models followed an agent-based programming paradigm. The proposed agent-based representation for assessing walker models allowed for an in-depth and logical comparison of common aspects of walker models. The applied scoring system is a quantitative tool to evaluate, compare and to identify the blank spots of particular models.

It is not possible to make accurate assessments, as often not all information on the model is present. However, the scores gave a good indication of the strength and weaknesses of the models.

We concluded the assessments by identifying that the utility-based models and most notably the Nomad model is most suited to be used for both investigations on individual behaviours and to simulate complex situations. The Nomad model did not perform badly in any of the agent-based elements. Where Nomad did not score well we did not identify an impossibility for it to be improved making Nomad the ideal model to be used in this dissertation. The social force models would also qualify by being not very dissimilar than the Nomad model in its original derivation. However, contrary to Nomad they lack a pedestrian theory to enhance their explanatory power.

CA models received the lowest scores, mostly due to the time and spatial discretisation that limit significantly the realism of the movements. Other promising types of models are the collision avoidance and the discrete choice models that scored only slightly worse than Nomad and the Social Force model.

The discussion on the different aspects of modelling walking behaviour revealed some gaps on modelling walking behaviour:

- The exploration of the effects of heterogeneity in pedestrian behaviour.
- Different actions besides walking required in pedestrian facilities.
- Other travel purposes, such as leisure and shopping behaviours.
- Group behaviour and leader-follower behaviour.
- Introduction of fatigue.
- Models that combine anticipation with reactive behaviours.

Not all of these gaps are covered in this dissertation and we made a prioritisation of implementing the different actions needed for complex pedestrian areas and improving the accuracy by modifying the interaction behaviours introducing anticipation to the Nomad model (chapter 3).

The other gaps (new travel purposes, group and leader-follower behaviour and fatigue) are a natural continuation of the developments of this dissertation and together with the necessary empirical data are left to be explored in the future.

Chapter 3

Nomad walker model and simulation

The Nomad model was proposed by Hoogendoorn and Bovy (2002) and Hoogendoorn and Bovy (2003). Its underlying principle states that pedestrians continuously minimise the effort required to walk. In the Nomad pedestrian theory the walking effort is expanded to the more generic concept of walking cost and utility earned by performing an activity (see section 2.2.4 for the definitions of utility). Simply put, pedestrians gain utility when performing activities and 'pay' a cost when walking. In the Nomad theory both costs and utilities are expressed in time units. Nomad pedestrians are maximising the sum of both, thus it is an activity based normative theory (*pedestrian economicus*). The normative approach stems from the *homo economicus* concept used in several economic theories. The concept refers to the idea that humans behave rationally and always aim at maximising their self-interests (Wikipedia (2016)).

All relevant tasks pedestrians must fulfil are modelled using the cost minimisation principle. Section 3.1 puts forward the description of the Nomad three level pedestrian theory that divides these tasks into logical units. The Nomad simulation tool features an implementation of these three levels allowing for complex simulations to be run. However, only the operational level (walker model) is the focus of this dissertation and is explained in detail in this chapter.

This chapter presents the theoretical and mathematical foundations of the Nomad walker model (Section 3.2). Nomad is a spatially and time continuous model that describes individual pedestrians. The model described in this chapter reproduces the commuter behaviour of purposeful pedestrians going straight to a goal. Nomad model is extended to model special behaviours such as waiting behaviours in section 3.3.

The derivation of the model can be found in Hoogendoorn and Bovy (2002) and some of the extensions in Campanella et al. (2009c). Here, we recall the most important aspects of the derivation of the walker model and emphasise the connection between the model and the behavioural assumptions. The behavioural hypothesis that guides the development of the model are explicitly presented in the sections in an ordered list with the prefix H.

Nomad is implemented as a simulation model and has been used in several occasions to predict pedestrian flows (chapter 8). The implementation was made with several goals: accuracy, richness of behaviours and computational performance. Section 3.4 presents new features that aim at these three goals. This section also presents an overview of important features of the system architecture of the Nomad simulation tool. This shows the modularity, and thus the ease to extend Nomad with other behaviours. Section 3.5 ends the chapter with a summary and future developments of the Nomad model.

3.1 Nomad three level pedestrian model

The Nomad model is based on the three level pedestrian theory approach. These levels break the important aspects of pedestrians behaviour into distinct tasks reducing the model complexity. The *strategic level* incorporates the tasks that must be completed before the trip starts (the plan), the *tactical* level describes the choices and decisions including changes in the original plan during the trip and the *operational level* describes the walking behaviour or how pedestrians navigate to accomplish the plan. Figure 3.1 shows the scheme of the Nomad pedestrian model.

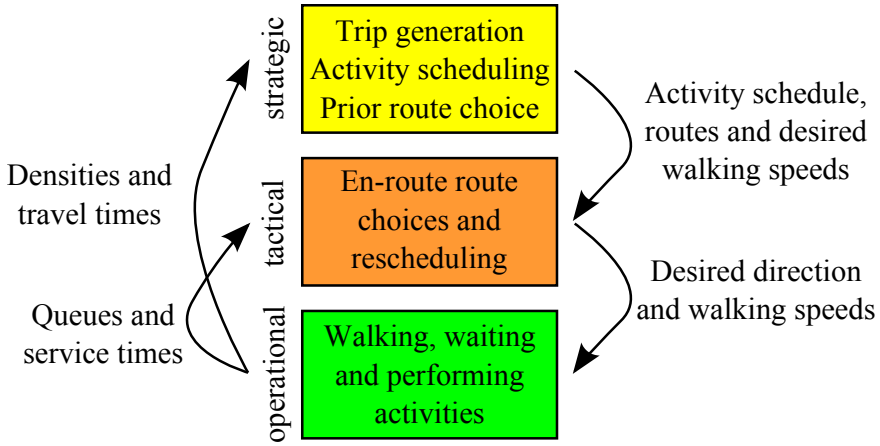

Figure 3.1: The scheme of the three levels modelling approach from Hoogendoorn and Bovy (2004).

This dissertation does not detail the two higher levels but here we present a short introduction. It also shows the relations between the strategic and tactical levels to the operational level by describing a typical trip of a Nomad pedestrian of a commuter type that (may) perform activities before reaching its destination. Commuters have at least one destination and walk towards it (see section 2.3.3).

The activities that commuters perform during the trip such as buying a transport ticket or stopping for information are usually performed sequentially in different locations. Therefore, the set of activities is chained and the activity locations become intermediate destinations before the end of the trip on the final destination.

The plan (*strategic level*)

The first action of commuters is to plan their trip and this is the task of the *strategic level*. The plan consists of the schedule (ordered list) of the activities and the corresponding routes linking the origin, activity areas and destination. According to the Nomad theory the planned trip has the highest possible utility that a pedestrian can gain from performing the intermediate activities, reaching the destination and discounting the walking costs. Thus, the trip is an optimal schedule of activities for which the ordering of activities and the choice of the routes are performed simultaneously (Hoogendoorn and Bovy (2002)). The optimal route can have constrain due to obligatory order of activities (passengers must book a ticket before boarding a train).

In the implementation of Nomad, we made a simplifying assumption that the prior activity set is also ordered. However, if more than one location can receive the activity function or be the final destination, the plan is the chain of activities in which the choice of the activity area locations and the connecting routes is optimal.

The list of input of the *strategic level* contains:

1. The origin and the destination.
2. A set of activities that will be performed during the trip.
3. The locations of the activity areas.
4. The complete description of the walking area.

Let us consider $\{l_{i,j}\}$ the set of locations where activity A_i can be performed. The set $S = \{A_i\}$ of activities to be performed includes the activity 'exiting' at the final destination. Let us also consider that performing the activity A_i in $l_{i,j}$ yields an utility $U(A_i, l_{i,j})$. The utility corresponds to an intrinsic value obtained by realising the activity at the specific location ('this restaurant is very good').

The cost $C_t(A_i, l_{i,j})$ is a measure of the expected *waiting time* to be served at location $l_{i,j}$. It is a negative utility (cost) proportional to the amount of people in the location or walking towards it.

The expected time spent in the location performing activity A_i also generates a negative utility. The cost $C_s(A_i, l_{i,j})$ is proportional to the expected *service time* at $l_{i,j}$.

The last cost is proportional to the expected *walking time* $C_w(l_{i-1}, l_{i,j})$ from the location $l_{i-1,k}$ of the previous activity A_{i-1} to $l_{i,j}$.

The utility U_{choice} obtained when *choosing* location $l_{i,j}$ to perform activity A_i coming from location $l_{i-1,k}$ is:

$$U_{choice}(A_i, l_{i,j}, l_{i-1,k}) = U(A_i, l_{i,j}) - [C_t + C_s](A_i, l_{i,j}) - C_w(l_{i-1,k}, l_{i,j}) \tag{3.1}$$

The resulting optimal activity chain S^* with the activities and location areas will be the one that results in the maximum sum of all U_{choice}:

$$U^*_{sum} = \arg\max \left(\sum_{i \in S} U_{choice}(A_i, l_{i,j}, l_{i-1,k}) \right) \tag{3.2}$$

The route choice model was developed by Hoogendoorn and Bovy (2004) using the minimum walking cost principle. The costs of walking reflect preferences of pedestrians: travel distance, minimum distance to obstacles, travel time, physical effort (using stairs is more costly than escalators), subjective preferences such as closeness to shopping windows (assuming an interest by the pedestrians then close positions generate lower walking cost).

The end result of the route choice calculation for a particular destination is a cost map that presents the walking cost for each position in the walking area to reach the destination. The optimal route results from moving from the current position to the closest position with the lowest cost. This is repeated until the destination that has the overall lowest cost is reached. Hoogendoorn and Bovy (2004) show that the optimal route is the one that presents the lowest sum of walking costs between the origin and the destination and that for each position with connection to the destination there is always one optimal route connecting them.[1]

Figure 3.2 shows an illustration of a cost map and three desired routes from three different origins towards the same destination. The coloured rings represent regular lines of walking costs (equi-cost). The walking cost is minimal over the destination (in yellow) and maximal the furthest from the destination (over the white dotted line).

Each destination has only one equi-cost map. Optimal routes can be obtained from any location of the walking area by simply following perpendicular curves to the equi-cost lines (minimal walking cost during the trip). The desired walking direction is always perpendicular to the equi-cost lines and the speed is obtained by the walker model.

Changes in the plan (*tactical level*)

There are many reasons why pedestrians make choices during the trip: the need to reschedule the plan because the original route is congested and an alternative route is less costly or an alternative activity area has considerably less pedestrians waiting to perform the activity. Choices always follow the utility maximisation principle. Also pedestrians may have to choose between queues, escalators and stairs. Section 3.3.2 will present in more detail the choice behaviour of queues and servers.

[1] There are situations in which there is not a single optimal route. Walking areas with independent accesses to a destination present regions that present more than one equally optimal route. In these cases random fluctuations in the model will decide which route is desired (see figure 3.2).

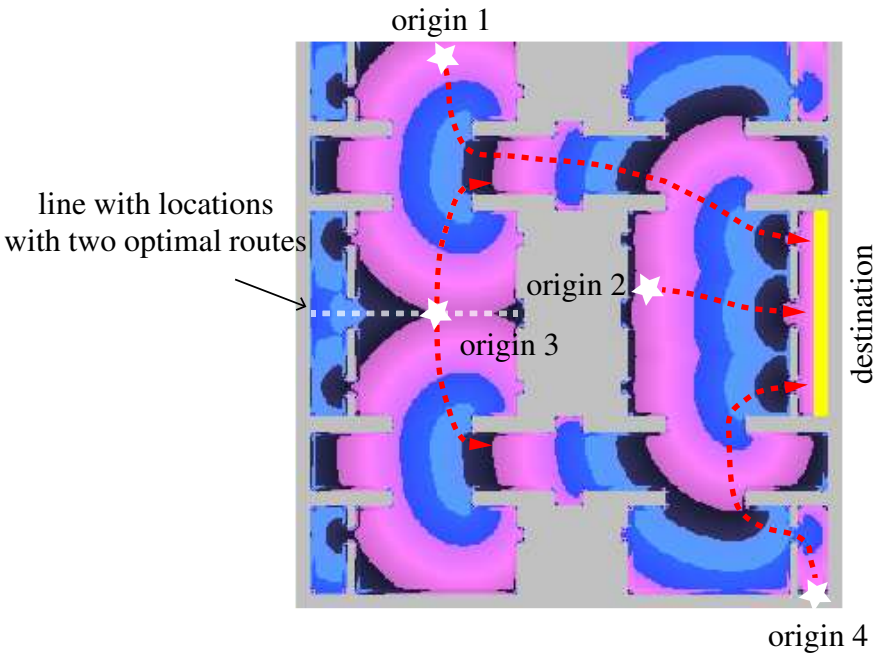

Figure 3.2: Three optimal routes starting from origins 1, 2, 3 and 4 (represented by the stars) leading to the same destination accessible via three doors. The background colour are rings representing the cost maps. In grey are all walls and obstacles and in yellow the destination. Locations above the white dotted line on the left have optimal routes via the upper corridor and below via the lower corridor. Locations on the line such as origin 3 always present two optimal routes.

Walking (*operational level*)

Once on their way pedestrians will walk towards their upcoming activity area. They navigate around the pedestrian traffic that is encountered. When reaching the area and if the activity is available, pedestrians start performing it. This walking and performing activity cycle repeats until all activities are finished. The behaviours displayed during the walking and performing activities is the domain of the *operational level* and are detailed in the next sections.

3.2 Nomad walker model

This section presents and discusses the original version of the Nomad walker model proposed by Hoogendoorn and Bovy (2003) and modifications introduced by Campanella et al. (2009c). Nomad is a continuous model in space and time. Therefore, it allows the representation of pedestrian movements by the dynamics of the position:

$$\frac{d\vec{r}(t)}{dt} = \vec{v}(t) \qquad \text{and} \qquad \frac{d\vec{v}(t)}{dt} = \vec{a}(t) \tag{3.3}$$

where:
$\vec{r}(t)$ is the position vector at time t.
$\vec{v}(t)$ is the velocity.
$\vec{a}(t)$ is the acceleration.

The Nomad model is the function f that estimates the acceleration: $\vec{a} = \vec{f}$. This function has two components: the controlled and the non-controllable acceleration.

The controlled acceleration $\vec{a_c}$ represents the subjective walking behaviour that steers pedestrians towards their destinations avoiding other pedestrians while trying to maintain their free-speeds. $\vec{a_c}$ is not equivalent to conscious movement because much of the walking is realised without awareness (Goffman (1972)). It represents all movements that can be initiated and modified by pedestrians.

The non-controllable or physical acceleration $\vec{a_p}$ results from contact forces with other pedestrians or with obstacles. The forces generated by contact are also referred as crowd pressure (Helbing et al. (2000a), Maury and Venel (2007)). By definition they are independent of each other. Therefore, the total acceleration model is the sum of the controlled and the uncontrolled acceleration:

$$\vec{a}(t) = \vec{a_c}(t) + \vec{a_p}(t) \tag{3.4}$$

where:
$\vec{a_c}$ is the controlled component.
$\vec{a_p}$ is the physical component (not controlled).

In the next subsection we present the walking cost function J. This function allows the derivation of the controlled acceleration as a cost minimisation problem following the normative Nomad pedestrian theory.

3.2.1 Walking costs

The Nomad cost function is determined by the sum of the walking costs along the trajectory. This is mathematically described by integrating the so-called walking costs L_p over the planning period $[t, t+T]$. This is represented by the cost functional $J^{(p)}$ for the pedestrian p:

$$J^{(p)} = \int_t^{\infty} e^{-\eta_p s} L_p\left(s, \vec{z}(s), \vec{a_c}(s)\right) ds \tag{3.5}$$

where:
$\eta_p > 0$ is the (temporal) discount factor that decrease the value of the predicted costs

over time and space.
$\vec{a}_c$ is the controlled part of the acceleration.
$\vec{z}(t) = (\vec{r}, \vec{v})$ is the state vector composed by the position and the velocity.

The controlled acceleration $\vec{a}_c$ results from the minimisation of the cost functional $J^{(p)}$:

$$\vec{a}_c{}^* = \arg\min \left(J^{(p)} \right) \tag{3.6}$$

The walking costs reflect a variety of factors k that pedestrian consider, and it is assumed that these costs add linearly (although this assumption is not determinant for the derivation):

$$L(s, \vec{z}, \vec{a}_c) = \sum_k c_k L_k(s, \vec{z}, \vec{a}_c) \tag{3.7}$$

where:
c_k denotes the relative weight between the cost components.

The complete derivation of the acceleration model is detailed in Hoogendoorn and Bovy (2003) and in Hoogendoorn et al. (2003), and will not be shown here.

In the following we will present the three acceleration components that are derived from walking costs that represent: following desired paths, avoiding pedestrian and avoiding obstacles. The walking costs are preceded by behavioural hypothesis (referred by the letter H) taken from empirical studies.

3.2.2 Controlled acceleration $\vec{a}_c$

Like real pedestrians Nomad pedestrians perceive their surroundings and use the perceptions to act.

change to:

H1: Pedestrian behaviour is feedback-oriented.

Pedestrians follow the minimum effort principle and this is translated to a utility optimisation strategy of minimising the costs of walking. In Nomad the walking costs are explicitly defined and correspond to independent behaviours related to walking. The independence assumption allows the walking costs to be added (equation (3.5)).

H2: Pedestrians minimise additive discounted costs resulting from walking.

In its basic version Nomad distinguishes three walking costs.

Pedestrians minimise costs resulting from:
H3: straying from the desired route,
H4: the vicinity of obstacles and
H5: the vicinity of other pedestrians.

In the model this corresponds to:

$$\vec{a_c}(t) = \vec{a_f}(t) + \vec{a_o}(t) + \vec{a_r}(t) \tag{3.8}$$

where:
$\vec{a_f}$ is the path following component.
$\vec{a_o}$ is the obstacle interaction component.
$\vec{a_r}$ is the pedestrian interaction component.

Inserting equation (3.8) into (3.4) we obtain **Nomad acceleration model:**

$$\vec{a}(t) = \vec{a_f}(t) + \vec{a_o}(t) + \vec{a_r}(t) + \vec{a_p}(t) \tag{3.9}$$

Equation (3.8) shows the accelerations resulted from the basic walking costs but others such as the cost of staying in the vicinity of a group, can also be included. These three costs are the most important to define individual walking behaviours and their mathematical formulations are detailed in the following.

3.2.3 Path following component $\vec{a_f}$ (H3)

Section 3.1 showed that the optimality assumption results in desired velocities along optimal routes towards a destination. Furthermore, according to Buchmueller and Weidmann (2006) pedestrians prefer to walk with their free-speeds that are close to the optimum in terms of energy consumption. Therefore, deviations from free-speeds and from the desired velocity constitute additional walking costs. (figure 3.3)

The Nomad model proposes an exponential equation (3.10) for the velocity that penalises deviations below and above the free-speeds and away from the optimal route.

$$\vec{v}(t) = \vec{v_0}(1 - \mathrm{e}^{-t/\tau}) \tag{3.10}$$

where:
τ is the constant acceleration time.
v_0 is the free-speed.

The further away from the optimal velocity the stronger is the acceleration bringing the velocity back to the optimal, with the maximum acceleration occurring when $\vec{v}(t) = 0m/s$. When densities are high, interaction accelerations (section 3.2.5) can push speeds above the free-speed resulting in negative acceleration from the path following component.

The exponential formulation with its characteristic asymptotic shape on $\vec{v_0}$ was shown to reflect empirical evidence for pedestrians walking alone and starting from standstill (Moussaïd et al. (2009)).

The **path following component** $\vec{a_f}(t)$ is the acceleration that the pedestrian will apply trying to reach the desired velocity. It results from the temporal derivative of the equation (3.10).

$$\vec{a_f}(t) = \frac{d\vec{v}(t)}{dt} = \frac{\vec{v_0} - \vec{v}}{\tau} \tag{3.11}$$

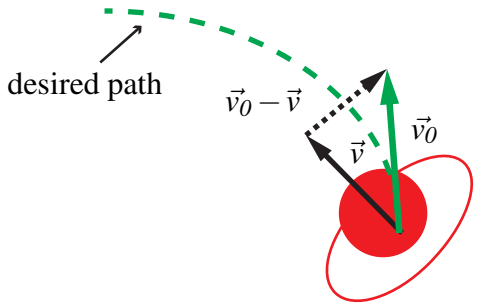

Figure 3.3: The path following component elements.

The acceleration time τ mostly affects the amount that pedestrians stay close to the optimal route. Pedestrians with very small τ ($\sim 0.0s$) will walk closely to their desired path with speeds around their free-speeds. It will require very large interaction accelerations (section 3.2.5) to make these pedestrians deviate from their paths, and thus to avoid other pedestrian representing uncooperative (aggressive) pedestrians.

3.2.4 Obstacle repulsion component $\vec{a_o}$ (H4)

Pedestrians maintain a shy-away distance to obstacles (see section 2.3.4). Further away obstacles are not influencing the walking. However, there are situations in which pedestrians may need to stay closer to obstacles when waiting or passing turnstiles. Therefore, we use a linear function that to keep the accelerations not increasing too much in short distances (equation (3.12)). For simplicity the distances between the pedestrians and the obstacles are calculated considering circular pedestrians. (figure 3.4)

If a pedestrian is in the vicinity of several obstacles than the interaction acceleration of all obstacles are added (H2). Equation (3.12) considers the set O of obstacles in the vicinity and calculates the acceleration due to avoidance of obstacles.

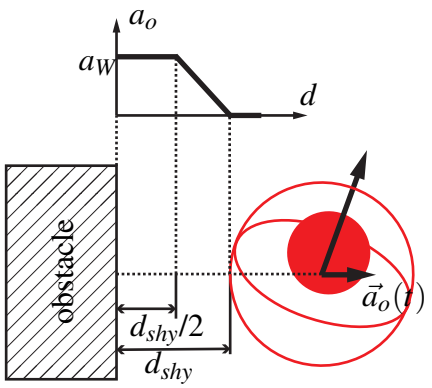

Figure 3.4: The interaction acceleration $\vec{a}_o(t)$ applied by the pedestrian due to the obstacle. The function against the distance d is shown in top.

$$\vec{a}_o(t) = -\vec{e}_n \cdot a_W \sum_{o \in O} \begin{cases} 1 & \text{if } 0 < d \leq d_{shy}/2 \\ 2(1 - d/d_{shy}) & \text{if } d_{shy}/2 < d \leq d_{shy} \\ 0 & \text{if } d > d_{shy} \end{cases} \tag{3.12}$$

where:
$\vec{e}_n$ is the unity vector in the normal direction pointing to the closest point of the obstacle.
a_W is the obstacle interaction strength is a balancing parameter between this components and the others (the larger a_W the more important is the obstacle interaction).
d_{shy} is the shy-away distance.

3.2.5 Pedestrian interaction component $\vec{a}_r$ (H5)

When pedestrians perceive pedestrians that potentially could collide in the near future they (may) apply avoiding manoeuvres. The reaction to these opponents is based on assumptions about their reactions. When opponents are not paying attention (distracted behaviour) or display a 'dominant' behaviour (aggressive behaviour) they are non-cooperative. In the assumption of non-cooperation the reference pedestrian carries the whole burden of the avoidance manoeuvres.

Hoogendoorn and Bovy (2002) show that under some conditions, cooperative models are similar to non-cooperative models. The Nomad model uses a non-cooperative strategy that is simpler to implement and realistic because all pedestrians apply the avoiding manoeuvres approximating the overall behaviour to a cooperative behaviour.

H6:	*Walkers anticipate on the behaviour of other pedestrians by predicting their walking behaviour according to non-cooperative or cooperative strategies.*

3.2.6 Anticipation strategies (H6)

Pedestrians anticipate the movement of others and themselves with the aim of minimising their future cost of walking. The anticipation time can extend from zero (no-anticipation) to a positive value (in seconds). In Nomad this is modelled by using anticipated positions instead of current positions in the pedestrian perception.

We use the zero acceleration assumption used commonly in collision avoidance models (section 2.2.3). The anticipated positions are extrapolated from the current speeds of the opponents (and for themselves) for a time determined by the *anticipation time* (t_A).

$$\vec{r_A} = \vec{r} + \vec{v} \cdot t_A \tag{3.13}$$

where:
t_A is the anticipation time.
$\vec{r_A}$ is the anticipated position of pedestrians.

Anticipation introduces the direction of movement to the pedestrian interaction behaviours. Figure 3.5 shows on the left the red pedestrian walking approaching and on the right distancing from the brown pedestrian. One would expect that even if in both cases, the distances between the pedestrians are the same, they interactions differ. With the former creating larger accelerations than the latter and this is exactly what the anticipation produces.

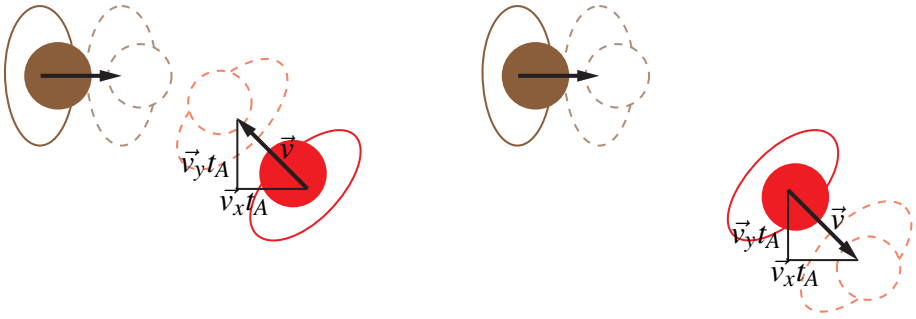

(a) approaching (b) distancing

Figure 3.5: The anticipation of pedestrian positions. For avoidance purposes the leftward pedestrian considers the anticipated dashed positions.

If the anticipated distances are larger than the real distances, pedestrians are moving away from each other (case (b) in figure 3.5). In these cases their interaction will be vanishing in the future and the anticipation reflects this. In the case that pedestrians are approaching (case (a)) their interaction will increase in the future and the anticipation behaviour reinforces this.

The anticipation is only used for interactions with pedestrians that are in front. Pedestrians do not guess the speed of pedestrians that are behind them. When pedestrians are very close and walking towards each other the anticipated positions could change from approaching to distancing. This would create a wrong behaviour in a crucial moment. Therefore, we avoid illogical behaviour by not allowing anticipated positions to fall behind the reference pedestrians.

3.2.7 Influence area (H7 and H8)

Pedestrian perception is largely based on vision, but the other senses also play a role (especially for vision impaired pedestrians). Pedestrians perceive what is happening behind them, but only in close range (see the discussion in section 2.3.2). The perception is limited in range, according to Goffman (1972) pedestrians scan a elongated area around 3 to 4 sidewalk squares ahead when walking on streets.

Nomad pedestrians thus have a limited area of interaction that is named the *influence area* that identifies which obstacles and pedestrians affect the pedestrian interaction behaviour.

H7:	*Pedestrians have limited predicting possibilities, reflected by discounting utility of their actions over time and space, implying that they mainly consider pedestrians in their direct environment.*
H8:	*Pedestrians react mainly to stimuli in front of them.*

The perception of pedestrians is dependent of the direction of the velocity and creates a distinction between the frontal (d_f) and the backward (d_b) parts of the influence area. Figure 3.6 shows the depiction of the two elliptical shapes that compose the influence area.

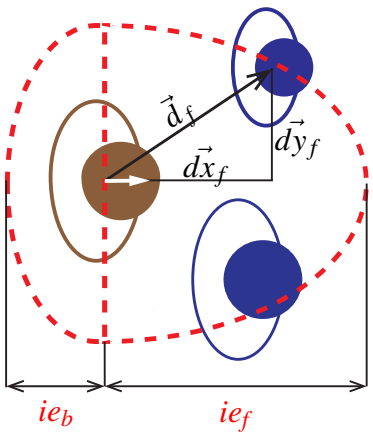

Figure 3.6: The influence area that determines the interaction zone extending to the front and to the back of the pedestrian. The maximum extensions of the influence area are respective ie_f and ie_b for the frontal and backward parts.

Another important aspect of the Nomad influence area is the increased influence on the interaction behaviours of pedestrians and obstacles that are in the vicinity of the walking direction. This is implemented by modifying the perceived distance in such a way that their distances become closer than reality. This is shown by the isolines in figure 3.7. The darker the colour the closer the pedestrians are perceived. Figure 3.7(b) shows an exaggerated effect of this distortion.

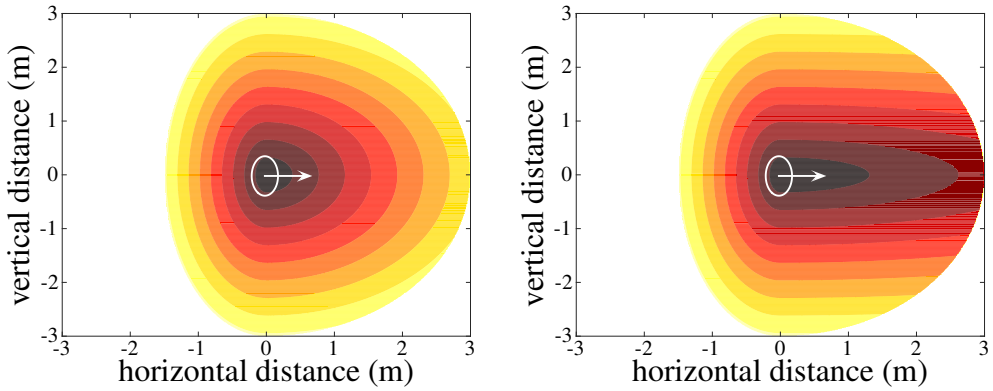

(a) $c_0^+ = 0.85$ (b) $c_0^+ = 0.25$

Figure 3.7: The influence area and the isofields with similar influence on the interaction behaviour. The pedestrian in white is walking to the right. (a) A value of c_0^+ that resulted from calibrations. (b) A more extreme case of influence from the frontal walking direction.

This change of the perception results from multiplying the projected distance between pedestrians in the velocity direction $\vec{d}_x$ by a factor c_0^+ that is smaller than 1. However, in general in the backward locations the opposite occurs when pedestrians on lateral positions are easier perceived. Therefore, the backward factor c_0^- is generally larger than 1 causing the backward elongation to be perpendicular to the walking direction as shown in figure 3.7. Equation (3.14) shows the mathematical formulation:

$$\vec{d}_f = \sqrt{(c_0^+ \vec{dx}_f)^2 + \vec{dy}_f{}^2} \qquad \vec{d}_b = \sqrt{(c_0^- \vec{dx}_b)^2 + \vec{dy}_b{}^2} \tag{3.14}$$

where:
$\vec{d}_f$ and $\vec{d}_b$ are the perceived distances respectively in the front and in the back between the pedestrians.
$\vec{dx}$ is the projected distances in the velocity direction.
$\vec{dy}$ is the orthogonal distances in the velocity direction.
c_0^+ is the multiplying factor for the forward distances and is < 1.
c_0^- is the multiplying factor for the backward distances.

3.2.8 Interaction acceleration

For interaction purposes the costs of proximity are inverse to the distance between pedestrians. The closer they are to each other the more intensively pedestrians want to increase their relative distances. This is the equivalent to say that pedestrians will apply larger avoiding accelerations due to pedestrians that are closer. These accelerations push them away from each other in a direction along their centres also called normal direction (see figure 3.8). In Nomad the interaction acceleration is modelled by an exponential function that amplifies the close-by accelerations, supported by empirical studies (Moussaïd et al. (2009)).

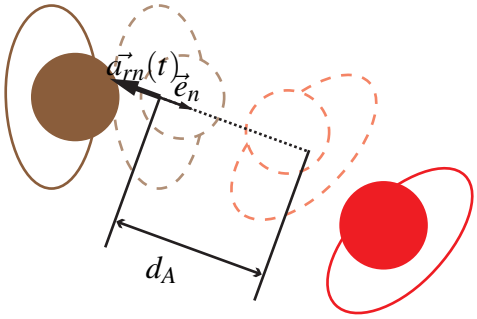

Figure 3.8: The interaction acceleration $\vec{a}_{rn}(t)$ applied by the left pedestrian due to the opposing pedestrian in the direction along their centres.

The **normal interaction acceleration** $\vec{a}_{rn}(t)$:

$$\vec{a}_{rn}(t) = -a_0 \mathrm{e}^{-d_A/r_0} \cdot \vec{e}_n \tag{3.15}$$

where:
a_0 is the interaction strength parameter.
r_0 is the interaction distance parameter.
d_A is the anticipated distance between pedestrians.
$\vec{e}_n$ is the unity vector in the normal direction pointing to the other pedestrian.

The interaction strength parameter a_0 is the balancing parameter between the pedestrians interacting component and the other components. The larger a_0 the more important this component is in comparison to the others.

The interaction distance r_0 relates the distance between the pedestrians and the intensity of the interaction acceleration. Diminishing values of r_0 ($\sim 0.0m$) diminish the distances required to generate large interaction accelerations. Diminishing r_0 decreases the space between pedestrians in crowded situations.

3.2.9 Extra lateral interaction

When two pedestrians walk towards each other in an almost parallel path they perform a strong lateral avoidance manoeuvre (usually the right side, Moussaïd et al. (2009)).

The interaction acceleration $\vec{a_{rn}}(t)$ presented in the previous section is not enough to create such large lateral accelerations when trajectories are aligned in a collision path. This occurs because the angle of the resulting $\vec{a_{rn}}(t)$ is aligned and opposing the velocities.

In the extreme case of perfectly aligned 180° ongoing paths the interaction component would display a non-realistic behaviour of only decelerating the pedestrians until they stop. To improve such situations an extra lateral interaction component is introduced for pedestrians walking towards each other (figure 3.9).

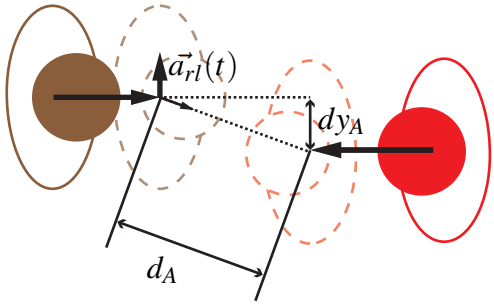

Figure 3.9: The lateral interaction acceleration $\vec{a_{rl}}(t)$ applied by the left pedestrian due to the opposing pedestrian.

The same exponential principle is applied and the lateral displacement of pedestrians as seen in figure 3.9 is used.

The **lateral interaction acceleration** $\vec{a_{rl}}(t)$:

$$\vec{a_{rl}}(t) = -a_1 \mathrm{e}^{-(d_A dy_A)/r_1} \cdot \vec{e}_y \tag{3.16}$$

where:
a_1 is the lateral interaction strength parameter.
r_1 is the lateral interaction distance parameter for lateral interactions.
d_A is the anticipated distance between pedestrians.
dy_A is the anticipated lateral distance between pedestrians.
$\vec{e}_y$ is the orthogonal speed direction pointing to the oncoming pedestrian.

The term $(d_A dy_A)$ makes sure that only when pedestrians are close to each other and with small lateral displacement the extra lateral acceleration will be significant.

The total interaction acceleration component is the sum of both interactions:

$$\vec{a_r} = \vec{a_{rn}} + \vec{a_{rl}} \tag{3.17}$$

3.2.10 Interaction with many pedestrians (H9)

When pedestrians interact with several pedestrians they react more intensively than when facing a single pedestrian. In Nomad this is achieved by adding the interaction of each pedestrian in the influence area as described by $\vec{a}_r$.

H9:	*Walkers will be more evasive when encountering a group of pedestrians than when encountering a single pedestrian.*

The behaviour hypothesis H9 states that pedestrians will add the influence of all pedestrians inside the influence area. Therefore the equations 3.18 and 3.16 are rewritten to:

$$\vec{a}_r(t) = -a_0 \sum_{p \in P} \mathrm{e}^{-d_{Ap}/r_0} \cdot \vec{e}_{np} - a_1 \sum_{p \in P_{front}} \mathrm{e}^{-\left(d_{Ap} dy_{Ap}\right)/r_1} \cdot \vec{e}_{yp} \tag{3.18}$$

where:
P is the set of pedestrians inside the influence area.
P_{front} is the set of pedestrians inside the influence area and walking towards the pedestrian.

3.2.11 Physical acceleration $\vec{a_p}$ (H10 and H11)

The contact forces occurring in collisions can achieve dangerous levels in extreme conditions. It is difficult to exactly model pedestrian collisions because the complexity of the body constitution. Bellies are usually softer than shoulders and the body vertical projection is elongated. Extreme situations may require sophisticated collision models (Helbing et al. (2007)), but Helbing et al. (2000a) proposes a particle based collision model to estimate the contact and friction forces. Similar contact accelerations are introduced in Nomad.

The most important assumption for the physical model is the division of the physical acceleration in two parts: the acceleration acting in the direction of the centres of the pedestrians (elastic) and the acceleration in the orthogonal direction (friction). These forces are additive due to the assumption that these forces are independent of each other in the same manner as collisions between perfectly circular elastic bodies.

$$\vec{a_p}(t) = \vec{a}_{p_n}(t) + \vec{a}_{p_t}(t) \tag{3.19}$$

During collisions:
H10: pedestrians bounce away from each other,
H11: whilst sliding and dragging each other.

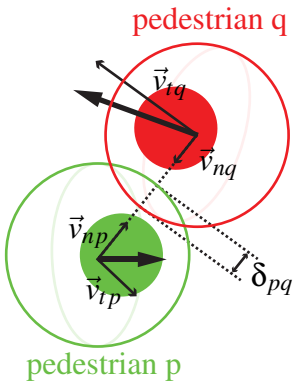

Figure 3.10: The graphic representation of a collision between two Nomad pedestrians. For simplicity, the collisions occur between circular shaped pedestrians.

The physical acceleration components for pedestrian p can be written as:

$$\vec{a}_{p_n}(t) = -k_0 \delta_{pq} \cdot \vec{e}_n \tag{3.20}$$

$$\vec{a}_{p_t}(t) = k_1 \delta_{pq} \left(\vec{v}_{tq} - \vec{v}_{tp}\right) \tag{3.21}$$

where:
$\vec{a}_{p_n}(t)$ is the physical acceleration in the direction of the centres of pedestrian p and q. (always in the direction opposite to the other pedestrian)
$\vec{a}_{p_t}(t)$ is the physical acceleration in the tangential direction of the centres of pedestrian p and q.
δ_{pq} is the deformation of pedestrians p and q.
k_0 is the elastic spring coefficient.
k_1 is the orthogonal friction factor.
$\vec{v}_t$ is the projection of the velocity vector into the orthogonal direction.
$\vec{e}_n$ is the unity vector in the normal direction pointing to the other pedestrian.

The accelerations are always applied in the direction contrary of the projected velocities. Therefore they always act in the opposite directions for each pair of pedestrians. The same model applies for collisions between pedestrians and obstacles where obstacles do not present deformations or velocities.

3.3 Special types of behaviour

In this section we present behaviours that are necessary in simulations of complex pedestrian facilities. Usually, large airports, train stations, metro stations, high-rise

buildings and shopping centres have pedestrians waiting, queueing or changing levels using stairs or escalators. These special behaviours were introduced to Nomad for complex simulations such as those presented in chapter 8.

The lack of data did not allow a proper calibration and validation of these behaviours. However, they were implemented and face validated with close resemblance to the data found in literature and in field observations. All behaviours were considered good enough for the applications that they were created for.

In the following, we will present models for waiting behaviours that are to be used in a variety of situations such as train platforms, in front of arrival halls below information boards. We then proceed by presenting servers (devices that provide a functionality to pedestrians such as turnstile machines) and associated queue behaviours, and finish with walking in stairs and escalators.

3.3.1 Waiting behaviour

The Nomad model presents several possibilities to simulate pedestrians performing activities (see appendix A). These include a wide range of waiting behaviours. The basic distinction between waiting and other activities is the reactiveness that pedestrians present to their surroundings. Pedestrians may not react to the presence of other pedestrians when standing in front of a metro ticket machine. This is mostly observed in activities that require higher concentration. However, when waiting on a train platform or in a public space pedestrians display an awareness of the current pedestrian traffic and may give way to walking pedestrians in crowded situations.

Waiting behaviours are also dependent of subjective preferences of individuals. Individuals may display a general non-reactive behaviour even when waiting but we simplify and consider that waiting behaviours are dependent on the type of activities and waiting pedestrians are reactive.

H12: Waiting Pedestrians display awareness and react to the surrounding traffic.

In Nomad the waiting behaviour is modelled by an adapted version of equation (3.9). The interaction with pedestrians and obstacles ($\vec{a}_r$ and $\vec{a}_o$), and the physical acceleration ($\vec{a}_p$) are not modified. However, the path following behaviour is modified for the different walking situations that make up the Nomad waiting behaviour. Figure 3.11 shows a pedestrian entering an area where many pedestrians are waiting. In Nomad we distinguish three situations:

1. Walking outside the waiting area (*normal walking* described by equation (3.9)).
2. Waiting in the waiting location.
3. Walking inside the busy waiting area.

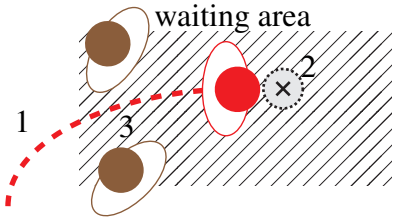

Figure 3.11: The trajectory of a pedestrian towards the waiting location inside the waiting area illustrating three possible situations.

Pedestrians choose a position to wait according to subjective reasons such as proximity to train doors, closeness to shopping windows. In this version Nomad has a random location assignment inside waiting areas.

The assigned waiting location is randomly determined within a location grid that is created over the waiting area. The cell size is a parameter that determines the minimal waiting distances (default value is $0.5m$). When pedestrians reach the waiting area they get the coordinates of the centre of a free cell anywhere in the grid.

The pedestrian will stay in a circle around the assigned location (region 2 in figure 3.11). The location radius is dependent on the pedestrian radius ($d = rad/2 \approx 0.1m$). Inside the circle, pedestrians stop applying the path following acceleration ($\vec{a}_f = 0$) and move only according to the remaining behaviours (such as in equation (3.9)). Thus, making way for the pedestrians still walking.

When waiting:
H13: pedestrians prefer to stay around a chosen location in the waiting area,
H14: and only move in reaction to pedestrians walking in close distances.

Very often the waiting area is shared with many pedestrians and the navigation inside the area is severely hindered. Crowded platforms are often heterogeneously occupied presenting some areas of high density regions (region 3 in figure 3.11).

Walking inside crowded areas requires different behaviours than walking in normal traffic. If pedestrians would walk *normally*, there would be a probability that they would not penetrate the crowded area. Therefore, pedestrians walking in and around high density areas are forceful. They walk much closer to standing pedestrians as they would do in normal situations. Furthermore, they 'brush' waiting pedestrians more often than they would in normal conditions. In Nomad this behaviour is achieved by temporarily setting a very small value of $\tau \approx 0.1$ in $\vec{a}_f$ (equation (3.11)) for pedestrians walking towards their waiting locations.

H15: When walking inside waiting areas pedestrians walk more forcefully than in normal conditions and accept smaller distances to waiting pedestrians.

3.3.2 Servers and queues

Nomad has servers and choice areas that can be used to simulate a group of turnstiles, ticket counters or sport stadium entrances. Servers implement a situation in which pedestrians stop during the service time and then move on towards the next destination. When 'being served', pedestrians are not implementing the waiting behaviours described previously. They simply stop and do not interact with nearby pedestrians. This represents situations that require the full attention of pedestrians.

If servers are used to simulate a group of turnstiles, after the service time finishes, pedestrians move through the turnstile. A line of turnstiles divide the walking zone into two separated zones each on one side of the servers.

What distinguishes them from activity areas is the possibility to form queues for those waiting to be served. In front of a group of servers always a choice area is modelled. Inside this area pedestrians start to choose a server and may eventually stand in queues (figure 3.12).

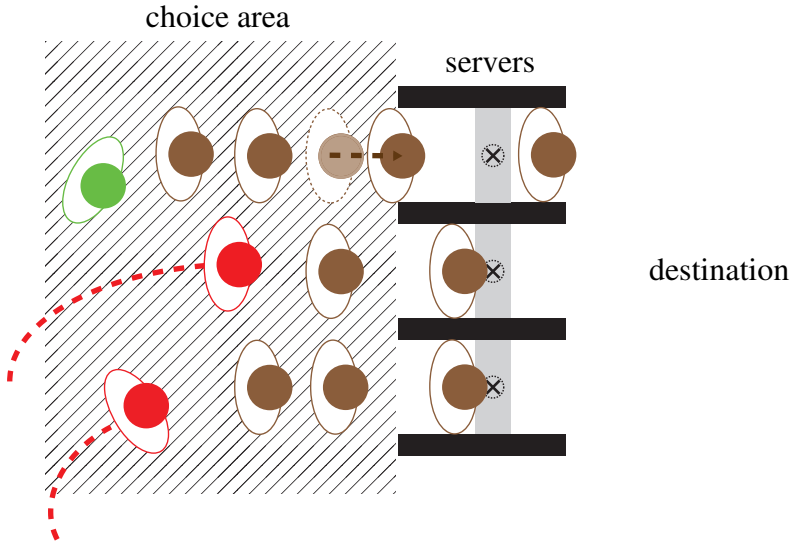

Figure 3.12: Choice areas (striped area) and servers (turnstiles). Brown pedestrians are in queues or being served. Red pedestrians are still reaching their chosen queues. The green pedestrian is changing queue after predicting a smaller queuing time.

Server choice behaviour

The choice of servers is performed by calculating the perceived time needed to reach the server and to be served. The total perceived time is named t_{total}. Pedestrians will choose the server that offers the lowest t_{total} at that moment. If no other pedestrian is inside the choice area nor in any server t_{total} is the time to reach the closest server from the current position plus the expected service time $t_{walking} + t_{service}$. Here we are

assuming that the average service time is the same for all servers. However, in Nomad this is not mandatory and pedestrians identify the different service times.

If the choice area is occupied with other pedestrians in queues or walking towards, the expected service time is added with the expected queuing time t_{queue} and the service time of the pedestrian currently in the server in front of the chosen queue t_{server}. The t_{total} is determined by:

$$t_{total} = t_{queue} + t_{walking} + t_{server} + t_{service} + \varepsilon \tag{3.22}$$

where:
t_{queue} is the estimated time spent in the queue.
$t_{walking}$ is the walking time to reach the estimated end of the queue.
t_{server} is the current service time if the server is occupied.
$t_{service}$ is the expected service time for the reference pedestrian.
ε is a stochastic noise accounting for t_{total} assessment and modelling errors.

H16: Pedestrians minimise the time needed to reach servers.

Reconsidering the choice

Pedestrians regularly reconsider their choice of queue based on the prevailing queuing conditions. In Nomad the choice interval is a parameter and the default value is 5 seconds. Their choice always follows the same model presented in equation (3.22).

H17: While waiting in queues pedestrians reconsider their queue choice.

3.3.3 Escalators and stairs

Escalators and stairs have the function to connect levels. Both are automatically incorporated during the route map calculations only requiring the user to specify which levels they are connecting. Stairs are bidirectional, while escalators are unidirectional and the direction (*up* or *down*) must be specified. [2]

Very often stairs and escalators are installed side-by-side and pedestrians have to choose. According to field observations and literature, escalators are more attractive than stairs (Daamen et al. (2005a), Zeiler et al. (2011)).

When calculating the routes Nomad assigns higher walking costs for stairs. This creates a bias towards escalators in the route choice map similar to the routes towards destinations shown in the walking map presented in figure 3.2. Figure 3.13 shows in grey the cost map pointing towards the escalator.

[2] Bidirectional escalators are getting more popular, particularly in the Netherlands. In the future they will be available in Nomad as well.

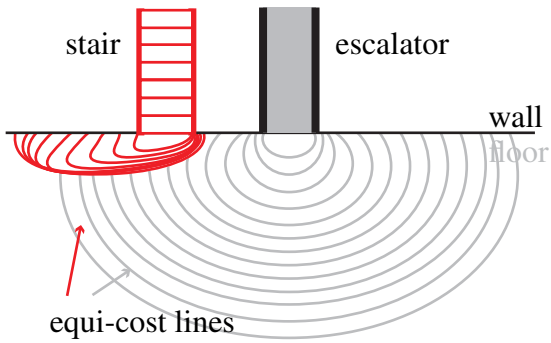

Figure 3.13: Scheme of a walking area that ends with a stair and a escalator. The floor Route map with equi-cost lines (section 3.1) for a stair and a escalator. The red lines represent the area where pedestrians will choose the stairs.

Figure 3.13 shows that the stair is also an exit option but only for pedestrians located close to its entrance. The red lines represent the area with lower walking costs for stairs. This area is not set directly but is the consequence of the route choice cost maps.

The size of the area that determines the preference for stairs depends of two factors: the relation between the stair and escalator walking costs $L_{stair}/L_{escalator}$ and the length of the stairs (and escalators). The stair preference area decreases when L_{stair} and the length of the stair increases.

In Nomad the use of stairs is dependent on the level of congestion in front of the escalator. The more pedestrians are waiting in front of the escalators the larger is the probability that pedestrians will reach inside the red dotted area in front of the stair. This behaviour is in agreement with field observations for commuters in metro stations.

H18:	*When changing levels pedestrians prefer escalators over stairs.*
H19	*For side-by-side layouts, the amount of pedestrians taking the stairs increases with the increase of congestion in front of the escalator.*

Stairs can propagate the tail of the congested queue upstream but escalators not. Like real escalators, pedestrians will always be poured to the next level. If many pedestrians are standing nearby the exit of escalators, they risk causing collisions.

Stairs

Nomad only implements straight stairs with handrails. Spiral stairs can be introduced by creating several straight stairs with horizontal landings.

Some factors influence the speed of pedestrians in stairs, its construction, the amount of steps (length of the stair), the size of risers. However, these are not taken into consideration in Nomad and the same average walking speed is used for all stairs.

We are assuming that the simulated stairs are designed according to standard comfort levels.

According to Fruin (1971) pedestrians on stairs have smaller vision cones and less manoeuvrability than when walking level. Therefore, free-speeds and the walker model in the equation (3.9) are adjusted both for the upward and the downward directions. Table 3.1 shows the staircase free-speeds from Weidmann (1993):

Table 3.1: Mean walking speeds in stairs taken from Weidmann (1993)

	horizontal speed (m/s)	vertical speed (m/s)
upward	0.61	0.31
downward	0.69	0.35

The speeds shown in table 3.1 are used as average speeds in stairs and the actual speeds in stairs will be proportional to v_0. Fast pedestrians ($v_{0fast} > v_0$) will climb or descend faster than the speeds in table 3.1 and the opposite happens with slow pedestrians.

The behaviours are temporarily modified according to the following hypothesis:

H20: To avoid tripping in stairs:
- *(a) pedestrians have less attention for other pedestrians,*
- *(b) apply less manoeuvres and*
- *(c) do not walk backwards.*

In Nomad this is achieved by restricting the size of the influence area ($ie_f = 1.0m$ and $ie_b = 0.3m$) and making pedestrians less prone to deviate from the path following the stair. For stairs the path following parameter τ is severely reduced to 0.1 m/s. (These values were validated for capacity).

When walking on stairs pedestrians only ascend or descend. If their interaction with close-by pedestrians is very intense they do not move and congestion develops downstream. The Nomad stair behaviour restricts the walking direction to the forward and lateral directions. This results in a behaviour similar to queues but with a (reduced) overtaking behaviour.

Escalators

Escalators are designed with space for one or two pedestrians per tread. Equation (3.23) shows that the maximum theoretical flow of $2.5 peds/s$ could be achieved if all spaces would be taken by standing passengers (Kauffmann (2011)).

$$\text{theoretical capacity} = \text{(belt speed)(tread depth)(pedestrians per tread)} \quad (3.23)$$

$$2.5 \text{ pedestrians}/s = (0.5m/s)(1 \text{ tread}/0.4m)(2 \text{ pedestrians}/\text{tread}) \quad (3.24)$$

It is generally accepted that the maximum theoretical capacity of full occupancy of threads is never achieved. Fruin (1971) notes that escalators present empty spots to allow larger personal space decreasing the maximum theoretical capacity sometimes to 50%. To calibrate the capacity Nomad has a parameter that controls the probability that pedestrians enter the escalator.

In real situations some pedestrians in wide escalators go to the left lane and overtake standing pedestrians. This increases the capacity of escalators (Davis and Dutta (2002)). However, in Nomad this feature is not implemented yet. Nomad escalators behave as queues and pedestrians stay on the same treads and are simply moved.

3.4 Nomad implementation

The Nomad simulation software is developed as a research tool to investigate pedestrian behaviours. Given the incremental development of the model it was structured to be friendly to extensions and modifications by presenting a modular architecture and a Object-Oriented (OO) programming paradigm.

The OO programming is a development of earlier programming paradigms that provide tools to describe the elements of the system and how they relate to each other. The units of the program are a direct abstraction of the real problem and are defined as classes. The realisation of the classes are the Objects.

In Nomad we have a *Pedestrian* class that contains the characteristics of the simulated pedestrians: how they behave, what they know, how they interact with other classes such as Obstacles. Each pedestrian that enters the simulation is a different instance that implement the methods of the *Pedestrian* class.

These requirements gave a strong motivation to choose Java (Oracle (2014)) due to its well structured OO programming language that makes it friendly to non-professional programmers. Furthermore, there are several tools and libraries that help the development of complex and large systems. The portability of Java was also a factor for its choice.[3]

The Nomad simulation can be distributed in different versions that differ by the different capabilities. For example, the basic version that is freely distributed [4] is restricted

[3] In general Java programs are simpler and friendlier to implement but are slower than C++ programs. However, the difference is steadily diminishing and for intensive floating point calculations such as in the Nomad simulation the loss is acceptable. Furthermore, to develop the full performance C++ programs requires a level of programming skills that are beyond that of the average programmers (Hundt (2011)).

[4] www.pedestrians.tudelft.nl

to a single level and has no scripting language capabilities for complex batch manipulations of simulations. Appendix B presents a list of features of the Nomad simulation. Some of the Nomad simulation features are presented in this section and more details can be found in the Nomad simulation user manual (Campanella (2011)).

3.4.1 Overview of the system architecture

The most important Nomad classes are *Pedestrian*, *Activity* and *Infrastructure*. Pedestrians are from the commuter type that will follow the optimal path towards their destinations and activity areas. *Activity* is the super class of the activity classes that implements the behaviour that pedestrians display when performing them. The *Infrastructure* class is a super class that implements all the elements that make up the simulation area.

The simulation area is structured in *Levels* that are 2D representations of a walking area. They are formed by groups of *Obstacles* and *Walkables* that are surfaces that allow pedestrians to walk on. *Levels* are connected by *Staircases* and *Escalators*. Pedestrians always enter the simulation via an *Origin* and exit via a *Destination* that are not necessarily on the same level. Activity areas are from class *Destination*.

The organisation of the classes is top down using the concept of inheritance (inheriting methods from super-classes) and interfaces (obligatory methods for interfaced classes).

Several tasks are necessary in the simulation: creating the demands, moving the pedestrians, performing the activities and updating the infrastructures. Each of these tasks are executed by special classes called *Managers*. They contain instructions to the classes that actually realise the tasks. This logical division of the tasks is part of the modular modelling strategy that helps the development and extension of Nomad.

The simulation step is conducted by the *NomadModel* Class that execute serially all 5 managers. One simulation step is the sequence of steps of the managers as presented in flow diagram shown in figure 3.14.

Pedestrian class

The *NomadAgent* is the super-class for all agent types that are implemented. The *Pedestrian* class implements pedestrians with the ability to walk and to perform activities and is a sub-class of the *NomadAgent*. Pedestrians in wheel chairs or blind pedestrians could have a special class to represent them.

Another important class for pedestrians is the *PedestrianType*. The *PedestrianType* is the class that contains parameter distributions for pedestrian characteristics, of which a single value is drawn for an individual *Pedestrian*. The simulation input contains the description of the several *PedestrianType*'s creating different age groups and/or gender

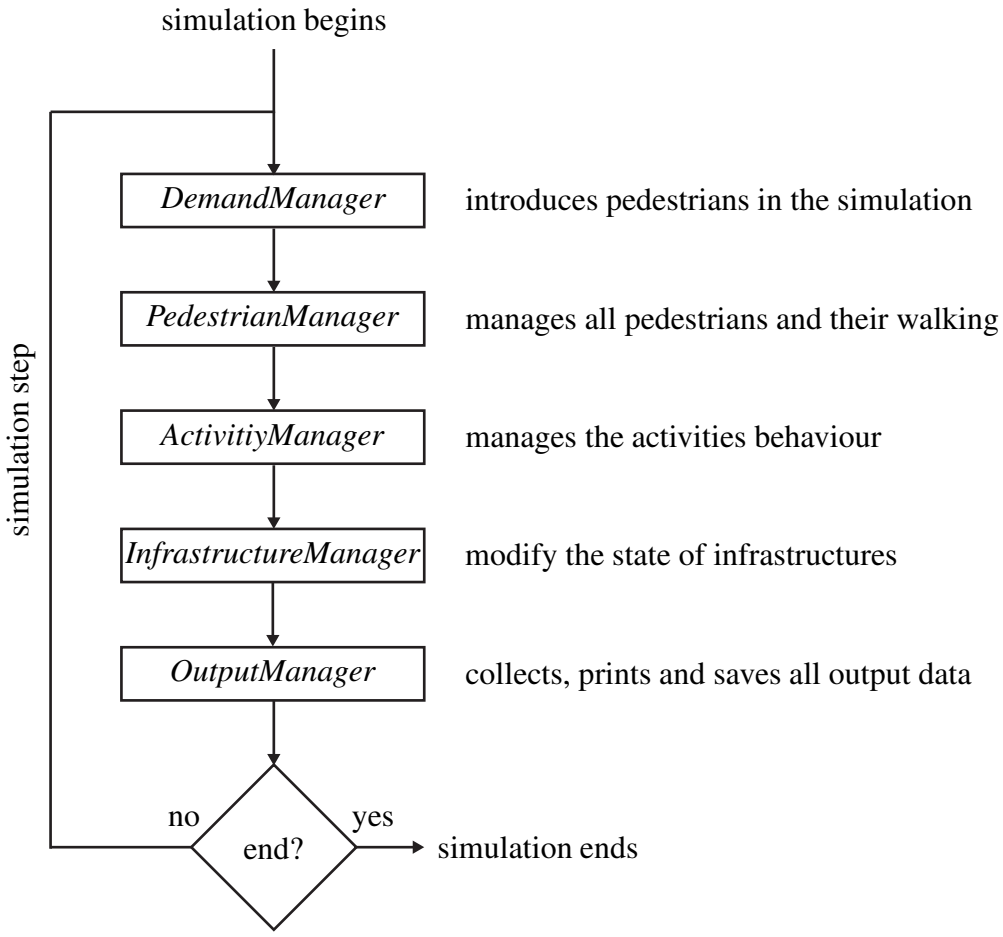

Figure 3.14: The representation of one simulation step conducted by the *NomadModel* class.

groups. This gives the user the possibility to have total control of the demographics in the simulation.

The *PedestrianType* is a list of random variables normally distributed with μ and σ set by the user in the input. Each parameter distribution with $\sigma \neq 0$ generates different parameter values creating heterogeneity.

Figure 3.15 shows the UML class diagram for the *Pedestrian* class and its relation with the *NomadAgent* and the *PedestrianType* classes.

Infrastructure class

All infrastructures are sub-classes of the *NomadInfrastructure* that defines the basic fields for all infrastructures such as the 'visible' that sets the rendering in the simulation window (flag that indicates if the object is visible or not). Figure 3.16 shows the UML diagram for the Nomad infrastructures.

Two different classes are directly sub-classed from the *NomadInfrastructure*: the *InfrastructureCollection* that is used for complex objects constituted of moving parts such

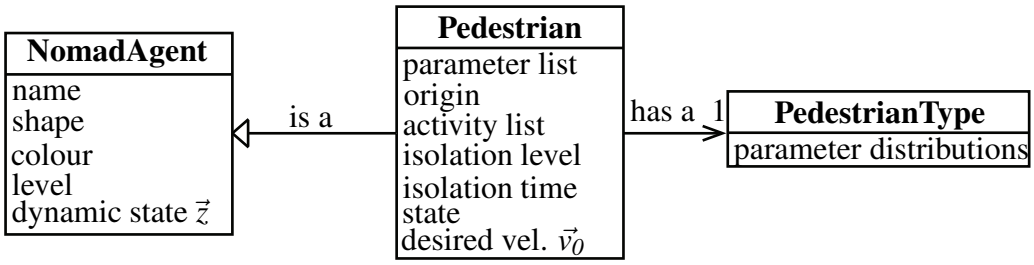

Figure 3.15: The UML class diagram of the pedestrian class with the most important fields.

as the *RevolvingDoor* class and the *InfrastructureObject* that is the base-class for all other infrastructures.

There are several infrastructure types such as origins, destinations, turnstiles, servers and levels.

An *Origin* is a line that generates pedestrians. A *Origin* will only place a new pedestrian in the simulation, if the pedestrian has enough space over the line. Otherwise, the pedestrians are put in a FIFO (First-In First-Out) list and will be introduced in the next simulation step.

Obstacle is the super-class for any form of infrastructure that blocks walking. They are considered solid objects that block the interaction between pedestrians on both sides of obstacles. Pedestrians only 'see' each other if there is an unimpeded line between their centres.

Destination are the locations where pedestrians can perform activities. In the Nomad simulation, exiting the simulation is an activity. The parameters that affect the destination choice as described by equation (3.2) in section 3.1 are set in the destinations. The behaviour of pedestrians while performing the activities is determined by the type of activity chosen (see section 3.4.1).

Level is the super class of the surfaces that create the simulation walking area. The walking area is constituted by at least one *Horizontal* level. One *Inclined* level will always connect two horizontal levels. There is no limit for the amount of horizontal and inclined levels in one simulation. In the Nomad simulation we have implemented *Stairs* and *Escalator* as inclined levels.

In Nomad the walking behaviour is implemented in special infrastructure called *Walkable*. The most common level is the horizontal that contains a *WalkableLevelHorizontal* that implements the 'normal' walking behaviour represented by the equation (3.9). Similarly each other type of level will have its own walkable and associated walking behaviour such as *WalkableLevelEscalator*.

Pedestrians can only walk in one level at a time. However, other walkables can be implemented in a level. *Turnstile* is a sub-class of the *NomadServerChoiceWalkable* that is a walkable that implements a server choice behaviour (section 3.3.2). Turnstiles

own one or more *Server* that is a walkable with the special server behaviour. Turnstiles and servers are not shown in figure 3.16. The simulation will always know which walking behaviour to use because they are always connected to the current activity that the pedestrians is performing.

Activity class

The *NomadActivity* is the super class of all activities implemented in the Nomad simulation. It implements the *Activity* interface requiring that all activities must have the essential functions such as those that implement the waiting behaviour. All activities in Nomad can be input with more than one activity area (destination). The service time of the activities are set in the destinations allowing for the activity area choice to be influenced by all parameters as described by the equation (3.2) in section 3.1.

Figure 3.17 shows the fields of the NomadActivity including the choiceType and destinations list.

The waiting activity described in section 3.3.1 corresponds to the *RandomWaiting* and is very useful for wide locations such as train platforms where pedestrians are dispersed.

Another waiting activity is the *CentroidWaiting* that fixes a single waiting location for all pedestrians, usually the centroid of the waiting area. Pedestrians will then stand around the centroid until their waiting time has passed following the same behaviours described in section 3.3.1. It is useful for areas under information boards that usually offer preferred locations.

Nomad also has the *Simple* activity that does not apply the walking behaviours described in section 3.3.1. When reaching the *Simple* activity area, pedestrians simply stop and do not interact with any pedestrian. It is mostly used to remove pedestrians from the simulation. If the activity is the last of the activities list then Nomad exits the pedestrian. Usually for exiting, the activity time is set to $0s$.

3.4.2 Numerical methods

Numerical instabilities cause erratic behaviours due to overreactions of pedestrian interactions. If the time-step is too large pedestrians will not walk smoothly and will bounce frequently. This problem is aggravated in dense situations when the probability of collisions between pedestrians is very high. A simple but costly remedy in terms of computational time is to use very small time-steps, usually in the order of fractions of seconds. However, when simulating complex pedestrian facilities and large flows usually only part of the pedestrians are subjected to high densities. Furthermore, these high densities may occur only during short time periods. Therefore, imposing very small time-steps to all pedestrians all the time creates an unnecessary performance penalty.

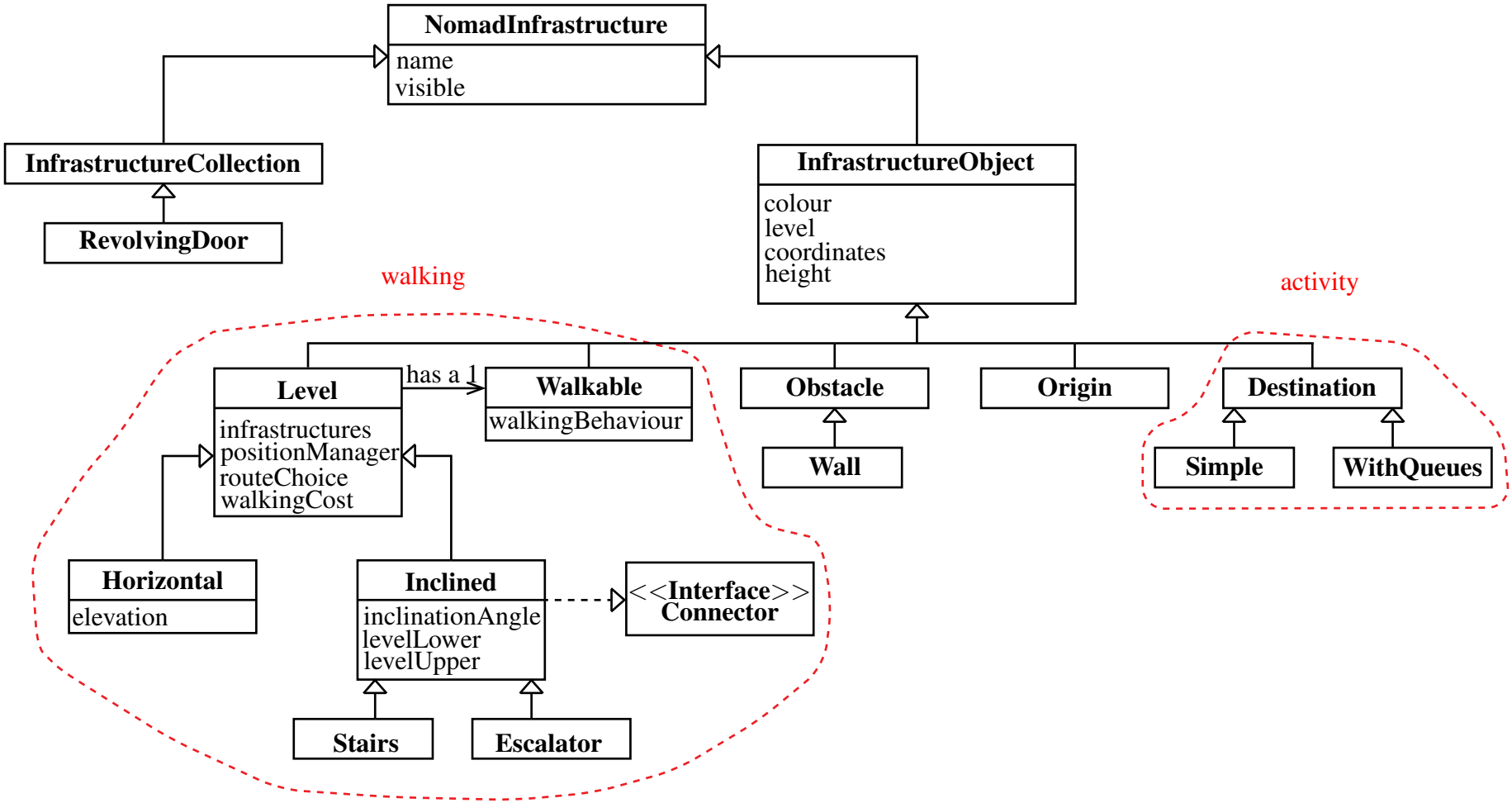

Figure 3.16: The UML class diagram of the infrastructure classes with their most important fields.

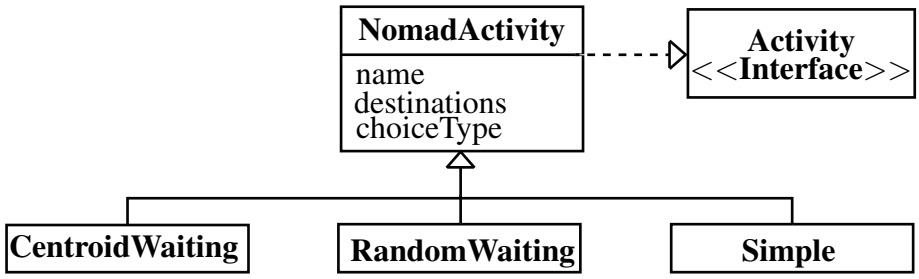

Figure 3.17: The UML class diagram of the activity class with the most important fields.

To mitigate this performance penalty the Nomad simulation introduces a different time-step for each pedestrian. The size of the time-step depends on the level of isolation of the pedestrians. The level of isolation is determined by the (current) distance to the nearest pedestrian or obstacle, effectively introducing a variable time-step for each pedestrian in the simulation.

The numerical methods also includes a smart management of the search of the surroundings of each pedestrian. Every pedestrian will only search the surroundings for pedestrians and obstacles if he or she was close to any in the previous time-step (low level of isolation). Pedestrians isolated from other pedestrians and from obstacles do not need to search their surroundings.

The following sections give an overview of the variable time-step and the smart management. Further details are found in Campanella et al. (2007b) and Campanella et al. (2009b).

3.4.3 Variable time-steps

In the Nomad simulation there is one update of the complete traffic state at each simulation step. Each simulation step corresponds to the passing of one time-step (ΔT_{sim}). However, some pedestrians have their state updated more than once during the simulation step effectively being subjected to smaller time-steps. As mentioned in the previous subsection, the time-steps are dependent of their level of spatial isolation from other pedestrians and obstacles. The Nomad simulation uses three levels of spatial isolation: *isolated*, *in-range* and *in-collision* (figure 3.18).

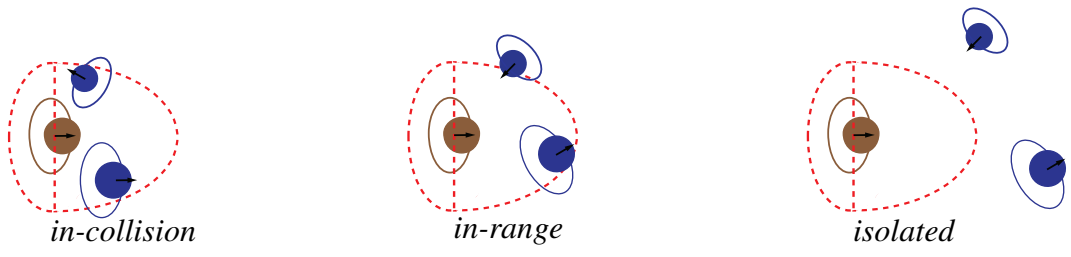

Figure 3.18: The three isolation levels that determine the variable time-steps.

Isolated pedestrians have no pedestrians or obstacles with the possibility to enter their influence area in the next time step. Without interactions pedestrians tend to follow the desired velocity (section 3.2.3). This is true in straight paths such as those found in corridors. Curves introduce deviations from the desired velocity. These deviations increase with larger values of the parameter τ and larger time-steps. For most applications the behaviour of isolated pedestrians is not important for the determination of bottlenecks and areas with high densities. Therefore, their accelerations can be calculated using larger time-steps.

The Nomad simulation applies the simulation time-step (that is the largest possible) to calculate the next position of *isolated* pedestrians ($\Delta T_i = \Delta T_{sim}$ in equation (3.11)).

Pedestrians *in-range* have other pedestrians (or obstacles) inside or close to their influence area requiring the application of interaction accelerations. However, pedestrians *in-range* have no possibility of colliding in the next time-step. Therefore, the acceleration model described by equation (3.9) can be simplified eliminating the physical acceleration (section 3.2.11).

The determination of the positions of pedestrians interacting requires a small time-step to minimise the numerical errors. After some tests we set the *in-range* time-step to be $\Delta T_r = 0.2\Delta T_{sim}$.

The remaining pedestrians are very close to others or to obstacles and need a very small time-step to account to the large numerical instabilities that arise in collisions. The Nomad simulation applies an even smaller time-step to *in-collision* pedestrians $\Delta T_c = 0.1\Delta T_{sim}$.

The Nomad simulation calibration and validation presented in the chapters 7 and 8 use the isolation fractions presented in this section with $\Delta T_{sim} = 0.1s$.

Determining the isolation levels

To determine the isolation level the Nomad simulation does not consider the current speed and direction of pedestrians. To prevent an incorrect classification due to a sudden change of the velocity the Nomad simulation considers the worst case scenario: pedestrians are walking at their maximum speed and on a collision path. Figure 3.19 shows how a pedestrian (p) is far enough of its nearest neighbour that even in a collision path at full speed his influence area cannot be reached during the next time-step. Pedestrian p is therefore *isolated*. A similar algorithm determines whether the pedestrians are *in-range* and the remaining ones are *in-collision*. For interactions between pedestrians and obstacles the Nomad simulation considers the closest point to the obstacle.

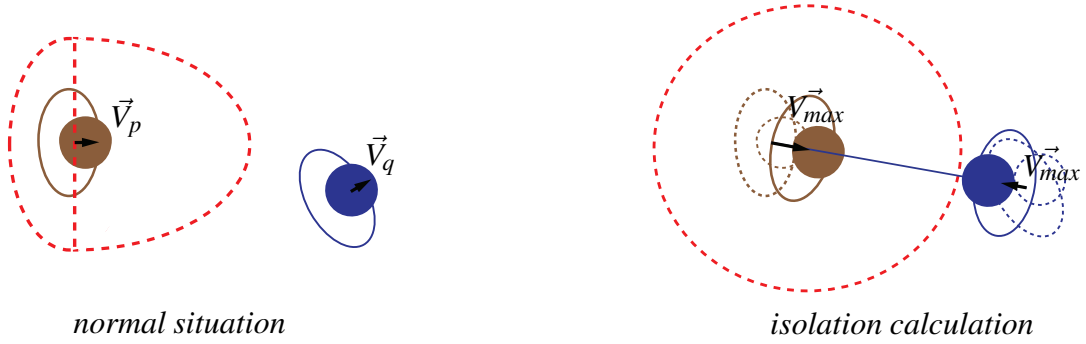

Figure 3.19: The left figure shows the real dynamics of the *isolated* pedestrian *p*. The right figure shows both pedestrians walking at maximum speed towards each other and a circular isolation area to determine the isolation level.

3.4.4 Smart pedestrian management

All pedestrians need to search their vicinities for pedestrians and obstacles and this is a large source of computational cost. Nomad uses the isolation levels of the variable time-step to reduce the the amount of spatial search of pedestrians.

Large simulation areas create situations in which pedestrians walk during long periods without coming close to other pedestrians or obstacles. The Nomad simulation takes advantage of these situations by letting very isolated pedestrians walk 'blindly', i.e. without searching for nearby pedestrians and obstacles. These pedestrians walk without perception for a limited period of time. This so called 'time-in-isolation' is the time that the nearest pedestrian would take to reach the influence area in the worse case scenario mentioned in the previous subsection.

When a pedestrian enters the simulation, Nomad determines the time-in-isolation. After the time expires, the isolation level and the new time-in-isolation is determined. This is repeated for each pedestrian in isolation. Pedestrians walking in the other isolation levels search their surroundings at each time step.

When new pedestrians are introduced in the simulation Nomad recalculates the isolation level and time-in-isolation for all pedestrians in the areas surrounding the origin. Campanella et al. (2007b) and Campanella et al. (2007a) show the details for the calculation of these times.

The Nomad simulation differentiates between pedestrian and obstacle isolation. It always uses the smallest time-step determined, but it will perform the assessment separately of pedestrians and obstacles allowing for further improvement of the computational efficiency.

In our tests with large simulation areas we observed that the variable time-step algorithm combined with the smart management proposed was four times computationally more efficient. The performance loss due to the extra tests to determine the isolation levels were negligible for small simulations.

3.4.5 State update strategies

Pedestrian states including the dynamic state (position and velocity), are updated sequentially during the simulation time-step. This is an alternative to the most common parallel update that changes the state all pedestrians simultaneously at the end of the simulation step based in the traffic state before the time step. The investigations in Campanella et al. (2009b) showed that the sequential update is more accurate for larger time-steps and only marginally less accurate for small time steps.

The sequential update is combined with the variable time steps. Therefore, at each intermediate time-step some pedestrians may have their state updated and others not depending in which level of isolation they are. The order of the sequential time step is fixed and according to the appearance of the pedestrians in the simulation.

3.5 Conclusions

In this chapter we have shown the relation between the components of Nomad and empirical behaviour. This direct connection between modelling and reality simplifies the understanding of the model and allows for improvements and extensions.

The acceleration equation (3.9) that was implemented and used in several simulations contains innovations that could benefit many types of walker model. Most notably the development of anticipation in section 3.2.6 introduces the direction of the velocity in the interaction component. This has the logical consequence of distinguishing between frontal and backward interactions bringing the model closer to real interactions. The acceleration model can now be used to investigate the accuracy of pedestrian models in the chapters 4, 6 and 7.

Section 3.4 detailing the implementation of the model serves as a basic conceptual outline of the structure and features of pedestrian models. The list of performance optimisations is extensible to similar models such as social force models. The improvements of computational performance outweighs the accuracy loss for pedestrians walking isolated since these are not determinant for crowded situations that are usually of interest in simulations. This algorithm (together with the optimised pedestrian management) can be adapted to other type of models and especially traffic driver models.

The introduction of the special behaviours greatly expanded the possibilities of the Nomad simulations. The waiting behaviour is divided in three situations that reproduce realistic behaviour that can be adopted by any type of pedestrian model. Chapter 8 will show the importance of the new behaviours and the benefits of the implementation features.

Chapter 4

Novel methodologies for calibration and validation of walker models

In the state-of-the-art we discussed that pedestrian traffic is usually very complex, presenting many situations such as unidirectional, bidirectional and crossing flows. On local levels, densities can go up to 10 peds/m^2 (Helbing et al. (2007)).

It is not desired to have parameter sets that are accurate only in specific situations such as those occurring in unidirectional flows. Such 'specialised' parameter sets have limited use in simulations of large pedestrian facilities that present several different situations such as bidirectional corridors and crossing flows. A parameter set suited for general use needs to perform well (be accurate) in different situations.

These requirements made us hypothesised that the most useful walker models are accurate and generic: walker models should be able to reproduce a large amount of different situations with a high level of accuracy. This chapter proposes a new formalisation of the calibration and validation processes of walker models. The novelty is the focus on obtaining parameters for general use.

The process of determining the accuracy of a model and its parameter set is called *validation*. Before the validation, the model parameters must be known and the systematic process of parameter estimation is called *calibration* (Kleijnen (1995)).

There are different types of validation. In this dissertation we use the most common approach of dividing the validation into three steps: a model is *verified*, *face validated* and *predictively validated*.

- Verification indicates to which extent the model does what the developer expects it to do. Galea (1998) details that this initial step aims at testing the simulation components and their functional behaviour.
- Face validation is a qualitative assessment of the model. If face valid, the model has the capacity to reproduce the behaviour of the system in the required detail

(Van Lint (2009)). For example, a walker model should not present pedestrians walking on top of each other or predict that pedestrian speeds are not affected by the density.

- Predictive validation is the quantitative assessment that ensures that the results of the model can be used for the prediction of performance indicators (Klügl (2008)). A model should only be used if it has been predictive validated.

These definitions are consistent with those used in transportation and in the pedestrian dynamics community (Hoogendoorn (2007), Van Lint (2009), Galea (1998), Klügl (2008), Klüpfel (2009) and Schadschneider and Seyfried (2009b)). The first verification step and the face validation deals with the implementation of the simulation model and is not the subject of this chapter.

Optimal parameters are calibrated for certain performance indicators of the traffic system. These can be the positions of the individual pedestrians, fundamental diagram relations or distributions of travel times. However, once the parameters are estimated there is no guarantee that the walker model is reproducing other aspects on an acceptable level (specialisation of the parameter set). The same applies for different flow configurations: parameters estimated with data from unidirectional flows may not perform well in other flow configurations (e.g. bidirectional or crossing flows).

The basic hypothesis of this chapter is that the simultaneous use of several indicators of pedestrian traffic for the calibration reduces the level of specialisation of the parameter set. Parameter sets calibrated with several indicators will likely perform better in many situations than specialised parameter sets. This hypothesis is confirmed in chapter 7.

No systematic calibration or validation guidelines incorporating the diversity of pedestrian behaviours was found in the literature. The Rimea project[1] proposes a set of guidelines for the application of microscopic models in evacuation analysis that is focused on ships (Rimea (2009)). Unfortunately, it only proposes few face validation tests in some simple evacuation scenarios. According to the manual, predictive validation tests are not proposed due to insufficient availability of empirical data.

In this chapter we identify and discuss all components of calibration (section 4.1) and validation (section 4.2) processes proposing novel methodologies. The key components for both methodologies are the so called *scenarios* and the *multi-objective* functions. Scenarios contain all data and methods to run simulations and compare their outcomes with reference data. Multi-objective functions combine the outcomes of scenarios producing a single measure of accuracy of models (Section 4.3). In the remaining, we will refer to multi-scenarios in contrast to single-scenario.

Another important aspect of the calibration methodology are the significance tests that show the sensitivity of the model for the calibrated parameters (section 4.4). Without

[1] (http://www.rimea.de)

those tests, it is not possible to know if a parameter has any influence in the outcomes of the model or if the data used on the calibration was appropriate.

Section 4.5 finishes the chapter with a summary and a discussion on the benefits of using multi-scenarios to improve the significance and accuracy of the calibrations.

4.1 A generalised calibration methodology

For the calibration methodology we use the knowledge on the walking behaviour to obtain parameters of general use. The methodology favours (but is not restricted to) the simultaneous use of several aspects of walking behaviours by the choice of smart performance indicators applied on different walking situations in what we call *multi-scenario* calibration.

Figure 4.1 shows the scheme of the methodology for the calibration of the parameter set θ. The calibration consists of two parts: the clockwise loop describing the iterative process for estimating the optimal parameter set and the sensitivity analysis to calculate the significance of each estimated parameter.

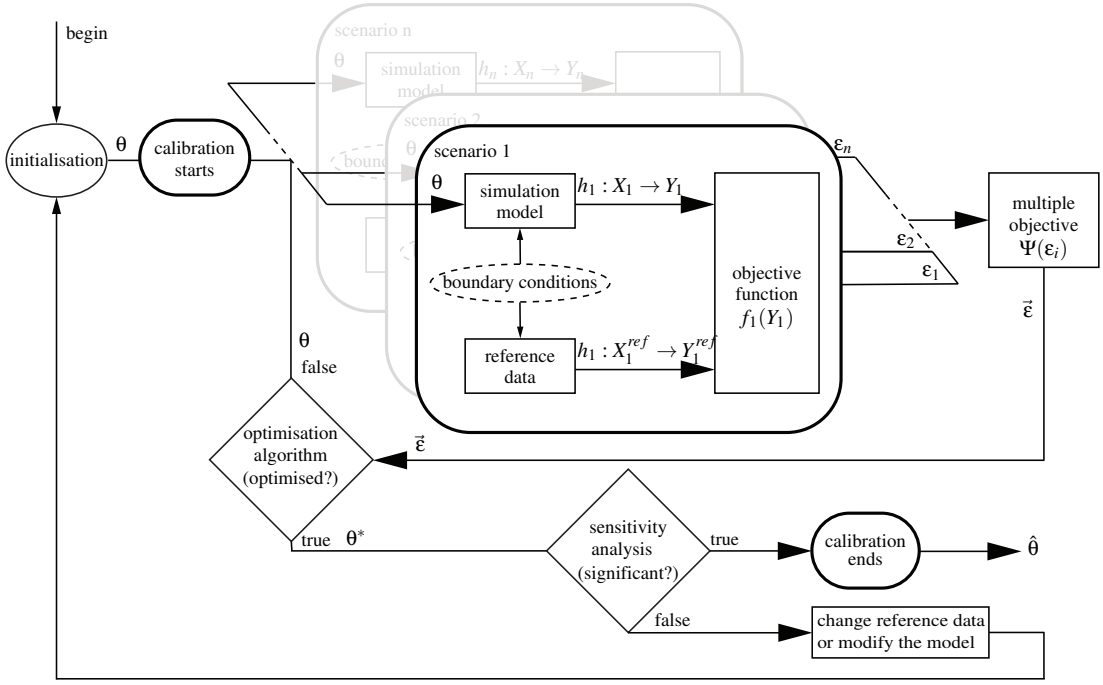

Figure 4.1: Calibration methodology for walker models. It is a loop initiating in the upper left corner and ending after the optimal parameter set θ^* is shown to be statistically significant for the outcomes of the model, therefore considered estimated ($\hat{\theta}$) ending the calibration.

The most important component of the methodology is the *scenario* that incorporate everything that is necessary to simulate pedestrians: boundary conditions such as demands, description of the walking facility and population demographics; and

everything necessary to calculate the deviations of the model from the reference system (reference data, indicators and objective functions).

Scenario 1 in figure 4.1 shows how parameter set θ is input to the simulation model (top left) to generate trajectories X_i according to the boundary conditions determined by the walking situation to this scenario. The trajectories are mapped by a function h_i to calculate the traffic indicator Y_i that will be input in the objective-function $f(Y_i)$ generating the performance measure ε_i that compares the predicted and reference data (right side of the calculation step). The other scenarios have their own reference data and other indicators and may represent different walking situations.

The methodology does not require trajectory data, e.g. capacity values, velocity distributions can also be used as reference data. However, having trajectories allows for a wider choice of performance indicators in the objective functions. To simplify the description of the methodology we consider the reference data in the form of trajectories.

Performance measures can be errors (differences) between simulated and reference data, log-likelihoods of indicators estimating optimal values. In a more general form the performance indicators can be ordinal variables that results in a ranking. We will discuss these performance measures in section 4.3. In the remainder of this chapter we will mostly mention the *error* as a general performance measure to simplify the text.

An example of an indicator is the position r of pedestrians resulting directly from the trajectories. The performance measure ε_i can be calculated by the mean of absolute position errors of all time instances k in the complete pedestrian trajectory:

$$\varepsilon = \frac{1}{n}\sum_{k=1}^{n}\left|r(t_k) - r^{ref}(t_k)\right| \tag{4.1}$$

There is no assumption on the form of h (only that it is a computable function). Fundamental diagram relations, distributions of headways and travel times are examples of functional mapping in the form indicated by (4.2). The variable s represents other parameters necessary to calculate the diagrams such as space and time discretisation for fundamental diagrams (Edie (1963)).

$$h : Y(s) = h(X) \tag{4.2}$$

A calibration with more than one scenario will combine errors from the objective-functions in a single error by a multi-objective function. The resulting error is submitted to an optimisation process that compares the current error with errors from previous iterations and calculates if a stopping condition is met. If not, a new set of parameters is generated and a new iteration is performed. If a minimum error is found the parameters are considered optimal:

$$\theta^* = \arg\min \varepsilon(\theta) \tag{4.3}$$

If the optimality condition is not met, a condition based on the maximum amount of iterations forces the end of the optimisation with a non-optimal parameter. This can indicate that there is no distinguished optimal value (highly non-linear result space), problems with the reference data (see the following discussion on poorness of data), problems with the model or a non-appropriate optimisation algorithm. In these cases some action must be taken before the calibration process can be initiated again.

4.2 A generalised validation methodology

It is a general advice to perform the validation with a different set of data than those used for calibration (Van Lint (2009)). This prevents the problem of the model being optimised for a single walking example (the overfitting problem). However, using different reference data for the validation does not only assure that the parameters are performing well in walking situations other than those in the calibration. Therefore, multi-scenario validations that combine several scenarios are necessary to evaluate walker models for general use.

There is no optimisation process for the validation methodology. We assume that it is not necessary to repeat the significance analysis because it has been included during the calibration. With these suppositions the validation methodology comprises one iteration of the loop presented in figure 4.2. The multi-objective errors represent the performance measure for all scenarios. The assessment criteria determine if the level of accuracy of the model is adequate for application.

We mentioned in the introduction the distinction between face validation and predictive validation. Face validation shows that the model is reproducing basic features of pedestrian movement usually in a qualitative manner and predictive validation makes use of quantitative indicators to show the accuracy of the simulations.

If we inspect the literature for walker models we observe that most validations are qualitative. The qualitative indicators vary in their complexity and scope. Developers put more emphasis on complex assessments such as the appearance of self-organised lanes in bidirectional flows (Still (2000), Treuille et al. (2006), Nakayama et al. (2008), Bandini et al. (2009), Asano et al. (2010)) and the shape of the fundamental diagrams (Blue and Adler (1999), Still (2000), Isobe et al. (2004), Berrou et al. (2005), Seyfried and Schadschneider (2008), Portz and Seyfried (2010), Townsend (2014)).

We argue in this methodology that these assessments need to be quantified and combined in multi-objectives. Chapter 7 presents a multi-scenario validation of Nomad using quantitative indicators. The validation criteria is based in three ordinal values ‘Bad’, ‘Medium’ and ‘Good’ converted from the multi-objective error.

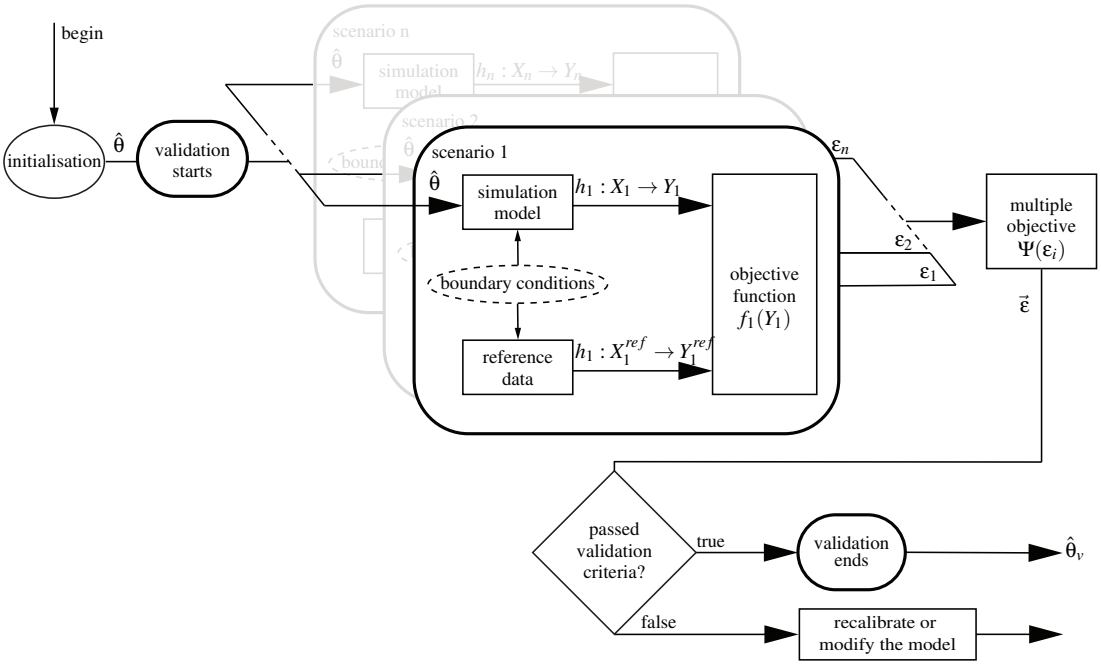

Figure 4.2: Validation methodology for walker models. It is a single iteration initiating on the left with the calibrated parameter set and ending with the validation criteria on the right.

4.3 Multi-objective functions

There is no unique way to combine performance measures from different scenarios. It depends what type of performance measures the objective-functions are calculating, e.g. log-likelihoods or errors.

Likelihood functions use likelihoods instead of errors allowing for a probabilistic way to combine different scenarios. If the scenarios are assumed to be independent they can be multiplied to give the combined probability. Furthermore, by calculating the logarithm of the likelihood we obtain the log-likelihood $\tilde{L}$ that can be added without any need of weights to express the joint probability of different scenarios. The assumption of independence usually does not hold, but Hoogendoorn and Hoogendoorn (2010) show how to overcome this problem. This approach is exposed in section 5.2.1.

Multi-objective error functions have several functional forms (Steuer (1986)) and its simplest and most popular form is a linear addition of the several errors of the objective functions with weights λ_i:

$$\vec{\varepsilon} = \lambda_1\varepsilon_1 + \lambda_2\varepsilon_2 + \ldots + \lambda_n\varepsilon_n \tag{4.4}$$

There is no simple way to find the values of λ other than setting them arbitrarily (Taboada et al. (2007)). The interpretation of λ depends on the errors. If the range of the errors are equal, they have the same relative magnitude and larger values of λ reflect

the importance of indicators over others. If the errors have different magnitudes then λ is also reflecting the differences between the error ranges.

One way to have errors with the same range is to calculate them as proportions of an indicator. If the indicator is an absolute value such as travel time and door capacity then we can calculate their relative errors:

$$\varepsilon_i(\theta) = \frac{\| Y_i(\theta) - Y_i^{ref} \|}{Y_i^{ref}} \tag{4.5}$$

where:
Y_i^{ref} is the reference indicator value.
$Y_i(\theta)$ is the simulated value.

Another approach to determine the parameter value is to create a Pareto set of solutions and choose one of them. A solution is part of the Pareto set if it is not possible to improve the outcomes from one objective function without decreasing the others. This condition creates a set of solutions that are locally optimal and the optimal is chosen according to an arbitrary choice or a specific condition (Taboada et al. (2007)).

Both weighted sums and Pareto optimality require extra conditions for the definition of the optimal solution. The possibility to set prior information in the calibration of walker models can be used to obtain parameter sets that perform well in several situations with a focus on a particular one. One could imagine the application of walker models to situations that are complex and with specific characteristics. For example, if a parameter set is to be used mainly for popular outdoor music festival, it should deliver good behaviours in bidirectional flows generally occurring in the dedicated paths and very good behaviours of individuals manoeuvring inside dense crowds.

4.4 Significance analysis

The significance indicates the sensitivity that the model has for a parameter. If the significance is low, the model is not much affected by variations of the parameter. For each parameter θ_i^* from the optimal set θ^* a significance analysis is performed calculating their sensitivity around the calibrated value $S_{\theta_i} \in \vec{S}$. The sensitivity can be visualised by the hypothetic example in figure 4.3. In the figure we plotted the variation of the error of the objective function for an optimal parameter $\theta_i^* = 1.6$ (the value of the other parameters of θ^* were kept the same). The dashed curve represents an ideal situation in which the error is minimal and small variations will increase significantly the error. The solid curve shows the opposite and the parameter is not significant.

The two most important reasons for a parameter not passing the significance test are the parameter is not useful and could be eliminated from the model or the empirical data was 'poor' (Ossen (2008)) and needs to be supplemented and new scenarios created.

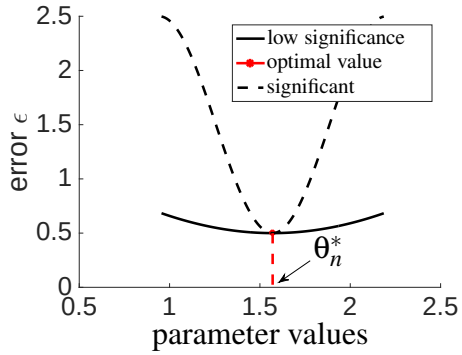

Figure 4.3: A generic example of a sensitivity analysis of two parameters. The multi-objective function is used to calculate the errors around of $\theta_n^* = 1.6$. The dashed curve shows a significant and the solid curve shows a low significant parameter.

If the parameter is significant with other reference data then the problem lies with the reference data used in the calibration.

Poorness of data is the insufficient amount of information about important behaviours such as collision avoidance or following behaviour. If no interactions occur in a reference data, the parameters responsible for these behaviours cannot be optimised. In the validation process the poorness of data prevents any conclusion regarding the model accuracy in the lacking behaviours.

There is a possibility to have too high significance (small variations of the parameters generate extremely high variations in the errors). This is generally an indication of *overfitting* of the parameters. The model will show very large variations of the performance indicators when not simulating the exact conditions used for the calibration. The parameters are therefore too specialised (Van Lint (2009)). Models with many parameters such as walker models are more susceptible for overfitting.

Therefore, the significant test is a very important component and needs to be passed by all estimated parameters before a model can be used. A statistical test such as the one presented in section 5.2.1 must determine if the parameter is significant.

4.5 Conclusions

In this chapter we identified the key components of the calibration and validation of walker models and used them to propose generalised calibration and validation methodologies.

The basic component of the methodologies are the scenarios that comprise all elements necessary to obtain a performance measure from estimations of the walker model with a particular parameter. The scenario contains a flow that is represented by the reference

data and the simulations of the model. The flow will provide the model with walking situations that need to be accurately reproduced.

The calibration was proposed with two steps. The first step is the optimisation process that estimates a parameter that best reproduce the performance indicator applied to the reference data. The second calibration step is a significance analysis that certifies that the parameters are significant therefore useful to the model. The validation methodology has one step that calculates a performance indicator and subjects it to an assessment criteria defining the accuracy of the parameter and the model.

We hypothesised that pairing different scenarios in what we called multi-scenario calibration will increase the probability of obtaining parameter sets that perform well in situations not used in the calibration. This hypothesis is confirmed in chapter 5 and in chapter 7 where we show that parameter sets using multi-scenario calibrations result in parameter sets with higher accuracy than single-scenario parameters.

Chapter 5

Investigating factors that affect calibration of walker models

The calibration process is an optimisation process with an unknown solution. It is not possible to know how close a parameter set is from the optimal solution giving the highly non-linear search space of walker models (Hofmann (2005)). However, it is possible to study the process of calibration using synthetic trajectories. The main idea is to generate trajectories with Nomad and use the known parameters as the optimal values to be retrieved.

Synthetic trajectories allow the comparison of the calibration results with the optimal parameters that created the trajectories. In this chapter we create trajectories that represent the most common walking situations to investigate factors that affect the process of calibration.

The aim is to gain insights on the calibration process and to investigate the impact of using multi-scenarios in the accuracy of the calibrations and the significance of the calibrated parameters. We present the aims in form of research questions in section 5.1.

The calibrations use a trajectory based calibration in accordance with the methodology presented in chapter 4 that optimise the parameters corresponding to the behaviours of individual pedestrians. The trajectories represent bidirectional, crossing and unidirectional congested flows. The set-up of the experiments is presented in section 5.2.

The factors that affect the accuracy of calibrations are discussed in section 5.3. Section 5.4 shows how the use of multi-scenarios improves the significance of the calibrated parameters maintaining a good level of accuracy.

Section 5.5 finishes the chapter with a discussion on the benefits of using multi-scenarios to improve the significance and accuracy of the calibrations. The investigations concluded that multi-scenarios are effective in overcoming the problem of 'poorness of data' (lack of information about the behaviour in the reference data) proving the usefulness of the proposed calibration methodology.

5.1 Calibration investigation research questions

The fundamental question of calibration can be summarised as: how to improve the probability that a calibration is finding optimal parameters that are statistically significant? We break this question in two parts and the first investigates the factors affecting the accuracy of the calibration procedure and the second how to improve the accuracy and the significance of the parameters by using more than one set of reference data in the calibration.

The calibration of models simulating complex processes is not expected to be perfect because of the non-linear result space (Hofmann (2005)). Given that different flows such as bidirectional, crossing and unidirectional submit pedestrians to different situations, we suppose that the optimal parameter values will be different. The question is how can we know if the optimisation algorithm is correctly estimating the optimal values for each of them if they are different and cannot be compared. Therefore, we need to know: *What are the factors that affect how close the estimated parameter values are to their true optimal values?*

Supposing that the calibration procedure is not finding correct parameters for single-scenarios, we can test the hypothesis that combining reference data from different flows provides more information about pedestrian behaviours, thus improving the accuracy and the significance of the parameters. However, the different flows will contain different levels of information about specific behaviours and pairing them in multi-scenario calibrations is no guarantee that the reference data that is 'rich' will prevail over the one that is 'poor' in behaviour information and deliver good results. Therefore, *to what extent the accuracy and the significance of the parameters are affected by combining scenarios with different levels of 'poorness' of data?*

5.2 Experimental set-up

The questions formulated in the previous section concern the calibration procedure and the use of multi-scenarios to improve the quality of the calibrations. Therefore, we need to know what are the values of the optimal parameters. The only way to know with certainty is to create the reference data with simulations and compare the calibrations with a ground truth (Ossen (2008)).

We are also interested in investigating the questions in conditions that are similar to those found in real situations with heterogeneous populations. Therefore, we need to be able to estimate parameters for individual pedestrians. A trajectory based procedure that estimates parameters of single pedestrians is presented in section 5.2.1. The estimated parameter set is compared with the original parameter set (the correct optimal) that generated the reference trajectory.

Three reference sets were created namely one with identical parameters for all pedestrians that we call *clean*, a set called *heterogeneous* formed by normally distributed parameters creating heterogeneity, and the *noisy* that has distributed parameters and a stochastic noise added to their states. We estimate the amount of heterogeneity from previous calibrations of Nomad using trajectory data from real experiments. The stochastic noise stands for tracking errors usually encountered in empirical data. The inclusion of both should create conditions close to calibrations using empirical data.

It is expected that the heterogeneity and the noise complicate the calibration by increasing the complexity of the search space. The *heterogeneous* set was created to compare the influence of heterogeneity and tracking noise in the calibration accuracy. The *clean* set allows for the investigation of other causes of loss of accuracy.

The trajectories are composed by three flow configurations namely a unidirectional congested flow with a narrow bottleneck (*bneck*), a bidirectional corridor (*bidi*) and 90° crossing flows (*cross*). These configurations represent the most common traffic situations occurring between pedestrians and obstacles creating a large amount of behaviours that need to be properly predicted by walker models. In these configurations, pedestrians need to avoid oncoming pedestrians, follow or overtake leading pedestrians, interact with pedestrians coming from the sides and deal with conflicts due to congestion near bottlenecks.

Two types of multi-scenarios are used to investigate their impact on accuracy and the level of significance of the calibrations by reducing the effect of poorness of data. The first is composed by the trajectories of the three flows. The second type uses ten different individuals from the bidirectional flow. The bidirectional flow was chosen because it presented the most accurate single scenario calibrations and therefore, minimises errors arising from the other factors that reduce the accuracy of the calibrations.

We visualise these calibrations by imagining three (or ten) scenarios from figure 4.1 generating errors from their objective-functions. Each scenario has a randomly chosen pedestrian to be calibrated. This creates a high probability that each will have different parameters for the *heterogeneous* and *noise* sets. The different parameters make it impossible to compare the calibrations with a single correct parameter. To overcome this, we compare the calibrations to the means of the parameter distributions.

Creating different multi-scenario calibrations allow to compare two approaches to overcome poorness of data. Using three different flows necessarily result in the optimisation algorithm finding optimal solutions for different walking situations. By taking 10 trajectories from the same flow we increase the probability to submit similar situations to the optimisation problem.

5.2.1 Trajectory based calibration

We explained earlier that we need a calibration procedure that allow us to obtain individual parameters. We found similar frameworks that calibrate traffic models with

single trajectories Hoogendoorn et al. (2005), Ossen and Hoogendoorn (2008) and Johansson et al. (2007). Although they share similarities, the former is more flexible because it uses a log-likelihood objective function that easily allows for multi-scenario calibrations. Furthermore, the log-likelihood has been used with good results for both for walker (Hoogendoorn and Daamen (2010)) and for car driver models (Hoogendoorn and Hoogendoorn (2010)). In the following sub-sections we will recall and describe the parts of the framework that are used in this and in the following chapters. For more details we refer to the original references.

The calibration is performed by selecting one trajectory from the set X of trajectories and use it to calculate the likelihood that Nomad can predict the dynamic states of this pedestrian along his or her trajectory. The state of the other pedestrians match the reference trajectories. By doing so we make sure that we estimate the parameters that best represent the walking behaviour of this single pedestrian during the whole trajectory while the external conditions correspond to the reference data.

A potential problem of such procedures is the effect of autocorrelation in the errors resulting in non-optimal parameters. Autocorrelated or serially correlated errors occur when the prediction errors by the model and the reference system at subsequent time steps of the simulation are not independent from each other (Hoogendoorn and Ossen (2006)). In these cases the errors are not distributed around zero but around a base value. Autocorrelation can also be introduced by a treatment of the reference data such as smoothing or any other type of interpolation.

Another type of auto-correlation arises from the propagation of one error in a simulation time step to the next. For instance, when a pedestrian interacts with other pedestrians during his or her trajectory. At the moment that a simulated pedestrian is not in the exact position of the real pedestrian then he or she is perceiving a different traffic situation and this may cause an additional prediction error. This error is not independent of the previous error and the longer the trajectory of a pedestrian the higher is the probability of autocorrelation.

This type of autocorrelation can be diminished or even prevented by putting the state variables back at the values of the reference data at regular instants (reset-times). That is, correcting the state of the pedestrian after he or she walked the equivalent of the reset-step and the error was measured. The smaller the reset-step, the smaller is the chance this type autocorrelation can occur. If the reset-time is equivalent of the simulation time-step, it is eliminated.

Hoogendoorn and Hoogendoorn (2010) show that it is possible to determine the level of autocorrelation and that the framework described in the next sections allows the calibration using likelihood functions for the estimation of parameters even with correlated errors.

Maximum likelihood mapping for single trajectories

To estimate the set of parameters θ_p for a single pedestrian p we use a microscopic mapping Y that reflects the pedestrian behaviour. The most common is one of the dynamic state variables: position $\vec{r}_p$, velocity $\vec{v}_p$ or acceleration $\vec{a}_p$ but any microscopic mapping or a combination of mappings can be used as well. The difference between the mappings at time t_k subject to parameter set θ is expressed by:

$$\varepsilon(t_k \mid \theta_p) = \left\| Y^{ref}(t_k) - Y(t_k \mid \theta_p) \right\| \tag{5.1}$$

If we assume that the model predictions $\varepsilon(t_k \mid \theta_p)$ of the mappings are independent and normally distributed $\mathcal{N}(0,\sigma^2)$ we can obtain the probability p_k of the calibration error at time t_k from the probability density $f(\varepsilon)$ of the normal distribution:

$$p_k(\theta_p,\sigma_p) = \frac{1}{\sigma_p\sqrt{2\pi}} \exp\left(\frac{-\varepsilon^2(t_k \mid \theta_p)}{2\sigma_p^2}\right) \tag{5.2}$$

A common definition of a likelihood function L combines all n time instances observed for pedestrian p:

$$L(\theta_p,\sigma_p) = p(\varepsilon(t_1 \mid \theta_p),\ldots,\varepsilon(t_n \mid \theta_p)) = \prod_{k=1}^{n} p_k(\theta_p,\sigma_p) \tag{5.3}$$

The log-likelihood is then:

$$\tilde{L}(\theta_p,\sigma_p) = -\frac{n}{2}\ln(2\pi\sigma_p^2) - \frac{1}{2\sigma_p^2}\sum_{k=1}^{n}\varepsilon^2(t_k \mid \theta_p) \tag{5.4}$$

The parameter calibration equation defined in (4.3) can be expressed in terms of the log-likelihood:

$$\theta^* = \arg\max \tilde{L}(\theta) \tag{5.5}$$

By applying the optimality condition in the log-likelihood we obtain the Maximum-Likelihood-Estimate (MLE) condition:

$$\frac{\partial\tilde{L}}{\partial\sigma_p^2} = 0 \Rightarrow \hat{\sigma}_p^2 = \frac{1}{n}\sum_{k=1}^{n}\varepsilon^2(t_k \mid \theta_p) \tag{5.6}$$

Substituting (5.6) in (5.4) we are able to write the MLE only as a function of the errors (5.7).

$$\tilde{L}(\theta_p, \sigma_p) = -\frac{n}{2} \ln \left(\frac{2\pi}{n} \sum_{k=1}^{n} \varepsilon(t_k \mid \theta_p)^2 \right) - \frac{n}{2} \tag{5.7}$$

The maximum value of the MLE can then be found by determining θ_p that maximises its value by means of a numerical optimisation.

We used the acceleration as calculated by the equation (3.9) for the mapping of the trajectories. We did preliminary calibrations comparing the accuracy of the position and the velocity mappings and observed that the acceleration gave the best results (Campanella et al. (2010)). We suspect that because the simulation model calculates directly the acceleration it generates smaller numerical errors.

Multi-objective

If we combine S different scenarios s in the likelihood function we need to assume that the pedestrians p_s chosen to be calibrated have the same parameter set $\overline{\theta}$. In this case we can modify equation (5.3) by substituting the individual parameters θ_p in equation (5.3) by $\overline{\theta}$ and combining them in a multiple likelihood function:

$$L_{multi}(\overline{\theta}) = \prod_{s=1}^{S} L_i(\overline{\theta}) \tag{5.8}$$

The resulting $\overline{\theta}$ is not optimal for an individual but reflects an average behaviour of the chosen individuals of the S different scenarios.

Parameter significance

After calibrating a parameter θ_i^* we need to know if its influence on predicting pedestrian behaviours is significant and therefore the parameter is 'useful'. The task is to show that the model outcomes (in our case the log-likelihoods) are varying significantly around the estimated parameter value (other parameters are kept fixed). Below we describe the statistical method that decides if the influence of the estimated parameter is statistically different from the outcomes of the 'zero' parameter $\theta_i^* = 0$ that is equivalent to removing the parameter from the model.

Ben-Akiva and Lerman (1985) proposes a test that calculates the range in which a parameter is considered significantly different from any value of interest θ_{test} with a desired probability. The test assumes that the distribution of the outcomes $\hat{\theta}_i$ of this parameter around the optimal value θ_i^* is normally distributed with mean $\mu = \theta_i^*$ and variance σ_i^2. The test states that:

H0: $\theta_i^* = \theta_{test}$
H1: $\theta_i^* \neq \theta_{test}$

Where, H0 is the null hypothesis and H1 is the alternate. If we do not reject H0 then θ_i^* is not significantly different from θ_{test} (in our case $\theta^{test} = 0$).

To simplify we translate the parameter value according to:

$$Z = \frac{\theta_i^* - \theta_{test}}{\sigma_i} \tag{5.9}$$

The variable Z is then normally distributed with $\mathcal{N}(0,1)$ (standard normal distribution) and the condition to confirm the null hypothesis for a 5% level of significance becomes: $c_{0.025} = -1.96$ and $c_{0.975} = 1.96$ for $Pr = 0.95$.

Substituting $\theta_{test} = 0$ we can reject the null hypothesis for $\frac{\theta_i^* - 0}{\sigma_i}$ if:

$$\left| \frac{\theta_i^*}{\sigma_i} \right| \geq 1.96 \tag{5.10}$$

To apply equation (5.10) we need to find σ_i. Hoogendoorn et al. (2005) indicate that for likelihood objective functions the Cramer-Rao lower bound can be used to estimate the variance of the parameters (5.11):

$$\sigma_i^2 \geq -E(\nabla^2 L_i^*) \tag{5.11}$$

However, calculating analytically the matrix with the partial derivatives is often not possible, because walker models are too complex to permit an analytical derivation of the partial derivatives.

This matrix can be approximated by a sensitivity analysis around the values of θ^* maintaining the other parameters constant at their optimal values and calculating the approximated second derivative of the objective-function at θ_i^* (Ossen (2008)):

$$\sigma^2 = -\left(\frac{\partial^2 L}{\partial \theta_i^2} \right) \Bigg|_{\theta_i^* = \theta^*} \tag{5.12}$$

After estimating the variance, the significance test can be applied by introducing the variance into equation (5.10). If the test is satisfied the parameter θ^* is significant otherwise, we are unsure about its value.

5.2.2 Calibrated parameters

Nomad has many parameters and all contribute to the predictions of the estimated states. However, four parameters display a much larger influence to the estimated states. The interaction strength (a_0) and interaction distance (r_0) are directly responsible for the interaction between pedestrians, the acceleration time (τ) controls the

intensity that pedestrians try to walk along their intended path and the obstacle interaction strength that affects the interaction between pedestrians and obstacles (a_W). Chapter 3.2 details these parameters in Nomad.

The heterogeneity was introduced in three of the calibrated parameters: a_0, r_0 and τ. The a_W was not varied due to a lack of evidence of how much it varies in the pedestrian population. The free-speed v_0 and the pedestrian radius *rad* were also varied as they are two of the most important input parameters of walker models and they have been widely documented giving a good empirical estimation of their distributions. The heterogeneity of all five parameters is created with normal distributions $\mathcal{N}(\mu^{sy}, \sigma^{sy})$ and are referred in the following sections as *distributed parameters*.

The noise is inserted at each time step of the simulation by a normally distributed variable added to the acceleration $\vec{a}$ presented in equation (3.4) resulting in $\vec{a}^{noise}$:

$$\vec{a}^{noise} = \vec{a} + \mathcal{N}(0, \phi^2) \tag{5.13}$$

Table 5.1 shows the means and standard deviations of the six parameters of interest and the noise in the investigations. The rest of the parameters necessary to run the Nomad model were kept fixed and equal through all the calibrations. Their values resulted from previous calibration of the Nomad model. We also added the coefficient of variation ($c_v = \sigma/\mu$) to give an idea of the dispersion of the distributions.

Table 5.1: Distribution means and deviations for the parameters that produced heterogeneity or were estimated.

parameters	mean $\overline{\mu}^{sy}$	deviation $\overline{\sigma}^{sy}$	coef. variation $\overline{\sigma}^{sy}/\overline{\mu}^{sy}$
a_0	10.0	0.7	0.07
r_0	0.16	0.02	0.13
τ	0.25	0.03	0.13
v_0	1.45	0.20	0.14
rad	0.22	0.02	0.09
ϕ	0	0.001	-
a_W	20.0	-	-

5.2.3 Synthetic trajectories

The reference data are composed of three sets of synthetic trajectories created by the Nomad model. The heterogeneity was created with normal distributions shown in table 5.1. Table 5.2 shows their heterogeneity and noise composition.

Table 5.2: Heterogeneous parameters and input errors for the reference sets.

	heterogeneity	noise
clean		
heter	a_0, r_0, τ, v_0, *rad*	
noisy	a_0, r_0, τ, v_0, *rad*	ϕ

5.2.4 Number of calibration runs

The analysis of the mean calibrated parameter values for the distributed parameters should not be affected by statistical errors due to insufficient sample size. A too small sample, may result in values outside of the desired accuracy due to large stochastic variations. While in reality, if enough calibrations would have been performed, the sample average could have fallen within the accuracy boundary. Therefore we determine for each distributed parameter the minimum sample size that guarantees an accuracy of 5% of the mean parameter value $\overline{\theta}^{sy}$.

To determine the amount of calibrations necessary of the distributed parameters we apply a dependent t-test for paired samples with 95 % confidence. The samples are generated with $\mathcal{N}(\overline{\theta}^{sy}, \overline{\sigma}^{sy})$ for the three distributed parameters until the sample size consistently gives the desired accuracy. The following calculations show that samples with 25 individuals are sufficient:

$$n \geq \left(\frac{z\sigma_p}{d}\right)^2 \tag{5.14}$$

where:
n is the number of runs needed to obtain the sample accuracy
z is the confidence multiplier (1.96 for 95% confidence for the two tailed distribution)
σ_p is the standard deviation of the sample test (table 5.1)
d is the desired accuracy of the sample (5% of the mean parameter value $\overline{\theta}^{sy}$ (table 5.1))

$$n_{a_0} = \left(\frac{1.96 * 0.7}{0.5}\right)^2 = 8 \qquad n_{r_0} = \left(\frac{1.96 * 0.02}{0.008}\right)^2 = 24$$
$$n_{\tau} = \left(\frac{1.96 * 0.032}{0.0125}\right)^2 = 25 \qquad n_{v_0} = \left(\frac{1.96 * 0.17}{0.0725}\right)^2 = 21$$
$$n_{rad} = \left(\frac{1.96 * 0.02}{0.011}\right)^2 = 13$$

5.2.5 Flow configurations

Figure 5.1 shows the scheme of the three flows: the bidirectional (*bidi*), the narrow bottleneck (*bneck*) and the crossing flows (*cross*). The dimensions of the walking areas are: $10m \times 4m$ for the bidirectional flow, $10m \times 4m$ narrow bottleneck flow with a corridor of $1m$ at $x = 6m$ and $8m \times 8m$ for the crossing flow. These dimensions were chosen to match the walking experiments realised in Daamen and Hoogendoorn (2003). The experiments were designed to present representative walking behaviours and their trajectories will be used in the calibrations performed in chapter 6.

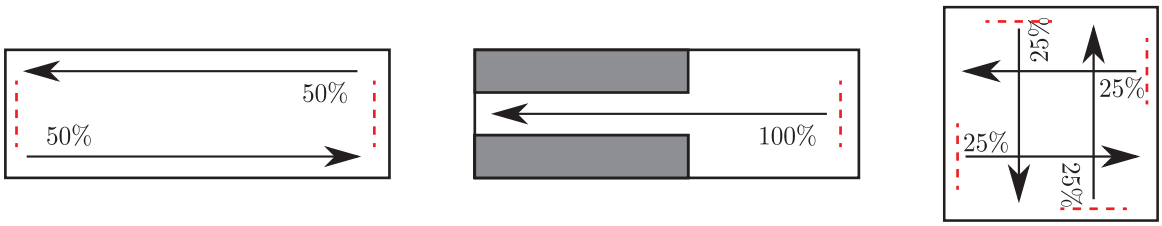

Figure 5.1: The three experimental set-ups (from left to right): the bidirectional flow, the narrow bottleneck and the crossing flows. The arrows represent the direction of the flows with the percentage of the demands on the flows and the dotted lines the origins of the flows.

The input flows were created in a stepwise ascending manner to assure that both free flow and congestion could occur in all flow configurations and that the densities could reach approximately 2 peds/m^2. Figure 5.2 shows the graph with the demands per simulation period for the bidirectional flow. The demand value is multiplied by the percentages shown in figure 5.1 to obtain the amount of pedestrians that is generated in each origin (represented by the dotted lines on figure 5.1).

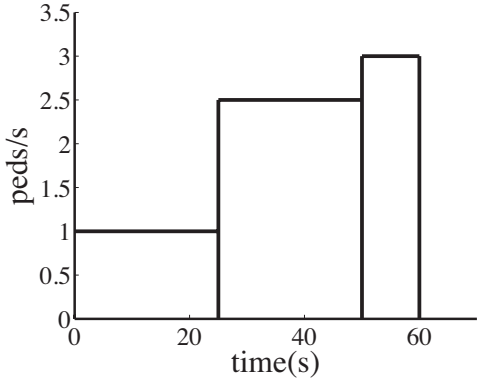

Figure 5.2: The stepwise inflow demands for the bidirectional flow.

The total time of the input flows is 60 seconds for all experiments to allow enough time for interactions between pedestrians but not extend too much the computational time of the calibrations. The total amount of pedestrians that walk in the simulations are respectively, 173 for the narrow bottleneck corridor, 200 for the crossing flow and 236 for the bidirectional corridor.

5.2.6 Indicators

In this section we present the two indicators used in this chapter the accuracy indicator that calculates relative errors of the calibrated parameters and a local density indicator.

Accuracy indicator

The results are analysed using the absolute values of the relative errors (ε) of the calibrated parameters:

$$\varepsilon(\theta_i^*) = \frac{\|\theta_i^{sy} - \theta_i^*\|}{\theta_i^{sy}} \tag{5.15}$$

where:
θ_i^{sy} is the correct value used in the simulation that created the trajectories.
θ_i^* is the calibrated parameter.

The parameters calibrated for the *noisy* trajectories for the multi-scenario calibrations can not be subtracted from the correct parameters. The scenarios chose randomly the pedestrians from the flows and they likely present different parameter values. Therefore, for the analysis of the multi-scenario calibrations we use the mean values of the normal distributions to calculate $\overline{\varepsilon}$:

$$\overline{\varepsilon}(\theta_i^*) = \frac{\|\mu_i^{sy} - \theta_i^*\|}{\mu_i^{sy}} \tag{5.16}$$

where:
μ_i^{sy} is the mean of the parameter distribution $\overline{\theta}_i \sim \mathcal{N}(\mu^{sy}, \sigma^{sy})$.
θ_i^* is the calibrated parameter with the multi-scenario.

Density indicator

In this chapter we are interested in calculating the local densities as a way to assess the local conditions experienced by each individual. Given that the walking areas of the different types of flows are relatively small, the usual grid based density calculation produces non smooth results (Edie (1963)). Therefore, we use the definition of local density proposed by Helbing et al. (2007) and shown in equation (5.17). This density calculates how much of a pedestrian should be included to the occupation of a circular area around a location. This ocupation varies between 0 and 1 depending to the distance to the location. Duives et al. (2015) call it *Exponentially Weighted Distance* (EWD) and showed that it is accurate producing smooth values for local densities.

$$k(\vec{r},t) = \frac{1}{\pi R^2} \sum_j \exp\left[-|\vec{r}_j(t) - \vec{r}|^2 / R^2\right] \tag{5.17}$$

where:
R is the radius around the location We adopted $R = 1m$ as recommended by Helbing et al. (2007) to emphasise the local range.
j are all pedestrian within the circle with radius R.
The exponential factor $\exp\left[-|\vec{r}_j(t) - \vec{r}|^2/R^2\right]$ determines the extent of occupation of pedestrian j into the density k in (ped/m^2) in location $\vec{r}$.

5.2.7 Simulation set-up

The numerical set-up of the simulations was the same for all flows. We used a simulation time-step $\Delta T = 0.02s$. These values have proven to simulate stable trajectories and do not demand too much computational power. The reset-step used is the smallest possible i.e. the simulation time-step.

5.2.8 Optimisation algorithm

The calibration of complex non-linear models such as the Nomad model requires an optimisation algorithm that does not get trapped in local minima solutions. Also the algorithm must be able to find a solution in reasonable computational time given the intention of performing several calibrations.

A genetic algorithm (GA) was chosen due to its simplicity and excellent qualities in dealing with non-linear models. The disadvantage of GA's is their relatively high demand of computational power. Tests with the Nomad model indicated that the GA could consistently find the correct parameter values. To improve the performance we used a hybrid optimisation procedure combining a GA and a Simplex optimiser. The Simplex is a much faster optimisation algorithm that works well in finding local minima. The idea of combining both algorithms is to apply the GA in the first part of the optimisation until the best candidate of the GA population is close enough to the stopping condition. The best candidate is sent to the Simplex optimiser and the optimal parameter set θ^* is found. This hybrid procedure improved the computational performance by often taking less than 50% of the time when compared with the pure GA with similar results.

5.3 Investigating the calibration accuracy

In this section we investigate the factors that affect the calibration accuracy by comparing the results of the calibrations of the three experiments using the single-scenario. Figure 5.3 shows the box-plots with the results of 25 calibrations for each type of flow for two sets of synthetic trajectories (*clean* and *noisy*).

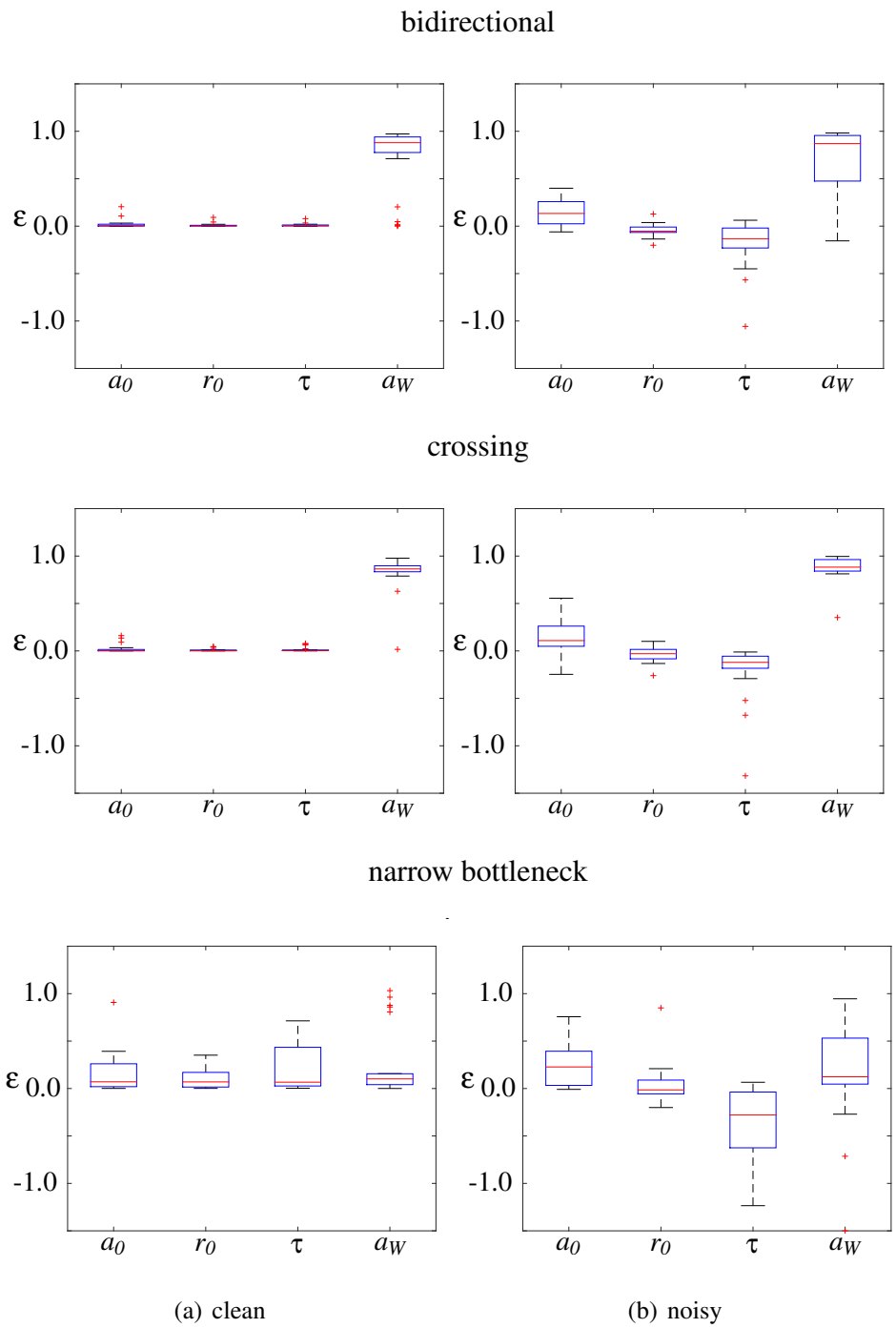

Figure 5.3: Estimation errors for all *clean* and *noisy* single-scenario calibrations.

The left column for the *clean* trajectories shows that both bidirectional and crossing flows present very accurate calibrations for the three parameters a_0, r_0 and τ. The average results are close to the correct value and their distribution is very small. However, the narrow bottleneck simulation presents significantly worse results with larger calibration errors shown in table 5.3. What is not visible in the figure is that for the narrow bottleneck less parameters are significant.

We can point to two causes for these differences in the *clean* set for the parameters

a_0, r_0 and τ, namely poorness of data due to insufficient interactions and complex movements in the area around the entrance of the corridor.

Table 5.3: The average relative errors ε for the three parameters a_0, r_0 and τ. The results include only the significant calibrations. The values below are the percentages of significant calibrations from the total.

		flows								
		bidirectional			crossing			narrow		
		a_0	r_0	τ	a_0	r_0	τ	a_0	r_0	τ
clean	ε	0.02	0.01	0.01	0.02	0.01	0.01	0.11	0.10	0.20
	(% sig.)	(100)	(100)	(100)	(100)	(100)	(100)	(96)	(96)	(96)
heter	ε	0.01	0.01	0.01	0.02	0.01	0.02	0.11	0.14	0.25
	(% sig.)	(100)	(100)	(100)	(100)	(100)	(100)	(100)	(100)	(100)
noisy	ε	0.16	0.06	0.20	0.18	0.06	0.20	0.21	0.08	0.35
	(% sig.)	(100)	(100)	(100)	(100)	(100)	(100)	(92)	(96)	(92)

The third cause of loss of accuracy is the introduction of noise visible on the right column (figure 5.3(b)). Table 5.3 shows that the noise affected negatively the calibration of all parameters from all flows. The table also shows that heterogeneity had no significant impact in the calibrations and will not be discussed further.

The discussion about the a_W results is restricted to the narrow bottleneck trajectory, that is the only simulation that generates enough interactions between pedestrians and obstacles. This can be seen by the very low percentages of significant calibrations for the bidirectional and crossing flows in table 5.4. The table also shows that the accuracy of the a_W calibrations is the wort of all parameters.

Table 5.4: The average relative errors ε for the a_W parameter. The values in brackets include only the significant calibrations. The values below are the percentages of significant calibrations.

		a_W (significant)					
		bidirectional		crossing		narrow	
clean	ε	0.73	(0.05)	0.83	(0.32)	0.24	(0.12)
	(% sig.)		(20)		(4)		(84)
noisy	ε	0.71	(0.18)	0.88	(0.35)	0.41	(0.26)
	(% sig.)		(28)		(4)		(80)

In the next sections we will discuss separately the influence of the three factors of loss of accuracy for all four parameters. For the first two factors, poorness of data and complexity of movement, we used the clean trajectories. We proceed with the influence of noise comparing the results of the *clean* and the *noisy* trajectories.

5.3.1 Poorness of data

The largest errors for the three flows resulted from trajectories with extreme poorness of data due to very little interactions with other pedestrians. Figure 5.4 shows the trajectory for the narrow bottleneck flow of a pedestrian walking alone in the beginning of the narrow flow simulation.

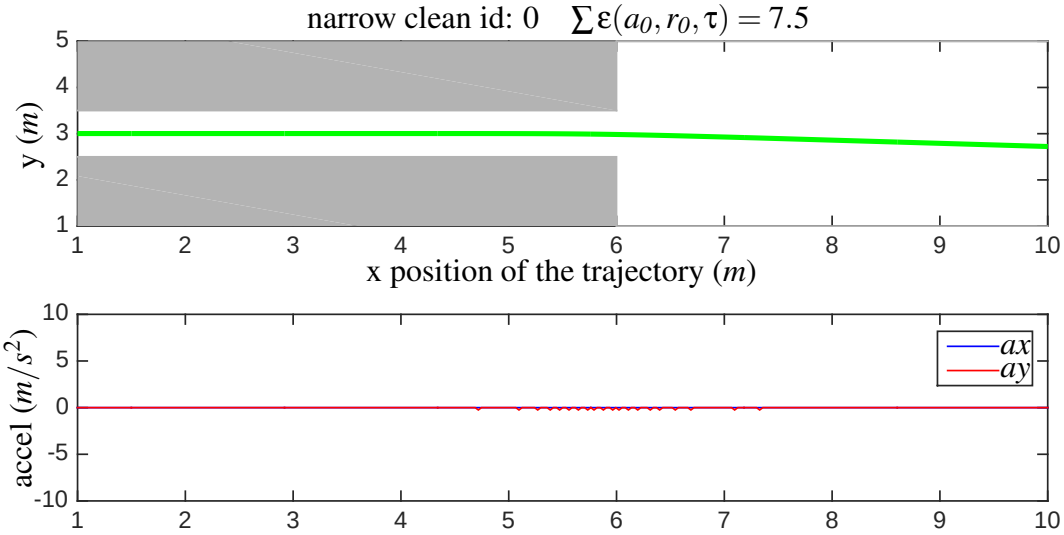

Figure 5.4: A trajectory (walking from the right to the left) and the accelerations for a pedestrian walking alone in the narrow bottleneck simulation. The error ε is the sum of the errors from parameters a_0, r_0 and τ.

The trajectory presents no accelerations due to the absence of other pedestrians and the coincidence that the trajectory was aligned with the middle of the corridor. In this situation almost any value of the parameters will keep the pedestrian following the desired trajectory. The resulting calibration errors are at least 10 times higher than for other trajectories. By being such a special case with very large outlier values it is the only calibration that was taken out from the average results presented in table 5.3.

The main reason why the narrow bottleneck is more affected by the poorness of data is that pedestrians have less possibility to interact inside the corridor that takes half the length of the trajectory. Also it is only possible to interact with slower pedestrians in front. Therefore, in general the narrow bottleneck presents less probability of interactions in low flows. Figure 5.5 shows that even the worse calibration for the bidirectional flow presented some interactions.

Similarly, the non-significant calibrations for the the a_W parameter for the narrow bottleneck occurred for pedestrians walking alone in the corridor. These pedestrians did not interact with the walls and walked straight and further than the shy-away distance (the relatively constant distance from the walls in section 2.3.4). Therefore, they did not apply the interaction behaviour with walls. This can be seen in the trajectory presented in figure 5.4. Removing the results without interactions with walls improve the calibration results significantly (inside brackets in table 5.4).

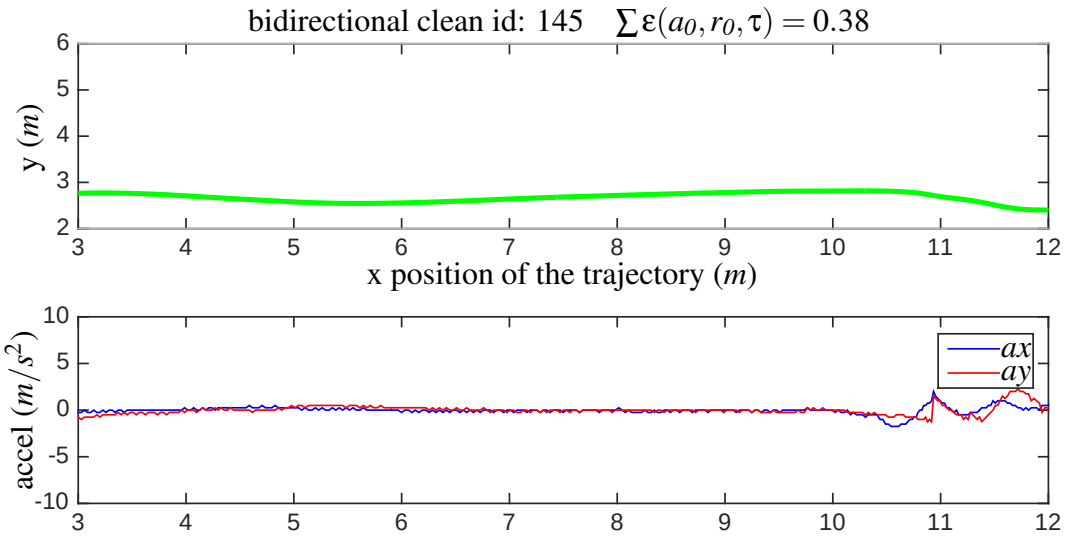

Figure 5.5: A trajectory (walking from the left to the right) and the accelerations for a pedestrian walking practically alone in the bidirectional simulation. The error ε is the sum of the errors from parameters a_0, r_0 and τ.

These results show that poorness of data is a strong factor in the loss of accuracy and that it may cause calibration errors that may not be accounted when using real trajectories.

5.3.2 Complexity of movement

For situations with larger flows, the narrow bottleneck simulation presents a more complex behaviour due to the strong interactions in the area upstream of the bottleneck. The trajectories tend to be less smooth than the normal walking that occurs in the bidirectional and crossing flows. A small change of one of the parameters such as τ that strongly affects the longitudinal acceleration (in this chapter called ax) can be enough for the pedestrian to advance or not into the corridor.

The same applies to the interaction parameters (a_0 and r_0) when pedestrians from the back part of the influence area may *push* the pedestrian into the corridor. Figure 5.6 illustrates this situation for the simulation and for the experiments where two pedestrians a and b are interacting strongly.

The complexity is further enhanced by the fact that pedestrian behaviours are also determined by the a_W parameter that controls the interaction with obstacles. This is certainly true for pedestrian p_1 in figure 5.6(a) that is bordering the corridor wall and also has a strong push from this proximity.

It is not easy to quantify the complexity of movements. We can identify its effects using two indicators: walking time and the walking accelerations. The walking time is a measure of congestion and time spent while manoeuvring in crowded situations (in the *clean* trajectories all pedestrians have the same free-speed). A long walking time

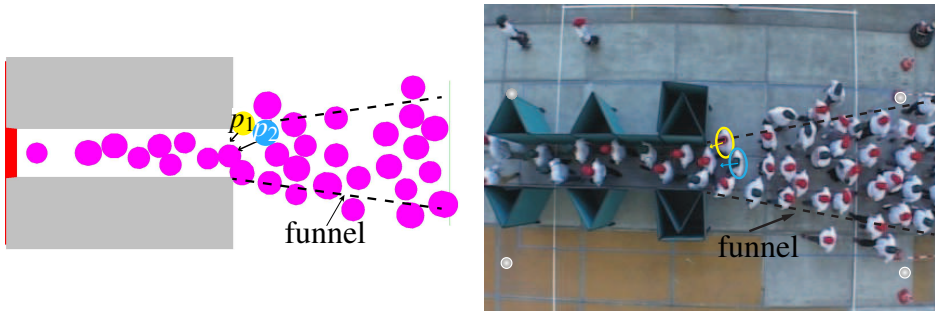

(a) (b)

Figure 5.6: A snapshot of the narrow bottleneck simulation with two pedestrians interacting in the entrance of the corridor for a simulation and for the experiments when the congestion sets in (from Daamen et al. (2005b)).

indicates more interactions and a likely increase of complexity of interactions. The acceleration a directly represents the disturbances in the trajectory and the larger its absolute mean value the more disturbances a pedestrian encountered in its trajectory.

Figure 5.7 shows plots with these indicators on the axis for the three flows. We used the calibration errors to paint the dots. Large errors are painted with bright colours. The scales of the axis and the colour-bar were chosen to improve the visibility by enhancing the variations.

The diagonal shape of the plots indicates that the average acceleration and the walking time have a positive correlation. Larger walking times reflect more manoeuvres causing larger accelerations.

We distinguish three regions in the plots. The first region is the lower left with low acceleration and short walking time. These calibrations presented large errors due to poorness of data mentioned earlier for the three flows. The narrow bottleneck plot reveals the extreme case represented by pedestrian with id:0.

In the second region above $a \geq 0.5 m/s^2$, the errors start to decrease. For the bidirectional and crossing flows the dots get darker until a third region where the errors are close to zero. This increase in accuracy reflects the increase of traffic, thus increase of interactions. For these two flows the errors stay low indicating trajectories with plenty of room for manoeuvres that even with an increase of accelerations, stay relatively smooth. These situations are favourable for accurate calibrations.

Figure 5.8 shows the trajectory for the pedestrian with the largest acceleration and one of the largest walking times in the bidirectional flow. It is interesting that this pedestrian generated a perfect calibration with ε= 0.0.

The narrow bottleneck presents a different situation. When the congestion sets in, some pedestrians present complex movements around the entrance of the corridor sharply decreasing the accuracy. These pedestrians are not able to enter the funnel created in front of the corridor entrance (figure 5.6) until they reach the walls around the corridor.

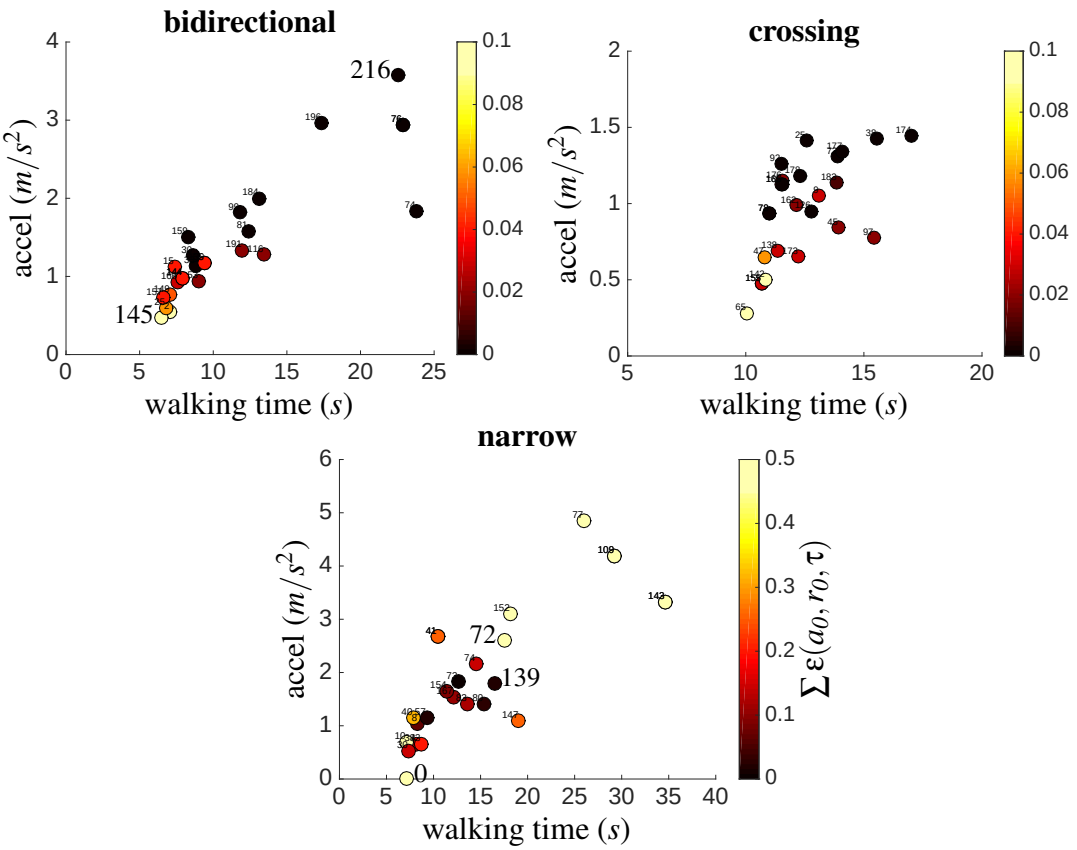

Figure 5.7: The average of the absolute values of the acceleration against the walking time for the *clean* trajectories. The colour represents the sum of the errors from parameters a_0, r_0 and τ. We enlarged the ids of pedestrians that have their trajectories plotted in separate figures.

They struggle for a long time to force themselves into the congested flow creating movements with sharp directional changes and large accelerations ($a \geq 3.0 m/s^2$ and walking times $\geq 20s$). The trajectory shown in figure 5.9 illustrates these cases.

Figure 5.10 shows the average local densities experienced by the pedestrians during their whole trajectory. For the narrow simulation we limited to a the region at $2m$ from the entrance. This eliminates the corridor and enhances the effects of congestion.

We plotted the average local densities to illustrate the two situations occurring in the narrow bottleneck. The first situation is the situation described previously in which pedestrians walk around the funnel because they entered at positions outside it. They experience lower densities but their situations results in long walking times and inaccurate calibrations due to the complex movements around the corridor entrance. The trend 2 line in the narrow bottleneck plot in figure 5.10 represents these cases.

These sharp manoeuvres can be approximated by different values of the parameters of Nomad. This makes the calibration process end in local optima decreasing the calibration accuracy for the narrow bottleneck.

The second situation is similar to what we described for the bidirectional and crossing

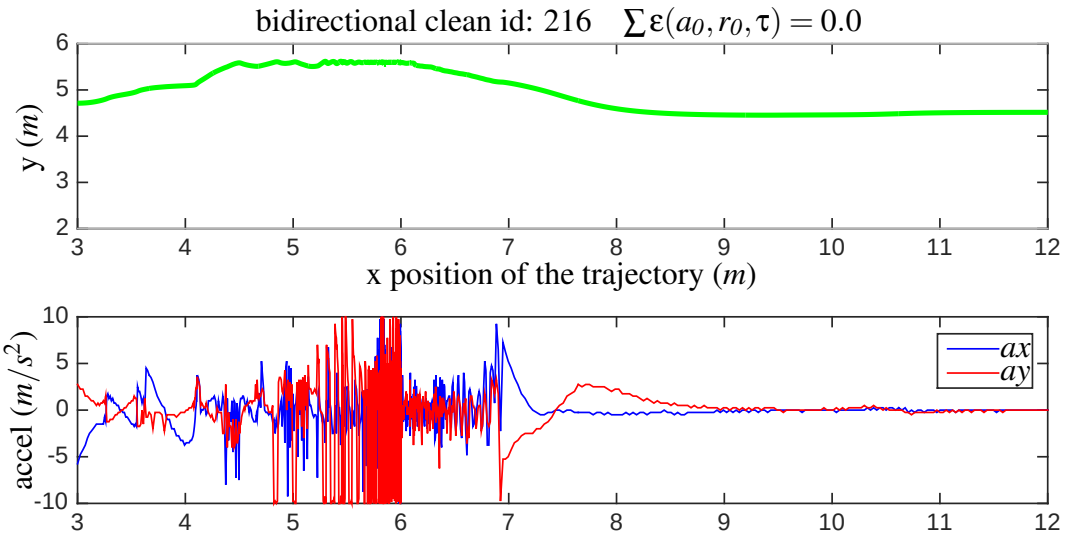

Figure 5.8: A trajectory (walking from the left to the right) and the accelerations for the pedestrian that applied the highest accelerations and spent one of the longest walking times in the bidirectional simulation. The error ε is the sum of the errors from parameters a_0, r_0 and τ.

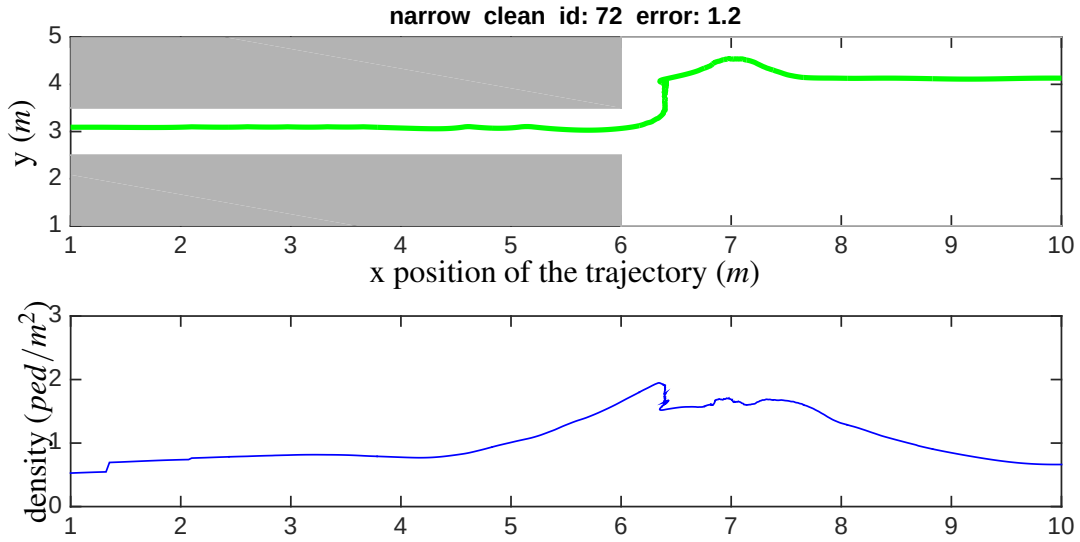

Figure 5.9: A trajectory (walking from the right to the left) and the local density for the pedestrian that encountered one of the highest local densities near the corridor entrance and moderate walking times in the narrow simulation. The error ε is the sum of the errors from parameters a_0, r_0 and τ.

flows. Pedestrians walk in relatively smooth trajectories even with greater densities. The accuracy improves due to the increase of interactions. This can be seen in the plots of the bidirectional and crossing flows in figure 5.10 and in the trend 1 line in the narrow bottleneck flow.

Above $\geq 2 ped/m^2$ trend 1 represents the pedestrians walking inside the congested funnel. These pedestrians experience large densities but their movements are smooth

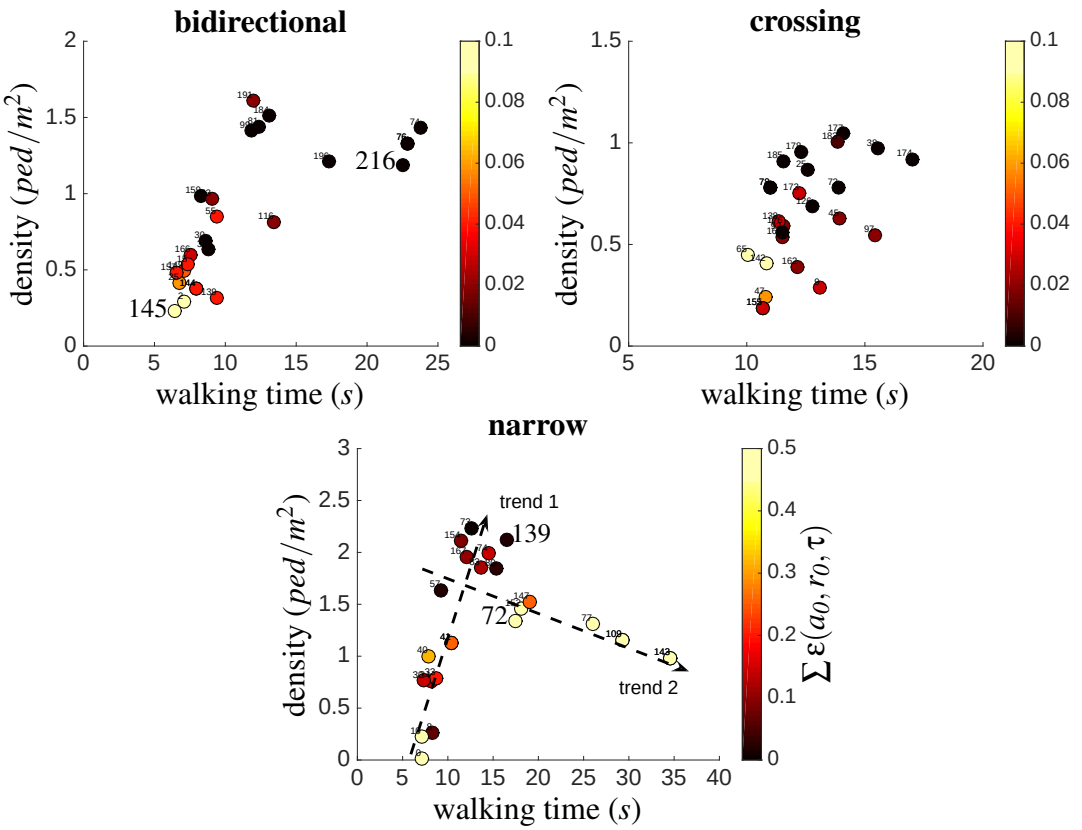

Figure 5.10: The average of the local density against the walking time for the *clean* trajectories. The colour represents the sum of the error values from parameters a_0, r_0 and τ. For the narrow trajectories the density is limited to the region at two meters distance from the corridor entrance. The numbers near the dots are the ids of the pedestrians.

allowing accurate calibrations. To illustrate this, we plot the trajectory of the pedestrian with id = 139 that encountered one of the largest densities as we can see in figure 5.10 (walking time = $17s$ and density = $2.2ped/m^2$). Figure 5.11 shows that the pedestrian is well positioned in relation to the entrance of the corridor and presented good calibration results.

The situation of the a_W parameter is distinct from the other parameters because its accuracy depends mainly on lateral accelerations inside the corridor that create interactions with the corridor walls. This can be seen in figure 5.12 where lateral accelerations $a_y \geq 0.3m/s^2$ have higher accuracy.

Two pedestrians with id:8 and 10 in figure 5.12 display enough lateral accelerations to deliver good calibrations even with low densities inside the corridor. These occurred because they entered the corridor in a oblique path that leads to short distances to the wall creating interactions.

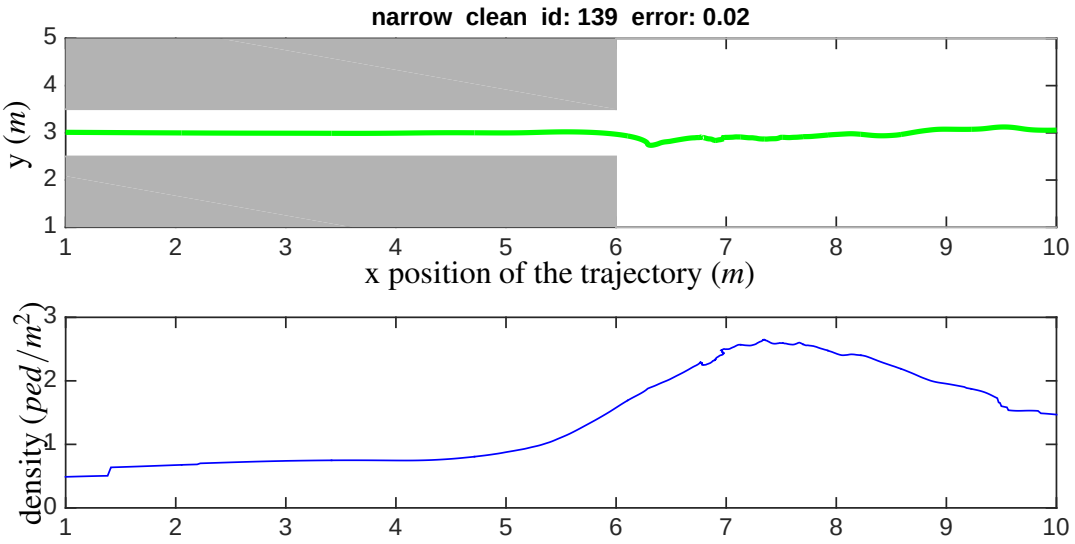

Figure 5.11: A trajectory (walking from the right to the left) and the local density for the pedestrian that encountered one of the highest local densities near the corridor entrance and moderate walking times in the narrow simulation. The error ε is the sum of the errors from parameters a_0, r_0 and τ.

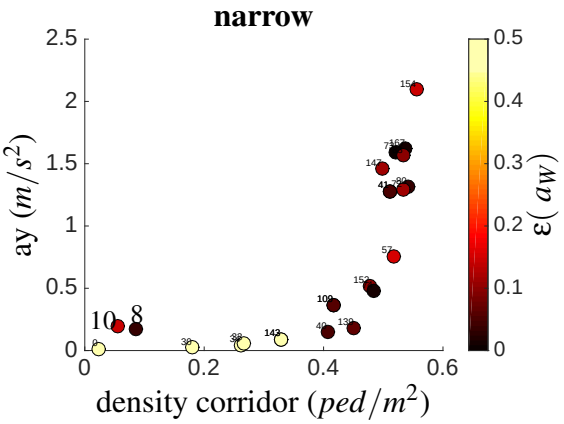

Figure 5.12: The average of the local density against the lateral acceleration inside the corridor of the narrow bottleneck flow with *clean* trajectories. The colour represents the error values from parameter a_W.

5.3.3 Effects of heterogeneity and noise in the calibration

As expected, the introduction of noise decreases the accuracy of the calibrations for all parameters. This is clearly seen in the figure 5.3(b). Table 5.3 shows that heterogeneity has little influence on the accuracy and we will not discuss the heterogeneity separately any further.

Table 5.3 shows that the narrow bottleneck flow still presents the worst accuracy with noise for the three interaction parameters. However, the introduction of noise has a large negative effect in the accuracy of all parameters and all flows diminishing the differences between the different flows.

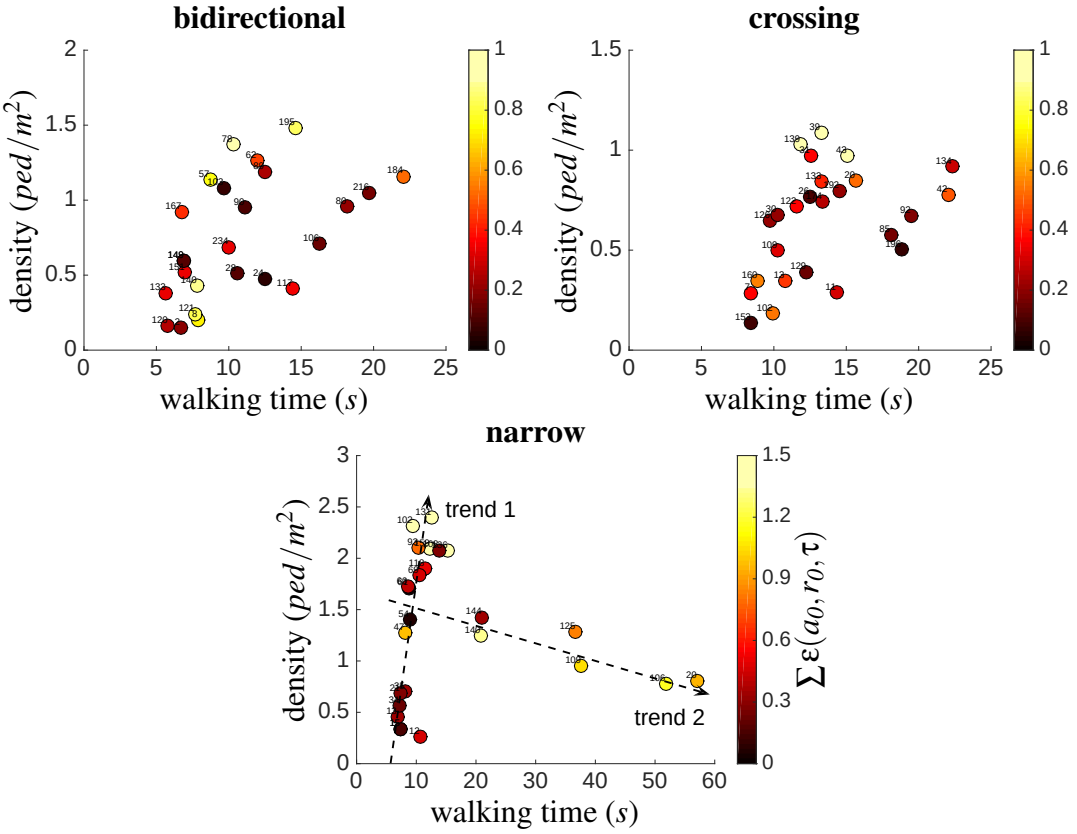

Figure 5.13: The average of the local density against the walking time for the *noisy* trajectories. The colour represents the sum of the error values from parameters a_0, r_0 and τ. For the narrow trajectories the density is limited to the region at two meters distance from the corridor entrance.

Contrary to the *clean* sets, the primary effect of noise is to create a loss of accuracy with increase of density. This derives from the fact that the negative effect of the noise at every trajectory step is proportional to the amount of steps with interactions and the increase of density increases the number of interactions. This can be seen in figure 5.13 that presents the same density plot as figure 5.10 but without the well defined regions with high accuracy. On the contrary the region with high density has inaccurate calibrations reflecting the negative effect of the noise at each time-step.

Figure 5.3(b) shows how the optimisation process is affected by the noise in the trajectories. The optimisation algorithm compensates the difficulties in finding the optimal values by estimating larger values of τ and smaller values of a_0. This tendency creates pedestrians that are more manoeuvrable and walk closer (see discussion in section 3.2.5). This finding can be used to restrict the lower and upper boundaries of these two parameters during calibrations with prior-information.

The calibration of a_W is also significantly affected by the noise. Table 5.4 shows that the introduction of noise increased the calibration errorsr. Also for the *noisy* set the poorness of data remained the largest cause of inaccurate a_W calibrations.

For all parameters, the significance was not very affected by the noise showing that the

poorness of data is the largest cause for loss of significance in the calibrations.

5.3.4 Conclusion

The use of the different sets allowed us answering the first research question by identifying and discussing three factors that affected the accuracy of the calibrations, poorness of data about pedestrian behaviours, the complexity of movements when pedestrians forced their way inside a congested flow near a bottleneck and errors caused by tracking noise. Each of the factors affect the accuracy in different ways and intensity.

The noise has the largest impact resulting in differences between the clean and noisy errors of $\sim 15\%$ for all flows indicating that care must be taken when tracking and smoothing pedestrian trajectories. More importantly the noise did not affect the amount of significant calibrations.

The poorness of data also has a large impact but its effect can be easily avoided by identifying parameters that originated from trajectories with very small accelerations. Its main contribution is in reducing the amount of significant calibrations.

The most difficult factor to avoid is what we call complexity of movements. These accounted for $\sim 10-20\%$ of the errors for the *clean* narrow bottleneck. When inspecting the trajectories for the bidirectional and the crossing flows we could observe some instances in which pedestrians would also apply sharp changes in direction. However, these did not affect the accuracy significantly because the rest of the trajectories were smooth. This indicates the difficulty in identifying the effect of complex manoeuvres.

5.4 Multi-scenario calibrations

The multi-scenario calibrations followed the procedure presented in section 5.2.1. The log-likelihoods of the three flows (called *multi-3-flows* in the remainder) or ten trajectories (*multi-10-bidi*) were added and used by the optimisation algorithm. The results for the *clean* trajectories in figure 5.14(a) and in table 5.5 shows that the multi-scenarios presented the same excellent results for the parameters a_0, r_0 and τ as for the single objective bidirectional and crossing flows.

Pairing 10 trajectories in multi-10-bidi with the same optimal parameters (clean trajectories) produced better results than for the three trajectories of the multi-3-flows. 10 trajectories produced by the same parameter sets presents a large amount of information to the optimisation algorithm increasing the chance to reach optimal results.

The multi-3-set presented good results for a_0, r_0 and τ as well, indicating that the problems of poorness of data and complexity of movements presented by the calibrations with the narrow trajectories are overcome with the multi-3-flows and that the

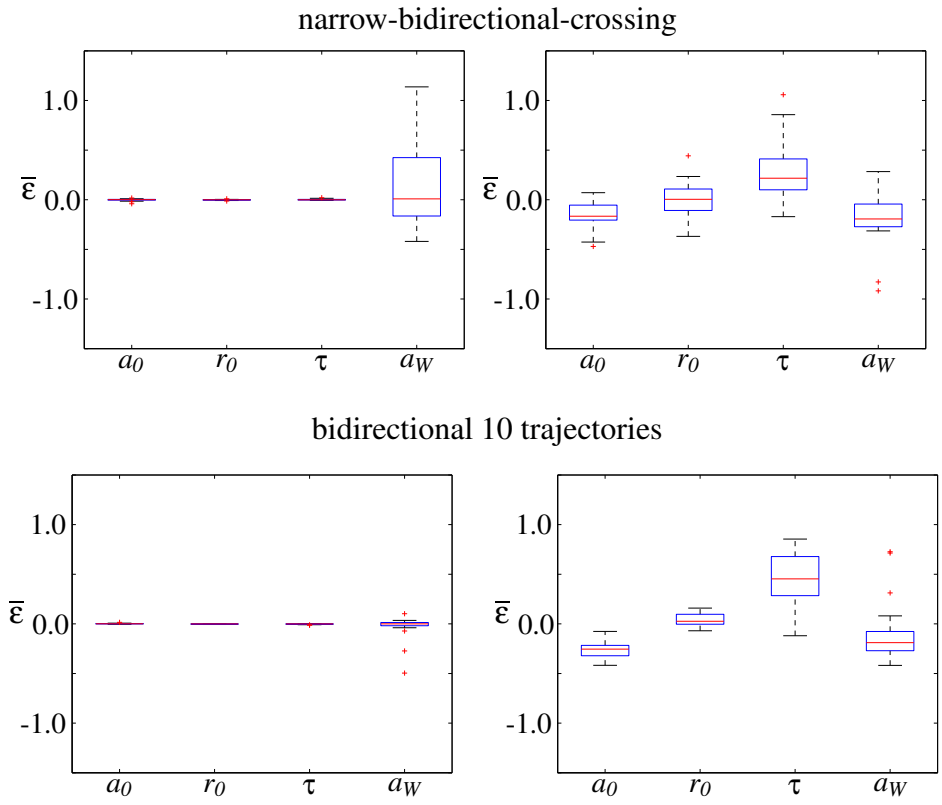

(a) clean (b) noisy

Figure 5.14: Estimation errors for all *clean* and *noisy* multi-scenario calibrations.

Table 5.5: The average relative errors ε for the multi-scenario calibrations using the mean of the original parameter distributions. The values in brackets include only the significant calibrations. The values below are the percentages of significant calibrations from the total.

		multi-3-flows			multi-10-bidi		
		a_0	r_0	τ	a_0	r_0	τ
clean	ε	0.01	0.00	0.01	0.00	0.00	0.00
	(% sig.)	(100)	(100)	(100)	(100)	(100)	(100)
noisy	$\overline{\varepsilon}$	0.16	0.12	0.31	0.23	0.06	0.47
	(% sig.)	(100)	(100)	(100)	(100)	(100)	(100)

optimisation algorithm can correctly find the parameter values of a_0, r_0 and τ for both multi-scenarios.

The a_W parameter was more affected by poorness of data for the multi-3-flows. Table 5.6 shows that the results with the *clean* set of the multi-scenarios is worse than those for the narrow bottleneck flow. Differently, the multi-10-bidi resulted in much better accuracy and amount of significant calibrations than both the narrow bottleneck flow and the multi-3-flows.

Table 5.6: The average relative errors ε and standard deviations for the a_W parameter. The values in brackets include only the significant calibrations. The values below are the percentages of significant calibrations.

		a_W (significant)					
		narrow		multi-3-flows		multi-10-bidi	
clean	ε	0.24	(0.12)	0.36	(0.19)	0.05	(0.05)
	(% sig.)		(84)		(80)		(100)
noisy	ε	0.41	(0.26)	0.23	(0.17)	0.25	(0.23)
	(% sig.)		(80)		(92)		(96)

The fact that only one of the three flows provided information about obstacle interaction created more difficulties for the calibration procedure. The decrease in accuracy for a_W with the *clean* for the multi-3-flow set can also be attributed to a larger amount of trajectories without many lateral accelerations in the corridor than with those used in the single-scenario narrow bottleneck calibrations (not shown). An indication of this larger poorness of data is the lower amount of significant multi-scenario calibrations.

The multi-10-bidi produced very good results for a_W because the groups of 10 trajectories presented on average 3 trajectories with pedestrians walking close to the lateral walls. These 3 trajectories contained enough information for the optimisation algorithm to find the optimal value of a_W.

The next section presents the analysis of the effect of noise in the multi-scenario calibrations and compare with the single scenario calibrations. After that we discuss the effect of the three flows in the results of the multi-3-flows and end the section with the conclusions on the impact of multi-scenario calibrations in the accuracy and the amount of significant of parameters.

5.4.1 Effects of noise in the calibration

Table 5.5 shows us that the multi-scenarios maintained the 100% significant calibration statistic obtained with the bidirectional and the crossing flows. This indicates the robustness of the multi-scenario calibration.

The comparison of the accuracy for the *noisy* trajectories must be done using errors $\overline{\varepsilon}$ calculated with the mean μ^{sy} of the normal distributions. Therefore, we need to recalculate the single-scenario errors shown in table 5.5 using the mean instead of the correct values. Table 5.7 shows the differences in the errors for the two calculation methods for the flows.

The table shows that in general the errors with the means are larger than with the correct values. This reflects the accuracy of the calibrations. The smaller the errors

Table 5.7: The average relative errors ε for the individual flows calculated with the correct values θ_i^{sy} and with the mean μ^{sy} of the distributions.

	flows									
	bidirectional			crossing			narrow			
	a_0	r_0	τ	a_0	r_0	τ	a_0	r_0	τ	a_W
noisy (correct)	0.16	0.06	0.20	0.18	0.06	0.20	0.21	0.08	0.35	0.41
noisy (mean)	0.17	0.16	0.22	0.18	0.12	0.23	0.28	0.12	0.61	0.41

with the correct values the larger will be average distance between the calibrated value and the mean of the distribution μ^{sy}. This explains the large variation for the r_0.

The amount of this difference is also dependent of the coefficient of variation ($c_v = \sigma^{sy}/\mu^{sy}$) of the original distribution (table 5.1). Small c_v will decrease this difference by creating small dispersions of the correct values around μ^{sy}. This explains the small differences for a_0 that presents the smallest c_v.

When the errors and the coefficient of variation are large then anything can happen. The calibrated parameters do not follow the original distribution and larger errors most likely will increase the variation. This explains the very large difference for the τfor the narrow. The a_W was constant and no variation could occur.

Comparing the mean results for the *noisy* set in table 5.7 with those in table 5.5 we observe that the multi-3-flow produce errors for a_0, r_0 and τ that are smaller than those from the narrow bottleneck flow and comparable with those from the bidirectional and crossing flows for all parameters. This shows the beneficial influence of combining three different flows in the multi-scenarios.

The noisy set of multi-10-bidi resulted in larger errors for a_0, r_0 and τ than those of the multi-3-flow set but still smaller than the errors from the narrow bottleneck. Using 10 trajectories of the bidirectional flow creates a large dispersion of the optimal parameter sets around the mean of the distribution. This increases the difficulty for the optimisation algorithm in finding the optimal values resulting in the opposite effect obtained with clean trajectories. The multi-3-flow is less affected by this problem by only using 3 different optimal values for each calibration.

Table 5.7 shows that contrary to the multi-scenario calibrations with the *clean* set, the calibrations with the *noisy* set improved both the accuracy and the significance of the a_W parameter. The improvement of the accuracy is not large but the percentage of significant calibrations increases with the amount of trajectories that present proximity to walls. Thus, explaining why the multi-10-bidi presents the best results for significance.

The good qualities of the multi-3-flows calibration with noise and heterogeneity can be observed by the cumulative distribution of the calibrated parameters compared to the calibrations using the bidirectional and crossing flows (figure 5.15).

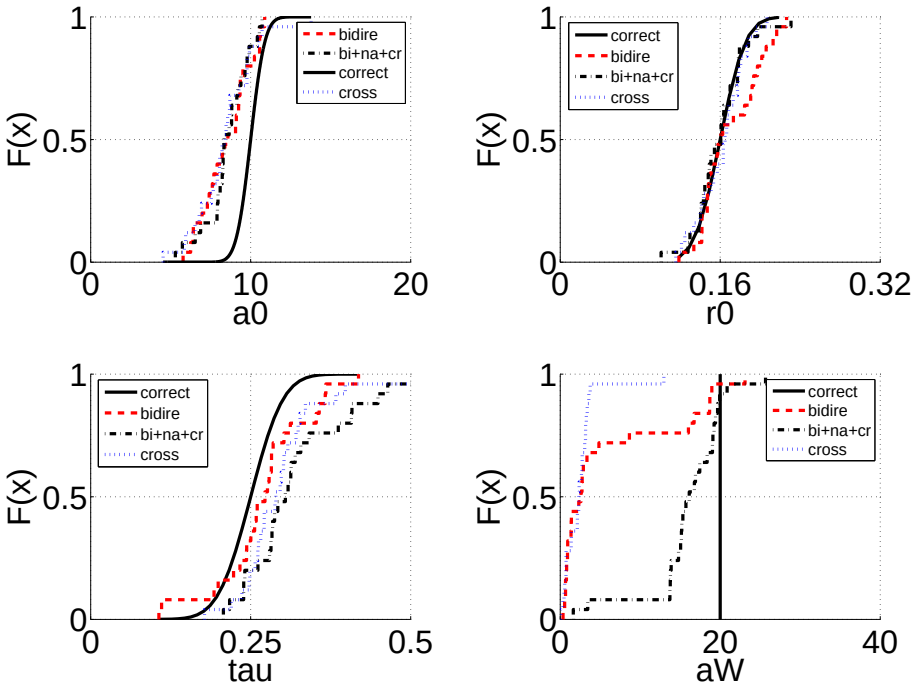

Figure 5.15: The cumulative distribution of the parameters estimated for the bi-directional, crossing and the multi-scenario with the *noisy* trajectories.

5.4.2 The influence of the flows in the multi-3-flow calibrations

To have a better understanding of the multi-3-flow calibration process, we compared the overall influence of each flow to the final calibration results. This is done by computing the errors for each flow with the correct parameter value for this scenario θ_i^{sy} instead of the mean of the distribution μ^{sy}. We rename this error to parameter distance $d_s(\theta_i^*)$ for scenario s.

Low values of d_s for a flow indicates that the calibrated parameter was closer to the correct values of this flow. If we compare the average of d_s for the flows we can measure which flow had a larger influence on the calibration procedure.

Table 5.8 shows that the bidirectional flow has the smallest average of all distances for a_0, r_0 and τ. The narrow bottleneck flow showed larger distances than the crossing flow for τ and exactly the same for the other two parameters. This also supports the result that in general the multi-scenario calibration approximates the flows that are less influenced by the noise. The a_W distances are necessarily the same because this parameter was the same for all flows.

Table 5.8: The average relative distances between the correct values of the parameters to the calibrated results using the multi-scenario.

		relative distance			
		a_0	r_0	τ	a_W
$\bar{d}_s$	bidirectional	0.23	0.13	0.21	0.84
	crossing	0.26	0.17	0.24	0.84
	narrow	0.26	0.17	0.27	0.84

5.4.3 Conclusion

We can conclude that the multi-scenarios have a positive impact in the calibration accuracy and significance and are more influenced by the scenarios with smaller errors. Even in the unfavourable situation of a_W with only one flow providing information about the obstacle interactions, the errors were closer to the narrow bottleneck than for the other two flows.

The *clean* trajectories produced very small errors for the multi-scenario calibrations showing that the poorness of data and complex movement factors can be mitigated if they are not present in all scenarios.

For the multi-3-flows, the introduction of heterogeneity and noise resulted in errors of a_0, r_0, τ that are between 1 and 9% larger than for the single-scenarios with the best results (bidirectional and crossing flows). Simultaneously the errors for the a_W were reduced by 18% and the significance increased by 12%.

Figure 5.14 shows that for the two multi-scenarios the optimisation algorithm also finds τ that are in general larger and a_0 that are smaller than the mean of the distributions. This reveals the same process discussed for the single-scenario calibrations of estimating pedestrians that are more manoeuvrable.

5.5 Conclusions and findings

The original in this chapter is the quantitative analysis of the calibration process using synthetic trajectories as the ground truth. The investigations identified the factors that reduce the accuracy of calibrations and proved the beneficial effects of using multi-scenario calibrations in increasing the amount of significantly calibrated parameters.

The investigation consisted in two parts: determining the most important factors that affect calibrations and using these factors to discuss the implications of using multi-scenarios.

We determined that three factors: poorness of data, complexity of movements and random noise in the data are the most critical for the calibration accuracy and parameter

significance. The first refers to the availability of data containing information about of pedestrian behaviours such as pedestrian interactions. The second refers to complex manoeuvres with sharp and abrupt movements. The third arises from the imperfect process of acquisition of pedestrian data containing errors and noise.

The most important result from this chapter resulted from the second part of our investigations. We showed that multi-scenario calibrations were positively influenced by the scenarios that produced the most accurate calibrations. These results show that even if some scenarios presented difficult situations to the calibration, other scenarios compensated resulting in good accuracy and increased significance of parameters. This supports the use of multi-scenario calibrations to obtain parameters that are generic and useful.

The investigations showed the importance of the significance analysis in determining the accuracy of sample of parameters. The parameter responsible for obstacle interaction was estimated with extremely low amount of significant calibrations for two of the flows. Without the significance analysis determining the statistical significance the calibrated parameters would be completely inaccurate.

We found that tracking noise had the largest influence in the calibration. This important result shows that the process of tracking pedestrians and smoothing trajectories must be well performed to minimise the introduction of noise in the trajectories.

We defined complexity of movements as large variations of direction coupled with large accelerations. These movements deviate from smooth movements encountered in most flows and create difficulties for the calibration procedure. We identified a particular situation that caused these complex movements. Future investigations could determine quantitative or qualitative indicators that give measures of movement complexity. These measures could be used to identify non-optimal calibrations due to complex movements.

We observed that the calibrations that were inaccurate due to one or more of the three factors previously mentioned produced a bias in the estimated parameters. From the four parameters estimated in this investigation, one parameter was often underestimated whilst the other was mostly overestimated. These biases increase the manoeuvrability of the pedestrians and decrease their interaction distances. The knowledge of these tendencies can be used as prior-information by the optimisation algorithm to improve the calibration in defining upper and lower boundaries for the parameters.

Two important results of this chapter will be used in the following chapters. In chapter 6 we will investigate individual characteristics using single trajectories. We observed that using 10 trajectories created difficulties for the optimisation algorithm resulting in values that are less accurate.

Chapter 7 investigates the effect of multi-scenario calibrations on the accuracy of predictions. The good results of the multi-scenario calibration with different flows motivate us to use three flows to improve the accuracy of parameter sets.

Chapter 6

Investigating microscopic behaviours with calibration

The microscopic pedestrian simulation model Nomad has (like other simulation models shown in chapter 2) a large amount of parameters. The calibration of such complex models is not a simple process given the problem of complexity of behaviours and the information poorness of the available data as discussed in chapter 4.

Furthermore, pedestrian behaviours vary according to several factors such as walking area configurations, traffic conditions and pedestrian heterogeneity. Therefore, it is important to know to which situations a model can be applied for prediction. One way to investigate the general applicability of a walking model is to compare the parameter estimations when varying the different factors.

We showed in chapter 4 that differences in the estimated parameter samples can reflect the inability of the model to correctly predict the different behaviours. If the parameter samples are significantly different then the model is not general enough and the samples reflect variations of pedestrian behaviours. The estimated parameter samples can therefore be used to investigate how pedestrians are behaving in the different situations possibly resulting in insights to improve the model.

This chapter presents the calibration results of Nomad using data from several controlled experiments. The experiments give the opportunity to compare distinct behaviours from different flows such as bidirectional, unidirectional and crossing flows.

We estimate parameters for each pedestrian using the trajectory based calibration introduced in chapter 4. The parameters are simultaneously estimated for each individual pedestrian. The calibration results are used to investigate the parameter significance, parameter correlation and general applicability of Nomad.

The calibrations were performed using trajectories representing three flows that provide behaviours found during normal walking, evacuation through a door and interactions between individual pedestrians. The walking experiments replicating these situations and the other components of the calibration set-up are presented in section 6.1.

Section 6.2 explains how we perform statistical tests based in Kolmogorov-Smirnov goodness-of-fit test to investigate the influence of type of flows and traffic conditions to the pedestrian behaviours and to infer the extent of pedestrian heterogeneity.

Section 6.3 shows that the calibration procedure is able to significantly estimate a large amount of parameters for the Nomad model simultaneously. This section also presents the amount of independence of the parameters by means of their correlation.

Section 6.4 shows that there is a significant variation in the parameter samples along different types of flows and gives an analysis of the causes of these differences. The impact of population composition and urgency levels is discussed in section 6.5.

We also show that traffic conditions influence pedestrian behaviours and we analyse in section 6.6 how the values of the estimates vary with walking speeds as a proxy of local conditions. The discussion of the results of this chapter is in section 6.7.1.

This chapter ends in section 6.7 with the conclusions and the general implications of these results suggesting that microscopic models must account for heterogeneity and variation of behaviours. The results support modifying model parameters according to the actual traffic conditions experienced by pedestrians. Modifications are suggested by creating dependences of parameters to traffic conditions.

6.1 Parameter estimation set-up

In the following, first a short description of the calibration procedure is given. Then, the laboratory experiments of which the data are used. Finally, we present the Nomad parameters that will be estimated, followed by a discussion about the parameters that are not estimated.

6.1.1 Calibration procedure

The model calibrated in this chapter is the modified Nomad model with anticipation and extra lateral repulsion forces presented in chapter 3. The acceleration behaviour does not predict swaying effects. This required that the trajectories of the empirical data sets were transformed via a smoothing procedure to remove the swaying effects. Appendix D presents details about the smoothing algorithm adopted in this chapter.

The trajectory based calibration is described in chapter 4 and the log-likelihood objective function used the error in acceleration. The position of the pedestrian being calibrated was reset at each time-step to minimise auto-correlation in the errors (one step ahead prediction with reset-time $= 0.02s$). The same hybrid genetic algorithm with a simplex optimiser described and used in chapter 4 was applied.

6.1.2 Trajectory data

In this thesis we are interested in behaviours occurring in normal conditions by commuters. These conditions are found in large pedestrian facilities and result in several types of flows, such as unidirectional and bidirectional flows found in corridors, crossing flows in large atriums; and congested flows around exits. Furthermore, there are situations in which the motivation to exit is high but no extreme behaviour is found (see discussion in section 2.3.6). Such situations are found in evacuations or in certain situations when pedestrians have short transfer time. In this chapter we chose empirical data that present data cover normal walking in several types and intensities of flow and different levels of urgency.

The trajectories used in this chapter originate from three types of controlled experiments: a series of normal walking flows (Daamen and Hoogendoorn (2003)), room evacuations through a door (Daamen and Hoogendoorn (2009a)) and one-to-one interaction experiments (Versluis (2010)). Pedestrians in the normal walking and interaction experiments walked under normal conditions. In the evacuation experiments pedestrians were instructed to evacuate as quickly as possible and were induced during the experiments to low and high urgency levels. The interaction experiments were set up forcing the pedestrians to apply avoiding manoeuvres.

The overview of the eleven calibrations performed is presented in table 6.1. The table shows the abbreviation of the trajectory set used in this chapter, the type of experiment that originated the trajectories, the name with a brief description of the walking area arrangement with the type of flow and the amount of trajectories (pedestrians) available to calibrate. The abbreviations will be used as much as possible in the remainder as the identification of the calibrations. We will present some details about the experiments in the next sections and more details can be found in appendix C and in previously mentioned references.

Normal walking experiments

Figure 6.1 shows the infrastructure layout and flow directions of the four configurations of the normal experiments: unidirectional flow, bidirectional flows, crossing flows and a narrow bottleneck. All experiments have been performed under normal walking conditions, while only in the narrow bottleneck experiment congestion occurred. Since the congestion occurred upstream of the corridor, the area of this experiment has been split into two: one (possibly) congested area upstream of the bottleneck and an area inside the bottleneck where capacity occurred. Therefore, five calibrations were performed with the normal experiments.

The bold lines in figure 6.1 represent floor markings that demarcated the borders of the walking areas. Pedestrians were instructed to stay inside these markings as if these were walls. Only the narrow corridor walls were made solid and could not be walked over.

Table 6.1: Description of the 11 calibrations and the amounts of trajectories estimated

abbreviation	experiment type	description	# of traj.
bidir	normal	bidirectional flow	709
unidir	normal	unidirectional flow	1167
cross	normal	90° crossing flow	1052
bneckDown	normal	unidirectional flow downstream the bottleneck	1123
bneckUp	normal	unidirectional flow upstream the bottleneck	1123
evacHoLoSt	evacuation	homogeneous population with low urgency	78
evacHoHiSt	evacuation	homogeneous population with high urgency	81
evacHetLoSt	evacuation	heterogeneous population with low urgency	99
evacHetHiSt	evacuation	heterogeneous population with high urgency	99
interBidir	interaction	bidirectional	168
interCross	interaction	crossing	144
		total	**5843**

The dotted rectangles are used for the calibrations. Experiment *cross* used only the positions inside the region in which interaction behaviour happened (the dotted square 'c' with dimensions $4m \times 4m$ inside the crossing area shown in figure 6.1. The calibration for *bneckDown* used the positions inside the corridor that are downstream of the bottleneck (dotted rectangle 'a' in figure 6.1), while the calibration for *bneckUp* upstream the narrow corridor used only pedestrian positions inside the rectangle 'b'.

Evacuation experiments

The evacuation experiments were not being held under normal walking conditions. The four evacuation experiments have the same walking layout but two different population compositions and two levels of induced urgency as different human factors[1]. These urgency levels created a sense of urgency that was not present in the two other experiment types.

The homogeneous population (*Ho*) was composed by adults only and the heterogeneous population (*Het*) was composed of 25 % children, 55 % adults, and 20 % elderly that correspond approximately to the average of the Dutch population. We called the two urgency levels normal (*Lo*) and high (*Hi*). The density in all evacuations varied between $0.0 < k < 3.0\ peds/m^2$.

The four evacuation experiments are composed of a combination of these four experimental variables (see table 6.1). The evacuation experiments were split into upstream

[1]The authors of the original experiments called the variable as *stress* in Daamen and Hoogendoorn (2009a) but we will adopt the term *urgency* as explained in the chapter 2.

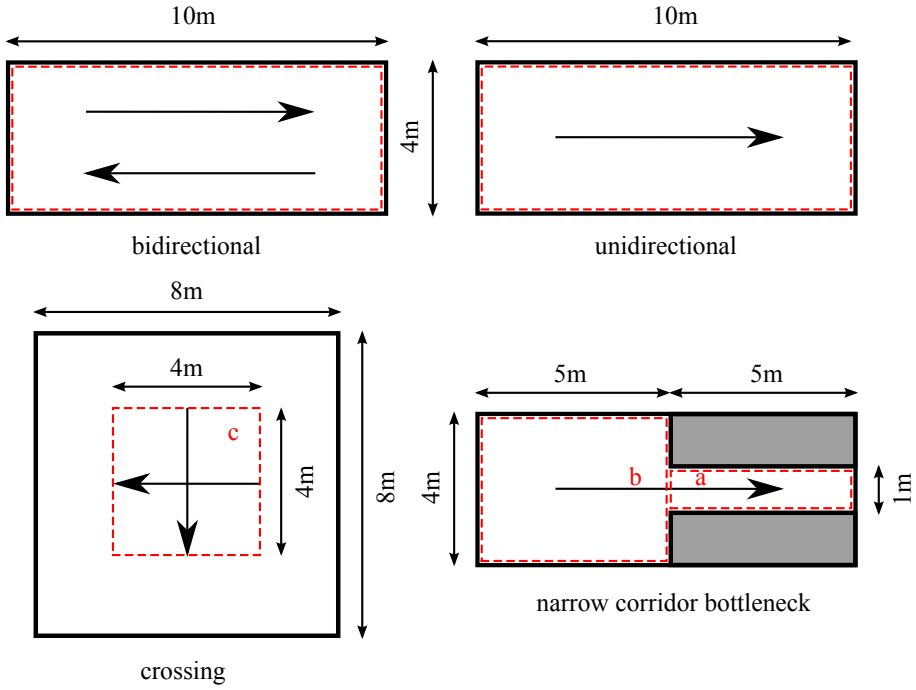

Figure 6.1: Schemes of the areas in which the trajectories where located for the normal walking calibrations. The arrows represent the dominant direction of the flows. The red dotted areas define the perimeter of the trajectories used for calibration.

and downstream flows in relation to the evacuation door, just like in the narrow bottleneck experiment. This was done because the behaviours exhibited by the participants was significantly different in these two situations. Upstream of the door pedestrians made a real effort to evacuate as fast as possible and downstream they dispersed in a relaxed manner. The upstream behaviours are more relevant for evacuation analysis and therefore only those trajectories were included in the estimation. Figure 6.2 shows the rectangle 'e' that enclosed the pedestrian positions used in the calibrations.

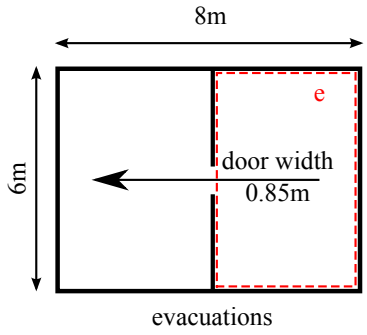

Figure 6.2: Schemes of the areas in which the trajectories where located for the evacuation calibrations (red dotted areas). The arrows represent the dominant direction of the flows.

Interaction experiments

In these experiments the focus was to create conditions to pedestrians interact in one-on-one situations. The aim was to investigate how pedestrians apply avoidance manoeuvres when walking towards each other under different approach angles. Pedestrians were placed at locations at $10m$ distances and walked towards each other meeting somewhere halfway. The schemes of the experiments are shown in figure 6.3.

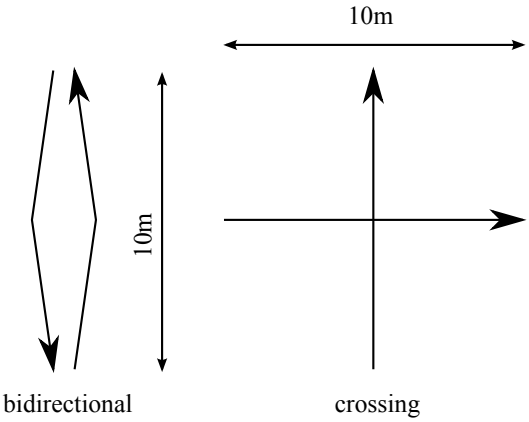

Figure 6.3: Schemes of the areas in which the trajectories were located for the interaction calibrations. The arrows represent the dominant direction of the flows.

6.1.3 Overview of parameters to be estimated

The parameters calibrated in this chapter are those responsible for three behavioural components of the Nomad model: path following, pedestrian interactions and obstacle interactions. Table 6.2 gives a brief description of the role of the parameters that are estimated. For a complete overview and mathematical definitions, see section 3.2.

Table 6.3 shows the calibrated parameters for each experiment and the three corresponding model components. Chapter 5 showed us that poorness of data was a large influence in the amount of significant calibrations. Therefore, a_W is only included in the evacuation experiments and the two calibrations using the narrow bottleneck experiment. The other experiments did not present obstacles to provide such behaviours.

Figure 6.4 shows how Nomad would incorrectly predict collisions for radius around $0.25m$ that is the average body width according to Fruin (1971) (image from the evacuation experiments).

Such situations mostly occur in the evacuation experiments. Therefore, *rad* is calibrated for the evacuation experiments. However, non-existing collisions can also occur in the remaining experiments, especially in the narrow bottleneck. To prevent non-existing collisions to interfere in the calibrations we adopt a smaller value of $rad = 0.22m$ to all pedestrians. This radius expresses body depth according to Fruin (1971). A small radius also reduces the lateral width of each pedestrian. This is not a

Table 6.2: Overview of the parameters calibrated in this chapter. The double lines separate the parameters according to the pedestrian characteristics and the three model components: path following, pedestrian and obstacle interactions. The single lines separate the four parts of the pedestrian interaction component: pedestrian avoidance, influence area, lateral avoidance and anticipation.

Symbol	Explanation
rad	pedestrian radius (m).
τ	acceleration time (s), the time required to accelerate towards the free speed v_0 in the direction of the desired path. Small values of τ will force pedestrians to walk very close to their desired path and to their free-speeds. Deviations from the path will generate large path following accelerations.
a_0	interaction strength (m/s^2), controls the intensity in which pedestrians are avoiding each other. Larger values of a_0 indicate an increase of the avoidance accelerations due to other pedestrians.
r_0	interaction distance (m), controls how sensitive the avoidance accelerations are to the distance between pedestrians. Small values of r_0 signify that only small distances between pedestrian cause avoidance accelerations.
c_0^-	transforms the shape of the influence area behind pedestrians from circular (value = 1) to an ellipsoid. For values smaller than one the main axis of the ellipsoid is in the walking direction otherwise; in the perpendicular direction.
c_0^+	transforms the shape of the influence area in front of pedestrians from circular to an elongated ellipsoid similar to c_0^- .
ie_f	influence area extension at the front (m), the largest distance at the front at which a pedestrian will provoke avoiding behaviours.
ie_b	influence area extension at the back (m), the largest distance at the front at which a pedestrian will provoke avoiding behaviours.
a_l	lateral interaction strength for pedestrians (m/s^2), controls the intensity of the extra lateral component of the avoidance accelerations when pedestrians are walking towards each other.
r_l	lateral interaction distance for pedestrians (m), controls how responsive the extra lateral avoidance accelerations are to the lateral distances of pedestrians walking towards each other.
t_A	anticipation time (s), the time in the future that pedestrians project the current locations of neighbouring pedestrians.
a_W	obstacle interaction strength (m/s^2), controls the intensity in which pedestrians are avoiding obstacles. Larger values of a_W indicate an increase of importance of the obstacle avoidance accelerations.

problem for the estimation of the parameters because Nomad model uses the centre of pedestrians and not their shoulder distances.

Table 6.3: The parameters that are calibrated in each experiment.

parameters		path follow	pedestrian interactions									obst-acle
			ped avoid		influence area				lateral avoid		antici-pation	
experiments	*rad*	τ	a_0	r_0	c_0^-	c_0^+	ie_f	ie_b	a_1	r_1	t_A	a_W
bidir		×	×	×	×	×	×	×	×	×	×	
unidir		×	×	×	×	×	×	×	×	×	×	
cross		×	×	×	×	×	×	×	×	×	×	
bneckDown		×	×	×	×	×	×	×	×	×	×	×
bneckUp		×	×	×	×	×	×	×	×	×	×	×
evacHoLoSt	×	×	×	×	×	×	×	×	×	×	×	×
evacHoHiSt	×	×	×	×	×	×	×	×	×	×	×	×
evacHetLoSt	×	×	×	×	×	×	×	×	×	×	×	×
evacHetHiSt	×	×	×	×	×	×	×	×	×	×	×	×
interBidir		×	×	×	×	×	×	×	×	×	×	
interCross		×	×	×	×	×	×	×	×	×	×	

Figure 6.4: Two pedestrians walking close but not colliding in the evacuation experiment. The circular body formulation in Nomad predicts a collision.

6.1.4 Parameters not estimated

Three parameters were not included in the calibrations: the free-speed (v_0) and the two parameters that are used to calculate the physical forces (k_0, k_1). In the following, we discuss the main motivation for these exclusions.

Free-speeds

Since the free-speed is specific for each pedestrian, this speed is estimated using the beginning of the trajectories when the densities are low and it can be assumed that a pedestrian is walking in free flow conditions.

In the normal experiments the free-speeds of pedestrians were calculated as the av-

erage speed in their first second in the walking area. This procedure was motivated by the arrangement of the walking areas where pedestrians were only tracked after walking a few meters and the densities at the regions of their initial positions were low. This initial non-tracked walking enabled pedestrians to 'warm-up' reaching their free-speeds. Given that the trajectories used in the calibrations were obtained after smoothing out the original positions the interval of 1s was sufficient to overcome the observation noise.

The evacuation experiments did not allow such a free-speed calculating method because in all four experiments there was a spill-back of the congestion towards the initial positions of the pedestrians. This congestion decreased the speeds far below free-speeds values given by literature. Therefore, for all pedestrians a constant value of $v_0 = 1.5m/s$ obtained from Daamen and Hoogendoorn (2003) was used.

Fixing the free-speeds may affect the calibrations, specially for the children and elderly in the heterogeneous population in the evacuation experiments. According to equation (3.11) if the free-speeds are higher or lower than the correct values, the resulting τ will be larger to reduce the path following accelerations. This may explain partially, the larger values of τ as presented in table 6.6 for the evacuation experiments. However, the results for the heterogeneous population (that include the children and elderly) showed smaller values of τ indicating that other reasons discussed in the next sections are more important for these large values.

For the interaction experiments we could obtain the free-speed for each individual in dedicated runs. Each subject walked alone and unimpeded eight times a distance of $12m$. The average speed on each run was used to create a sample of free-speeds and the average of this sample would constitute the pedestrian's free-speed.

Physical forces

The parameters used to calculate the physical forces are set to very large values that were proven to prevent large compressions of pedestrians in previous calibrations. Therefore, it was not necessary to estimate them and the values $k_0 = 1000, k_1 = 1000$ were kept fixed.

6.2 Parameter analysis for the calibrations

A parameter set θ_p^* is constituted by the calibrated parameters for a pedestrian p ($\theta_p^* = [\tau_p, a_{0p} \ldots]$). All parameters θ_p^{i*} for one experiment are are grouped in samples of parameters θ^{i*}. One experiment will therefore result in a collection of samples $\theta^{i*} \in \theta^*$. Table 6.1 presents the maximum sample size of each experiment. An estimated value will only be part of the sample if it is significant according to the method shown in section 5.2.1. Values that are on the boundaries of the estimation interval available for

the optimisation algorithm are not part of the sample since we cannot guarantee that they are optimal.

The following subsections explain how the parameter samples are used in the investigations of this chapter.

6.2.1 Analysing the calibration results

In this chapter we discuss the results of the calibrations using the average values of the samples, their correlations and the percentage of significant calibrations. The correlations between the parameters are only calculated among pairs of significant estimations for the same experiment. This limits the size of the set of pairs of parameters to be used in the correlation calculation to the smallest amount of significant parameters from both parameters.

If two samples present a large degree of correlation (or anti-correlation) then the behaviours associated with the parameters are linearly related. If the correlation is close to 1 in all experiments then one of the parameters could be replaced by a linear relation of the other. However, we show in section 6.3 that the high non-linearity of the Nomad model does not result in wide spread correlations. The significance is calculated according to the procedure used in section 5.2.1.

The extra lateral acceleration parameters presented in section 3.2.9 resulted in very small samples of significant calibrations. We tested if the cause of these results were due to the lack of sufficient situations requiring the extra accelerations (poorness of data) in the experimental data or that their limited influence in the outcomes of the Nomad model. We applied likelihood-ratio test to compare Nomad with the two extra lateral acceleration parameters (*unrestricted* model) with a version without them (the parameters are set to zero and the model called *restricted*).

The test involves calculating the likelihood ratio (D) that corresponds the differences of the log-likelihoods:

$$D = 2\left[\ln(\text{likelihood}_u) - \ln(\text{likelihood}_r)\right] \tag{6.1}$$

Then a chi-squared distribution ($\tilde{\chi}^2$) with degrees of freedom equal to the difference of the number of parameters (for the lateral avoidance parameters the difference is two) is used to approximate the test probability distribution of of D with $\alpha = 95\%$.

null hypothesis - The unrestricted model is not significantly better than the restricted model.

alternative hypothesis - The unrestricted model is significantly better than the restricted model.

Since the unrestricted model has more parameters it is supposed to fit the data better. Therefore, if the log-likelihood of the restricted model (llr) is not reduced then the test failed and the unrestricted model is worse. However, if $llu - llr > 0$ we apply the likely-ratio test to see if the improvement is significant.

6.2.2 Testing the impact of type of flow on pedestrian behaviours

We discuss the influence of the type of flows in pedestrian behaviours using Kolmogorov-Smirnov tests and the sum of Kolmogorov-Smirnov statistics of parameter samples in what we called Similarity Statistics (ST).

An inspection of the estimated parameter distributions shows that they are very deviant from a normal distribution making parameterised statistical tests such as student t-tests and analysis of variance (ANOVA) tests not applicable. Therefore, we choose Kolmogorov-Smirnov tests to perform our statistical analysis of similarity between samples, since this test is independent of the distribution type.

To establish if two estimated parameter samples come from the same distribution we perform a two sample Kolmogorov-Smirnov test with 5% significance level. The null and alternative hypothesis are:

null hypothesis - The two samples are realisations of the same distribution.

alternative hypothesis - The two samples are not realisations of the same distribution.

We test the impact of the type of flow on the estimated parameter values by two criteria: showing that the samples θ^{i*} for each experiment are significantly different from each other (rejecting the null hypothesis) and comparing the sum of the KS statistics of all samples for two experiments.

Both criteria define the degree of similarity between the experiments and consequently represent the degree of similarity between the behaviours in the experiments.

The first criteria uses the KS test and applies it for all samples of the same parameter obtained in the different experiments. Every time the null hypothesis is rejected the samples are statistically different and the walking behaviours that created the trajectories are significantly different. The first criteria of is the percentage of rejection of the KS tests between two experiments. The more rejection the less similar the experiments.

The second criteria uses the result of the KS statistic as a measure of similarity between the samples (see figure 7.1 for a representation of the KS statistic for two samples). Independently if the samples passed the equality KS test, the KS statistic can always be used to show the degree of similarity between the samples.

To simplify the analysis we add the KS statistics $D_{a,b}$ from all KS tests between the samples θ^i of experiments $[a,b]$. This results in the sum of the KS statistics ($ST_{[a,b]}$). The assumption is that the sum of the KS statistic can be considered another indicator of similarity between the types of flows represented by the experiments. The smaller the ST the more similar are the behaviours in the experiments.

$$ST_{[a,b]} = \sum_{\theta^i \in \theta^*} D_{[a,b]}(\theta^i) \tag{6.2}$$

All KS tests are only performed between samples of the same experiment types, eliminating other sources of differences that could mask the results for the types of flows. This strategy generates 10 comparisons for the normal, 6 comparisons for the evacuation and 1 comparison for the interaction experiments for each parameter. These numbers are obtained by the combination of the amount of experiments in pairs of each type.

6.2.3 Testing the population composition and urgency level on pedestrian behaviours

The influence of types of flow are investigated for the normal and interaction experiments. The evacuation experiments are very similar to each other and an investigation of the differences between the samples measures the effect of the two experimental variables: population composition and urgency level, rather than type of flow. Therefore, the similarity statistic results for the evacuation experiments are presented separately.

6.2.4 Measuring pedestrian behaviours based on walking speeds

The most frequently used definitions of traffic conditions come from the so called fundamental relations (chapter 2). In this investigation we use the speed as the independent investigation variable because it can be directly measured without requiring assumptions on the density or flow definitions. Since the duration of the trajectories is several seconds, we use the average speed along the entire trajectory.

The basic hypothesis here is that for each pedestrian the parameter estimated is optimal for the entire trajectory therefore averaging the speed reflects the average behaviour during the trajectory. The relationship between behaviour and speed varies according to the conditions created by the flows. Therefore, for each speed range we will include the influence the different conditions on the behaviours.

The average walking speed during each trajectory is calculated and classified into intervals of $0.20 m/s$. Each interval (given that there are pedestrians walking within the

interval) forms a sample of parameters. The influence of the speeds on the behaviours is analysed by comparing the average values of the estimated parameters in the different intervals. These average values are plotted against the speed intervals.

No normal experiment presented speeds between $0m/s$ and $0.20m/s$ and no experiment had more than 4 pedestrians with speeds above $2.0m/s$. Table 6.4 presents the intervals and the total amount of pedestrians that walked with speeds that were in the intervals. These values represent the maximum possible size of the parameter samples. However, for the analysis the samples are composed of significant parameters thus the intervals most likely have smaller sizes. Furthermore, we only considered samples with at least five significant parameters to reduce the influence of outliers.

The evacuation and interaction experiments did not present enough estimations in the different speed intervals to allow a proper statistical analysis of the speed intervals. Therefore, only the results for the normal walking experiments are considered in this analysis.

6.3 Calibration results

Table 6.5 with average values of calibrated parameters allow for general discussion of the calibration results. This discussion is presented in subsection 6.3.1.

This section also discusses the reasons why certain parameters present low percentage of significant calibrations for some experiments (table 6.6). The discussion of significance in calibrations is presented in subsection 6.3.2.

6.3.1 Average parameter values and correlations

The three different types of experiment present parameter values that reflect the different situations pedestrians are encountering. After the initial discussion for τ, a_0 and r_0 we will discuss the results of the remaining parameters.

Results for τ, a_0 and r_0

This section presents discuss the calibrations of τ, a_0 and r_0. These three parameters are arguably the most important driving the behaviours of pedestrians and focusing on them simplifies the analysis.

Nomad pedestrians following closely to desired paths, need larger path accelerations to reduce the movements in case of interactions with pedestrians or walls. Thus, acceleration time parameter τ tend to be small for trajectories that stay close to desired paths (section 3.1).

Table 6.4: The speed intervals used to classify the estimated parameters and the maximum size the parameter samples can have per interval. The table only presents the normal experiments. The evacuation and interaction experiments did not present enough calibrations to create many samples with the minimum sample size of 5 parameters.

	Amount of observations										
speeds (m/s)	0.0-0.2	0.2-0.4	0.4-0.6	0.6-0.8	0.8-1.0	1.0-1.2	1.2-1.4	1.4-1.6	1.60-1.80	1.8-2.0	2.0-
bidir	0	0	0	0	3	154	391	145	16	0	0
unidir	0	0	0	0	2	64	496	505	95	5	0
cross	0	0	0	0	41	172	378	283	82	11	4
bneckDown	0	0	0	96	648	204	110	48	14	2	1
bneckUp	0	307	257	162	104	76	98	69	41	7	2

Table 6.5: The average values of the significant parameters for the eleven calibrations. The first column has the average walking speed for all trajectories. The parameters that showed no significant estimations were replaced by a cross (×). Empty spaces are parameters that were not calibrated.

			path follow	**pedestrian interactions**									**obst-acle**
				ped avoid		**influence area**				**lateral avoid**		**anticipation**	
	$\overline{v}$	*rad*	τ	a_0	r_0	c_0^-	c_0^+	ie_f	ie_b	a_1	r_1	t_A	a_W
bidir	1.30		0.32	2.02	1.24	0.94	1.01	1.30	1.98	7.08	0.69	0.53	
unidir	1.41		0.27	2.39	1.45	1.01	1.03	1.42	1.82	×	×	0.61	
cross	1.35		0.62	2.42	0.99	1.00	1.00	0.96	1.10	4.71	×	0.52	
bneckDown	1.00		0.63	4.51	1.28	1.07	1.06	1.04	1.51	×	×	0.56	9.43
bneckUp	0.74		0.57	2.84	1.06	0.99	0.96	1.36	1.14	5.97	0.62	0.60	9.02
evacHoLoSt	0.60	0.12	1.06	1.36	0.59	1.28	0.89	1.28	0.89	1.64	0.85	0.70	×
evacHoHiSt	0.64	0.12	0.86	1.52	0.59	1.26	0.93	1.30	0.85	2.40	0.71	0.70	×
evacHetLoSt	0.50	0.09	0.99	1.26	0.63	1.32	0.94	1.55	0.78	1.06	0.71	0.76	0.96
evacHetHiSt	0.46	0.11	0.82	1.65	0.61	1.36	0.91	1.53	0.75	1.45	0.83	0.59	×
interBidir	1.50		0.08	2.45	×	0.92	1.03	1.51	2.01	2.49	×	0.54	
interCross	1.57		0.14	5.66	0.91	1.03	1.00	1.66	1.52	7.12	0.92	0.69	

Table 6.6: Percentages of significant parameters in each experiment.

		path follow	**pedestrian interactions**									**obst-acle**
			ped avoid		**influence area**				**lateral avoid**		**antici-pation**	
	rad	τ	a_0	r_0	c_0^-	c_0^+	ie_f	ie_b	a_1	r_1	t_A	a_W
bidir		49	58	10	66	62	62	68	7	1	57	
unidir		75	62	17	60	71	71	71	0	0	56	
cross		52	36	3	40	55	43	28	2	0	48	
bneckDown		72	91	32	72	81	72	79	0	0	61	28
bneckUp		66	75	21	55	66	58	53	3	1	53	13
evacHoLoSt	71	92	96	92	90	87	62	55	6	8	73	0
evacHoHiSt	72	95	98	89	81	86	77	59	7	5	65	0
evacHetLoSt	60	94	84	82	82	86	63	48	7	4	68	1
evacHetHiSt	74	99	92	90	80	91	77	53	3	8	78	0
interBidir		67	17	0	45	21	24	41	8	0	37	
interCross		69	34	2	28	42	58	39	5	2	69	
average	69	66	65	21	59	67	61	58	4	3	56	8

This is exactly what happens to the bidirectional, unidirectional experiments. In these two experiments, densities were small allowing for very unobstructed walking. For larger densities in the bidirectional flow, the self-organised lane formation resulted in trajectories fairly parallel to the main walking directions also resulting in lower values of τ.

The interaction experiments produced very smooth trajectories because pedestrians were separated by long distances giving them plenty of time to avoid the incoming pedestrians as shown in figure 6.5. The smooth trajectories resulted in the smallest values of τ.

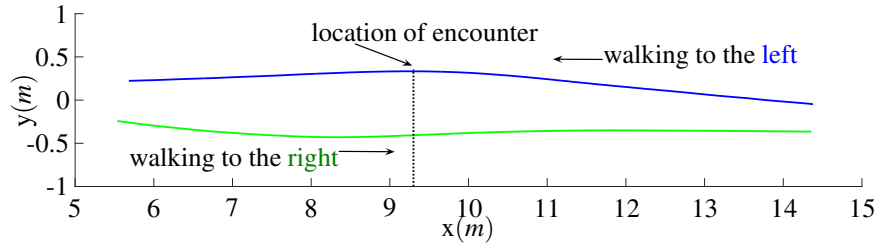

Figure 6.5: Two interacting trajectories from the bidirectional experiment.

The other experiments resulted in larger values of τ, reflecting the larger variations in speed and direction of movement. The crossing flow presents avoidance manoeuvres even with low densities creating deviations from the desired path. Figure 6.6 presents two interacting trajectories represented by dots corresponding to time steps of 0.2s. The pedestrian walking from the top to the bottom realises the avoidance maneuverers, whilst the pedestrian walking from the right to the left walks at a higher speed almost unperturbed.

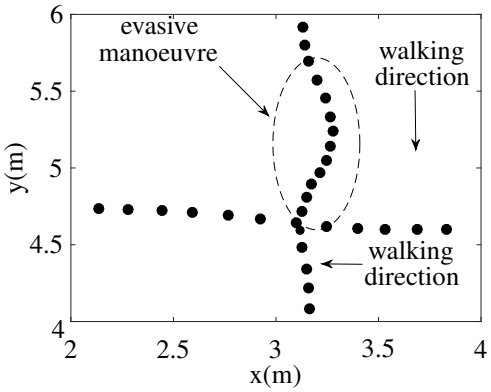

Figure 6.6: Two trajectories from the normal crossing experiment, illustrating the large avoidance manoeuvres that occur even in low densities. The dots corresponds to time steps of 0.2s.

The evacuation and narrow bottleneck experiments result in larger values of τ due to the slower speeds that pedestrians are experiencing. In these experiments, the path following acceleration is always large due to the difference between the walking and

the free-speed. To limit the value of the path following acceleration, τ results larger. This is why the largest values of τ occur for the evacuation experiments that presented the lowest walking speeds (first column of table 6.5).

The values of the interaction strength parameter a_0 give a measure of the intensity of the interaction accelerations. The bidirectional, unidirectional and interaction bidirectional experiments present mostly longitudinal interactions in smooth trajectories. a_0 for these experiments, reflect the deceleration in case of slower pedestrians downstream. The self-organised lanes in the bidirectional flow create more interactions than the unidirectional flow. Pedestrians also mostly follow each other but do not spread laterally reducing the interactions. Thus, the smaller value of a_0 for the bidirectional flow.

A similar situation occurs with the evacuation experiments. In these flows, pedestrians walk very close in a synchronised pattern that result in smooth trajectories with very little overtaking maneuverers. These small distances result in even smaller values of a_0 for the evacuation experiments.

The crossing and narrow bottleneck upstream flows present similar values of a_0 as the unidirectional flow indicating the need for larger interaction accelerations to allow for avoiding maneuverers. The complex movements in front of the corridor entrance described in section 5.3.2 requires even larger interaction acceleration, thus the larger value of a_0 for the narrow bottleneck upstream experiment in comparison to the unidirectional and crossing flow.

The self-organised 'zipper' pattern observed in the narrow corridor creates very short distances between pedestrians and corridor walls (section 2.3.5. These short distances are better modelled with large pedestrian and obstacle accelerations. Otherwise, Nomad would create oscillations in the corridor. This also explains the positive correlation of 0.84 between these two parameters indicating their linear dependency inside the corridor. Thus, the large values of a_0 and $a_W$for the narrow bottleneck downstream experiment.

The 90° arrangement of the crossing trajectories results in much closer interaction distances than those of the bidirectional interaction experiment. Also the maneuverers are larger for the crossing flow, resulting in significant larger a_0. The normal crossing flows offer more interaction possibilities than the interaction crossing that only have a one-to-one interaction not resulting in such large a_0.

The main effect of the interaction distance parameter r_0 is to change the sensitivity of the interaction acceleration with the distances between pedestrians. Higher densities will result in shorter distances. Thus, higher densities result in smaller values of r_0 as the evacuation calibrations show. Also the crossing, narrow bottleneck upstream and interaction crossing with smaller interaction distances also result in smaller r_0 than for the bidirectional and unidirectional flows. The unidirectional flow presents larger distances between pedestrians, thus resulting in the largest r_0.

The evacuation experiments presented the smaller values of a_0 and r_0. This is due to the higher densities that also created smooth trajectories with little overtaking. These parameters resulted with negative correlation. Table 6.7 shows that the negative correlations are not large but were significant for the four experiments. We included the correlation for the crossing experiment that also presented interactions with short distances. No correlations between these two parameters were found for the other experiments.

Table 6.7: Correlations between the parameters a_0 and r_0 for the evacuation experiments.

experiment	**parameter**	r_0
cross		-0.41
evacHoLoSt		-0.34
evacHoHiSt	a_0	-0.42
evacHetLoSt		-0.41
evacHetHiSt		-0.32

Pedestrian radius

The estimated *rad* for the experiments with homogeneous population was $\approx 0.12m$ (equivalent of a diameter of $0.24m$). The calibration results are much smaller than the average body diameter of $0.46m$ according to Buchmueller and Weidmann (2006), they are closer to the average body depth of $0.28m$ for males reported in the same source. The experiments with heterogeneous population estimated an even smaller radius due to the presence of children and elderly people.

These results for the radius show that for simulations of dense situations, the depth of the bodies is more accurate than the width that would result in too large longitudinal distances.

Influence area parameters

The values for the influence area extension at the front ie_f for all the experiments were similar and stayed between $1.3m$ and $1.6m$. Only the crossing and the downstream bottleneck presented lower values, around $1.0m$. Thus, the calibrated ie_f are not far from results of previous investigations. Johansson et al. (2007) obtained $ie_f = 1.0m$.

There are different mechanisms that influence the length of ie_f. Duives et al. (2014a) showed that pedestrians in congested flows adapt their speeds anticipating the congestion ahead. This may justify the relatively large values of ie_f for the upstream bottleneck and the evacuation experiments. The bidirectional, unidirectional and the interaction experiments also presented large values of ie_f due to the need to anticipate when walking with higher speeds.

Poor visibility is a factor reducing ie_f. Pedestrians inside the narrow corridor in the downstream bottleneck can only see the leader in front. Visibility of pedestrians walking in the crossing experiment inside the tracked area is also reduced due to small distances between pedestrians (figure 6.1). Poor visibility results in smaller ie_f for both experiments.

A strange result were the large values of influence area extension at the back ie_b for the normal and interaction experiments. It is not so clear why we obtained these non-intuitive results. Furthermore, only the upstream bottleneck and the interaction experiments obtained $ie_f > ie_b$. As discussed in section 2.3.2 the perception of the events in front are more important for pedestrians and these results cannot be justified as realistic. These results may reflect a deficiency of the model rather than pedestrian behaviours. Campanella et al. (2009c) showed the necessity of the effect called 'push from behind' in the Nomad model to deliver good validation results. This push from behind is an artificial repulsion force that push pedestrians when they are being followed at close distances. The calibration results suggest that this effect is enhanced in the experiments in which pedestrians are more aligned with each other (bidirectional, unidirectional and the downstream bottleneck).

The calibration of the influence area factors for the evacuation experiments resulted in values that create the elongated elliptical shape in the frontal part $c_0^+ < 1$ and the lateral elliptical shape for the backward part $c_0^- > 1$ as represented in figure 3.6. This is also happening for the upstream bottleneck, which is the only normal experiment that presents $c_0^+ < 1$. The results for these experiments show that in congestion pedestrians are much more influenced for those exactly in their front.

The urgency did not affect the influence area parameters, but the heterogeneity did. We observe that heterogeneity makes pedestrians more aware to what is happening to their sides both in front and at their back $ie_{f_{Ho}} < ie_{f_{Het}}$ and $ie_{bHo} < ie_{bHet}$. However, the largest influence is in the extension of the influence area. Again, with increase of heterogeneity pedestrians increase their scanning areas in both directions. We could hypothesise that the different age groups create situations that are more confusing for the individuals requiring a wider scanning to keep their safety margins.

For the normal walking and interaction experiments the results stayed around the unitary value approximating the influence area to circles. Interestingly, we obtained a small positive correlation between ie_f and c_0^+. This a logical behaviour in which pedestrian scanning further in their walking direction (large ie_f) also include more of their surroundings (larger c_0^+). This explains why there are no correlations for the interaction experiments (table 6.8).

Lateral avoidance

There were not many significant results for lateral avoidance parameters (especially for r_1). We discuss in section 6.3.2 the difficulties to significantly calibrate the lateral

Table 6.8: The significant correlations between the parameters ie_f and c_0^+ for the normal and interaction experiments.

experiment	parameter	c_0^+
unidir	ie_f	0.42
cross		0.51
bneckDown		0.33
interCross		0.36

avoidance parameters for the normal and interaction experiments. However, a_1 correlates positively with a_0 in the bidirectional (0.50) and crossing experiments (0.99).

These correlations indicate that the lateral behaviour is creating large lateral movements when the interaction accelerations are the greatest. This is an indication of the usefulness of the extra lateral accelerations for frontal conflicts when pedestrians are needing to apply large interaction accelerations.

Anticipation time parameter

If we inspect the calibrated values of t_A for the normal and interaction experiments we observe that they stay roughly around two distinct values: $0.55s$ and $0.70s$. If we multiply the average speeds of the experiments with the anticipation times we obtain an anticipation distance ($d_{t_A} = \overline{v} \times t_A$).

The anticipated distance depends on the intensity and direction of the velocities. However, Nomad does not apply anticipation if pedestrians are so close that their anticipated position would change the sign of the relative velocities. Therefore, we can interpret the anticipated distance as the preferred distance at which the anticipation occurs and it is dependent from the type of flows and walking speeds.

Table 6.9 shows the average anticipation distances obtained by multiplying the calibrated value of t_A with the average speed of the pedestrian for every trajectory in the experiments.

In general for car traffic, anticipation allows drivers to keep safety margins to have time to react to potential hazards from the cars ahead (Van Der Hulst (1999)). The same is assumed to happen in pedestrian traffic, Hoogendoorn and Daamen (2005a) show that distance headways increase with speeds to account for larger steps and to increase the safety margin for unidirectional flows.

The results in table 6.9 show a similar behaviour for the anticipation distance. The evacuation experiments and the upstream bottleneck resulted in the smallest anticipated distances. This is the reflection of their slow speeds and higher densities. The table shows that the anticipation distance increases with the walking speeds for the unidirectional flows.

Table 6.9: The average values of the product $\overline{v} \times t_A$ that represent the average anticipated distance for all experiments.

experiment	$\overline{v}$ (m/s)	t_A (s)	$\overline{v} \times t_A$ (m)
bidir	1.30	0.53	0.68
unidir	1.41	0.61	0.86
cross	1.35	0.52	0.72
bneckDown	1.00	0.56	0.56
bneckUp	0.74	0.60	0.45
evacHoLoSt	0.60	0.70	0.37
evacHoHiSt	0.64	0.70	0.43
evacHetLoSt	0.50	0.76	0.33
evacHetHiSt	0.46	0.59	0.32
interBidir	1.50	0.54	0.81
interCross	1.57	0.69	1.00

However, the anticipation distance is also dependent of the direction of the flows. Nomad assumes that in non-unidirectional flows the avoiding manoeuvres are shared. In theory when both pedestrians anticipate their positions the effect of the anticipation in the interaction acceleration should double.

Effectively we see that the anticipation times of the bidirectional and crossing flows are smaller when compared to the unidirectional flows. However, the difference in the interaction distance from the bidirectional and crossing flows with the unidirectional is considerably smaller than half. This indicates that the self-organised lanes and the diagonal stripes reduce the necessity of anticipation.

These results for t_A support the anticipation model adopted in Nomad. We showed that t_A does not vary much with the types of flow making the formulation proposed in Nomad in accordance to empirical evidence, encouraging the application in other walker models.

Obstacle Avoiding parameter

Upstream and downstream narrow bottleneck walking experiments resulted in similar average values for a_W. The value for the evacuation experiment is unreliable because it is the outcome of only one significant calibration (see section 6.3.2).

We saw that a_W correlated strongly with a_0 for the pedestrians walking inside the corridor (0.84). The upstream bottleneck experiment also presented a small positive correlation (0.29). These two correlations show that the interaction behaviours work together in dense situations that are near walls.

6.3.2 Significances of the calibration results

In total the calibrations resulted in 120 parameter samples for all experiments. This number is obtained by counting all cells of table 6.6. The table shows different percentages of significance calibrations for the parameters. The percentages of non-significant calibrations are concentrated mostly on the two lateral avoidance parameters and the obstacle interaction parameter. r_0 samples resulted with more significance calibrations than the samples for these three parameters, especially for the evacuation experiments, but lesser than for τ and a_0. The experiments have less influence on the significant calibrations. Only the interaction experiments resulted in fewer percentages.

The low amount of significant calibrations of the lateral avoidance parameters was expected since the majority of the experiments did not present sufficient frontal interactions. We will discuss the significances in the following. However, the overall results for the important parameters τ, a_0 and in somewhat lesser amount for r_0, give confidence that the calibration procedure is able to find optimal values that are relevant for the model outcomes and that the model outcomes are sensitive for most of the parameters.

We recall from section 4.4 that two possible causes exist for the small number of significant estimations of parameters and these causes will be referred in the analysis:

1. The model outcomes are insensitive to the parameters.
2. The amount of information in the data about the behaviour modelled by the parameters in the trajectories is low.

The level of significant calibrations varies for the different experiment types. In general, the normal experiments presented more than 50% significant calibrations. Only the crossing flow experiment showed a smaller amount of significant calibrations than the other four experiments. The reasons are the somewhat shorter trajectory length of $4m$ and the low densities encountered in the crossing flow experiment. Inspections of the results showed that the percentage of significantt calibrations increases for larger densities.

Both bottleneck experiments presented a slightly longer walking distance of $5m$ and much higher density levels while the bidirectional and unidirectional experiments had $10m$ long trajectories. These factors contributed to longer walking time and higher probability for interactions and consequently higher percentages of significant calibrations for these experiments.

The high percentages of significant calibrations for the evacuation experiments are due to the high densities achieved and the long walking time due to congestion. Furthermore, the urgency that was present in the evacuation experiments created less overtakings resulting in less complex manoeuvres that have a negative impact on the calibration procedure as shown in chapter 4.

The interaction experiments resulted in the smallest amount of significant calibrations from all three experiment types. This is due to very low amounts of information in the tracked data. Figure 6.5 illustrates the lateral movements that occurred between pedestrians in the interaction bidirectional experiment (*interBidir*). The figure shows that the pedestrians were already laterally displaced when they entered the tracking area and only a small lateral displacement occurs and thus interaction around the moment of encounter. Moreover, there is a maximum of one single conflict per trajectory. This problem especially affected the parameters responsible for pedestrian interactions, a_0, r_0, a_1 and r_1.

Tracking noise in the trajectories certainly affected the significance of the calibrations. However, it is not possible to determine the extent of its effect since the same tracking algorithm was used for all trajectories. The software was improved over the years and we believe that the version used for the evacuation and interaction experiments reduced tracking errors. This would further justify the better quality of the calibrations of the evacuation experiments.

In the following we will discuss the four parameters that had very low amounts of significant calibrations: r_0, a_1, r_1 and a_W.

Pedestrian avoidance parameter r_0

From the three most important parameters: τ, a_0 and r_0, only the interaction distance r_0 had a relatively low amount of significant calibrations for the normal and interaction experiments, with more significant calibrations for higher densities. This is in accordance with the high amounts of significant calibrations for the evacuation experiments that achieved the highest densities.

The relationship with density occurs because lower densities reduce the time available for the avoidance manoeuvres. Therefore, the interaction accelerations must be larger at longer distances to allow for the avoiding manoeuvres to be effective. Thus, larger r_0 are estimated for lower densities. The other experiments obtained r_0 values that follows a negative relationship with densities.

The normal crossing and the two interaction experiments provided few significant calibrations of r_0. Most of the avoiding manoeuvres occurred outside of the tracked area (see section 6.3.2). Therefore, calibrations that resulted in significant parameters were those in which pedestrians applied avoidance movements at short distances, thus having small r_0.

It is not entirely clear why we obtained so few significant calibrations for r_0, especially because it was accurately calibrated with the synthetic trajectories in chapter 4. However, the smaller values of r_0 for the evacuation experiments presented in table 6.5 suggest that the proximity between the pedestrians not only results in larger interaction accelerations originated from r_0, but also increases its significance for the behaviours.

For other less dense situations any value of r_0 combined with a sufficiently large value of a_0 is enough to create the necessary interaction accelerations.

Lateral avoidance a_1 and r_1

Even if it was expected that most of the experiments, that are predominantly composed by unidirectional flows, would not deliver significant calibrations, for the parameters dealing with lateral avoidance it was surprising that the bidirectional, crossing and interaction experiments also had few significant calibrations.

The majority of the significant calibrations for the bidirectional occurred in higher densities. Furthermore, the trajectories that resulted in significant calibrations ended with 23% more lateral movements than the rest of the trajectories. Similar situations but in less amount, occurred with the crossing and interaction experiments. This suggests that there were not enough frontal collision situations resulting in lateral avoidance movements. Therefore, poorness of data on frontal collisions caused the low amounts of significant calibrations.

We extended this investigation by comparing the log-likelihoods of the calibration objectives with and without these parameters. We modified Nomad excluding a_1 and r_1 (restricted model) and calculated the log-likelihood for each optimal parameter set estimated in these four experiments.

To test the relevance of these parameters for the model we applied the log-likelihood ratio test as presented in section 6.2.1. The test compares both models with 95 % confidence and $m = 10 - 8 = 2$ degrees-of-freedom.

By removing these parameters from Nomad we would expect two things to happen with the log-likelihoods: a small variation for the trajectories that presented no significant calibrations and a large variation for the trajectories that presented at least one significant parameter. This should result in rejecting the null hypothesis of the log-likelihood test that states that the unrestricted model is not significantly better than the restricted model, in similar amounts to the percentage of significant estimations.

However, table 6.10 shows a surprisingly high level of rejection indicating that even if the parameter is not significant any value different than zero (that is the equivalent of removing it) improves significantly the simulated behaviour. The second column shows the percentages of log-likelihood amount of trajectories in which the log-likelihood of the unrestricted model is larger than the restricted model. The third column shows the percentages of significant calibrations of both parameters serving as comparison to the log-likelihood tests.

The large rate of success in the likelihood-ratio tests gives a solid indication that these parameters are relevant for the model. The reasons for the low amount of significances are specific for each flow. As we saw in the discussions about the parameter values, the bidirectional flows are similar to unidirectional flows distributed over lanes. These large amounts of leader-follower behaviour diminishes greatly the frontal conflicts.

Table 6.10: Results of the log-likelihood ratio test between the unrestricted model and the restricted model without a_1 and r_1. The table also shows the amount of times that the log-likelihood of the unrestricted model is larger than the restricted. The last column shows the percentages of significant calibrations of both parameters.

	log-likelihood test success (%)	log-likelihood unres.>rest. (%)	significant estimations a_1 (%)
bidir	66	88	7
cross	53	89	2
interBidir	80	92	8
interCross	88	98	5

Obstacle Avoiding parameter a_W

The obstacle interaction strength a_W responsible for the interaction behaviour with obstacles proved to be very difficult to calibrate for the evacuation experiments. The reason is that there were very few situations in which pedestrians were close to the obstacle walls.

Figure 6.7 shows the funnels created by the trajectories that prevented wall interactions for the evacuation experiment with homogeneous population and no urgency (*evacHoLoSt*) as well as the complete trajectories of the bottleneck experiments. The plot clearly shows that very few trajectories from the evacuation experiment are following the walls and that that exit door gives only few trajectory positions that could be used for the calibration.

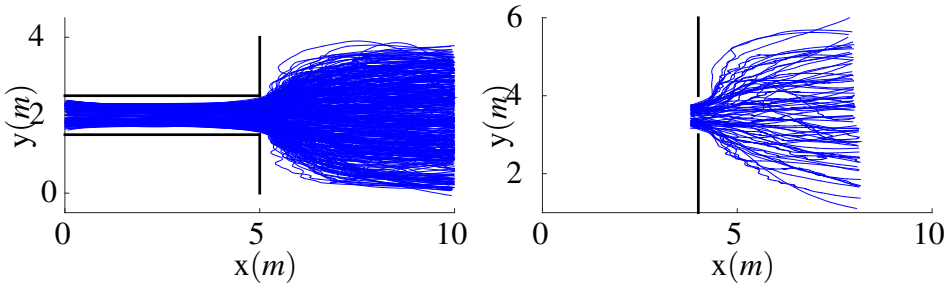

(a) bottleneck (b) evacuation

Figure 6.7: Trajectories of the experiments used to estimate the parameter a_W (interaction with obstacles).

The calibrations involving the bottleneck experiment obtained better results. However, the figure shows that also not many pedestrians were close to the lateral walls. Most of the interactions with the walls occurred in the vicinity of the corridor entrance during conflicts with other pedestrians.

Not surprisingly the trajectories inside the corridor produced the largest amount of significant calibrations of a_W. In the *bneckDown* trajectories, pedestrians were constantly

in the vicinity of the walls. However, the relatively low amount of 28% of significant calibrations can be attributed to the fact that pedestrians would only interact with the wall in the not so common situations of conflicts with slower pedestrians in front. This is a consequence of the lateral organisation arising from the zipper effect mentioned in section 2.3.5 and in figure C.1.

6.4 Influence of type of flow on pedestrian behaviours

In this section we will discuss to which extent we can identify differences in pedestrian behaviours due to the different type of flows. Each experiment has a distinct walking configuration and different density patterns. We are going to show how these aspects create significantly distinct behaviours.

In this section we show that different types of flow result in parameter samples that are statistically different, that is, these samples cannot be considered to be realisations of the same distributions. For this we use the Kolmogorov-Smirnov goodness-of-fit testing. We calculate the sum of the KS Statistics ST as defined in section 6.2.2 to obtain an indicator of the similarity between behaviours encountered in the flows.

Table 6.11 presents the amount of times that each pair of samples have confirmed the null hypothesis of the KS tests (the samples are from the same distribution). The last column shows the percentage of times the test has rejected over the total amount of tests. Values close to 0% express a large influence of the traffic flows in the walking behaviours.

Table 6.11: The amount of positive results of the KS tests for pairs of parameter samples for each experiment type. The last column shows the percentages for each type of experiments of the positive results from the total amount of tests.

parameters	**max # tests**	**path follow**	**pedestrian interactions**							**% of positive KS results**
			ped avoid		**influence area**				**anticipation**	
experiments		τ	a_0	r_0	c_0^-	c_0^+	ie_f	ie_b	t_A	
normal	12	0	1	4	3	3	2	0	2	19
evacuation	6	3	3	6	4	6	6	4	5	77
interaction	2	0	0		1	1	0	0	0	29

The results show clearly that the walking behaviours in each experiment from the normal and interaction experiments are different from each other. The contrary can be confirmed for the evacuation experiments, for which statistically can be indicated that the behaviours along the experiments are similar. These results support the assumption

that differences between the evacuation experiments are not significant and are accounted for by the other experimental variables: population composition and urgency levels. These are discussed in section 6.5.

Table 6.11 shows results from the samples of parameters that had enough significant estimations to be compared. Therefore, no samples of the a_1, r_1 and a_W parameters were included in this section (see table 6.6). In the following we will discuss the details of the results for the normal and interaction experiments.

6.4.1 Normal experiments

Table 6.11 shows that the five experiments presented no samples of τ and only 1 for a_0 were significantly similar. These parameters as described in chapter 6.2 determine the intensity between the two components, path following and pedestrian interactions and are very determinant for the behaviours predicted by their components. The fact that all samples are significantly different suggests large differences between their path following and pedestrian avoidance behaviours.

Table 6.12 contains the results of the similarity statistics that are the sum of the KS distances of every parameter of a pair of normal experiments. The table shows that in general the experiments display a similar value of the ST. However, experiments *bidir* and *unidir* presented a much smaller value of the ST indicating that these two experiments present most similar behaviours. This is in agreement with the calibration results shown in section 6.3 and confirms that the occurrence of the self-organising lanes in the bidirectional flow effectively put most pedestrians into a follower and leader situation similar as in unidirectional flows.

The largest statistics occurred between experiments *unidir*, *bidir* and *cross*, but the value was not significantly larger than the other values.

Table 6.12: The sum of all KS distances (ST) for the normal walking experiments. The bold values present the lowest and highest values of ST.

experiments	*bidir*	*unidir*	*cross*	*bneckDown*	*bneckUp*
bidir	0.00	**1.21**	1.81	1.75	1.60
unidir		0.00	**1.88**	1.67	1.60
cross			0.00	1.61	1.50
bneckDown				0.00	1.63
bneckUp					0.00

The similarity between the *bidir* and *unidir* samples can be seen in figure 6.8 that shows the plots of the distributions of the significant calibrations of the τ, a_0 and r_0.

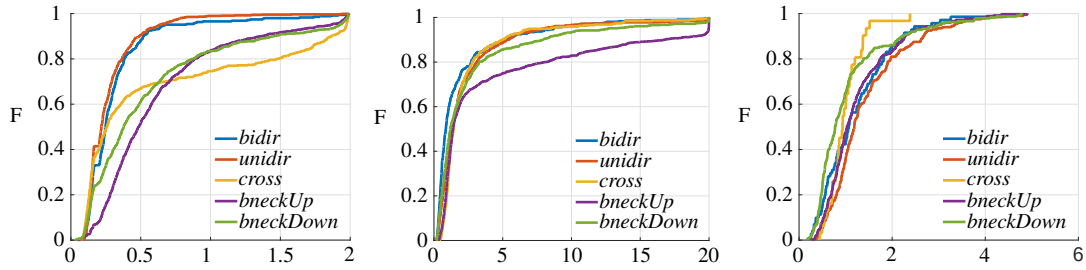

(a) τ (b) a_0 (c) r_0

Figure 6.8: The distributions of the significant parameters τ, a_0 and r_0 for the normal experiments.

6.4.2 Interaction experiments

The interaction experiments showed a very large value of *ST* even without a comparison between the samples of r_0 that had no significant values for the experiment *interBidir*. Only two parameters that control the shape of the influence area (c_0^- and c_0^+) presented samples that could be attributed to the same distribution. The other samples did not reject the KS tests indicating that when walking individually the angle of approach causes different behaviours. This corresponds with the normal experiments where the highest differences occurred between the *unidir*, *bidir* and the *cross*.

Table 6.13: The similarity statistics *ST* for the interaction experiments.

experiments	*interBidir*	*interCross*
interBidir	0.00	**2.37**
interCross		0.00

6.5 Impact of population composition and urgency levels

Results in table 6.5 show that the composition of the population and the urgency affect the behaviours. If we compare the experiments with the same population composition we observe that the increase of urgency to *Hi* creates pedestrians that follow more their paths (smaller τ) but they react more to the surroundings (larger a_0).

r_0 is not much affected. The parameter differences are smaller for the increase of heterogeneity in the population (*Ho* $\rightarrow$ *Het*), not allowing for a significant conclusion about its influence. Table 6.14 shows the relative differences between the parameters for the same population composition and varying the level of urgency and for the other way around.

The evacuation experiments gave a small percentage of rejection of the null hypotheses indicating that the distributions are similar (table 6.11). The two parameters that failed

Table 6.14: Parameter differences for τ, a_0 and r_0 for the evacuation experiments with different levels of urgency and population composition

experiment		**difference** (%)		
		τ	a_0	r_0
Urgency	*Homogeneous*	-19	11	0
Lo $\rightarrow$ *Hi*	*Heterogeneous*	-17	24	-3
Composition	*Lo* urgency	-6	-7	7
Ho $\rightarrow$ *Het*	*Hi* urgency	-5	9	3

most of the KS tests were τ and a_0 (three times each). This is in agreement with the large differences in the average τ and a_0 values discussed in section 6.3. In this section, we compare the evacuation experiments according to the similarity of all samples.

The 23% of rejections for the evacuation experiments can be attributed largely to the differences arising from the population composition and to a smaller extent to the urgency level in agreement with the empirical analysis from the experiments in Daamen and Hoogendoorn (2009a). When analysing the results from table 6.15 we find evidence that both variables contribute to differences in behaviours. The effect of urgency is different for the populations.

Table 6.15: The similarity statistics ST for the evacuation experiments.

experiments	*evacHoLoSt*	*evacHoHiSt*	*evacHetLoSt*	*evacHetHiSt*
evacHoLoSt	0.00	**1.11**	1.42	**1.80**
evacHoHiSt		0.00	1.43	1.33
evacHetLoSt			0.00	1.36
evacHetHiSt				0.00

The homogeneous adult population presented the smallest value of $ST = 1.11$ for the two urgency levels (*evacHoLoSt* x *evacHoHiSt*) suggesting that the urgency is not influencing their behaviours very much. This seems to contradict the results for the average parameter values of τ and a_0 as discussed in section 6.3. However, the samples of τ and a_0 did not produce very large KS statistics in the tests and the similarity between the other parameter samples of these two experiments is very high compensating for these two parameters. Therefore, we conclude that urgency must be affecting the behaviours, but not equally in all parameters.

The heterogeneous population (*evacHetLoSt* x *evacHetHiSt*) has a larger value of $ST = 1.36$ indicating that the induced urgency creates different responses for the different age groups that compose the population. These responses increase the differences in the average behaviours reaffirming the determinant role of heterogeneity in the nature of pedestrian flows as discussed in chapter 2.

When we compare the different pedestrian compositions for the same urgency level we obtain results that do not differ much: *evacHoLoSt* x *evacHetLoSt* and *evacHoHiSt*

x *evacHetHiSt* have similar values of $ST = 1.42$ and 1.33 respectively. This indicates that the differences between the populations are more determinant than the urgency for the differences of the behaviours. However, the smaller difference for the high urgency suggests that urgency exerts a tendency of uniformity in the behaviours as we observed in section 6.3.

$ST = 1.80$ was the largest value and it occurred between the experiments *evacHoLoSt* x *evacHetHiSt* indicating that the effect of both variables reinforce each other in creating different behaviours.

6.6 Influence of traffic conditions on pedestrian behaviours

In this section we will analyse the variation of the parameter values with different traffic conditions. For simplicity we use the average walking speeds as a proxy for the local conditions. The analysis is made with plots with the average parameter values for speed intervals for the five normal experiments. For readability, we will always distribute the five plots over two figures.

6.6.1 Path following parameter

The plot of the acceleration time τ on the left side of figure 6.9 suggests a sigmoid type of curve in which for high and low speeds τ is constant. The values of the plateaus are different for the two experiments.

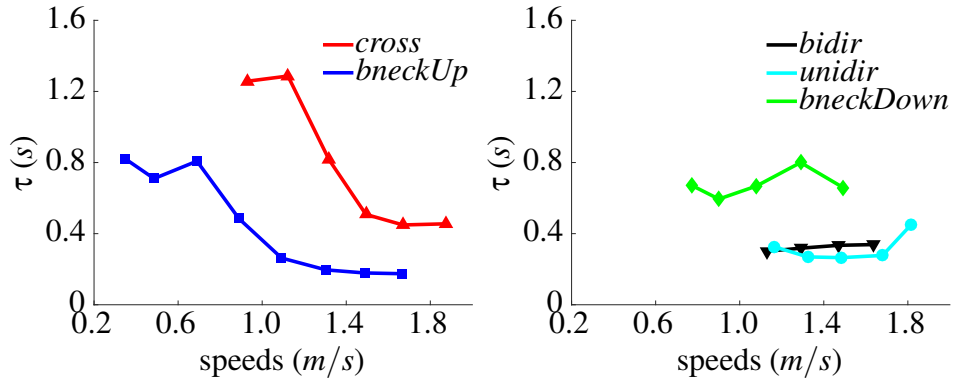

Figure 6.9: The average values of τ in the speed intervals.

The upstream bottleneck experiment presents an initial period of free flow until the bottleneck saturates at which moment pedestrians walk in congested flow. In the initial period, pedestrians are walking freely and behave similarly as those in the unidirectional flow. This is reflected by the low values of τ necessary for pedestrians to keep close to their desired paths and free-speeds. At this initial period the values of τ are

very similar to those of the (almost constant) unidirectional and bidirectional flows shown in the right plot in figure 6.9.

When the bottleneck starts getting oversaturating, pedestrians reduce their speeds and have more interactions. This happens around $v = 1.1m/s$. Trajectories in these situations start being calibrated with larger τ to allow for the slower speeds. When the congestion is settled, trajectories result in similar high values of τ creating the high plateau.

The crossing flow shows a similar behaviour but the values of τ in both plateaus are higher. This reflects the differences in the type of flows. The crossing flow requires more change in walking directions, therefore τ must be higher to allow the deviations from the desired paths, even for higher speeds. It is not certain if the top plateau represents the saturation of the crossing flow because the speeds are still high. However, it is expected that saturation would occur at higher speeds given the complex maneuverers required in the crossing interactions.

We discussed in section 6.3 the reasons for the higher values of τ for the downstream bottleneck. Interestingly, τ remains high and practically constant for the whole speed range. This indicates that the conflicts imposed by the walls and the slower pedestrians have similar effects requiring large variations of the longitudinal accelerations.

6.6.2 Pedestrian avoidance parameters

The three experiments on the left plot of figure 6.10 suggest that the interaction strength a_0 varies according to 'U' shapes. The minimum values of a_0 are located roughly at $1.1m/s$ corresponding to the beginning of the saturation for the upstream bottleneck flow.

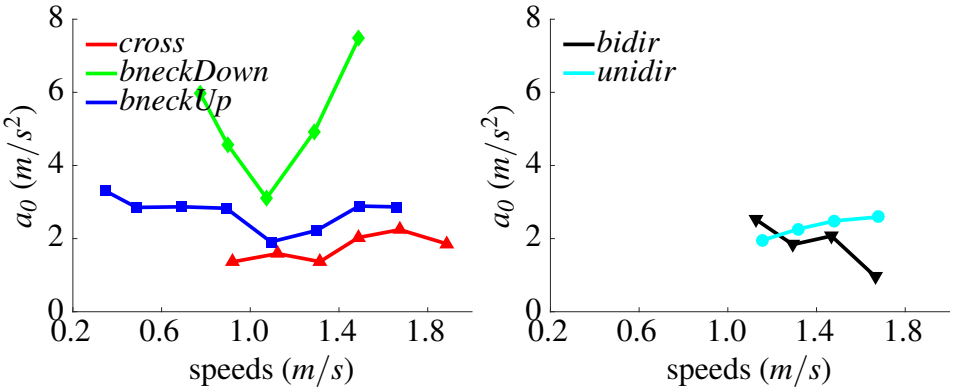

Figure 6.10: The average values of a_0 in the speed intervals.

For the upstream bottleneck, the 'U' shape reflects three distinct situations. During free flow a_0 is high to compensate larger distances. When speeds decrease, a_0 also decreases preventing the interaction forces from increasing too much. The minimum value of a_0 coincides with the beginning of the saturation of the bottleneck. After this

moment, pedestrians recognise the saturation ahead and anticipate the congestion by walking slower than they would in the same densities (Duives et al. (2014a)). The deceleration due to the anticipation results in larger a_0. With the distance to the congested flow diminishing due to the spill-back the deceleration is more intense increasing a_0. This stops when the whole flow is congested and a_0 practically stays constant preventing further increase of the interaction accelerations.

The curve for r_0 at the left of figure 6.11 for the upstream bottleneck has approximately the opposite shape of a 'U' with the maximum around $0.8m/s$. The curve shows how r_0 starts from a large value in free flow and increases slightly to values close to those of the bidirectional and unidirectional flows. When the saturation occurs around $1.1m/s$ r_0 grows rapidly showing the increase of sensitivity with distance required for the anticipation. After the flow is congested r_0 decreases rapidly indicating an increase in sensitivity to nearby pedestrians.

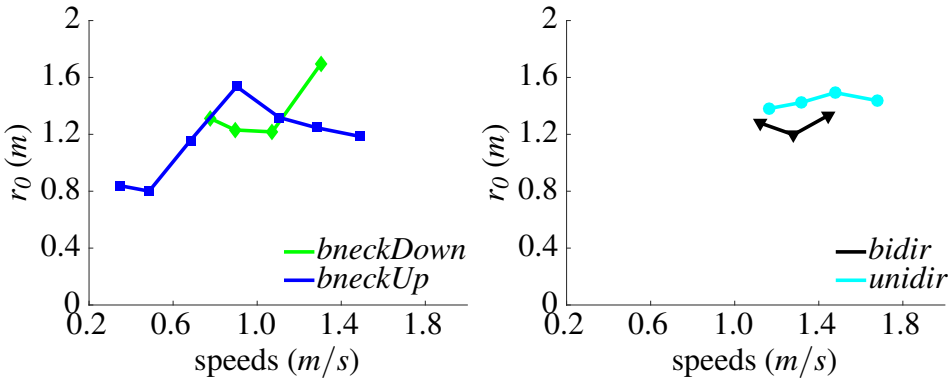

Figure 6.11: The average values of r_0 in the speed intervals.

The shape of the crossing flow a_0 curve may indicate a similar anticipation mechanism due to saturation of the area of conflict. However, the drop appears to occur at a higher speed around $1.4m/s$. Unfortunately, there was not a single sample of r_0 with more than 5 significant parameters for the crossing flow.

The downstream bottleneck flow presents a more extreme version of the 'U" shape curve for a_0. Inside the corridor a_0 and r_0 are large in free flow and both decrease with lower speeds preventing large interaction accelerations. The fact that a_0 reaches a minimum at exactly the same speeds as the for the upstream bottleneck, suggests the same anticipation mechanism. Inside the corridor, pedestrians see slower pedestrians ahead and decelerate to avoid collision, thus increasing a_0. r_0 stays almost constant for a range around $0.8m/s$. We suspect that r_0 would also decrease if slower speeds would have been attained.

a_0 is much larger for the downstream bottleneck flow, because of the proximity of the walls inside the corridor. Natural variations of movements at all speeds require that pedestrian and obstacle interaction accelerations act like spring forces damping the movements, thus requiring larger a_0 than in situations without walls. This explains the positive correlation between a_0 and a_W.

The unidirectional flow shows a diminishing trend of a_0 with decreasing speeds that resembles both bottlenecks and the crossing flow. r_0 stayed at a large value also in agreement with the other flows. Unfortunately the speeds never got less than $1.1 m/s$ to eventually reveal the anticipation mechanism.

The bidirectional flow presents a small increase of a_0 with slower speeds. It is not clear if this variation is connected to the appearance of the self-organised lanes where pedestrians are less free and react to the leader in front. Nothing can be interpreted from the r_0 curve with only three points.

6.6.3 Influence area parameters

Figure 6.12 shows that the values of c_0^- for all experiments stayed close to unity indicating that pedestrians are equally aware of what is happening in backward lateral positions. However, the c_0^+ showed some small variations that we will discuss in the following.

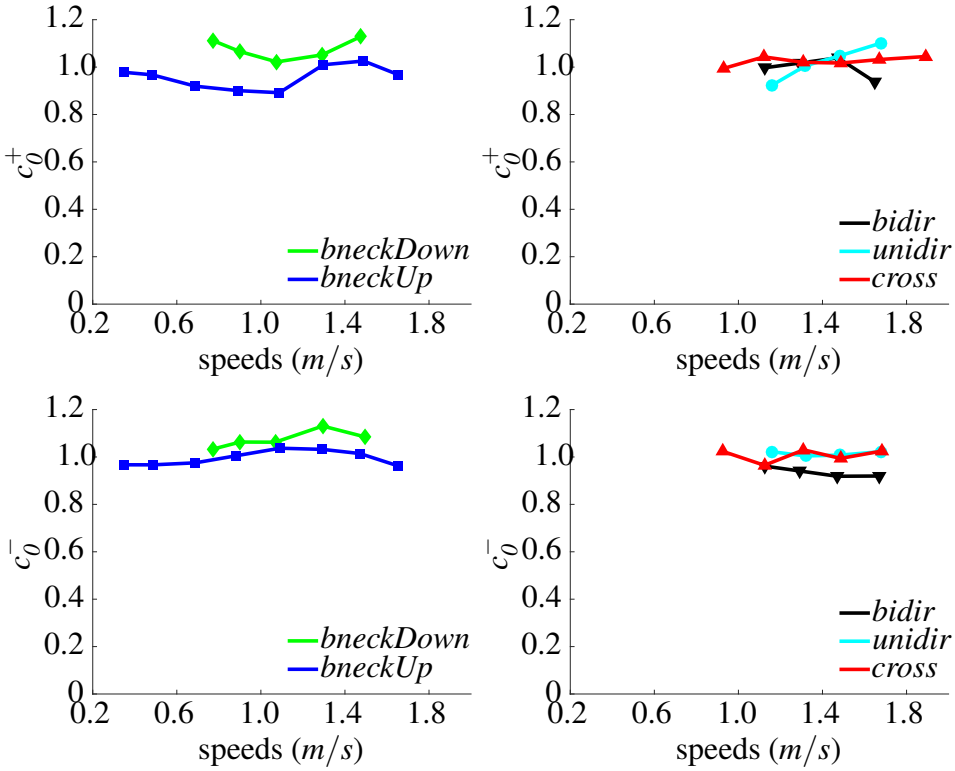

Figure 6.12: The average values of c_0^+ and c_0^- in the speed intervals.

The bidirectional and crossing flows resulted in values of $c_0^+ \sim 1.0$ for all speeds. The bidirectional has only three points not allowing for trends to appear. The values of c_0^+ indicates that for the large speeds in the experiment, pedestrians are considering their surroundings to avoid collisions. The layout of crossing paths require scans in all directions regardless of the speeds, thus resulting in a constant $c_0^+ = 1.0$.

The upstream bottleneck flow presents a sharp decline of c_0^+ for speeds below $1.4m/s$. Above this speeds pedestrians are looking around for potential conflicts. However, when more pedestrians are present, the anticipation mentioned in the previous sections causes a focusing in pedestrians in front of their paths decreasing c_0^+. This happens for speeds until around $1.1m/s$ when the bottleneck saturates. In congestion pedestrians continue to react more to the leader keeping c_0^+ values below 1.

The downstream bottleneck, presents c_0^+ values above 1.0 indicating that when there is interaction pedestrian are staggered in the 'zipper' layout needing to scan their sides. It is not so clear why the curve presents a decrease of c_0^+ for high speeds, given that there are no lateral interactions in the corridor at such speeds. The lowest point is in agreement with the anticipation mentioned in the previous section and the increase of c_0^+ for lower speeds is due to lateral proximity between pedestrians.

The results for the unidirectional flow, suggest a decrease of c_0^+ for speeds above $1.1m/s$ in accordance to the upstream bottleneck flows.

It would be expected that the influence area extension at the front would be increasing with the speeds. However, this relation seems to be significantly occurring only for the downstream bottleneck and the unidirectional flows. The upstream bottleneck also shows this trend, but not very accentuated.

The values for ie_b are very high, suggesting that they do not reflect reality. Furthermore, we would expect that ie_b would decrease with speeds but we see this tendency only with the crossing flow. We discussed in subsection 6.3.1 that this reflects a deficiency of the model rather than pedestrian behaviours, a necessity of an extra forward acceleration when pedestrians are followed at short distances.

6.6.4 Anticipation time parameter

We saw in the discussions in section 6.3.1 that t_A did not display much variation with the types of flow. In this section we show that they also do not show much variation with speeds. All experiments apart from the upstream bottleneck, experiment show a almost flat values of t_A.

We suggested in the discussion about the interaction parameters that pedestrians were adapting their speeds before reaching the end of the spill-back when the bottleneck was saturating at speeds around $1.1m/s$. Figure 6.14 for the *bneckUp* shows a increase of t_A before saturation and a decrease thereafter, providing evidence for the anticipation.

6.6.5 Obstacle Avoiding acceleration

The curves for the two bottleneck experiments presented remarkable similar results even though these are totally different situations.

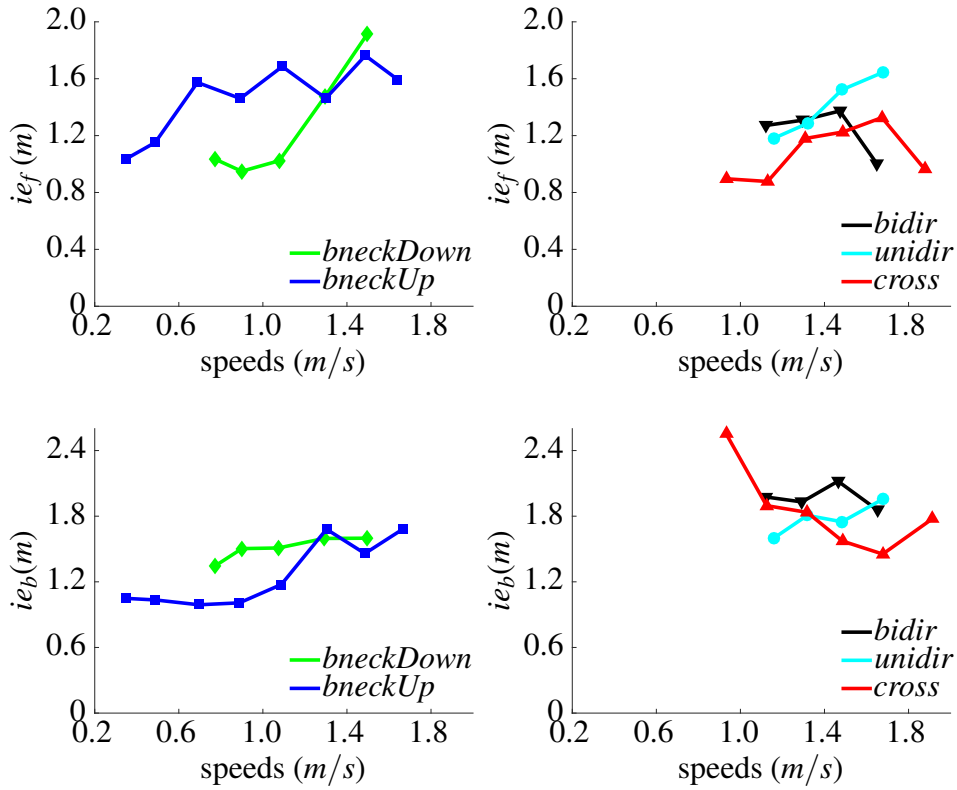

Figure 6.13: The average values of ie_f and ie_b in the speed intervals.

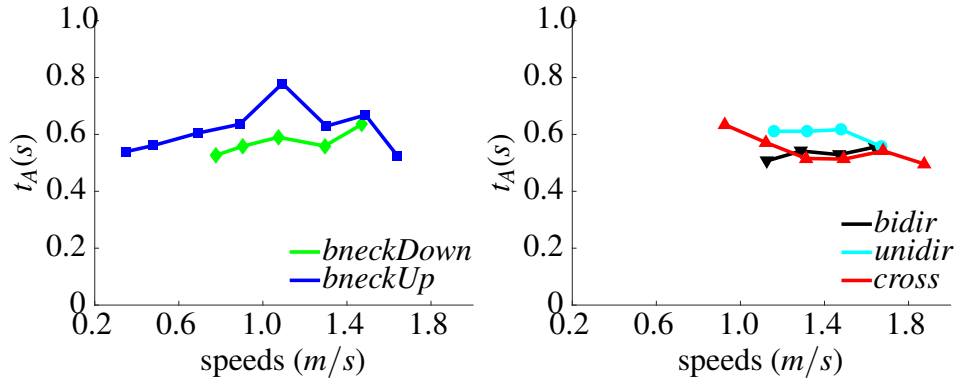

Figure 6.14: The average values of t_A in the speed intervals.

In the upstream bottleneck experiment pedestrians walking in free-flow conditions, only interact with the walls when they are entering the corridor. Inspecting the trajectories that resulted in large values of a_W we observed that most displayed oblique approaches to the entrance of the corridor. Johansson et al. (2014) show that the path following component similar for Nomad and Social Force Models does not provide correct amounts of drifting when compared with observations. Therefore, large values of a_W for high speeds are compensating the low values of τ as shown in figure 6.9.

For the downstream bottleneck experiment the situation is different. At free-flow speeds pedestrians are very isolated and only obstacle interaction accelerations are responsible to natural oscillations in lateral directions. Since the shy away distance to

the walls is large (equation (3.12)), a_W increases to produce the lateral accelerations.

At lower speeds, the distance to the walls do not vary much. A fairly constant value of $a_W \sim 9$ is enough to avoid collisions with the walls in both experiments.

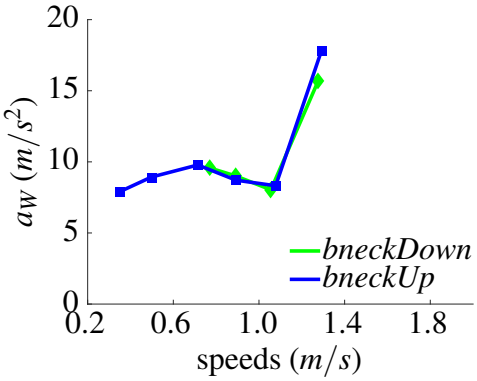

Figure 6.15: The average values of a_W in the speed intervals.

6.7 Conclusions and implications

The main contribution of this chapter is the extensive calibration of pedestrian behaviours using multiple sets of trajectories from several experiments, including different flow configurations, population characteristics and traffic conditions. The results of the calibrations were used to investigate pedestrian behaviours and the general applicability of the Nomad model.

What is innovative in this chapter is the analysis of pedestrians behaviours using multiple sets of trajectories derived from several experiments. The calibration methodology developed in chapter 4 was used to calibrate individual parameter sets of pedestrians and the obtained parameter samples were used to investigate the sensitivity, correlation and distributions of the different parameters. Several behavioural findings based on the statistical properties of the parameter samples are used to propose modifications in the Nomad model, that could also benefit other walker models.

6.7.1 Conclusions

The extensive significance analysis showed that all the Nomad parameters are important. The outcomes of the parameter values and their significance was significantly influenced by the walking regimes and types of flow. This outcome reveals the importance of using several types of flows to investigate walker models and its components.

We obtained few significant correlations between parameters of different components. The most important was the strong correlation between interaction strength a_0 and the obstacle interaction strength a_W. In the only experiment that subjected pedestrians to

long periods of close proximities with walls, these parameters correlated positively. suggesting that it would be possible to eliminate a_W.

Section 6.3 showed that in high densities the pedestrian radius for circular pedestrians should have the dimensions of the body depth and not from the body width. For models using circular pedestrians these results suggest that for the simulation of dense flows the pedestrian radius should be set closer to the body depth instead of the body width to compensate for the overestimation of distances when pedestrians are walking behind each other. Using these smaller values also approximate the real lateral distances. Real pedestrians are ellipses and in dense situations pedestrians assume staggered positions that resemble the zipper-effect found in narrow corridors.

Smaller radii are easy to introduce, but will only be effective if the calibration of the model parameters uses the smaller radius. Alternatively the model could be improved by introducing elliptical body shapes instead of circular bodies.

Influence of type of flows

After the extensive calibrations we obtained significant differences between the estimated parameters for the experiments (section 6.3). We discussed the significant differences due to the directions pedestrians walk (normal experiments) and walking characteristics (normal and evacuation behaviours).

We showed that bidirectional and unidirectional flows presented the smallest differences between the calibrated parameters. Pedestrians in these type of flows walk mostly along their preferred paths and do not need to make large deviations. The majority of the pedestrians in bidirectional flows are walking inside lanes, clearly indicating positive effects of self organisation. This suggests that parameter sets calibrated for bidirectional flows could potentially be used for unidirectional flows (this result is further supported by the validation results in section 7.4.2).

However, the same cannot be said for the other normal walking flows. Particularly the crossing flow displayed the largest differences to both bidirectional and unidirectional flows. The same was obtained for the interaction experiments.

Pedestrians in evacuations walk in a constrained situation and with a larger sense of urgency. These create less possibilities for pedestrians to manoeuvre and resulted in the different sets of parameters that these experiments generated when compared to the other experiment groups. Furthermore, the tests comparing the similarity of the samples of parameters showed small variations between the four evacuation experiments indicating the similarity between the congested evacuation flows.

This relation between the estimated parameters and the type of flows is common to traffic models that describe complex and non-linear phenomena (Van Lint (2009)). The obvious consequence for walker models is the specialisation of the calibrated parameters to the conditions that were present in the calibrations. This strongly points to the

necessity to submit the walker models and the parameter set that will be used in generic situations to multi-scenario validations that take several flow variables into consideration.

Importance of population composition and urgency levels

We showed that the population composition and the level of urgency have a significant effect on the outcomes of the calibrations (section 6.5). Calibration with homogeneous population resulted in similar parameter samples for two urgency levels. However, we observed that urgency did affect the forcefulness of the pedestrians. The urgency made pedestrians deviate less from their desired paths and simultaneously they were reacting more with the nearby pedestrians. These effects of urgency show the importance of human factors into the behaviour of pedestrians. Models developed for simulation of evacuations and normal walking should be calibrated with data obtained in these different situations.

The parameter samples for the same level of urgency, but with different levels of heterogeneity, were significantly different. This shows the importance of calibrating walker models with heterogeneous populations for accuracy. Therefore, models must be prepared to accept parameters that are represented by distributions. The Nomad model is capable to generate pedestrians with parameters generated from normal distributions.

Influence of traffic conditions

The results from section 6.6 show that pedestrian behaviours vary significantly in different traffic conditions and that the estimated parameters reflect these differences. Particularly, the estimated parameters of the upstream bottleneck experiment present a significant dependency to the average speeds of pedestrians in the form of (relatively) smooth curves. This experiment also showed the widest range of observed speeds.

For most parameters these curves presented inflexions at a critical speed $v_c \approx 1.0 m/s$. This speed was shown in Hoogendoorn and Daamen (2005a) to correspond to the capacity speed that separates the two regimes of free-flow and congestion. Therefore, an easy and effective way of improving walker models is to incorporate parameters that are dependent of different regimes. Eventually, a more complete solution is to define the parameters as functions with the local density as independent variable ($\theta_i = f(k)$). These functions account for all regimes from free flow until congestion improving the accuracy of the model in a wide range.

6.7.2 Findings

This chapter shows that the hypothesis of structuring walker models in behavioural components is correct. Parameters of the different components did not present enough

correlations to reject this hypothesis. All parameters of the Nomad model could be calibrated, and are therefore necessary to be included in the model. Results of the calibrations from trajectories of different experiments show that flow configurations have a strong influence on pedestrian behaviours, and resulted in different parameters.

Pedestrians in unidirectional flows behaved similar to pedestrians in bidirectional flows, showing that lane formation effectively separates the area in unidirectional regions. In congestion, pedestrian behaviour is quite different: in low densities pedestrians are more reactive due to the presence of other pedestrians, while in congestion pedestrians tend to follow other pedestrians and do not strain from their paths. The latter is also shown in the clear relation between some of the parameters and the (local) speed.

Population composition (heterogeneity) and urgency have significant impact on pedestrian behaviours. In general the increase of urgency turns pedestrians into more forceful walkers. They tend to stay closer to their desired paths and simultaneously they are more reactive to nearby pedestrians. This effect is enhanced if the heterogeneity is also increased. The overall effects of urgency and heterogeneity explains the loss of efficiency due to heterogeneity (Campanella et al. (2009a)) and due to the so called *freezing-by-heating* effects (Helbing et al. (2000b)).

Pedestrian avoidance behaviours also vary according to walking regimes. Most behaviours were shown to vary with speeds and some presented a distinct change at a critical speed that corresponds to the saturation of the bottleneck.

6.7.3 Implications

We found that the crossing flow experiments obtained less significant calibrations. We attributed to poorness of data due to a limited amount of interactions in the relatively small walking area and low densities encountered in the flows. This shows that empirical data must be composed by long trajectories that contain sufficient behavioural information.

We summarise the results with implications for the development walker models:

1. The use of body depth instead of width for models using circular shapes or the introduction of elliptical bodies in simulations of dense situations.
2. Introduction of heterogeneity in the input of the models.
3. Introduction of urgency for evacuation simulations.
4. Determination of parameters as functions of the local conditions such as current speeds or local densities. This would incur in a regime based model.

The previous list makes it clear that the level of complexity of walker models would increase even further. The current models with large amounts of variables are already

very difficult to calibrate and validate and this goes beyond the capacities of normal users. However, the fundamental question is: *is the effort of improving the microscopic characteristics of such models necessary?*

In this chapter we focused on the microscopic accuracy of walker models. However, walker models are predominantly used to assess macroscopic traffic characteristics such as capacities, egress times, area use and occurrence of bottlenecks. Being this the case, we may be content to show that current models are able to predict macroscopic indicators within accepted levels of accuracy. Chapter 7 does that for Nomad by comparing the accuracy of several parameter sets including those estimated in this chapter.

Chapter 7

Investigating the accuracy of multi-scenario calibrations

The aim of this chapter is to investigate the hypothesis proposed in chapter 4 that parameter sets calibrated with several situations represented by different flows perform better than parameter sets calibrated with a single situation. The hypothesis aims at obtaining parameter sets that are intended for general use.

To investigate the hypothesis, we compare the accuracy of parameters resulted from multi-scenario calibrations against those resulting from single-scenario calibrations. In the remaining of the chapter we will abbreviate the name of the calibrated parameter sets to *multi sets* (for multi-scenario) and *single sets* (for single-scenario).

The single sets are originated from two different calibration procedures. The first single sets are calibrated in chapter 6. These parameter sets represent an average of individual behaviours for the flows that they were calibrated. The second single sets are calibrated using travel time distributions, resulting in sets that are specialised in predicting a macroscopic characteristic of the flows.

The two procedures use the bidirectional, unidirectional and narrow bottleneck flows from the experiments introduced in chapter 6. These calibrations resulted in a total of six single-scenario parameter sets (two for each flow). Two multi-scenarios calibrations are performed resulting in two multi sets. The first uses the travel time distributions of the three flows simultaneously in a three scenario calibration. The second multi set combines the travel time distributions with an additional indicator based in the $u \times k$ relation in a total of six scenarios.

We argued in chapter 4 that the validation of models must also include several situations in what we called multi-scenario validation. The validations use the same experimental data from the calibrations and a additional crossing flow not used in any calibration. This flow is also originated from the experiments introduced in chapter 6. These flows represent the most commonly flows occurring in pedestrian facilities.

The scenarios use the following performance indicators: $u \times k$ relation, travel time distribution and bottleneck capacity. The indicators were chosen because they provide the required data for analysis of pedestrian flows (TRB (2010)). The multi-scenario validations result in average errors of these indicators. The capacity is only included in the assessment with the narrow bottleneck flow that presents congestion. We use these six single sets and two multi sets in three assessments of the parameter accuracies.

The first compares the performance of the multi sets with the performance of the single sets on the flows that were used to calibrate the single sets. We show that the multi sets are as accurate as single sets. These results show that it is not necessary to calibrate parameter sets for every specific situation (specialised sets).

We also show that the single sets resulting from the trajectory based calibration are inaccurate in predicting macroscopic characteristics of flows leading to the conclusion that averaging individual behaviours is not a good strategy for predicting macroscopic indicators.

The second compares the performance of multi sets and single sets over several flows simultaneously. The improved results in favour of the multi sets confirm the hypothesis that multi-scenario calibrations result in parameter sets more appropriate for general purpose applications. This is in agreement with the investigation in section 5.4 for synthetic trajectories.

The third compares the results of the two multi sets that were obtained with the same reference data from the same flows. We show that the multi set that resulted from two different indicators is almost two times more accurate than the multi set obtained with one indicator. Furthermore, the most accurate multi set also presented realistic movements indicating that Nomad can be applied with this parameter set for real case applications.

Three questions referring to the multi-scenario calibration are asked in section 7.1. Details of the multi-scenario calibrations and the macroscopic indicators are presented in section 7.2. The assessments set-up, explaining the components of the scenarios and the descriptions of the simulations are presented in section 7.3. Results are presented and discussed in section 7.4.

The chapter ends with the overall conclusions in section 7.5, a list of the findings and its implications for validation of walker models in general.

7.1 Research questions related to multi-scenario calibrations

This chapter argues that if no parameter set is calibrated for a specific situation (specialised set), then the set to be used for predictions must have shown to perform well

in various validation assessments utilising several walking situations giving a measure of general usability.

The first question that arises from this hypothesis relates to the presumed loss of accuracy of multi sets in comparison with single sets in the situations used to calibrate the single sets: *To what extent multi sets are less accurate than single sets in the specific situations used to calibrate the single sets?* This question addresses the necessity of calibrating sets for specific situations (specialised sets).

The second question investigates the claim made by the hypothesis that multi-scenario calibrations produce sets for general use: *What are the benefits of using multi sets in the combined accuracy of many flows?*

The third question addresses the overall performance of the multi sets: *What is the influence of indicators in the composition of multi-scenario calibrations?* This question does among other things evaluate the usability of Nomad in simulating complex situations.

7.2 Parameter sets

Eight parameter sets are used in this chapter that deals with the influence of multi-objective scenarios in the calibration of parameters. The first group of parameters were calibrated in chapter 6. These parameter sets are the average of the samples of calibrated parameters using the trajectory based scenarios presented in chapter 5. The scenarios use the acceleration prediction errors as indicators, thus being distinguished by the suffix 'Ac'.

For this chapter we use three parameter samples estimated with the normal bidirectional, unidirectional and narrow bottleneck upstream experiments (table 6.5). In the remainder these three single-scenario parameter sets are named *bidiAc*, *uniAc*, *bneckAc*.

The other five parameter sets use macroscopic performance indicators in the calibration scenarios. Two macroscopic indicators are used: differences in travel time distributions (TT) and a Fundamental Diagram indicator (FD) represented by the $u \times k$ relation.

Three single-scenario sets and one multi-scenario set use the travel time indicator (suffix 'TT'). The single sets use the same experiments as the 'Ac' sets being called: *bidiTT*, *uniTT* and *bneckTT*. The travel time multi-scenario set is *multiTT* and the other multi-scenario set uses both macroscopic indicators being named *multiTF*. The eight parameter sets are presented in table 7.1. All the calibrations applied the methodology presented in chapter 6 and are explained in the following subsections.

Table 7.1: Overview of the parameters sets used in the validations in this chapter.

	path follow	pedestrian interactions									obst-acle
		ped avoid		influence area				lateral avoid		antici-pation	
	τ	a_0	r_0	c_0^-	c_0^+	ie_f	ie_b	a_1	r_1	t_A	a_W
bidiAc	0.32	2.02	1.24	0.94	1.01	1.30	1.98	7.08	0.69	0.53	
uniAc	0.27	2.39	1.45	1.01	1.03	1.42	1.82			0.61	
bneckAc	0.57	2.84	1.06	0.99	0.96	1.36	1.14	5.97	0.62	0.60	9.02
bidiTT	0.50	0.67	0.07	0.84	0.24	0.69	0.55	0.83	0.58	0.25	
uniTT	0.79	1.09	1.54	1.97	1.36	1.88	1.53			0.99	
bneckTT	0.77	2.22	1.42	1.47	1.25	0.90	0.44			0.95	0.12
multiTT	0.26	1.50	1.38	1.84	0.72	1.55	1.45	0.92	1.44	0.14	0.14
multiTF	0.15	20.0	0.16	0.95	0.80	3.0	0.52	1.80	0.22	0.013	10.0

7.2.1 Travel Time indicator (TT)

The objective function consisted of the Kolmogorov-Smirnov distance ($D_{e,s}(\theta_i)$) between the travel time distributions. Figure 7.1 shows the representation of $D_{e,s}(\theta_i)$ for two travel time distributions. This distance was then associated with the objective function error (ε). However, during the try outs it was noticed that $D_{e,s}(\theta_i)$ would sometimes not reflect properly the occurrence of non-realistic behaviour.

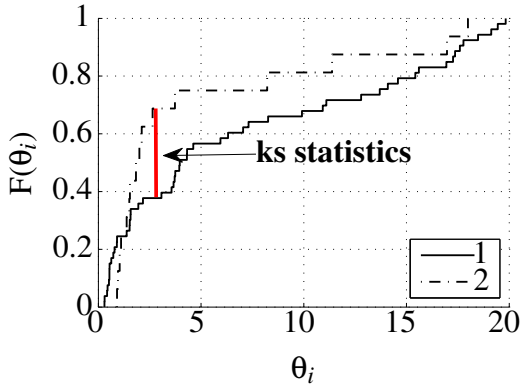

Figure 7.1: The representation of the Kolmogorov-Smirnov statistics for two travel time distributions.

Some combinations of parameters produce pedestrians walking erratically but eventually finding their way to the exit. In some cases the KS distances would not expose these erratic behaviours because the travel time distribution would not necessarily be too different from the empirical. Therefore, we introduced in the objective function two penalties: due to differences between the exit time of the last pedestrian in the simulation ($|ET_e - ET_s|$) and due to the amount of simulated pedestrians that exited the area after the last time a real pedestrian exited the experimental area. The penal-

ties are described by exponential functions that increase the error significantly if the differences become too large. Equation (7.1) and figure 7.2 show how the error is calculated.

$$\varepsilon(\theta) = D_{e,s}(\theta_i) exp\left(\frac{|ET_e - ET_s|}{(0.5ET_e)}\right) exp\left(\frac{(A_e - A_s)}{(0.05A_e)}\right) \tag{7.1}$$

where:

$\varepsilon(\theta)$ Objective function error for the simulation with parameter set θ.
$D_{e,s}$ Kolmogorov-Smirnov distance between empirical and simulated travel times distributions.
ET_e Exit time of the last pedestrian in the experiments.
ET_s Exit time of the last pedestrian in the simulation.
A_e Total amount of pedestrians in the experiments.
A_s Amount of simulated pedestrians that exited the area at simulation time$= ET_e$.

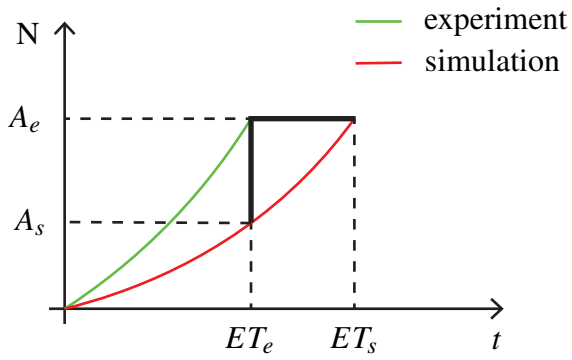

Figure 7.2: Representations of the cumulative distributions of the exit times.

The erratic movements due to very bad parameter sets created deadlocks or congestion. Deadlocks caused more difficulties to the calibration process, especially with the narrow bottleneck experiment. For a significant time no pedestrians would enter the corridor and than suddenly the deadlock would solve and pedestrians would exit at the end of the corridor. The variation of the KS distance would become highly non linear and optimisation convergence was a problem. Therefore, we created a high penalty for deadlock formation that is expressed by the differences in the amount of exit pedestrians at the end of the experiments (ET_e). The penalty represents an increase of 700% of the KS distance for a 10% increase in A_s in relation to A_e.

In other situations congestion would cause many collisions slowing pedestrians forward movement. These situations were not so extreme as with deadlocks and a smaller penalty was introduced to the Kolmogorov-Smirnov distance. The penalty represents an increase of 22% of the KS distance for 10% difference in ET_s in relation to ET_e. The weights chosen for the penalties were arbitrary and tests with the synthetic data from chapter 4 showed that the objective function successfully estimated the correct synthetic parameters.

7.2.2 Fundamental Diagram indicator (FD)

The Fundamental Diagram indicator, called the *FD* in the remaining, is the slope of the $u \times k$ relation. We define the values of the slope over bins of density intervals equal to 0.1 peds$/m^2$. We assume that these density intervals represent particular walking conditions that can be considered similar. Therefore, the slope of the $u \times k$ relation can be approximated by the average speed in the bin. Preliminary tests showed that intervals smaller than 0.1 peds$/m^2$ were not necessary and often created empty bins.

The fundamental diagrams were obtained according to the definition by Edie (1963) using the whole area to compute the densities (accumulation/walking area) and a time aggregation interval of 1 second to compute the speeds. These choices diminish the scatter and problems associated with density definitions (Duives et al. (2015)). We use the $u \times k$ relation for the assessment because it is the most used of the relations for pedestrian flows (Schadschneider et al. (2009)). Details of the $u \times k$ calculations can be found in Campanella et al. (2009d). The mean curve and the two shifted curves above and below the mean by the standard deviation are shown in figure 7.3.

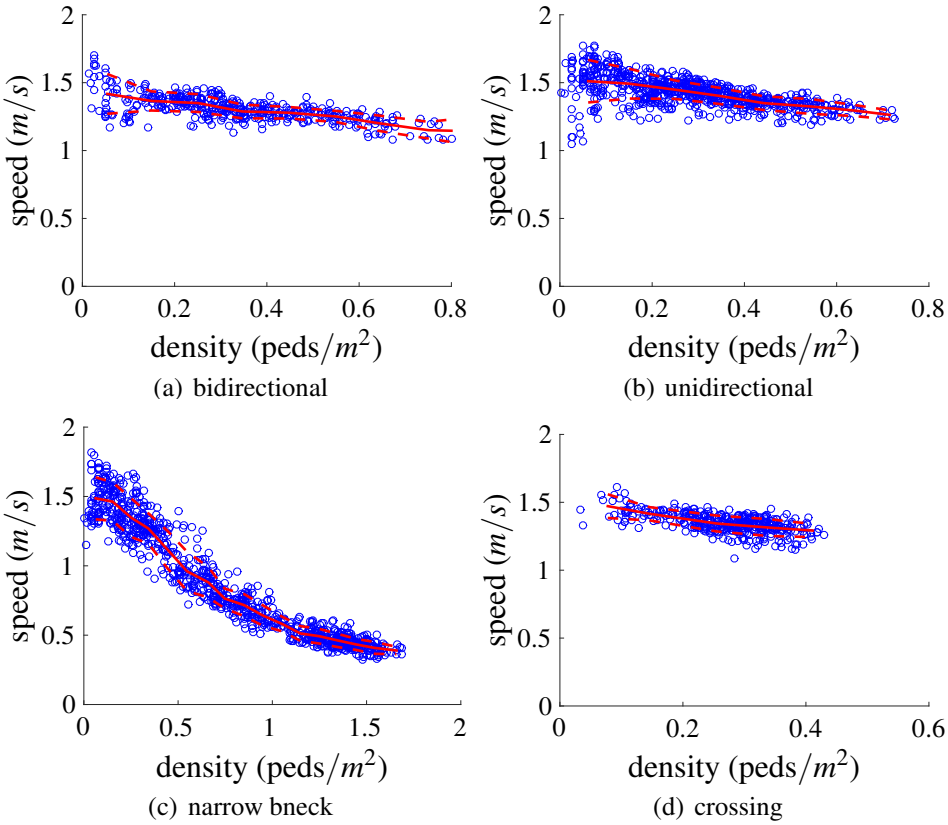

Figure 7.3: Speed-density plots for the experimental trajectories with the fitted curves.

For a simulation s, each bin error$_{\overline{u}_b}$ is computed according to:

$$\varepsilon_{\overline{u}_b} = \frac{\overline{u}^{sim} - \overline{u}^{exp}}{\overline{u}^{exp}}|_{b \in bins_s}$$

with:

$bins_s$ = bins on simulation s

$\overline{u}$ = average speed in bin b

The slope error for the simulation s is the average of the errors of all bins. Empty bins were assigned $\overline{u}^{sim} = 0$ generating $\varepsilon_{\overline{u}_b} = -1$. The same error was given to empty experimental bins in the case that simulations generated higher densities than the experiments. This prevents small slope errors when parameter sets correctly predict the free-flow densities of the $u \times k$ relation but does not produce the densities in the congested branch due to incorrect high flow capacity. This strategy assumes that the demands of the experimental and synthetic flows are similar.

$$\varepsilon_{\overline{u}}(s) = \frac{\sum_{b=1}^{bins_s} \varepsilon_{\overline{u}_b}}{bins_s} \tag{7.2}$$

7.2.3 Parameter estimations using macroscopic indicators

The calibrations for the three single scenario and the the multi-scenario TT parameters use the combination of the genetic algorithm with a simplex optimiser used in the two previous chapters and described in section 5.2.8. The single TT sets were calibrated with the error presented in equation (7.1) with the travel time distribution from the experiments. The *multiTT* sets was calibrated similarly but with the sum of the errors of the three experiments in a three scenario calibration.

The *multiTF* set was calibrated similarly but with the additional slope indicator. In total the multi-objective was the sum of errors from six scenarios, two indicators for each experiment.

A previously calibrated multi parameter set (Campanella et al. (2009c)) was used as the initial seed in a local search interactive approach for the *multiTF*. The previously calibrated set also used three flows and two performance indicators. However, because it was resulted from a limited amount of iterations, it was considered a good candidate to be improved.

The procedure initiated by varying every parameter from the seed around their values while keeping the others fixed. The parameter that presented the largest improvement was modified with the new value. The process repeated until no improvement could be achieved after 11 cycles. The FD indicator for the narrow bottleneck experiment produced the largest errors. Even though local search is not the most suited optimisation algorithm for non-linear search spaces the good assessment results obtained in this chapter (table 7.8) indicate that the calibration succeeded in finding at least an accurate local optimum.

7.3 Validation procedure

The validation procedure applied in this chapter is an implementation of the methodology proposed in chapter 4. The multi-objective function is the average of the relative errors of the scenarios. We propose a simple validation criteria based in the multi-objective error. A parameter set is considered accurate if the multi-objective error is smaller than 5%. For discussion purposes, we associate the range of errors into three ordinal variables (table 7.2).

Table 7.2: The three score intervals for the errors of the quantitative indicators.

score	interval
Bad	$10\% <$ error
Medium	$5\% <$ error $\leq 10\%$
Good	error $\leq 5\%$

This validation aims at testing the influence of multi-scenario calibration and the usability of Nomad as an accurate predictor of pedestrian flows in complex pedestrian facilities. Therefore, we need to validate the relevant behaviours found in these areas applying performance indicators that allow operational and planning analysis as defined in TRB (2010). We choose the duration, characteristic and intensity of flows represented by: travel times, $u \times k$ diagram and bottleneck capacity.

Pedestrian facilities such as train stations and airports will generally be composed by flows that resemble those found in the flows from the four normal experiments used for the calibration of individual parameters in chapter 6. In the next subsections we describe the three performance indicators and the set-up of the validations used to calculate the validation errors.

7.3.1 Performance indicators

Every validation scenario has one performance indicator as defined in chapter 4. The average travel times and the slope of the $u \times k$ diagram are part of the validations of all flows. The capacity indicator is only present in validations using the narrow bottleneck experiment. Table 7.3 shows that we created 9 different scenarios and that each parameter set is submitted to four different validations using 2 or 3 different scenarios.

All indicators are formulated as relative errors as defined in equation (4.4). This allows the direct calculation of the average of the scenario errors as the multi-objective of the validations. The indicators are calculated over 30 different simulations of each flow to account for the stochasticity of Nomad (section 7.3.2).

Table 7.3: Overview of the experiments used in each validation assessment.

	Experiments			
Indicator	bidirectional (*bidir*)	unidirectional (*unidir*)	crossing (*cross*)	narrow bneck (*bneck*)
Travel times	×	×	×	×
Capacity				×
Speed density	×	×	×	×

Travel times

The travel time indicator (TT) is the difference between the average travel times of the reference and simulated trajectories. The travel time error $\overline{\varepsilon}_{TT}$ is presented in (7.3).

$$\overline{\varepsilon}_{TT} = \frac{\sum_{s=1}^{30} \varepsilon_{TT}(s)}{30} \times 100 \text{ (in } \%) \tag{7.3}$$

$$\varepsilon_{TT}(s) = \frac{\overline{TT}^{sim} - \overline{TT}^{exp}}{\overline{TT}^{exp}}|_{s \in Simulations}$$

Table 7.4 shows the mean travel times $\overline{TT}^{exp}$ for the four flows used in equation (7.3).

Table 7.4: Overview of the mean travel times TT^{exp} for the four flows.

exp.	mean of travel times (s)	std of travel times (s)
bidir	7.8	0.9
unidir	7.2	0.7
cross	5.8	0.7
bneck	15.8	6.6

Fundamental diagrams

The fundamental diagram indicator $\overline{\varepsilon}_{FD}$ averages the slope indicator $\varepsilon_{\overline{u}}(s)$ for the 30 simulations ($s \in S$). The slope indicator was defined in equation (7.2).

$$\overline{\varepsilon}_{FD} = \frac{\sum_{s=1}^{30} \varepsilon_{\overline{u}}(s)}{30} \tag{7.4}$$

Bottleneck capacity

The bottleneck capacity (C) is only evaluated with the narrow bottleneck experiment. The capacity was calculated as the maximum flow in the entrance of the corridor (bottleneck) during the congested period. For the purpose of the validation we need a simple and consistent method for calculating the capacities.

The flows were calculated by counting a fixed amount of pedestrians and measuring the time needed for the first and the last pedestrians to pass the cross section. The choice of fixed amount of pedestrians instead of more common fixed time interval increases the statistical significance of the measured capacities. Hoogendoorn (1999) points that with fixed intervals, observations of traffic data show large variance. This happens specially when the flows are not high. Low flows have a double effect of presenting larger variations of speeds and smaller amounts of counts. Therefore, Hoogendoorn (1999) proposes fixing the amount of observations (pedestrians passing the bottleneck in our case) to keep the observations with comparable statistical significance.

This procedure has the advantage of being very simple. Basically it measures the time that passed between pedestrian p and the pedestrian $p+N$, N being the size of the batch. We measure the time passed for all pedestrians and the smallest time will determine the maximum flow, thus the capacity. The choice of the batch size is very important. If the amount is too small unrealistic high flows are measured. If too many pedestrians are counted over a long period of time there is large variations in the conditions.

To determine the size of the batch that reflects saturated conditions for the narrow bottleneck experiment we created an iterative process that increased the batch size progressively. We started with $N = 10$, and increased until the maximum difference between two consecutive measures during the congested period was not larger than 5% of the maximum flow. This error follows from the validation criteria in table 7.2. We observed that smaller errors did not change significantly the capacity.

The smallest amount that fulfilled this criteria for the experiments was 50 pedestrians and the interval of time measured was $t_c = 30.7s$ resulting in a capacity of $q_c = 1.63$ peds$/s$. This value is consistent with the two results calculated with two different and more complex methods in Hoogendoorn and Daamen (2005a) for the same experiments: 1.56 peds/s for a distribution-based estimate and 1.61 peds/s the Product Limit Method estimate.

The capacity estimator $\overline{\varepsilon}_{q_c}$ is the relative error of the capacities for each simulation resulting from the procedure described above:

$$\overline{\varepsilon}_{q_c} = \frac{\sum_{s=1}^{30} \varepsilon_{q_c}}{30} \times 100 \text{ (in } \%) \tag{7.5}$$

with:

$$\varepsilon_{q_c} = \frac{q_c^s - q_c^{exp}}{q_c^{exp}}|_{s \in simulations}$$

$$q_c^{exp} = 1.63\ peds/s$$

7.3.2 Simulation set-ups

Each simulation was set-up to resemble the original experiment: the same layout of the walking area, the same inflow pattern and the total amount of pedestrians. The inflows of the simulations were determined by counting the inflow of the experiments over periods of 10 seconds.

Simulation runs for the quantitative validations

To account for stochasticity we performed 30 runs of simulations for each parameter set. This number was determined to be sufficient to provide a statistical accuracy of 5% using the procedure explained in section 5.2.4. The 5% threshold follows the validation criteria established in table 7.2. Table 7.5 shows the 5% values of the average travel times, bottleneck capacity and average speeds in the density bins.

Table 7.5: Overview of the statistical accuracy used to determine the amount of runs in the validation mappings (the values shown represent 5% of the experimental average values).

	Experiments		
Mappings	bidirectional	unidirectional	narrow bneck
Travel times (s)	0.38	0.36	0.80
Capacity ($peds/s$)			0.080
FD: mean speed (m/s)	0.071	0.078	0.72

After running 30 simulations we could calculate the standard deviations of the indicators and determine the minimum amount of simulation runs that would be enough to satisfy the accuracy threshold. Table 7.6 shows that the worse results never required more than 29 runs. The table also shows that the bottleneck experiment produced the largest stochastic variation for all mappings, indicating that congested flows are more affected by stochastic variations of the model.

7.4 Validation results

This section presents the individual scores of the indicators and discuss the performance of parameter sets over the different flows. Initially we will discuss the results of the three indicators and than proceed in answering the research questions.

Table 7.6: Minimum amount of simulation runs necessary for the validation mappings. Only the worse case per mapping is posted.

Mappings	Experiment	Parameter sets	Std deviation of mappings	Actual amount of simulations
Travel times	*bneck*	*bneckTT*	2.2	**29**
Capacity	*bneck*	*multiTT*	0.15	1
FD: mean speed	*bneck*	*bneckTT*	0.06	13

Examining table 7.7 with the summary of the validation results we see that there is an agreement between the results of the indicators. Small travel time errors are accompanied by small fundamental diagram errors and the opposite is also true. The agreement between the errors is mostly visible in the narrow bottleneck flow where the capacity errors are correlated with the travel time errors and the FD indicator.

This is coherent since travel times are directly related with situations represented by the high density bins of the $u \times k$ relation and these presented the largest errors (not shown in the table). Too small capacity as observed with the single sets resulted in congestion setting sooner during the simulations. This increased the total occupancy of the walking area, increasing the slope errors. These validation results are in agreement with the discussions in chapter 4 about the difficulties to predict complex interactions.

The last column of the results table presents the overall score calculated according to table 7.2. The overall results clearly indicate that the multi sets give better validation results when compared to the specialised sets. We will discuss these results in detail in the following sections.

The densities of the unidirectional flow are comparable to those of the bidirectional and higher than those of the crossing flows (figure 7.3). However, the unidirectional flow produces the best results. This indicates that the behaviours occurring in this flow are less complex and therefore easier to be reproduced. We also observe that the narrow bottleneck flow produced the lowest scores. This is due to the calibration dificulties associated with higher densities such as the complexity of movements discussed in chapter 5.

The crossing flow that presents novel situations to all parameter sets posed difficulties to most sets. Only the *multiTF* resulted in a 'Good' score indicating that it can be considered a general purpose parameter set.

The three 'Ac' parameters showed bad accuracy in all experiments. This shows that the sum of individual behaviours does not result in an average pedestrian behaviour. This was further supported by visual inspections of the flows produced with these parameters. The trajectories presented jagged and unnatural movements for most situations. Given these bad results, we will not discuss these parameters in detail in this chapter.

The good validations of the bidiTT for the bidirectional, unidirectional flows and me-

Table 7.7: Overview of all validation errors in percentage (%).

exp	parameter sets	travel times $\overline{\varepsilon}_{TT}$	fundamental diagram $\overline{\varepsilon}_{FD}$	capacity $\overline{\varepsilon}_{q_c}$	validation errors $\overline{\varepsilon}_{total}$	validation score
bidir	*bidiAc*	-16	24		**20**	Bad
	bidiTT	0	3		**2**	Good
	uniTT	29	15		**22**	Bad
	bneckTT	115	23		**69**	Bad
	multiTT	5	4		**4**	Good
	multiTF	-1	3		**2**	Good
unidir	*uniAc*	-14	13		**13**	Bad
	bidiTT	-4	4		**4**	Good
	uniTT	0	4		**2**	Good
	bneckTT	-3	4		**3**	Good
	multiTT	5	5		**5**	Good
	multiTF	0	3		**2**	Good
bneck	*bneckAc*	214	25	-20	**125**	Bad
	bidiTT	149	39	-34	**74**	Bad
	uniTT	100	38	-20	**52**	Bad
	bneckTT	156	40	-16	**71**	Bad
	multiTT	-4	9	1	**5**	Good
	multiTF	6	8	1	**5**	Good
cross	*bidiAc*	-17	21		**19**	Bad
	uniAc	-16	18		**17**	Bad
	bneckAc	23	7		**15**	Bad
	bidiTT	6	6		**6**	Medium
	uniTT	26	27		**26**	Bad
	bneckTT	11	7		**9**	Medium
	multiTT	14	11		**12**	Bad
	multiTF	2	4		**3**	Good

dium for the crossing flow show that in the density range of the experiments, the bi-directional flow provides rich enough data to calibrate parameter sets. The other two single TT sets produced good accuracy only on the unidirectional flow, making them less suitable for single scenario calibrations.

The surprisingly bad result of *bneckTT* in the narrow bottleneck flow is caused by the difficulty to obtain accurate calibrations for the type of conflicts that occur in the entrance of the corridor as discussed in chapter 5. The travel time indicator could not overcome these difficulties suggesting that it does not a good indicator to be used in single calibrations involving complex situations.

We also made qualitative assessments about the quality of the movements resulted

by the simulations. In general the movements generated by the single sets were not realistic.

All single sets presented too many frontal collisions in the bidirectional flow and lateral collisions in the crossing flows. In the congested part of the narrow bottleneck we observed that for the uniTT and the bneckTT pedestrians would stay too far from each other. The bidiTT creates oscillations in the corridor of the narrow bottleneck.

Both multi sets presented better movements with the multiTF being the most realistic with minimal amount of collisions and less erratic movements in general.

7.4.1 Accuracy of specialised sets

The three single TT parameter sets can be considered to be specialised to the flows that were used in their calibration scenarios and the multiTT the chosen general purpose set to answer the first scientific question that states: *To what extent multi sets are less accurate than single sets in the specific situations used to calibrate the single sets?*

As expected, the bidiTT and the uniTT sets presented the lowest travel time errors in the same flows used for their calibration. Both present $\overline{\varepsilon}_{TT} = 0\%$. However, the multiTT also presents a 'Good' result, although with a larger error of $\overline{\varepsilon}_{TT} = 5\%$ for both flows. The difference between the errors of the multiTT and the specialised sets for the $u \times k$ indicator is only around 1%.

The multiTT also resulted with a smaller TT error for the narrow bottleneck flow. This shows that the multi-scenario calibration resulted in a set that was calibrated correctly on the three flows. The other two indicators also resulted in good results presenting a overall good accuracy of the multiTT set on the congested flow.

The good result of the multiTT for the narrow bottleneck flow is important because the calibration of the *bneckTT* did not succeed in estimating an accurate predictor for this flow.

We plotted the complete results for the TT (figure 7.4) and the capacity validations (figure 7.5) in form of box-plots to show that the results for the multiTT are not varying very much, presenting good statistical accuracy for the obtained distribution. The results discussed in this section answer the question by showing that the accuracy of specialised flows can be matched and even improved by multi sets.

Therefore, we can answer the first question by stating that multi sets have small losses ($\sim 5\%$) of accuracy when comparing with specialised sets for non congested situations. Furthermore, for the travel time indicator we showed that the multi set is much less affected by the difficulties presented by the complex manoeuvres in the bottleneck area resulting in more than 25 times more accurate travel times than the specialised single set. These results make the calibration of specialised sets not advantageous from the accuracy point of view.

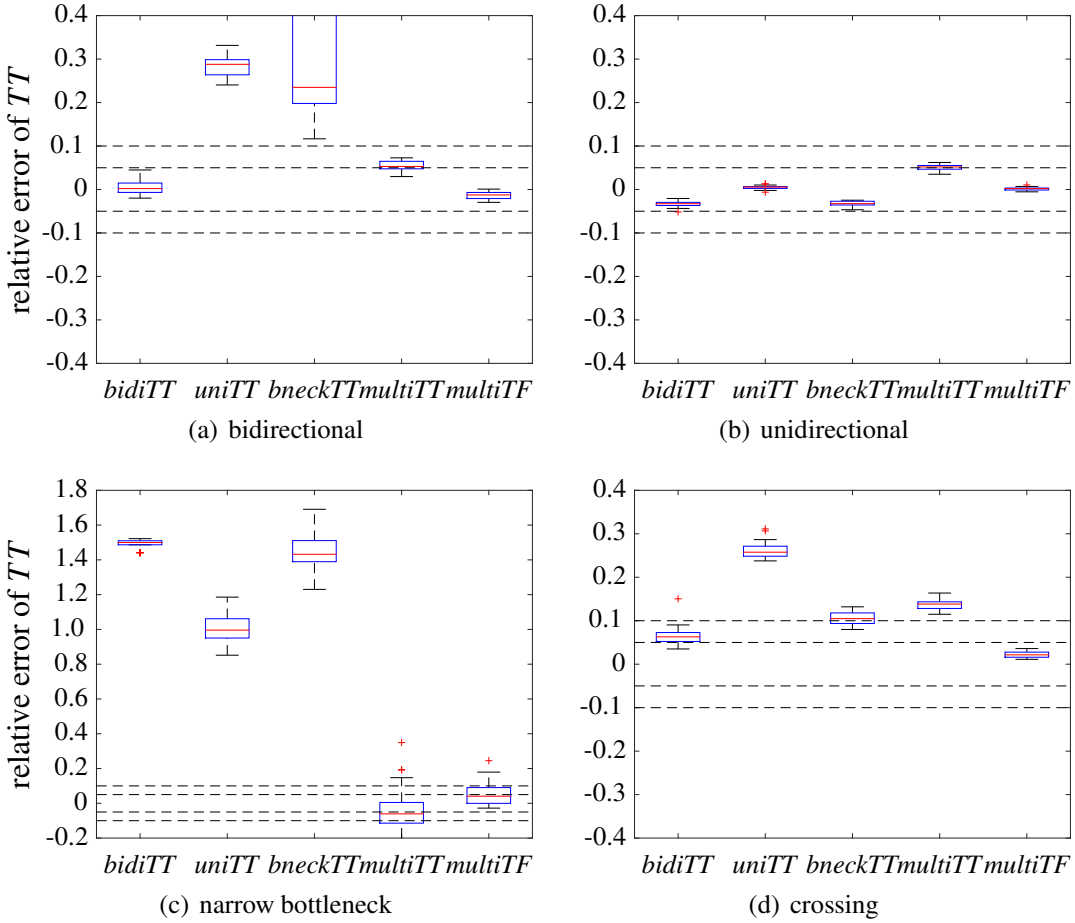

Figure 7.4: Box-plots with the relative errors of the travel times for the parameter sets. The dotted lines show the score intervals ('Good' at 5% and 'Medium' at 10%).

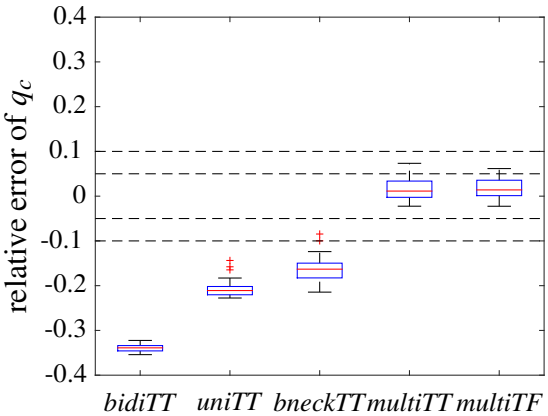

Figure 7.5: Box-plots with the relative errors of the capacities for the parameter sets in the narrow bottleneck. The dotted lines show the score intervals (5% and 10%).

7.4.2 Comparing results for all flows

In this section we compare the accuracy of each of the TT sets over the combined errors of the four flows. With that we are answering the second scientific question

that addresses the hypothesis that multi sets are more adequate to be used as general purpose sets. This answer requires novel flows not included in the calibrations.

We mentioned in the beginning of this section that the bidiTT presented good results for the bidirectional, unidirectional and crossing flows (table 7.7). However, things change when we include the error from the narrow bottleneck flow. The difficult walking situations in this flow are not well reproduced by the bidiTT that ends with very large errors (Table 7.8).

Table 7.8: Overview of combined validation errors for all flows in percentage (%).

exp	parameter sets	validation	
		errors $\overline{\varepsilon}_{total}$	score
[*bidir* +	*bidiTT*	**21**	Bad
unidir +	*uniTT*	**26**	Bad
bneck +	*bneckTT*	**38**	Bad
cross]	*multiTT*	**7**	Medium
	multiTF	**3**	Good

General purpose parameters are difficult to be obtained due to the complexities and non-linearities of walker models in the different situations that they are applied. We observe this by noticing the difficulties of the single sets in being accurate over all flows. The better overall accuracy of the multiTT was expected given that its calibration scenarios used three of the four flows used in the overall validation.

It would be expected that for each flow the multiTT would be slightly worse than the specialised set but ending with an overall lower error than the three specialised sets. This sort of behaviour indicates a compromise in the calibration algorithm balancing the importance of the scenarios.

The much better accuracy on the narrow bottleneck suggests that the multiTT not only reached a compromise but found a good solution. If we examine the parameters that compose the multiTT, we notice that τ is much smaller than the values of the other TT sets. From our experience with Nomad, this difference is large and has a greater impact in the movements of pedestrians than the differences on a_0 and r_0.

However, the multiTT presented worse results for the crossing flow than the bidiTT and the bneckTT sets. The bneckTT set performs so poorly in the narrow bottleneck flow that we cannot consider the parameter to be close to any optimal. Therefore, the good result of the bneckTT for the crossing flow must be regarded as coincidental.

The same cannot be said about the better performance of the bidiTT in the crossing flow. The bidiTT clearly shows a good accuracy when predicting flows with similar low to middle densities. This interesting result indicates that the walking behaviours

required in bidirectional flows are complex enough to be transferable to unidirectional and crossing flows that are not congested.

The compromise that the multiTT represents seemed to be affected by the situations represented by the narrow bottleneck reducing the accuracy on the crossing flow when compared to the bidiTT. This suggests that the multiTT is not close to a global optima.

The 'Medium' overall accuracy of $\overline{\varepsilon}_{total} = 7\%$ in contrast of the much larger error for the single sets, supports the hypothesis that combining several flows with different walking situations and densities improves the chances of estimating parameters that reflect general walking behaviours.

7.4.3 Impact of the calibration indicators on the validation results

As expected the inclusion of the $u \times k$ indicator in the calibration improved the validation accuracy of the multiTF in comparison to the multiTT for the bidirectional, unidirectional and narrow bottleneck flows. This is because the multiTF was calibrated with two indicators used in the validation.

Table 7.8 shows that the multiTF outperforms the multiTT in all indicators for the bidirectional, unidirectional and narrow bottleneck. Furthermore, if we exclude the results for the crossing in the calculation of the overall error we obtain $\overline{\varepsilon}_{total} = 5\%$ for the multiTT and $\overline{\varepsilon}_{total} = 3\%$ for the multiTF (not visible in the tables).

These errors show that the calibration algorithms find good solutions with both scenario arrangements. However, when we look at the parameters in table 7.1 we notice that almost all of their parameters are significantly different. Clearly indicating that the calibration procedures finished in different areas of the solution space.

The accuracy of the two multi sets are different for the crossing flow. In the analysis of the previous section we mentioned that the multiTT did not perform well with the crossing flow. The multiTT actually ended with a 'Bad' score and the multiTF with the only 'Good' score for this flow. It is with novel situations that we see the benefits of including more scenarios in the calibration.

The best way to visualise the good performance of the multiTF is to inspect the bins with the results of the $u \times k$ indicator. Figure 7.6 shows in blue the dots corresponding to the $u \times k$ bins formed by the average of the speeds (slope) according to the formulas presented in section 7.3.1 for the multiTF. We added the simulated and experimental shifted curves above and below the means by the standard deviation in each bin.

The $u \times k$ curves are close to the experimental curves (in red). The figure also shows that the slope errors are larger in the higher densities for all flows. The relatively low values of the densities for all flows results from the global densities (# peds in simulation/area), local densities that are much higher.

The multiTF resulted with a 'Good' validation for all flows and ended with a overall accuracy measure of $\overline{\varepsilon}_{total} = 3\%$ as shown in table 7.7. Another important consequence

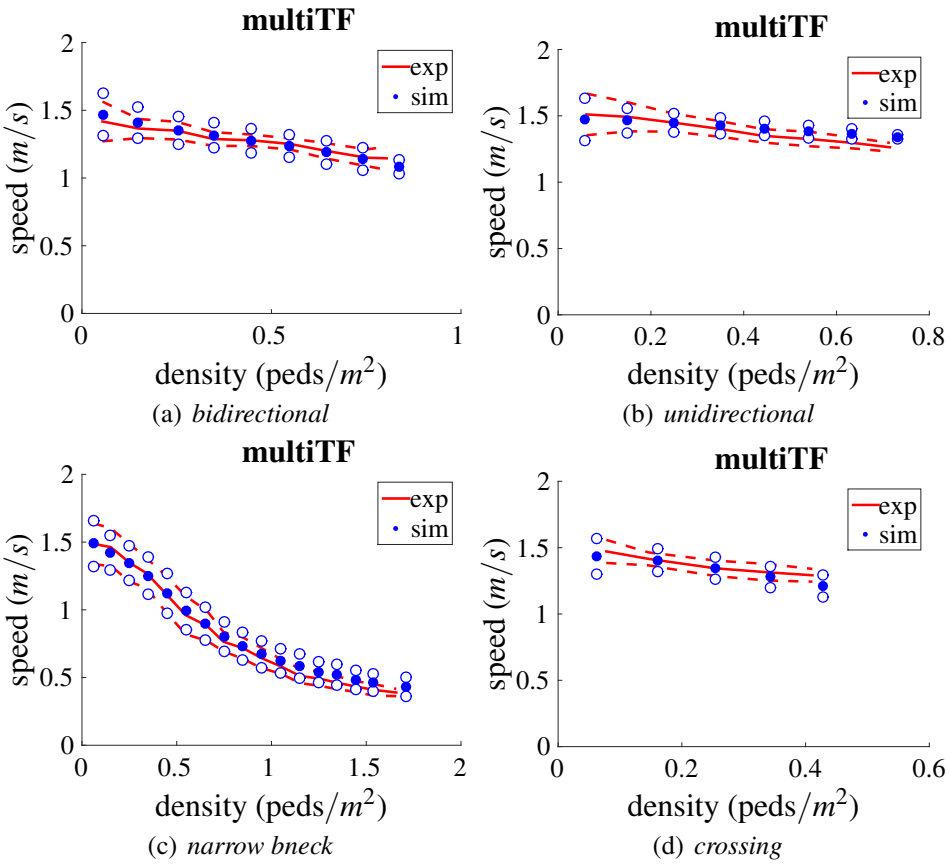

Figure 7.6: The speed density relations resulting from the parameter set*multiTF*. The filled dots correspond to the average speeds for the density bins. The white dots are the standard deviation displacements. The thick middle line is the average speeds for the experiments and the dotted lines are the standard deviation displacememnts.

of the improved calibration is the superior qualitative individual and collective movements resulting from the multiTF.

The results in this section showed that adding a second indicator in the calibration scenarios almost doubled the accuracy measured by the indicators and flows used in the calibration scenarios. However, the most important result was that adding a second indicator in the calibration improved by four times the accuracy for the crossing flow that was not used in the calibrations. Furthermore, the movements generated by the multiTF are also more realistic, showing that it is a better general purpose parameter set.

7.5 Conclusions

In this chapter we performed an extensive quantitative validation of the Nomad model using eight parameter sets. The validations followed the methodology presented in

chapter 4 where we proposed the concept of scenarios. In this chapter the scenarios were composed by four flows and three performance indicators.

The advantages of the validation implemented in this chapter are its simplicity and flexibility that allows for pairing any amount of assessments. The multi-objective was the average of the errors, resulting in each indicator being equally important. Furthermore, we used a simple conversion of the quantitative relative errors to three ordinal variables: 'Good', 'Medium' and 'Bad'. This conversion allowed for easy interpretation of the results.

The original on this chapter is the detailed comparison between five parameter sets. The most important result from this chapter is the support of the use of multi-scenario calibrations for the estimation of parameters intended for general use (not specialised in particular flows).

We showed that single-scenario sets that were calibrated with one particular flow are not appropriate to predict all the remaining flows. We also showed that using errors from three different flows simultaneously in multi-scenario calibrations, resulted in accurate predictions of the different flows.

The parameter sets resulting from the trajectory based calibration (calibration of individuals) are inaccurate in predicting macroscopic characteristics of flows leading to the conclusion that the sum of individual behaviours does not result in average pedestrian behaviour.

The calibrations involving travel time indicators produced better results with several parameter sets with good level of accuracy. The parameter set that was calibrated with the bidirectional flow had good accuracy in reproducing the unidirectional and the crossing flows. This indicates that the walking behaviours occurring in non congested bidirectional flows are similar and transferable to unidirectional and crossing flows. The conclusion is thus that bidirectional flows should be included in multi-scenario calibrations.

Since high densities and complex manoeuvres create the most difficult conditions for good accuracy they should always be included in walker model validations. Similarly, validations involving only unidirectional and bidirectional corridors with low or moderate densities should be avoided.

It was found during qualitative observations that the multi-scenario parameter sets produced flows with realistic walking movements while the single-scenario sets produced flows that were more erratic and displayed too many collisions. The implication is that realistic walker models diminish the sensitivity of simulation results by creating pedestrians that behave more predictably, similar to real pedestrians.

This chapter showed the importance of using several scenarios for validation of walker models. Even though the results of the scenarios showed positive correlations they allowed for detailed quantitative analysis of the accuracy of the different parameter sets. The analysis resulted in the recommendation of pairing more than one performance

indicator and using for several flows in the calibration scenarios to obtain parameters for general use.

We also demonstrated that Nomad fulfils the aim of this dissertation in obtaining a walker model that is accurate and realistic. We consider that overall errors below a threshold of 5% with the most important pedestrian flow assessments, namely travel times estimation, speed density relation and the capacity of a bottleneck corridor allow the application of Nomad for quantitative predictions.

Chapter 8

Applications of Nomad for pedestrian planning

Fruin (1971), Predtechenskii and Milinskii (1978) and TRB (2000) promote traffic conditions such as densities, travel times and travel distances experienced by pedestrians as important indicators of comfort and safety. More than predicting the evolution of traffic conditions with a detailed level, walker models can be used to predict the location and duration of activities of individual pedestrians. Detailed information on pedestrian walking and activity occurrences are useful to identify the impact of layout changes and increase of demand in complex facilities, helping decision making processes.

This chapter shows how a validated walker model such as Nomad can be applied to reveal insights about pedestrian operations in transport nodes. The examples illustrate how a walker model can be applied to perform different tasks required for transport planning and facility design. Simultaneously, the investigations in this chapter also justify the need and applicability of special behaviours by Nomad introduced in chapter 3.

The chapter is structured as follows. We present in section 8.1 how Nomad provides the data needed to estimate traffic conditions in circulation areas to identify the impact of installing turnstiles in the entrance hall of Amsterdam Airport Schiphol (Schiphol Plaza). Section 8.2 shows an optimisation problem, where Nomad predicts queuing times to reveal the influence of positioning reservation poles on train platforms. The last investigation in section 8.3 illustrates how Nomad is used to determine demands that are compliant to comfort criteria in a still to be built metro station.

The chapter ends in section 8.4 with the conclusions and insights resulting from the assessments described in this chapter.

8.1 Predicting traffic conditions at Schiphol Plaza

Schiphol Plaza is the shopping and food court of the land-side of the Amsterdam airport Schiphol. In this area arriving passengers meet their relatives and friends and departing passengers circulate towards one of the four terminals. Other pedestrians visit shops and restaurants, go to their working places or exit to destinations in the neighbourhood.

Plaza is a wide area of more than $80,000m^2$ with an underground train station. On the busiest day in 2007 (a Friday in July) 164,000 pedestrians visited the Plaza during the period between 5:00 am and 12:00 pm.

The aim of the study was the determination of comfort levels based on LOS values in future scenarios with 30 % passenger increase and the impact of the introduction of turnstiles at the exits of the subterranean train platforms in the circulation area. Several simulations were run for a whole day in the Plaza and a detailed analysis was performed. (More details can be found in Daamen et al. (2008)).

Figure 8.1 presents one of the outcomes of the simulations in the form of a map with maximum densities observed along the simulated day. The figure shows for each location of the circulation area, the maximum density reached during one day of the airport operation. Thus, the figure is not a snapshot of a moment but a maximum density map.

The crowded areas are mostly waiting areas. We can see that the walking patterns are clearly visible, while the lighter grey areas indicate the shops. In this simulation we were not interested in the crowdedness inside the shops and therefore they are not included in the density colour coding.

Figure 8.1 shows some critical areas. The areas around the ticket machines and the ticket offices became very crowded (areas a and b). This happened because the demand for tickets was far higher than the capacity of sales. The area c is the surroundings of one of the revolving doors that was saturated and generated large waiting times.

The introduction of turnstiles near the entrances of the train platforms narrowed the circulation area. Most of the affected areas did not create large discomfort, with the exception of the area d in figure 8.1.

The investigation concluded that the situation for the future scenario presented critical areas with high densities. However, we showed that the impact of the turnstiles was not as critical as for example the insufficient amount of ticket machines.

We showed that Nomad was successfully applied to simulate a complex situation and provided relevant answers to the original questions of the analysis. For this investigation we performed a validation of the OD table by simulating the base day of 2007 and compared the average stay time with empirical data obtained from surveys. We also compared qualitatively the waiting behaviours modelled in Nomad with those found in the real areas.

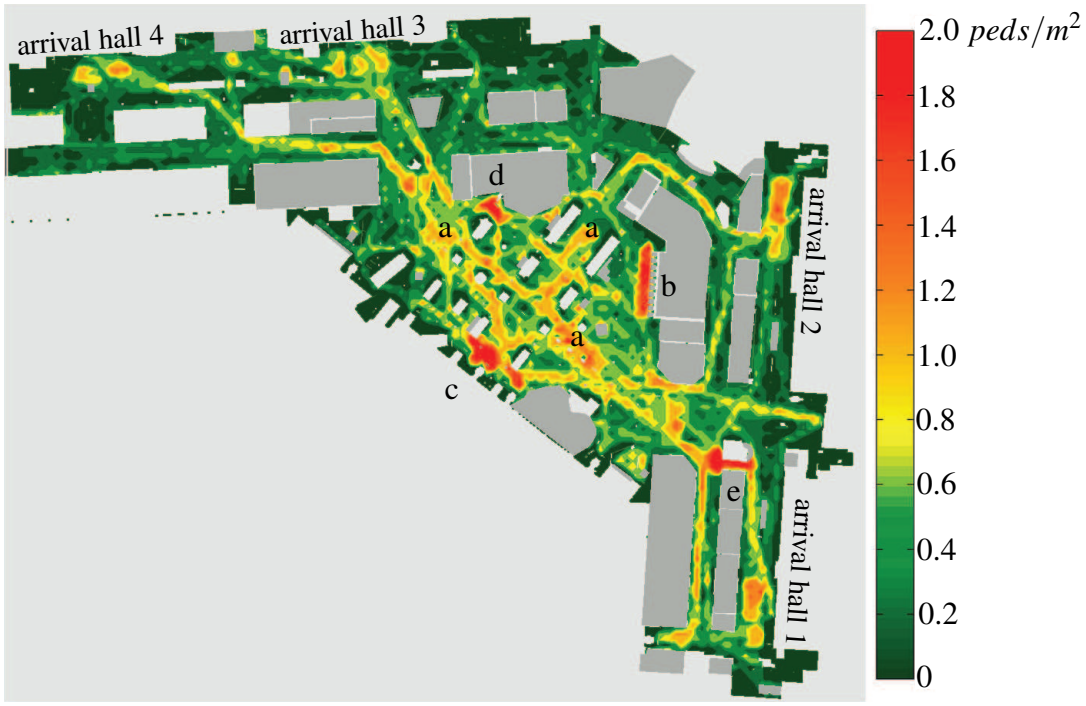

Figure 8.1: Overview of the maximum densities for the future Schiphol scenario. The walking area is divided in 2x2m squares and the densities (ped/m^2) during the day are recorded. Only the maximum densities are shown and they do not necessarily occur at the same time.

8.2 Assessment of ticket reservation posts on platforms

NS Hispeed is the train operator between Amsterdam Central Station and Brussels Station. NS Hispeed operates international trains and national trains between the stations of Amsterdam, Schiphol Airport, Rotterdam and Breda. During the planning phase, a 'new' tariff system including an obligatory reservation, both for international and national trains was considered[1]. Tickets would be sold on the internet, using dedicated Hispeed counters and via existing counters and ticket machines of Dutch Railways (NS). However, NS ticket machines would not be able to provide the corresponding seat reservations. Therefore, dedicated seat reservation posts would be developed.

These posts would be able to read public transport chip cards or bar codes and, after an approval of the back office, to provide a seat reservation. The reservation posts were planned to be located on the platforms and it was questioned what would be their impact on the passenger flows and transfer capacities.

The aim of this investigation was to determine the minimal amount of posts (efficiency from operator perspective) without keeping passengers spending too much time in queues and to keep operations in the platform smooth. The details of this study can be found in Daamen et al. (2009).

[1]The Hispeed system was eventually implemented without the obligation of seat reservation.

Figure 8.2 shows an overview of platform 5/6 in Schiphol with the scheme of the reservation posts. The light grey area indicates the platform. The brown areas are not available for pedestrians: they either represent obstacles on the platforms (escalators, columns) or the tracks next to the platform. The train is indicated in red, while the white squares indicate locations of the train doors. Four access points lead towards the platform, indicated in green. The middle two entrances are escalators, while the outer two access points consist of inclined moving walkways. It also shows the six clusters of reservation posts in orange.

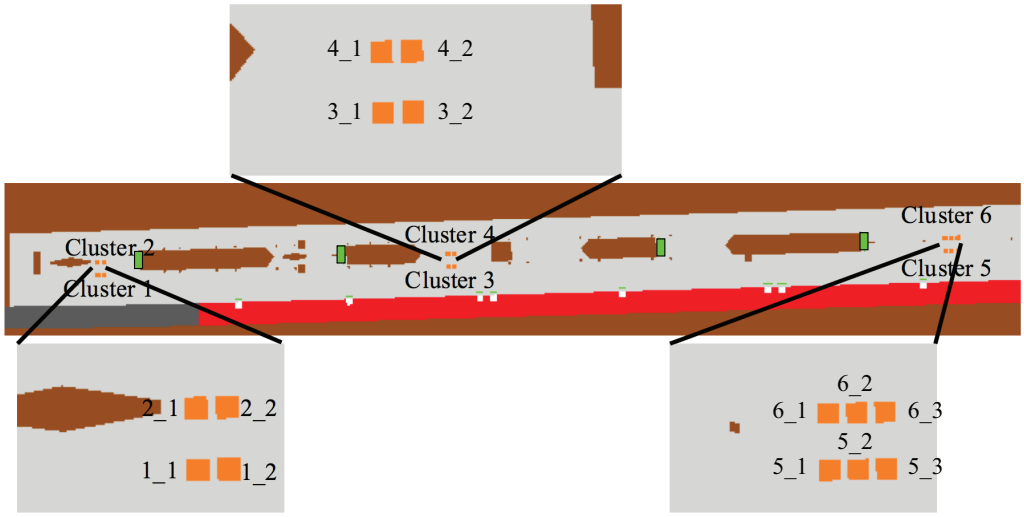

Figure 8.2: Location and numbering of reservation posts.

To determine the optimal utilisation of the posts we performed an iterative cycle of simulation. We removed the less busy poles one by one, and then identified the (steep) increase in waiting time. This time is dependent on the queues and indicates the use of each post.

The reference scenario with fourteen posts is taken as a starting point. The simulations showed that passengers spent around 12s at the posts. Then, the reservation post with the lowest load (usually the furthest from the platform entrances) is removed from the simulation, and the next simulations are run. A reduction to eleven posts does not affect the average time at a reservation post. When ten reservation posts are present, the average time increases, but only when the number of posts is reduced to eight, a considerable increase is visible in the average time per passenger (15s).

Figure 8.3 shows the average time passengers needed at a reservation post as a function of the number of reservation posts on the platform for the Schiphol station.

The investigations showed that the original amount of posts was unnecessarily high. The final recommendation was to reduce the amount to not less than eight units. The best location of the poles was also determined by the optimisation process resulting in the elimination of the most distant posts.

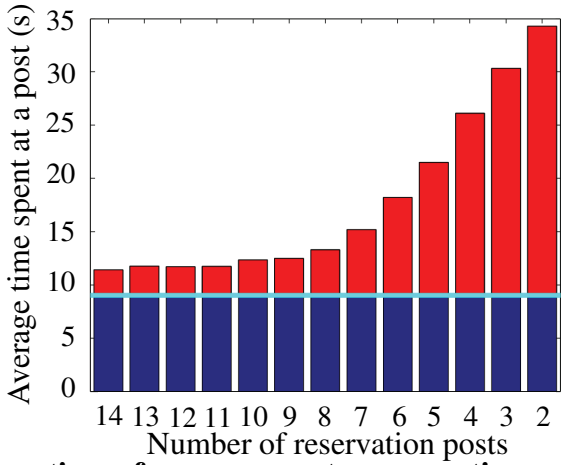

Figure 8.3: Average time of passengers at a reservation post as a function of the number of reservation posts on the platform.

In this investigation, Nomad was successfully applied to an optimisation problem. The amount of poles is optimised, given acceptable waiting times and reasonable cost. This use case shows a novel application of walker models for planning tasks. Regarding the assessment question the conclusion was that the proposed number of reservation posts could be reduced without decreasing passenger service for the three stations studied. It was not shown here but the results of the stations investigated showed that the most important factor for an efficient use of reservation posts is their location on the platform. The closer they were to the exits (stairs, escalators) the more they were used.

Preliminary to this investigation, a face validation of the distribution of pedestrians on the platform, including the immediacy of the doors before the alighting, was realised based on empirical data from other studies.

8.3 Determining the capacity of a Metro Station

Jardim Oceânico is a metro station being built in the city of Rio de Janeiro, Brazil. It will be inaugurated before the Olympic Games in August 2016. Three years before the inauguration, the private operator of the future station asked what would be the maximum amount of pedestrians walking in the station with an acceptable level of comfort. This amount would then be defined as the station capacity in operational conditions. It was expected that this capacity would be different from the capacity previously determined for emergency evacuations.

The aim of this investigation was to determine the maximum demand that could generate pedestrian flows and platform occupation that are compliant to comfort criteria that are less stringent than safety criteria. For detailed description of the investigation refer to Campanella (2012).

Jardim Oceânico is a terminal station with two lateral platforms. Platform 1 will only

serve for alighting and platform 2 for boarding. Both have an area of $513m^2$. The station's layout is approximately cruciform with three levels: platform, mezzanine and street level (figure 8.4).

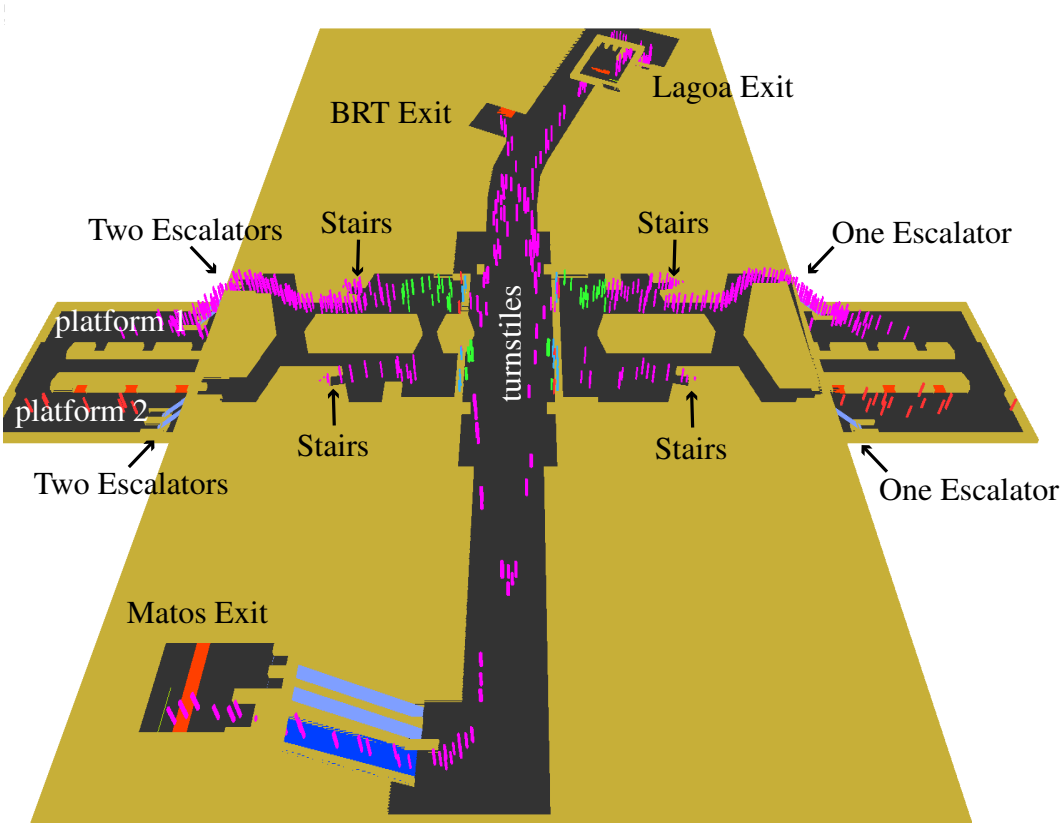

Figure 8.4: The Jardim Oceanico station with a simulation snapshot.

Figure 8.4 shows that the station has three levels connected by stairs and escalators. Furthermore, the entrance to the area accessible for travellers with a valid transport ticket is limited by a series of turnstiles. Before the simulations, we performed a series of calibrations of these components using operational data from MetrôRio, the future operator.

The comfort criteria were defined based on the duration of LOS levels at the walking and waiting areas. For example, it was decided that no waiting area of the station should reach LOS D for periods longer than 2 minutes.

We ran successive simulations of complete days with increasing demand resulting from multiplying a base demand with a factor larger than 1. The analysis determined that the bottleneck of the station was platform 2 (entering the station) in the morning peak. Figure 8.5 shows contour maps presenting the maximum consecutive periods that LOS D was reached on the platform 2 for the morning peak.

This investigation showed how a pedestrian simulation can be used to estimate an operational capacity of a metro station. The purposely defined comfort criteria determined

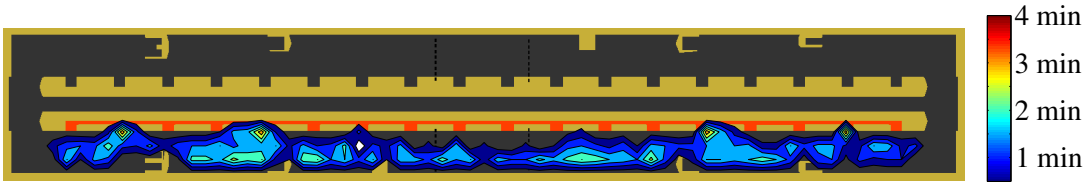

Figure 8.5: The maximum periods in minutes that areas of the platforms reached LOS D for the capacity demand. These areas are a 2x2m cell grid the maximum LOS D periods were not necessarily reached simultaneously.

the maximum inflow that fulfilled the criteria and showed that one of the platforms is the bottleneck of the station.

The capacity of the stairs and escalators were calibrated using data obtained by the operator of the metro. Furthermore, observations in existing stations provided evidence for face validations of the behaviours of pedestrians in the queues formed in front of the turnstiles.

8.4 Conclusions

In this chapter we showed how Nomad and any microscopic pedestrian simulation model can be used to generate simulation results, analyse the data, calculate indicators and derive insights about pedestrian flows and comfort in pedestrian facilities.

Three investigations involving Nomad were presented. The first investigation was the assessment of bottlenecks and circulation problems of the large entrance hall of Schiphol Airport in Amsterdam. The second investigation looked at the effects of reservation posts on passenger flows on train platforms in the Netherlands. The third investigation was the determination of the maximum demand that would fulfil comfort criteria of a metro station in Rio de Janeiro, Brazil.

For each of these investigations different qualitative validations of the special functionalities introduced in chapter 3 were performed. The walking areas of these investigations showed the need of these functionalities in walker models that are simulating complex pedestrian areas. This indicates that Nomad is a useful tool for operators, designers and authorities.

This chapter provides an important conclusion that pedestrian simulation models are ready to be fully integrated into planning and design services. However, pedestrian simulation models should not be handled as ‘black-boxes’ that always give correct predictions. Users need to know the level of accuracy of the simulation model, which features best represent the real processes and understand the principles of safety and comfort in pedestrian flows to provide appropriate answers to the questions asked.

Chapter 9

Conclusions and recommendations

The research focused in contributing to the development of pedestrian microscopic models. The contributions made in this thesis concentrated in improving the accuracy of walker models and modelling processes that are necessary to simulate large pedestrian facilities.

Accuracy is essential for the use of walker models and received the largest attention in this thesis. We focused in a key aspect of accuracy of walker models, that is, how to obtain parameter sets that are accurate in predicting flows and situations that were not used in the calibration. To implement novel walking processes, we chose Nomad as the most suitable model, and used it in extensive calibrations and validations performed in this thesis.

This chapter presents the main findings and conclusions in section 9.1. The practical implications and applications resulting from this thesis are discussed in section 9.2. The chapter ends with considerations about future research directions derived from the perspectives opened by this dissertation in section 9.3.

9.1 Main findings and conclusions

The main conclusion of this dissertation is that parameters calibrated with several flows and performance indicators increase the general applicability and the usefulness of walker models.

We concluded this by investigating the process of calibration with synthetic data (chapter 5) and comparing the results of validations using empirical data (chapter 7). In both studies we showed that parameter sets that were calibrated with data from three different flows (multi-scenarios) were more accurate than parameters that were calibrated with only one flow as reference data (single-scenarios). These investigations resulted in the recommendation of pairing more than one performance indicator and using several flows in the objective function to obtain parameters for general use.

The findings and conclusions from the thesis are presented in subsections that follow the general research questions presented in the introduction (section 1.4).

9.1.1 Agent based representation of walker models

The agent based representation proposed in chapter 2 resulted in model characteristics being directly related to pedestrians, their behaviours and the environment that they walk.

The agent based process of describing how pedestrians apply what they perceive to perform their walking actions resulted in the conclusion that walker models evolved into four families since their introduction in the 1970's: rule-based reactive, force-based reactive, goal-based and utility-based models.

The model assessments and scoring outcomes based in the agent representation showed that no model received high scores in all agent based characteristics suggesting that walker models that simulate large pedestrian facilities need to be improved.

The most promising modelling direction identified was a combination of strategies between reactive behaviours that are predicted directly from the state of the traffic and the environment with behaviours that are modelled with anticipation of future actions of the neighbouring pedestrians.

In this thesis we introduced anticipation in the Nomad model proposed by Hoogendoorn and Bovy (2002) that originally was purely reactive. Nomad together with other models achieved the highest score and was chosen to be further developed in this thesis by being the only model derived from a pedestrian walking theory.

9.1.2 Modelling walking behaviour

We conclude that the principles of the Nomad pedestrian theory can be applied for the development of special behaviours other than walking, showing the importance of having a behavioural theory to provide the basis of pedestrian models (chapter 3).

The hypothesis of structuring walker models in behavioural components according to the Nomad pedestrian theory, is strongly supported by the results in chapter 6. Parameters of the different components did not present enough correlations to reject this hypothesis. All parameters of the Nomad model could be calibrated, and are therefore necessary to be included.

Chapter 7 provided extensive validations showing that the Nomad model fulfils the aim of obtaining a walker model that is sufficiently accurate and realistic.

9.1.3 Generalised calibration and validation methodology

Chapter 4 resulted in a methodology for calibrations and validations based in a multi-objective function that includes several walking situations and performance indicators in what we called multi-scenarios.

Multi-scenarios are necessary to increase the probability of obtaining parameter sets that perform well in situations not used in the calibration. For validations multi-scenarios are necessary to increase the amount of walking situations (and levels of density) that parameter sets are shown to be accurate.

Calibrations require a significance analysis that certifies that the calibrated parameters are significant therefore influencing the outcome of the predictions on the situations encountered in the empirical data.

Validations require an assessment criteria based with quantitative indicators. The criteria establishes if the model is accurate for applications.

9.1.4 Factors affecting calibration of walker models

The analysis using individually calibrated parameters using trajectories produced with simulations allowed for finding that three factors affect calibrations: poorness of data, complexity of movements and random noise.

The first refers to lack of data containing information about pedestrian behaviours resulting in non-significant parameters. The second finding deals with congested bottlenecks involving complex manoeuvres presenting situations that are difficult to be accurately predicted. We showed quantitatively that noise in the tracking process affects significantly the accuracy of the calibrations. This finding reveals the importance of the accuracy of the tracking process in obtaining empirical data.

We concluded that multi-scenario calibrations combining errors from three flows reduce the problems arising from the three factors.

9.1.5 Investigations in microscopic behaviours

The research conducted in this dissertation shows for the first time quantitatively that flow configurations have a strong influence on pedestrian behaviours resulting in significantly different parameters. This allows us to conclude that pedestrians display different behaviours in different walking situations.

Pedestrian avoidance behaviours vary with speeds (used as a proxy for traffic conditions). In general pedestrians will be more sensitive to pedestrians further away and further from their walking direction when walking in free-flow. In congestion, pedestrian behaviour is quite different: pedestrians tend to follow other pedestrians and do not strain from their paths.

The transition of behaviours from free-flow to congestion is not gradual but presents a distinct change at a critical speed that corresponds to saturation of the flow. Before reaching a bottleneck, pedestrians increase their reactivity to pedestrians in their walking direction and decelerate due to temporal and spatial anticipation of the bottleneck conditions upstream. These results support the conclusions from Duives et al. (2014a).

Population composition (heterogeneity) and urgency have significant impact on pedestrian behaviours. In general the increase of urgency turn pedestrians into more forceful walkers. When urged to walk fast, pedestrians tend to stay closer to their desired paths reducing deviations (less cooperative). The effect of urgency is not the same for the different age groups and the reactivity between the pedestrians increases for heterogeneous populations probably accounting for unequal reactions.

Pedestrians in unidirectional flows behaved similarly to pedestrians in bidirectional flows, showing that lane formation effectively separates the area in unidirectional regions. The similarity between these two flows was also supported by results from the validation chapter (chapter 7) that showed that a parameter calibrated with a bidirectional flow was very accurate in predicting indicators of a unidirectional flow. Although the opposite is not true due to the absence of interactions with colliding trajectories in unidirectional flows.

The different outcomes for the types of flow reveal the importance of using several types of flows to investigate pedestrian behaviours.

9.1.6 Multi-scenario calibrations

Single-scenario sets that were calibrated with one particular flow are not appropriate to predict all the remaining flows. Multi-scenario calibrations using errors from three different flows resulted in accurate predictions of the different flows.

The best parameter set (validation error of 3%), reproduced with a satisfactory level of accuracy the most important pedestrian flow assessments, namely travel times estimation, speed density relation and the capacity of a bottleneck corridor for four different flows including one that was not used in the calibration.

It was found during qualitative observations that the most accurate parameter sets produced flows with the most realistic walking movements. The worst results of the quantitative validations coincided with flows that were more erratic and displaying many collisions. The implication is that realistic walker models diminish the sensitivity of simulation results by creating pedestrians that do behave more predictably similarly to real pedestrians.

Parameter sets resulting from the trajectory based calibration (calibration of individuals) are inaccurate in predicting macroscopic characteristics of flows leading to the conclusion that the sum of individual behaviours does not result in average pedestrian behaviour.

9.1.7 Application of walker models

The three case studies that used validated parameter sets combined with the special features introduced in chapter 3 showed that microscopic models are suited to be integrated into planning and design processes.

9.2 Contributions and recommendations for model developers

It is fundamental to any model developer to show extensively with calibrations, significance analysis and validations that the model components and the calibrated parameters are significant, and produce accurate results. Therefore, the most important practical contribution of this dissertation is the methodology that improves the probability of calibrating parameter sets that can be applied in various situations commonly found in large pedestrian facilities.

The methodology and the investigations in this thesis show the importance of performing sensitivity tests to determine the significance of the calibrated parameters.

The investigations using the methodology indicate the importance of quantitive validations using several performance indicators and different flows to assess the prediction accuracy in several situations, especially those not used in the calibration of the parameters.

The calibrations with synthetic trajectories is an useful procedure to investigate the ability of the calibration procedure in finding global optimal parameters. Such investigations increase the confidence that the results of calibrations with empiric data will correspond to the best predictions from the model. Results in chapter 5 show the necessity to introduce noise in the synthetic trajectories accounting for imperfections of the tracking procedure that reduce the ability to find global optimal results.

Chapter 7 proposes multi-objective function that averages errors from scenarios that is effective in producing quantitative assessments of different parameter sets. The simple and flexible objective function allows for extensive discussions about the accuracy of different parameter sets or of different models.

Fundamental diagram relations are important indicators of traffic flow variables but are usually only verified qualitatively with superimpositions of the predicted and the empirical fundamental relations. We recommend the mapping of fundamental relations into performance indicators to obtain a measure of accuracy of walker models in the whole range of the traffic variables.

The diameter of the circular shaped pedestrians in dense situations resulted in optimal values reflecting the body depth ($\sim 0.25m$) instead of the commonly assumed body width ($\sim 0.50m$). This has important consequences for developers that use similar

formulations. The theoretical maximum densities that a walker model can achieve without collisions for $\sim 0.25m$ diameters is 16 $peds/m^2$ instead of only 4 $peds/m^2$ for $\sim 0.50m$. Although 16 $peds/m^2$ is not a realistic value for maximum density, using diameter values smaller than the body width allows for extreme situations that were observed in real flows (Helbing et al. (2007)).

9.3 Future research

The future research directions follow the main contributions of this thesis on the empirics of pedestrian behaviour, walker model developments, and on calibration and validation methods.

9.3.1 Empirics

The mechanism of anticipation of traffic conditions downstream is important for the design of pedestrian facilities. The fact that pedestrians change their behaviour according to conditions in the near future should be further studied to determine if it occurs in real-world situations and how far the anticipation reaches. The anticipation mechanism can combine tactical level decisions with walker models. Furthermore, the knowledge of the anticipation mechanisms can also be investigated regarding crowd management actions and design guidelines. If it is determined that pedestrians are scanning long distances, rules can be developed to avoid visual obstructions blocking alternatives to bottlenecks. If an escalator is predicted to congest then an alternative staircase should be placed in a position that allows pedestrians to choose it before they reach the bottleneck.

We used trajectory data obtained from controlled experiments for calibrations and validations. A next step is collecting empirical data directly from flows occurring inside large pedestrian facilities. Real-world observations will assure that models are calibrated and validated with behaviours found in large pedestrian facilities. Controlled experiments may create conditions such as fatigue, boredom and bonding between subjects that make the data less reliable.

Trajectory data is difficult to obtain in public spaces and the spacial precision that trajectory data provides is not required to calculate macroscopic indicators. The precision and limitations of data obtained with new methods of position tracking such as Bluetooth, Radio-frequency identification (RFID) need to be investigated. New tracking methods will allow for new types of flows and situations to be included in calibrations and validations of walker models, increasing the accuracy of parameter sets.

9.3.2 Model developments

The findings on the influence of local conditions into behaviours obtained in this thesis are promising to improve model accuracy. Our study had the merit of showing quantitatively that different situations result in different parameters. A promising way to improve the accuracy of walker models (operational level) is to have parameters that vary with the local conditions. Pedestrians need to recognise the type of situations they are walking and switch the parameter set accordingly. It is not difficult to characterise the different types of flows such as bidirectional and crossing flows from the pedestrian perspective. When pedestrians perceive a change of type of flows or increase of density, they adopt other parameters.

Such modifications may risk increasing the complexity of the models but one can argue that no simple model can perform well in all situations pedestrians are walking. Therefore, making walker models more complex may increase their general use by simplifying the conditions that end users need to account when applying them.

The Nomad walker model was developed to improve the behaviours and activities usually occurring with commuters. Although this travel purpose is very common among pedestrians visiting large pedestrian facilities, the applicability of walker models can be extended to new travel purposes such as evacuation, shopping and leisure. These modes are important because these travel purposes occur in several situations with large crowds such as shopping centres and concerts.

The development of the new travel purposes requires the development of strategic and tactical model components including psychological and sociological aspects specific for these situations. Both empirical knowledge and modelling aspects need to be developed determining what behaviours should be applied in these situations.

To develop new strategic and tactical components, requires the expansion of the agent representation. These travel modes are more informal, not fitting to the current commuter behaviour of aiming destinations using utility based choices. Artificial Intelligence reasoning architectures such as the Belief Desire and Intention models (BDI) are good candidates to develop the agent representations of pedestrian models.

9.3.3 Calibration and validation guidelines

The other direction of future research is the development of calibration and validation guidelines. Guidelines are a further development of the methodology proposed in this thesis. There is a need to normalise the performance indicators and flow situations used in the calibrations and validations to compare different parameter sets and especially different types of models.

Developing the guidelines will require research into types of flows encountered in pedestrian facilities. Such study should include different types of facilities such as

train stations and airports that are often subjected to simulations. Preferably the flow conditions should include high densities and congestion that are critical conditions for walker models. Importantly, the investigation should also result in quantitative performance indicators that are able to represent the complexity of the flows. Fundamental diagram relations that expose the accuracy of models over the whole range of the traffic variables are the best candidate to be quantified in similar ways as proposed in this thesis.

Appendix A

Nomad activities

Nomadprovides five activities in total that give the user the possibility to simulate different types of waiting behaviours such as standing in train platforms, in front of public screens around information poles:

- *SimpleStatic* - The most basic activity. In this activity pedestrians stop immediately after stepping on the activity area.
- *RandomInternal* - Pedestrians are taken out of the simulation and do not react.
- *InPlaceWaiting* - Pedestrians start the activity in the current position.
- *RandomWaiting* - Pedestrians will choose a random location inside the activity area and stay on it while performing the activity.
- *CentroidWaiting* - Pedestrians will try to stay close to the centroid of the activity area.

SimpleStatic

The most basic and almost always present in the simulations as the activity of the final destination. Usually it is used with small destinations representing exits and ticket machines. When over it pedestrians do not move or take other pedestrians into consideration never being dragged away. Other pedestrians do react to those performing this activity. Like all other activity types pedestrians start moving to the next activity after the service time is finished.

RandomInternal

In this waiting activity pedestrians are not part of the simulation until the service time is passed. When entering the activity area pedestrians receive a random location and are

placed on it without walking. They are visible but do not exert any influence to other pedestrians. When the activity finishes they are moved to a point inside the activity area that is closest to the next destination and start walking. It is a useful activity for very complex simulations when pedestrians reach areas that are not of interest. For example when the simulation is focusing in the flow of corridors pedestrians entering shops can be temporarily removed.

InPlaceWaiting

This waiting behaviour is used in situations that are very crowded and the pedestrians cannot reach the main destination area. When boarding a public transport vehicle pedestrians usually aim at a seat. However, in crowded situations they may not find a free seat and wait somewhere in a free location in the standing areas. When the activity is finished (train reached the station) they simply go to the next activity area (exit) without the need to pass over the seat. While in their position pedestrian react to surrounding pedestrians and obstacles using the waiting behaviour.

RandomWaiting

The second most common type of waiting behaviour. Usually is used with large waiting areas like train platforms or areas under sign boards. When pedestrians reach the waiting area they *choose* a random location and walk towards it. Pedestrians need to navigate around other pedestrians that are waiting on the area. Pedestrians react to each other and those already close to their waiting locations may drift giving way to walking pedestrians and return to their location.

CentroidWaiting

Similar to the *RandomWaiting* but pedestrians do not have a fixed location but group around the centroid of the activity area. It is useful to simulate situations where pedestrians tend to stay compacted such as in groups. While in their position pedestrian react to surrounding pedestrians and obstacles using the waiting behaviour.

Appendix B

Nomad simulation

In this chapter we present a compilation of features present in the full version of the Nomad simulation. We divided the compilation in three areas: simulation features that list the tools to create complex simulation scenarios, usage features presents the facilities for user interaction, input and output; and computational performance improvements. Bellow is a list of features available in the Nomad simulation.

Simulation features

- Input of individual parameters for pedestrians (heterogeneity).
- Input of obstacles with different characteristics.
- Multi level simulations.
- Implementation of stairs.
- Implementation of escalators.
- Implementation of turnstiles (uni and bi-directional).
- Implementation of ordered queues.
- Queue choice model.
- Different activities.
- Two activity area choice behaviours.
- Capacity of setting attractiveness or repulsiveness to walking areas.

Usage features

- A comprehensive graphic user interface.
- AutoCAD plug-in for automatic input of infrastructure.
- Export of simulation images.
- export of route choice images.
- Export of pedestrian trajectories.
- Export of individual pedestrian data.
- Export densities over a user defined grid. The densities can be the instant or max densities recorded in a grid cell.
- Export of simulation data.
- Use of detectors to restrict the output data to desired locations.
- Easy batch runs with different random seeds.
- API - Application Programming Interface that allows Nomad to be accessed by other platforms such as Matlab (Mathworks (2014)).
- NomadNmd - Nomad scripting language for complex batch processing.

Performance improvements

- Variable time-steps.
- Smart pedestrian management
- Capacity to switch off the graphics to improve simulation performance.

Appendix C

Walking experiments and trajectory data

The empirical data used in this dissertation was obtained through controlled walking behaviour experiments performed by the Transport & Planning department of the Delft University of Technology. According to Daamen (2004) commuting behaviours require no conscious effort and therefore can be studied using data gathered in such controlled experiments. The experiments were performed in three different occasions for different purposes: collecting data for normal and hurried walking (Daamen and Hoogendoorn (2003)), for evacuation through single doors (Daamen and Hoogendoorn (2009b)) and for studies into interaction behaviour between pedestrians (Versluis (2010)). Figure C.1 show captions of some of the experiments.

All experiments were filmed and the trajectories from the pedestrians were extracted using a methodology developed in the Delft University of Technology and explained in Hoogendoorn et al. (2003).

In the following subsections we introduce the experimental set-ups that originated the trajectories for each experiment.

C.1 Normal walking experiments

Daamen and Hoogendoorn (2003) performed walking experiments with heterogeneous populations in so called normal conditions. Their goals were to get data for different walking conditions to study pedestrians behaviours, perform calibrations and validations of walker models. They controlled five experimental variables: free-speed of pedestrians (normal or hurried walking), direction of incoming flows (unidirectional, bidirectional and 90° crossing flow), intensity of incoming flows (equal or unequal inflows of pedestrians), density of the flow and presence of bottlenecks. The population demographics was set to be heterogeneous with equally divided groups of children, students, adults and elderly. The distribution of the different age groups was kept the

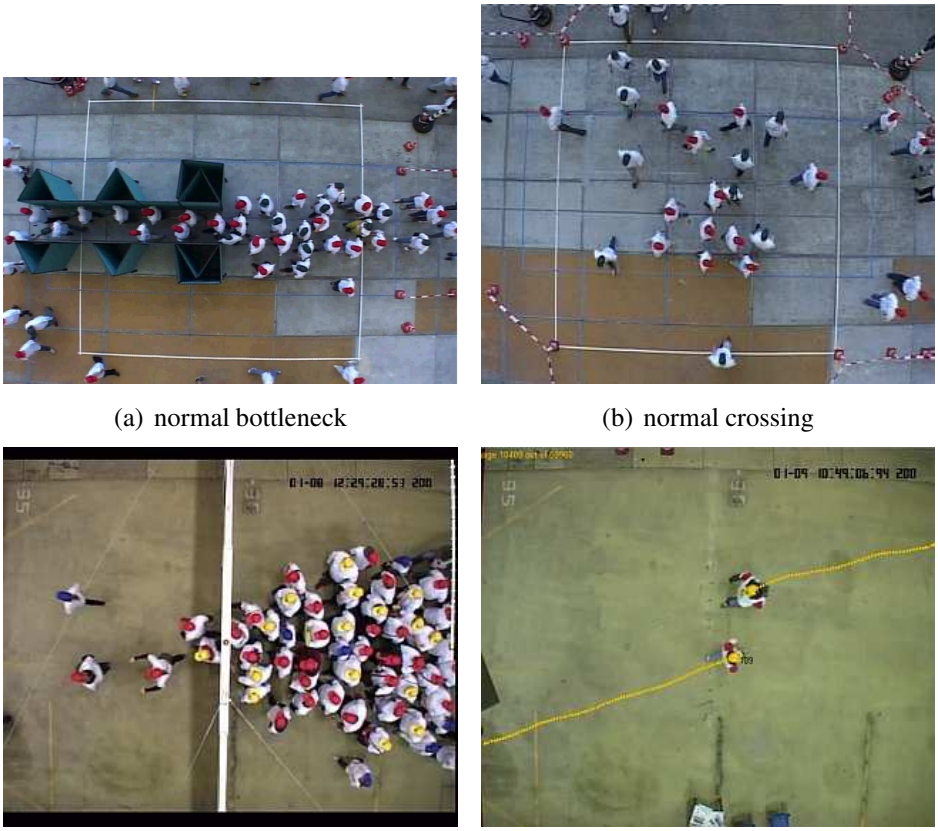

(a) normal bottleneck (b) normal crossing

(c) evacuation (d) interaction

Figure C.1: Experiments that originated the trajectory data used in this dissertation.

same for all experiments. For more details refer to Daamen and Hoogendoorn (2003). Bellow we list the experiments with the type, density range and amount of individual trajectories and figure C.2 show the arrangements of the experiments (the names in brackets represent the trajectories used in this dissertation):

1. Bidirectional flows with low global densities and equal inflows, $k < 1.0\ peds/m^2$, 709 participants. (*bidir*)
2. Unidirectional flow with low global densities, $k < 1.0\ peds/m^2$, 1167 participants. (*unidir*)
3. 90° crossing flow with low global densities and equal inflows, $k < 1.0\ peds/m^2$, 1052 participants. (*cross*)
4. Unidirectional flow with a narrow bottleneck corridor, $k < 2.0\ peds/m^2$, 1123 participants. (*bneck*)
5. Unidirectional flow with a wide bottleneck corridor, $k < 2.0\ peds/m^2$, 1898 participants.

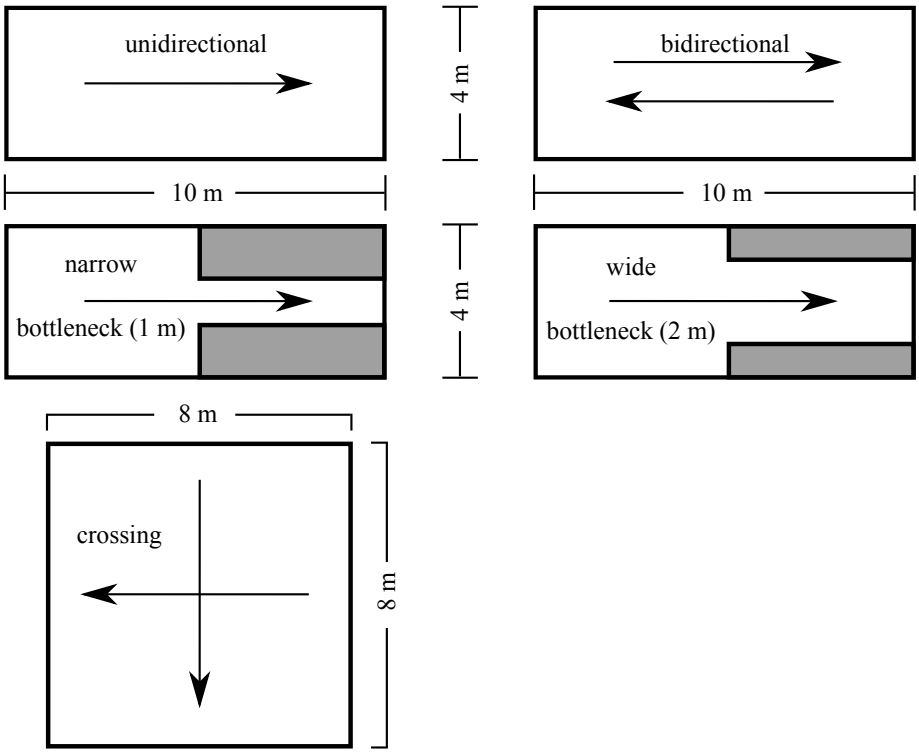

Figure C.2: Schemes of the normal walking experiments set-ups.

C.2 Evacuation experiments

Daamen and Hoogendoorn (2009b) conducted a series of experiments simulating evacuation through a single door varying several control variables: the composition of the population, stress levels conditions, lighting and door widths. The aim was to determine the dependency of the capacity of doors according to these variables. The composition of the population was varied over four distinct groups: children (under 18 years), adults (between 18 and 65 years), elderly (above 65 years) and disabled (people in wheelchair and blindfolded); the stress among the population was varied in three levels: normal conditions, using a slow-whoop siren (medium stress) and combining a slow whoop siren with a stroboscope light (high stress). Two alternative light situations were used: full lighting (200 lux) and dimmed (1 lux, corresponding to emergency lighting). The door sizes varied from a minimum of 55cm to a maximum of 275 cm. For this dissertation we chose four experiments with evacuations through a door opening of 85cm, two different populations compositions: one homogeneous and one heterogeneous and two levels of stress (normal and high stress). The homogeneous population was composed by adults only and the heterogeneous population was composed with 25 % children, 55 % adults, and 20 % elderly that correspond approximately to the average of the Dutch population. The global density in all evacuations varied between $0.0 < k < 3.0$ $peds/m^2$. Figure C.1(c) shows the experiment in which pedestrians are walking from the right to the left. The dimensions of the walking area are $8m \times 6m$ and the wall with the evacuation opening was placed at $4m$ (figure C.3).

The names in brackets represent the trajectories used in this dissertation:

6. Evacuation with a homogeneous population in normal stress conditions, 78 participants. (*evacHoLoSt*)
7. Evacuation with a homogeneous population in high stress conditions, 81 participants. (*evacHoHiSt*)
8. Evacuation with a heterogeneous population in normal stress conditions, 99 participants. (*evacHetLoSt*)
9. Evacuation with a heterogeneous population in high stress conditions, 99 participants. (*evacHetHiSt*)

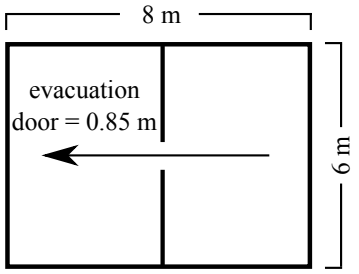

Figure C.3: Scheme of the evacuation experiments set-up.

C.3 Interaction experiments

Versluis (2010) performed experiments on interaction behaviour between one to one and one to two pedestrians. The author investigated how the interaction between individual pedestrians affect the walking behaviour. To force pedestrians in interaction situations the author set-up intersecting trajectories in angles varying from 0° (overtaking) through 180° (head-on) including three intermediate angles $45^\circ, 90^\circ$ and 135° (crossing). Twelve different pedestrians participated: nine young adults ($19 < \text{age} < 24$ years), two adults and one elderly. The genders were equally represented (6 males and 6 females). Figure C.4 shows the angles of approach of pedestrians walking in collision paths to perform the avoidance manoeuvres. In the experiments pedestrians walked $10m$ before reaching the interaction point and the trajectories were recorded from a distance of $4m$ before and after from the interaction points. Bellow is the list of the experiments that provided trajectories for the interaction experiments (the names in brackets represent the trajectories used in this dissertation):

10. Interaction between two pedestrians in overtaking, 96 trajectories.
11. Interaction between two pedestrians in 45° crossing flows, 144 trajectories.

12. Interaction between two pedestrians in 90° crossing flows, 144 trajectories. (*interCross*)

13. Interaction between two pedestrians in 135° crossing flows, 144 trajectories.

14. Interaction between two pedestrians in collision route, 168 trajectories. (*interBidir*)

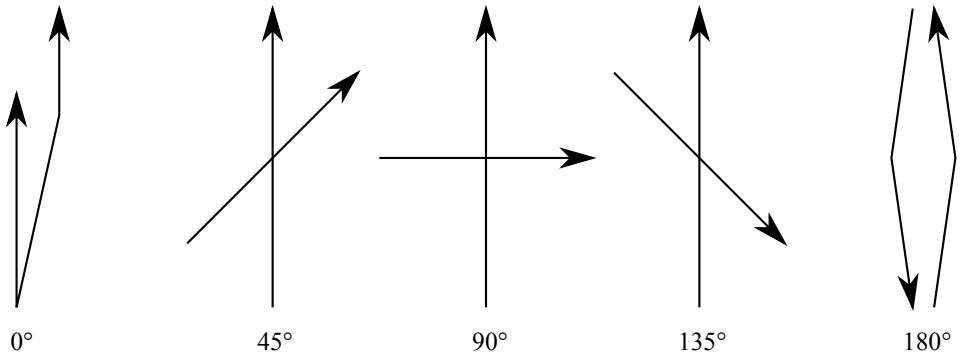

Figure C.4: Schemes of the interaction experiments set-ups.

Appendix D

Smoothing and interpolating trajectories

Pedestrians when walking and standing move sideways in a pendulum movement due to the bio-mechanics of the hip (Weidmann (1993)) in which the upper body 'falls' to the side of the supporting foot. This effect varies with the walking speed, length and age of the pedestrians. The length of the lateral movement has an average of 12 cm with average speeds of 1.19 m/s for the younger population (Woledge et al. (2005)).

We showed in chapter 5 that noise has a large effect in the calibration accuracy. Few authors mention the processes of smoothing trajectories (Brogan and Johnson (2003)) leaving this as an open research question. Therefore, we had to experiment with several standard smoothing algorithms available to find the most suited.

We chose randomly a number of trajectories from the experiments used in this thesis (appendix C) and applied different smoothing algorithms. We looked for the algorithm that would result in positions that mostly correspond to the movement of the centre of gravity of pedestrians (located approximately in the middle of the waist). Using the original videos we compared the smoothed positions and chose a local regression using weighted linear least squares and a 2nd degree polynomial model available in Matlab.

Figure D.1 shows an original trajectory and the resulting smoothed trajectory used in the calibrations. The trajectory has the lateral component in a broader scale to enhance the swaying effect.

After smoothed, the positions of the trajectories were interpolated to a time step of $0.02s$ that was shown to minimise the numerical errors that could influence negatively the estimation. This resulted in four extra locations to be inserted between the smoothed locations.

The interpolations considered the accelerations between the smoothed points to vary linearly. The algorithm divided the difference between the current and next time-step acceleration by four and distributed between the four interpolated points. The resulting

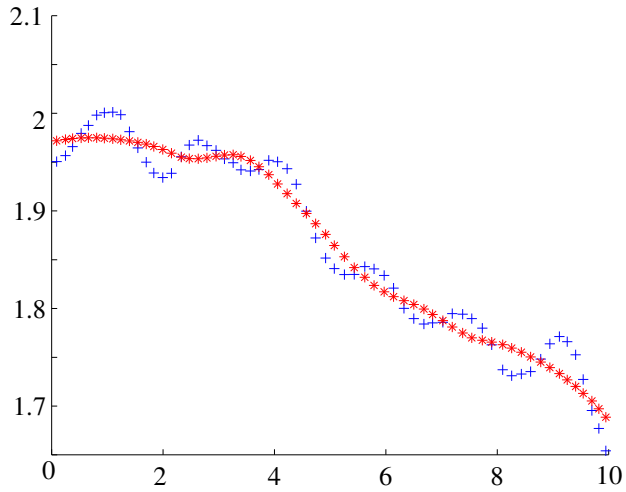

Figure D.1: Example of the smoothing of a trajectory from the narrow bottleneck experiment described in appendix C. The blue crosses are the tracked locations and the red stars the smoothed.

accelerations were used to calculate the speeds and interpolated locations. This created new locations that were not linearly distributed as can be seen in figure D.2.

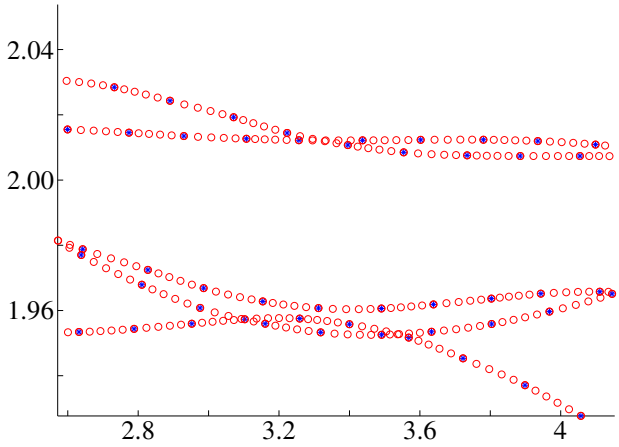

Figure D.2: Example of the interpolation after the smoothing algorithm. The blue stars are the smoothed locations and the red dots are the interpolated locations.

Bibliography

Antonini, G., Bierlaire, M., and Weber, M. (2004). Simulation of pedestrian behaviour using a discrete choice model calibrated on actual motion data. In *4th STRC Swiss Transport Research Conference*, volume 7, pages 249–258.

Antonini, G., Bierlaire, M., and Weber, M. (2006). Discrete choice models of pedestrian walking behavior. *Transportation Research Part B: Methodological*, 40(8):667 – 687. ISSN 0191-2615.

Ariely, D. (2008). *Predictably irrational - The hidden forces that shape our decisions*. HarperCollins New York.

Asano, M., Iryo, T., and Kuwahara, M. (2010). Microscopic pedestrian simulation model combined with a tactical model for route choice behaviour. *Transportation Research Part C: Emerging Technologies*, 18(6):842 – 855. ISSN 0968-090X. Special issue on Transportation Simulation; Advances in Air Transportation Research.

Aube, F. and Shield, R. (2004). Modeling the effect of leadership on crowd flow dynamics. In *Cellular Automata*, Lecture Notes in Computer Science, pages 601–611. Springer Berlin / Heidelberg.

Bandini, S., Gorrini, A., and Vizzari, G. (2014). Towards an integrated approach to crowd analysis and crowd synthesis: a case study and first results. *Pattern Recognition Letters*, 44:16–29.

Bandini, S., Manzoni, S., and Vizzari, G. (2009). *Modeling, Simulating, and Visualising Crowd Dynamics with computational Tools Based on Situated Cellular Agents*, chapter 3, pages 45–62. Emerald Group Publishing Limited.

Bansal, V., Kota, R., and Karlapalem, K. (2008). System issues in multi-agent simulation of large crowds. pages 8–19.

Batty, M. (2001). Agent-based pedestrian modeling. *Environment and Planning B: Planning and Design*, 28(3):321–326.

Bauer, D. and Kitazawa, K. (2010). Using laser scanner data to calibrate certain aspects of microscopic pedestrian motion models. In *Pedestrian and Evacuation Dynamics 2008*, pages 83–94. Springer.

Bellomo, N., Bianca, C., and Coscia, V. (2011). On the modeling of crowd dynamics: An overview and research perspectives. *SeMA Journal*, 54(1):25–46. ISSN 1575-9822.

Bellomo, N. and Dogbe, C. (2011). On the modeling of traffic and crowds: A survey of models, speculations, and perspectives. *SIAM review*, 53(3):409–463.

Bellomo, N., Piccoli, B., and Tosin, A. (2012). Modeling crowd dynamics from a complex system viewpoint. *Mathematical models and methods in applied sciences*, 22(suppl. 2).

Ben-Akiva, M. and Lerman, S. (1985). *Discrete Choice Analysis: Theory and Application to Travel Demand*. MIT Press series in transportation studies. MIT Press. ISBN 9780262022170.

Berrou, J. L., Beecham, J., Quaglia, P., Kagarlis, M. A., and Gerodimos, A. (2005). Calibration and validation of the legion simulation model using empirical data. In *Pedestrian and Evacuation Dynamics*, pages 167–181. Schreckenberg, M., Springer-Verlag.

Blue, V. and Adler, J. (1999). Cellular automata microsimulation of bi-directional pedestrian flows. *Transportation Research Record: Journal of the Transportation Research Board No.1678*, 1678:135–141.

Borgers, A., Kemperman, A., and Timmermans, H. (2009). Modeling pedestrian movement in shopping street segments. *Pedestrian behavior: Models, data collection and applications*, pages 87–111.

Borgers, A. and Timmermans, H. (2014). Indices of pedestrian behavior in shopping areas. *Procedia Environmental Sciences*, 22(0):366 – 379. ISSN 1878-0296. 12th International Conference on Design and Decision Support Systems in Architecture and Urban Planning, {DDSS}, 2014.

Brogan, D. and Johnson, N. (2003). Realistic human walking paths. page 94. IEEE Computer Society Washington, DC, USA.

Buchmueller, S. and Weidmann, U. (2006). Parameters of pedestrians, pedestrian traffic and walking facilities, ivt report no.132. Ivt Report no.132 Ivt Report no.132, ETH, Zurich.

Burstedde, C., Klauck, K., Schadschneider, A., and Zittartz, J. (2001). Simulation of pedestrian dynamics using a two-dimensional cellular automaton. *Physica A Statistical Mechanics and its Applications*, 295:507–525.

Campanella, M. (2012). Estudo para determinação da capacidade da estação jardim oceânico. Technical report, MetrôRio, Rio de Janeiro.

Campanella, M., Hoogendoorn, S., and Daamen, W. (2007a). A hybrid time-based and event-driven management of pedestrians in micro-simulation models. In Batty, M. and da Silva, A. R., editors, *Proceedings of Computers in Urban Planning and Simulation (CUPUM 2007)*, pages 1–14.

Campanella, M., Hoogendoorn, S., and Daamen, W. (2007b). Improving pedestrian micro-simulations with event steps. In *Proceedings of The Seventh International Conference on Traffic and Granular Flow (TGF '07)*.

Campanella, M., Hoogendoorn, S., and Daamen, W. (2008). Calibration of pedestrian models with respect to self-organisation. In *TRAIL in Perspective. Proceedings 2008, 10th International TRAIL Congress*, pages 1–20. TRAIL Research School, Delft.

Campanella, M., Hoogendoorn, S., and Daamen, W. (2009a). Effects of heterogeneity in self-organized pedestrian flows. *Transportation Research Record (TRR)*, pages 148–156.

Campanella, M., Hoogendoorn, S., and Daamen, W. (2009b). Exploring population variable time-steps and update strategies in pedestrian microscopic simulations. In *Proceedings of The Eight International Conference on Traffic and Granular Flow (TGF '09)*.

Campanella, M., Hoogendoorn, S., and Daamen, W. (2009c). Improving the nomad microscopic walker model. In *12th IFAC Symposium on Control in Transportation Systems*.

Campanella, M., Hoogendoorn, S., and Daamen, W. (2009d). Macroscopic relations in pedestrian traffic flows. In *Proceedings of The Eight International Conference on Traffic and Granular Flow (TGF '09)*.

Campanella, M., Hoogendoorn, S., and Daamen, W. (2010). A methodology to calibrate pedestrian walker models using multiple-objectives. In *Proceedings of The Pedestrian and Evacuation Dynamics (PED2010)*.

Campanella, M., Hoogendoorn, S., and Daamen, W. (2012). Quantitative and qualitative validation procedure for general use of pedestrian models. In *Pedestrian and Evacuation Dynamics (PED2012)*, pages 891–905. Springer.

Campanella, M. C. (2011). Nomad user manual - www.pedestrians.tudelft.nl. Technical report, Delft University of Technology.

Chattaraj, U., Seyfried, A., and Chakroborty, P. (2009). Comparison of pedestrian fundamental diagram across cultures. *Advances in complex systems*, 12(03):393–405.

Cheung, C. and Lam, W. (1998). Pedestrian route choices between escalator and stairway in mtr stations. *Journal of Transportation Engineering*, 124:277–285.

Choi, J., Hwang, H., and Hong, W. (2011). Predicting the probability of evacuation congestion occurrence relating to elapsed time and vertical section in a high-rise building. In Peacock, R. D., Kuligowski, E. D., and Averill, J. D., editors, *Pedestrian and Evacuation Dynamics*, pages 37–46. Springer US. ISBN 978-1-4419-9724-1.

Chraibi, M. and Seyfried, A. (2008). Pedestrian dynamics with event-driven simulation. In *Pedestrian and Evacuation Dynamics, PED2008*.

Cohen, B. (2004). Urban growth in developing countries: A review of current trends and a caution regarding existing forecasts. *World Development*, 32, Number 1:23–51.

Connell, R. (2001). Collective behavior in the september 11, 2001 evacuation of the world trade center.

Costa, M. (2010). Interpersonal distances in group walking. *Journal of Nonverbal Behavior*, 34, Number 1:1573–3653.

Daamen, W. (2004). *Modelling passenger flows in public transport facilities. PhD thesis*. Ph.D. thesis, Delft University Press.

Daamen, W., Bovy, P. H., Hoogendoorn, S. P., and Van de Reijt, A. (2005a). Passenger route choice concerning level changes in railway stations. In *Transportation Research Board Annual Meeting*, volume 1930, pages 12–20.

Daamen, W., Campanella, M. C., and Hoogendoorn, S. P. (2008). Assessing pedestrian flow conditions in Schiphol Plaza: Can Schiphol Plaza cope with future traveller demands? In *TRAIL in Perspective. Proceedings 2008, 10th International TRAIL Congress*, pages 41–57. TRAIL Research School., Delft.

Daamen, W. and Hoogendoorn, S. (2003). Controlled experiments to derive walking behaviour. *European Journal of Transport and Infrastructure Research*, 3(1):39–59.

Daamen, W. and Hoogendoorn, S. (2006). Free speed distributions for pedestrian traffic. In *PrePrints (CD-ROM) 85th Annual Meeting Transportation Research Board*.

Daamen, W. and Hoogendoorn, S. (2009a). Capacity of doors during evacuation conditions. In *Proceedings of the International Conference on Evacuation Behavior (ICEM 2009)*.

Daamen, W. and Hoogendoorn, S. (2009b). Pedestrian evacuation behavior near exit doors. In *to appear in the Proceedings of The Eighth International Conference on Traffic and Granular Flow (TGF '09)*.

Daamen, W. and Hoogendoorn, S. (2012). Emergency door capacity: influence of door width, population composition and stress level. *Fire technology*, 48(1):55–71.

Daamen, W., Hoogendoorn, S., and Bovy, P. (2005b). First-order pedestrian traffic flow theory. *Transportation Research Record*, 1934(-1):43–52.

Daamen, W., Hoogendoorn, S. P., Campanella, M. C., and Eggengoor, E. (2009). Ticket reservation posts on train platforms: Assessment using microscopic pedestrian simulation tool nomad. In *Transportation Research Board 88th Annual Meeting*.

Davis, P. and Dutta, G. (2002). Estimation of capacity of escalators in london underground. Technical report, London School of Economics and Political Sciences, London.

Degond, P., Appert-Rolland, C., Moussaid, M., Pettré, J., and Theraulaz, G. (2013). A hierarchy of heuristic-based models of crowd dynamics. *Journal of Statistical Physics*, 152(6):1033–1068.

Doniec, A., Mandiau, R., Piechowiak, S., and Espié, S. (2008). Controlling non-normative behaviors by anticipation for autonomous agents. *Web Intelligence and Agent Systems*, 6(1):29–42. ISSN 1570-1263. 1377793.

Duives, D., Daamen, W., and Hoogendoorn, S. (2014a). Anticipation behavior upstream of a bottleneck. *Transportation Research Procedia*, 2(0):43 – 50. ISSN 2352-1465. The Conference on Pedestrian and Evacuation Dynamics 2014 (PED 2014), 22-24 October 2014, Delft, The Netherlands.

Duives, D., Daamen, W., and Hoogendoorn, S. (2014b). Influence of group size and group composition on the adhered distance headway. *Transportation Research Procedia*, 2:183–188.

Duives, D. C., Daamen, W., and Hoogendoorn, S. P. (2013). State-of-the-art crowd motion simulation models. *Transportation Research Part C: Emerging Technologies*, 37:193–209.

Duives, D. C., Daamen, W., and Hoogendoorn, S. P. (2015). Quantification of the level of crowdedness for pedestrian movements. *Physica A: Statistical Mechanics and its Applications*, 427:162 – 180. ISSN 0378-4371.

Edie, L. (1963). Discussion of traffic stream measurements and definitions. In *in Proceedings of the Second International Symposium on the Theory of Traffic Flow*.

Fang, Z.-M., Song, W.-G., Zhang, J., and Wu, H. (2012). A multi-grid model for evacuation coupling with the effects of fire products. *Fire Technology*, 48(1):91–104.

Fruin, J. (1971). *Pedestrian planning and design*. Metropolitan association of urban designers and environmental planners, New York.

Fruin, J. J. (1993). The causes and prevention of crowd disasters. *Engineering for crowd safety*, 1:10.

Galea, E. (1998). A general approach to validating evacuation models with an application to exodus. *Journal of Fire Sciences*, 16(6):414 – 436.

Galea, E. and Galparsoro, J. P. (1994). A computer-based simulation model for the prediction of evacuation from mass-transport vehicles. *Fire Safety Journal*, 22(4):341 – 366. ISSN 0379-7112.

Galea, E. R., Hulse, L., Day, R., Siddiqui, A., Sharp, G., Boyce, K., Summerfield, L., Canter, D., Marselle, M., and Greenall, P. V. (2010). The uk wtc9/11 evacuation study: An overview of the methodologies employed and some preliminary analysis. In *Pedestrian and Evacuation Dynamics 2008*, pages 3–24. Springer.

Gehl, J. (2010). *Cities for people*. Island Press, New York.

Gibson, J. J. (1979). *The ecological approach to visual perception*. Houghton Mifflin, Boston, MA.

Gipps, P. and Marksjo, B. (1985). A micro-simulation model for pedestrian flows. *Mathematics and Computers in Simulation*, 27(2):95–105. ISSN 0378-4754.

Goffman, E. (1972). *The Individual as a Unit. Relations in Public: Microstudies of the Public Order*. Allen Lane The Penguin Press, London.

Gwynne, S., Galea, E., Owen, M., Lawrence, P. J., and Filippidis, L. (1999). A review of the methodologies used in the computer simulation of evacuation from the built environment. *Building and Environment*, 34(6):741–749.

Haklay, M., O'Sullivan, D., Thurstain-Goodwin, M., and Schelhorn, T. (2001). So go downtown simulating pedestrian movement in town centres. *Environ Plann B*, 28(3):343–359.

Hartmann, S. (1996). *Modelling and Simulation in the Social Sciences from the Philosophy of Science Point of View*, chapter The World as a Process, pages 77–100. Springer Netherlands, Dordrecht. ISBN 978-94-015-8686-3.

Helbing, D. (1997). *Verkehrsdynamik. Neue physikalische Modellierungskonzepte*. Springer-Verlag, Berlin.

Helbing, D., Buzna, L., Johansson, A., and Werner, T. (2005). Self-organized pedestrian crowd dynamics: Experiments, simulations, and design solutions. *Transportation Science*, 39(1):1–24. ISSN 1526-5447. 1247227.

Helbing, D., Farkas, I., and Vicsek, T. (2000a). Simulating dynamical features of escape panic. *Nature*, 407(6803):487–490.

Helbing, D., Farkas, I. J., Molnar, P., and Vicsek, T. (2002). Simulation of pedestrian crowds in normal and evacuation situations. In *Pedestrian and Evacuation Dynamics (PED 2001)*, volume 21, pages 21–58. Springer, Berlin.

Helbing, D., Farkas, I. J., and Vicsek, T. (2000b). Freezing by heating in a driven mesoscopic system. *Physical Review Letters*, 84:1240–1243.

Helbing, D. and Johansson, A. (2009). Pedestrian, crowd and evacuation dynamics. In *Encyclopedia of complexity and System Science*, volume 16, pages 6476–6495. Springer.

Helbing, D., Johansson, A., and Al-Abideen, H. Z. (2007). The dynamics of crowd disasters: An empirical study. *Physical Review E*, 75(046109).

Helbing, D. and Molnar, P. (1995). Social force model for pedestrian dynamics. *Physical review E*, 51:4282–4286.

Helbing, D., Molnar, P., Farkas, I. J., and Bolay, K. (2001). Self-organizing pedestrian movement. *Environment and Planning B: Planning and Design*, 28:361–383.

Helbing, D. and Mukerji, P. (2012). Crowd disasters as systemic failures: analysis of the love parade disaster. *EPJ Data Science*, 1(7).

Henein, C. M. and White, T. (2007). Macroscopic effects of microscopic forces between agents in crowd models. *Physica A: Statistical Mechanics and its Applications*, 373(0):694 – 712. ISSN 0378-4371.

Hill, M. R. (1982). *Spatial structure and decision-making aspects of pedestrian route selection through an urban environment*. Ph.D. thesis, Faculty of The Graduate College in the University of Nebraska.

Hillier, B. and Hanson, J. (1984). *The Social Logic of Space*. Cambridge University Press.

Hirai, K. and Tarui, K. (1975). A simulation of the behavior of a crowd in panic. In *Proceedings of the 1975 International Conference on Cybernetics and Society*, pages 409–411.

Hofmann, M. (2005). On the complexity of parameter calibration in simulation models. *The Journal of Defense Modeling and Simulation: Applications, Methodology, Technology*, 2(4):217–226.

Hoogendoorn, S. (1999). *Multiclass continuum modelling of multilane traffic flow. PhD thesis*. Ph.D. thesis, Delft University Press.

Hoogendoorn, S. (2007). *Lectures of the Course: Traffic Flow Theory and Simulation*. Delft University of Technology.

Hoogendoorn, S. and Bovy, P. (2002). Normative pedestrian behaviour theory and modelling. In *Transportation and Traffic Theory in the 21st Century*, pages 219–245. Proceedings of the 15th International Symposium on Transportation and Traffic Theory.

Hoogendoorn, S. and Bovy, P. (2003). Simulation of pedestrian flows by optimal control and differential games. *Optim. Control Appl. Meth.*, 24(3):153–172. TU Delft digital repository [http://repository.tudelft.nl/oai] (Netherlands) ER.

Hoogendoorn, S. and Bovy, P. (2004). Pedestrian route-choice and activity scheduling theory and models. *Transportation Research Part B*, 38:169 – 190.

Hoogendoorn, S. and Daamen, W. (2005a). Pedestrian behavior in bottlenecks. *Transportation Science*, (39):147–159.

Hoogendoorn, S. and Daamen, W. (2005b). Self-organization in pedestrian flow. In *Traffic and Granular Flow TGF 03*, pages 373–382.

Hoogendoorn, S. and Daamen, W. (2010). A novel calibration approach of microscopic pedestrian models. In Timmermans, H., editor, *Pedestrian Behaviour*, pages 195–214. Emerald Group.

Hoogendoorn, S., Daamen, W., and Bovy, P. (2003). Extracting microscopic pedestrian characteristics from video data. In *Transportation Research Board Annual Meeting*, number CD-ROM, Paper No 477. National Academies, Washington, USA.

Hoogendoorn, S. P. (2001). Normative pedestrian flow behavior, theory and applications. Research report vk2001.00.

Hoogendoorn, S. P. (2004). Pedestrian flow modeling by adaptive control. *Transportation Research Record: Journal of the Transportation Research Board*, 1878:95–103.

Hoogendoorn, S. P. and Bovy, P. (2006). Experiments and theory of self-organization in pedestrian flow. In *85th Annual Meeting Transportation Research Board, Washington DC: National Academy Press, pp. 1-12.*.

Hoogendoorn, S. P., Daamen, W., and Landman, R. L. (2005). Microscopic calibration and validation of pedestrian models: cross-comparison of models using experimental data. In Waldau, N., Gattermann, P., and Schreckenberg, M., editors, *Pedestrian and Evacuation Dynamics*, pages 253–265. Springer-Verlag.

Hoogendoorn, S. P., Hauser, M., and Rodrigues, N. (2004). Application of microscopic pedestrian flow simulation to station design evaluation in lisbon train stations. In *TRB 2004 annual meeting*, pages 04–3749.

Hoogendoorn, S. P. and Hoogendoorn, R. (2010). A generic calibration framework for joint estimation of car-following models using microscopic data. In *to appear in Transportation Research Board Annual Meeting (TRB)*.

Hoogendoorn, S. P. and Ossen, S. (2006). Empirical analysis of two-leader car-following behavior. *European Journal of Transport and Infrastructure Research*, 6(3):229–246.

Hoogendoorn, S. P., van Wageningen-Kessels, F. L., Daamen, W., and Duives, D. C. (2014). Continuum modelling of pedestrian flows: From microscopic principles to self-organised macroscopic phenomena. *Physica A: Statistical Mechanics and its Applications*, 416(0):684–694. ISSN 0378-4371.

Hughes, R. L. (2002). A continuum theory for the flow of pedestrians. *Transportation Research Part B*, 36(36):507–535.

Hundt, R. (2011). Loop recognition in c++/java/go/scala. In *Scala Days*.

Isobe, M., Helbing, D., and Nagatani, T. (2004). Experiment, theory, and simulation of the evacuation of a room without visibility. *Phys. Rev. E*, 69(6):066132.

Johansson, A. (2009). Constant net-time headway as key mechanism behind pedestrian flow dynamics. *Phys. Rev.*, E 80, 026120.

Johansson, A., Helbing, D., Al-Abideen, H. Z., and Al-Bosta, S. (2008). From crowd dynamics to crowd safety: A video-based analysis. In *Conference on Nonlinear Mechanics (ICNM-V)*. Shanghai.

Johansson, A., Helbing, D., and Shukla, P. (2007). Specification of the social force pedestrian model by evolutionary adjustment to video tracking data. *Advances in Complex Systems*, 10(2):271–288.

Johansson, F. (2013). *Microscopic Modeling and Simulation of Pedestrian Traffic, PhD thesis*. Ph.D. thesis, Linköping University, Department of Science and Technology.

Johansson, F., Duives, D., Daamen, W., and Hoogendoorn, S. (2014). The many roles of the relaxation time parameter in force based models of pedestrian dynamics. *Transportation Research Procedia*, 2:300–308.

Karamouzas, I. (2012). *Motion Planning for Human Crowds: from Individuals to Groups of Virtual Characters*. Master's thesis, Utrecht University.

Karamouzas, I. and Overmars, M. H. (2010). Simulating human collision avoidance using a velocity-based approach. *Workshop on Virtual Reality Interaction and Physical Simulation VRIPHYS*, 10:125–134.

Kauffmann, P. D. (2011). *Traffic Flow on Escalators and Moving Walkways: Quantifying and Modeling Pedestrian Behavior in a Continuously Moving System*. Master's thesis, Virginia Polytechnic Institute and State University.

Kerridge, J., Keller, S., Chamberlain, T., and Sumpter, N. (2005). Collecting pedestrian trajectory data in real-time. pages 27–39.

Keßel, A., Klüpfel, H., Wahle, J., and Schreckenberg, M. (2002). Microscopic simulation of pedestrian crowd motion. pages 193–202.

Kirchner, A., Klupfel, H., Nishinari, K., Schadschneider, A., and Schreckenberg, M. (2004). Discretization effects and the influence of walking speed in cellular automata models for pedestrian dynamics. *Journal of Statistical Mechanics: Theory and Experiment*, 2004(10):P10011.

Kirchner, A., Nishinari, K., and Schadschneider, A. (2003). Friction effects and clogging in a cellular automaton model for pedestrian dynamics. *Phys. Rev. E*, 67:056122.

Kitazawa, K. and Fujiyama, T. (2010). Pedestrian vision and collision avoidance behavior: Investigation of the information process space of pedestrians using an eye tracker. In *Pedestrian and evacuation dynamics 2008*, pages 95–108. Springer.

Kleijnen, J. P. (1995). Verification and validation of simulation models. *European Journal of Operational Research*, 82:145–162.

Klügl, F. (2008). A validation methodology for agent-based simulations. In *Proceedings of the 2008 ACM symposium on Applied computing*, SAC '08, pages 39–43. ACM, New York, NY, USA. ISBN 978-1-59593-753-7.

Klüpfel, H. (2009). *Crowd Dynamics Phenomena, Methodology and Simulation*, chapter 10, pages 215–244. Emerald Group Publishing Limited.

Klüpfel, H. and Meyer-Konig, T. (2003). Simulation of the evacuation of a football stadium using the ca model pedgo. page 423. Springer Verlag.

Kobes, M., Helsloot, I., de Vries, B., and Post, J. G. (2010). Building safety and human behaviour in fire: A literature review. *Fire Safety Journal*, 45(1):1 – 11. ISSN 0379-7112.

Kukla, R., Kerridge, J., Willis, A., and Hine, J. (2001). Pedflow: Development of an autonomous agent model of pedestrian flow. *Transportation research record: Journal of the transportation research board*, 1774(1):11–17.

Kukla, R., Willis, A., and Kerridge, J. (2003). Application of context-mediated behavior to a multi-agent pedestrian flow model (pedflow). In *Transportation Research Board (TRB) 82th Annual Meeting*, pages 212–222. Transportation Research Board, Washington DC.

Kuligowski, E. D. (2009). The process of human behavior in fires. Technical report, NIST Technical Note 1632, Gaithersburg, MD.

Kuligowski, E. D. and Gwynne, S. M. V. (2005). What a user should know when selecting an evacuation model. *Fire Protection Engineering Magazine, Society of Fire Protection (SFPE), USA*, Human Behaviour in Fire Issue 28:30–41.

Kuligowski, E. D., Peacock, R. D., and Hoskins, B. L. (2010). A review of building evacuation models, 2nd edition. Technical report, National Institute of Standards and Technology (Nist) - Technical Note 1680.

Leach, J. (1994). *Survival psychology*. Palgrave Macmillan.

Leach, J. (2004). Why people 'freeze'in an emergency: temporal and cognitive constraints on survival responses. *Aviation, space, and environmental medicine*, 75(6):539–542.

Løvås, G. G. (1994). Modeling and simulation of pedestrian traffic flow. *Transportation Research Part B: Methodological*, 28(6):429–443.

Luchies, C. W., Schiffman, J., Richards, L. G., Thompson, M. R., Bazuin, D., and DeYoung, A. J. (2002). Effects of age, step direction, and reaction condition on the ability to step quickly. *The Journals of Gerontology Series A: Biological Sciences and Medical Sciences*, 57(4):M246–M249.

Maniccam, S. (2003). Traffic jamming on hexagonal lattice. *Physica A: Statistical Mechanics and its Applications*, 321(3–4):653 – 664. ISSN 0378-4371.

Marconi, S. and Chopard, B. (2002). A multiparticle lattice gas automata model for a crowd. 2493:231–238.

Mathworks (2014). http://www.mathworks.nl/products/matlab/ - the language of technical computing.

Maury, B. and Venel, J. (2007). Handling of contacts in crowd motion simulations. pages 171–180.

Millonig, A. and Gartner, G. (2008). Shadowing-tracking-interviewing: How to explore human spatio-temporal behaviour patterns. In *Workshop on Behaviour Monitoring and Interpretation BMI 08*, pages 1–14.

Moussaïd, M., Guillot, E. G., Moreau, M., Fehrenbach, J., Chabiron, O., Lemercier, S., Pettré, J., Appert-Rolland, C., Degond, P., and Theraulaz, G. (2012). Traffic instabilities in self-organized pedestrian crowds. *PLoS computational biology*, 8(3):e1002442.

Moussaïd, M., Helbing, D., Garnier, S., Johansson, A., Combe, M., and Theraulaz, G. (2009). Experimental study of the behavioural mechanisms underlying self-organization in human crowds. *Proceedings of the Royal Society B: Biological Sciences*, 276:2755–2762. ISSN 0962-8452.

Moussaïd, M., Helbing, D., and Theraulaz, G. (2011). How simple rules determine pedestrian behavior and crowd disasters. *Proceedings of the National Academy of Sciences*, 108(17):6884–6888.

Moussaïd, M., Perozo, N., Garnier, S., Helbing, D., and Theraulaz, G. (2010). The walking behaviour of pedestrian social groups and its impact on crowd dynamics. *PLoS ONE 5(4): e10047*.

Nagel, K. and Marchal, F. (2005). Computational methods for multi-agent simulations of travel behavior. In *Workshop on Computational Techniques, 10th International Conference on Travel Behaviour Research (IATBR 2003)*.

Nakayama, A., Hasebe, K., and Sugiyama, Y. (2008). Effect of attractive interaction on instability of pedestrian flow in a two-dimensional optimal velocity model. *Phys Rev E.*, 77.

Nasir, M., Lim, C. P., Nahavandi, S., and Creighton, D. (2014). A genetic fuzzy system to model pedestrian walking path in a built environment. *Simulation Modelling Practice and Theory*, 45(0):18 – 34. ISSN 1569-190X.

Nasir, M., Nahavandi, S., and Creighton, D. (2012). Fuzzy simulation of pedestrian walking path considering local environmental stimuli. In *2012 IEEE International Conference on Fuzzy Systems (FUZZ-IEEE)*, pages 1–6. IEEE, Brisbane, Australia.

Okazaki, S. (1979). A study of pedestrian movement in architectural space, part 1: Pedestrian movement by the application on of magnetic models. *Trans. of AIJ*, 283(3):111–119.

Olivier, A.-H., Marin, A., Crétual, A., Berthoz, A., and Pettré', J. (2013). Collision avoidance between two walkers: Role-dependent strategies. *Gait & Posture*, 38(4):751 – 756. ISSN 0966-6362.

Ondřej, J., Pettré, J., Olivier, A.-H., and Donikian, S. (2010). A synthetic-vision based steering approach for crowd simulation. 29(4):123.

Oracle (2014). http://www.java.com/en/about - learn about java technology.

Ossen, S. and Hoogendoorn, S. (2008). Validity of trajectory-based calibration approach of car-following models in presence of measurement errors. *Transportation Research Record: Journal of the Transportation Research Board*, 2088:117–125.

Ossen, S. J. L. (2008). *Longitudinal Driving Behavior: Theory and Empirics*. Trail thesis series, Delft University of Technology.

Papadimitriou, E., Yannis, G., and Golias, J. (2009). A critical assessment of pedestrian behaviour models. *Transportation Research Part F: Traffic Psychology and Behaviour*, 12(3):242 – 255. ISSN 1369-8478.

Paris, S., Pettré, J., and Donikian, S. (2007). Pedestrian reactive navigation for crowd simulation: a predictive approach. 26(3):665–674.

Patla, A. and Vickers, J. (2003). How far ahead do we look when required to step on specific locations in the travel path during locomotion? *Experimental Brain Research*, 148(1):133–138. ISSN 0014-4819.

Pelechano, N., Allbeck, J., and Badle, N. (2007). Controlling individual agents in high-density crowd simuation. In *ACM SIGGRAPH / Eurographics Symposium on Computer Animation (SCA'07)*. San Diego (USA).

Penn, A. and Turner, A. (2001). Space syntax based agent simulation. In Schreckenberg, M. and Sharma, S., editors, *Pedestrian and Evacuation Dynamics (PED 2001)*, pages 99–114. Springer.

Pettré, J., Ondřej, J., Olivier, A.-H., Cretual, A., and Donikian, S. (2009). Experiment-based modeling, simulation and validation of interactions between virtual walkers. In *Proceedings of the 2009 ACM SIGGRAPH/Eurographics Symposium on Computer Animation*, pages 189–198. ACM.

Pettré, J., Wolinski, D., and Olivier, A.-H. (2014). Velocity-based models for crowd simulation. In *Pedestrian and Evacuation Dynamics 2012*, pages 1065–1078. Springer.

Portz, A. and Seyfried, A. (2010). Analyzing stop-and-go waves by experiment and modeling. In *Pedestrian and Evacuation Dynamics 2010*.

Predtechenskii, V. M. and Milinskii, A. I. (1978). *Planing for foot traffic flow in buildings*. Amerind Publishing, New Dehli.

Reynolds, C. W. (1987). Flocks, herds and schools: A distributed behavioral model. *ACM SIGGRAPH Computer Graphics*, 21(4):25–34.

Rimea (2009). Richtlinie für mikroskopische entfluchtungsanalysen: version 2.2.1. Technical report, Rimea.

Robin, T., Antonini, G., Bierlaire, M., and Cruz, J. (2009). Specification, estimation and validation of a pedestrian walking behavior model. *Transportation Research Part B*, 43:36–56.

Ronchi, E., Kuligowski, E. D., Nilsson, D., Peacock, R. D., and Reneke, P. A. (2014). Assessing the verification and validation of building fire evacuation models. *Fire Technology*, pages 1–23. ISSN 0015-2684.

Russell, S. and Norvig, P. (1995). *Artificial Intelligence: A modern approach*. Prentice-Hall, Upper Saddle River, first edition edition.

Sahaleh, A. S., Bierlaire, M., Farooq, B., Danalet, A., and Hänseler, F. S. (2012). Scenario analysis of pedestrian flow in public spaces. In *Proceeding of the 12th Swiss Transport Research Conference (STRC), Monte Verità, Ascona, Switzerland*. Citeseer.

Saloma, C., Perez, G. J., Tapang, G., Lim, M., and Palmes-Saloma, C. (2003). Self-organized queuing and scale-free behavior in real escape panic. *Proceedings of the National Academy of Sciences*, 100(21):11947–11952.

Schadschneider, A., Eilhardt, C., Nowak, S., and Will, R. (2010). Towards a calibration of the floor field cellular automaton. In *Pedestrian and Evacuation Dynamics 2010*.

Schadschneider, A., Klingsch, W., Klüpfel, H., Kretz, T., Rogsch, C., and Seyfried, A. (2009). Evacuation dynamics: Empirical results, modeling and applications. In Meyers, R. A., editor, *Encyclopedia of Complexity and Systems Science*, pages 3142–3176. Springer New York. ISBN 978-0-387-75888-6.

Schadschneider, A. and Seyfried, A. (2009a). *Empirical Results for Pedestrian Dynamics and their implications for Cellular Automata Models*, chapter 2, pages 27–44. Emerald Group Publishing Limited.

Schadschneider, A. and Seyfried, A. (2009b). Validation of ca models of pedestrian dynamics with fundamental diagrams. *Cybernetics and Systems: An International Journal,*, 40:367–389.

Seneviratne, P. and Morrall, J. (1985). Analysis of factors affecting the choice of route of pedestrians. *Transportation Planning and Technology*, 10(2):147–159.

Seyfried, A. and Schadschneider, A. (2008). Fundamental diagram and validation of crowd models. In *Proceedings of the 8th international conference on Cellular Automata for Reseach and Industry*. Springer-Verlag, Yokohama, Japan. 1430952 563-566.

Shi, J., Chen, Y., Ren, F., and Rong, J. (2007). Research on pedestrian behavior and traffic characteristics at unsignalized midblock crosswalk: Case study in beijing. *Transportation Research Record: Journal of the Transportation Research Board*, 2038:23–33.

Shields, T., Boyce, K., and McConnell, N. (2009). The behaviour and evacuation experiences of {WTC} 9/11 evacuees with self-designated mobility impairments. *Fire Safety Journal*, 44(6):881 – 893. ISSN 0379-7112.

Shmueli, G. (2010). To explain or to predict? *Statistical Science*, pages 289–310.

Sime, J. D. (1986). Perceived time available: the margin of safety in fires. In *Fire Safety Science-Proceedings of the First International Symposium*, pages 561–570.

Sparnaaij, M. (2015). Social forces model: Predictive vs.reactive. a comparative research. Cie5050-09 - individual research assignment, Delft University of Technology, Faculty of Civil Engineering & Geosciences, Department of Transport & Planning.

Steffen, B. (2010). A modification of the social force model by foresight. In *Pedestrian and Evacuation Dynamics 2008*, pages 677–682. Springer.

Steffen, B. and Seyfried, A. (2008). The repulsive force in continous space models of pedestrian movement. *arXiv preprint arXiv:0803.1319*.

Steuer, R. E. (1986). *Multiple Criteria Optimization: Theory, Computation and Application*. John Wiley, New York, 546 pp.

Still, G. K. (2000). *Crowd Dynamics. PhD thesis*. Ph.D. thesis, University of Warwick, Department of Mathematics.

Still, G. K. (2014). *Introduction to Crowd Science*. CRC Press.

Suma, Y., Yanagisawa, D., and Nishinari, K. (2012). Anticipation effect in pedestrian dynamics: Modeling and experiments. *Physica A: Statistical Mechanics and its Applications*, 391(12):248–263. ISSN 0378-4371.

Taboada, H. A., Baheranwalaa, F., Coita, D. W., and Wattanapongsakorn, N. (2007). Practical solutions for multi-objective optimization: An application to system reliability design problems. *Reliability Engineering and System Safety*, 92:314–322.

Teknomo, K. and Gerilla, G. P. (2005). Sensitivity analysis and validation of a multiagents pedestrian model. *Journal of the Eastern Asia Society for Transportation Studies (EASTS)*, 6:198–213.

Townsend, P. S. (2014). Crowd modelling for quasi-real-time feedback during evacuation in a situational awareness system. *Transportation Research Procedia*, 2:550 – 558. ISSN 2352-1465. The Conference on Pedestrian and Evacuation Dynamics 2014 (PED 2014), 22-24 October 2014, Delft, The Netherlands.

Toyama, M. C., Bazzan, A. L. C., and da Silva, R. (2006). An agent-based simulation of pedestrian dynamics: from lane formation to auditorium evacuation. In Nakashima, H., Wellman, M. P., Weiss, G., and Stone, P., editors, *AAMAS*, pages 108–110. ACM. ISBN 1-59593-303-4.

TRB (2000). *Highway Capacity Manual 2000 (HCM 2000)*. Transportation Research Board (TRB), US Department of Transportation, Washington, DC.

TRB (2010). *Highway Capacity Manual 2010)0 (HCM 2010)*. Transportation Research Board (TRB), US Department of Transportation, Washington, DC.

Treuille, A., Cooper, S., and Popovi, Z. (2006). Continuum crowds. pages 1160–1168. ACM New York, NY, USA.

Turner, A. and Penn, A. (2002). Encoding natural movement as an agent-based system: an investigation into human pedestrian behaviour in the built environment. *Environ Plann B*, 29(4):473–490.

UN (2007). World population prospects: The 2006 revision and world urbanization prospects: The 2007 revision. Technical report, Population Division of the Department of Economic and Social Affairs of the United Nations Secretariat.

UN (2010). Global report on human settlements 2009: Planning sustainable cities - abridged edition. Technical report, United Nations UN-HABITAT.

Van Der Hulst, M. (1999). Anticipation and the adaptive control of safety margins in driving. *Ergonomics*, 42:2:336–345.

Van Der Spek, S., Van Schaick, J., De Bois, P., and De Haan, R. (2009). Sensing human activity: Gps tracking. *Sensors (Basel, Switzerland)*, 9(4):3033–3055.

Van Lint, H. (2009). *Innovations in Dynamic Traffic Management - lectures of the Course: Intelligent Transport Systems & Services for Road Transport*. Delft University of Technology.

Van Wageningen-Kessels, F. (2013). *Multi-class continuum traffic flow Models*. Ph.D. thesis, Delft University of Technology.

Versluis, D. (2010). *Microscopic interaction behavior between individual pedestrians*. Master's thesis, Delft University of Technology.

Weidmann, U. (1993). Transporttechnik der fussgänger, transporttechnische eigenschaften des fussgängerverkehrs, leiteraturauswertung. Technical report, Schriftenreihe des Ivt Nr. 90, Zurich.

Wikipedia (2016). Homo economicus — wikipedia, the free encyclopedia. [Online; accessed 30-May-2016].

Woledge, R. C., Birtles, D. B., and Newham, D. J. (2005). The variable component of lateral body sway during walking in young and older humans. *Journal of Gerontology: MEDICAL SCIENCES*, Vol. 60A, No. 11,:1463–1468.

Wolff, M. (1973). Notes on the behavior of pedestrians. In *People in Places: The Sociology of the Familiar*, pages 35–48. Praeger, New York.

Wolfram, S. (2002). *A new kind of science*, volume 5. Wolfram media Champaign.

Yang, X., Daamen, W., Hoogendoorn, S. P., Chen, Y., and Dong, H. (2014). Breakdown phenomenon study in the bidirectional pedestrian flow. *Transportation Research Procedia*, 2:456–461.

Zanlungo, F., Brščić, D., and Kanda, T. (2014). Pedestrian group behaviour analysis under different density conditions. *Transportation Research Procedia*, 2(0):149 – 158. ISSN 2352-1465. The Conference on Pedestrian and Evacuation Dynamics 2014 (PED 2014), 22-24 October 2014, Delft, The Netherlands.

Zanlungo, F., Ikeda, T., and Kanda, T. (2011). Social force model with explicit collision prediction. *EPL (Europhysics Letters)*, 93(6):68005.

Zeiler, I., Rudloff, C., and Bauer, D. (2011). Modelling random taste variations on level changes in passenger route choice in a public transport station. In Peacock, R. D., Kuligowski, E. D., and Averill, J. D., editors, *Pedestrian and Evacuation Dynamics*, pages 185–195. Springer US. ISBN 978-1-4419-9724-1.

Zipf, G. K. (1949). *Human behavior and the principle of least effort*. Addison-Wesley Press.

About the author

Mario Carlos Campanella was born in Rio de Janeiro (Brazil) in 1964. In 1988, he obtained a bachelor's degree in Aeronautic Engineering from Instituto Tecnológico de Aeronáutica in São José dos Campos, Brazil. In 1999, he defended his M.Sc. thesis in Computer Science specialising in Artificial Intelligence methods in the Instituto Militar de Engenharia (IME) in Rio de Janeiro, Brazil. After finishing the Master thesis, Mario started working with several architectural offices developing models for architects and planners in Germany and in the Netherlands.

In 2006, he started his Ph.D. in the Department of Transport & Planning at Delft University of Technology. The goals of his research project was to implement a microscopic pedestrian model capable of simulating large walking facilities and to develop calibration and validation strategies with the aim of increasing the applicability of pedestrian models. During his doctoral studies, Mario worked as a teaching assistant and supervised the thesis of a graduate student. He also served as a reviewer for various international journals and conferences.

During his research years Mario also worked as a consultant applying the pedestrian model that was developed during this Ph.D and developing crowd management strategies for crowded metro stations in Brazil.

Currently, Mario is working as a consultant in the area of pedestrian flows and crowd management.

Publications

Journal articles

Campanella, M., Halliday, R., Hoogendoorn, S., and Daamen, W. (2015). Managing large flows in metro stations: The new year celebration in Copacabana. Intelligent Transportation Systems Magazine, 7(1), pp. 103–113.

Campanella, M., Hoogendoorn, S., and Daamen, W. (2009). Effects of heterogeneity in self-organized pedestrian flows. Transportation Research Record (TRR), pp. 148–156.

Peer-reviewed conference contributions

Campanella, M., Hoogendoorn, S. and Daamen, W. (2014) The Nomad model: theory, developments and applications. In Pedestrian and Evacuation Dynamics (PED 2014), Transportation Research Procedia, Elsevier, 2014, 2, pp. 462–467.

Campanella, M., Hoogendoorn, S., and Daamen, W. (2012). Quantitative and qualitative validation procedure for general use of pedestrian models. In Pedestrian and Evacuation Dynamics (PED 2012), Springer, pp. 891–905.

Campanella, M. and Daamen, W. (2011). Fundamental diagrams for pedestrian networks. In RD Peacock, ED Kuligowski and JD Averill (Eds.), Pedestrian and evacuation dynamics (PED2010), New York: Springer, pp. 255–264.

Campanella, M., Larusdottir, A.R., Daamen, W. and Dederichs, A.S. (2011). Empirical data analysis and modelling of the evacuation of children from three multi-storey daycare centres. In JA Capole and D Alvear (Eds.), Evacuation and human behavior in emergency situations, Santander: Universidad de Cantabria, pp. 223–236.

Campanella, M., Hoogendoorn, S.P. and Daamen, W. (2011). A methodology to calibrate pedestrian walker models using multiple-objectives. In RD Peacock, ED Kuligowski and JD Averill (Eds.), Pedestrian and evacuation dynamics (PED2010), New York: Springer, pp. 755–759.

Daamen, W., Campanella, M. and Hoogendoorn, S.P. (2011). Calibration of Nomad parameters using empirical data for various conditions. Proceedings Ninth International Conference on Traffic and Granular Flow (TGF'11), Moskou: Russian Academy of Sciences, pp. 21–30.

Campanella, M., Hoogendoorn, S., and Daamen, W. (2010). A methodology to calibrate pedestrian walker models using multiple-objectives. In Proceedings of Pedestrian and Evacuation Dynamics (PED 2010).

Campanella, M., Hoogendoorn, S. P. and Daamen, W. Identifying Pedestrian Interaction in Crowds 11th TRAIL Congress, TRAIL Research School, pp. 1-4.

Campanella, M., Hoogendoorn, S., and Daamen, W. (2009). Exploring population variable time-steps and update strategies in pedestrian microscopic simulations. In to appear in the Proceedings of The Eighth International Conference on Traffic and Granular Flow (TGF '09).

Campanella, M., Hoogendoorn, S., and Daamen, W. (2009). Improving the nomad microscopic walker model. In 12th IFAC Symposium on Control in Transportation Systems.

Campanella, M., Hoogendoorn, S., and Daamen, W. (2009). Macroscopic relations in pedestrian traffic flows. In to appear in the Proceedings of The Eight International Conference on Traffic and Granular Flow (TGF '09).

Daamen, W., Hoogendoorn, S. P., Campanella, M. C. and Eggengoor, E. (2009). Ticket Reservation Posts on Train Platforms: Assessment Using Microscopic Pedestrian Simulation Tool NOMAD, Transportation Research Board 88th Annual Meeting (TRB).

Campanella, M., Hoogendoorn, S., and Daamen, W. (2008). Calibration of pedestrian models with respect to self-organisation. In TRAIL in Perspective. Proceedings 2008, 10th International TRAIL Congress, pp. 1–20. TRAIL Research School, Delft.

Daamen, W., Campanella, M. and Hoogendoorn, S. P. (2008). Assessing pedestrian flow conditions in Schiphol Plaza: Can Schiphol Plaza cope with future traveler demands? TRAIL in Perspective. Proceedings 2008, 10th International TRAIL Congress, TRAIL Research School, pp. 41-57.

Campanella, M., Hoogendoorn, S., and Daamen, W. (2007). Improving pedestrian micro-simulations with event steps. In Proceedings of The Seventh International Conference on Traffic and Granular Flow (TGF '07).

Campanella, M., Hoogendoorn, S., and Daamen, W. (2007). A hybrid time-based and event-driven management of pedestrians in micro-simulation models. In Proceedings of Computers in Urban Planning and Simulation (CUPUM 2007), pp. 1-14.

Campanella, M., Hoogendoorn, S., and Daamen, W. (2007). Pedestrian movement simulations for two university campus designs. In Proceedings of Computers in Urban Planning and Simulation (CUPUM 2007).

Hoogendoorn, S.P., Daamen, W., Campanella, M. and Bovy, P. (2007) Delays, variation and anticipation in walker models. In the 6th Triennial Symposium on Transportation Analysis (TRISTAN), June, Thailand, pp. 1–6.

Technical reports

Campanella, M. (2012). Estudo para determinação da capacidade da estação Jardim Oceânico. Technical report, MetrôRio, Rio de Janeiro.

Campanella, M. (2011). Nomad user manual, Technical report, Delft University of Technology.

TRAIL Thesis Series

The following list contains the most recent dissertations in the TRAIL Thesis Series. For a complete overview of more than 150 titles see the TRAIL website: www.rsTRAIL.nl.

The TRAIL Thesis Series is a series of the Netherlands TRAIL Research School on transport, infrastructure and logistics.

Campanella, M.C., Microscopic Modelling of Walking Behaviour, T2016/20, November 2016, TRAIL Thesis Series, the Netherlands

Horst, M. van der, Coordination in Hinterland Chains: An institutional analysis of port-related transport, T2016/19, November 2016, TRAIL Thesis Series, the Netherlands

Beukenkamp, Securing Safety: Resilience time as a hidden critical factor, T2016/18, October 2016, TRAIL Thesis Series, the Netherlands

Mingardo, G., Articles on Parking Policy, T2016/17, October 2016, TRAIL Thesis Series, the Netherlands

Duives, D.C., Analysis and Modelling of Pedestrian Movement Dynamics at Large-scale Events, T2016/16, October 2016, TRAIL Thesis Series, the Netherlands

Wan Ahmad, W.N.K., Contextual Factors of Sustainable Supply Chain Management Practices in the Oil and Gas Industry, T2016/15, September 2016, TRAIL Thesis Series, the Netherlands

Liu, X., Prediction of Belt Conveyor Idler Performance, T2016/14, September 2016, TRAIL Thesis Series, the Netherlands

Gaast, J.P. van der, Stochastic Models for Order Picking Systems, T2016/13, September 2016, TRAIL Thesis Series, the Netherlands

Wagenaar, J.C., Practice Oriented Algorithmic Disruption Management in Passenger Railways, T2016/12, September 2016, TRAIL Thesis Series, the Netherlands

Psarra, I., A Bounded Rationality Model of Short and Long-Term Dynamics of Activity-Travel Behavior, T2016/11, June 2016, TRAIL Thesis Series, the Netherlands

Ma, Y., The Use of Advanced Transportation Monitoring Data for Official Statistics, T2016/10, June 2016, TRAIL Thesis Series, the Netherlands

Li, L., Coordinated Model Predictive Control of Synchromodal Freight Transport Systems, T2016/9, June 2016, TRAIL Thesis Series, the Netherlands

Vonk Noordegraaf, D.M., Road Pricing Policy Implementation, T2016/8, June 2016, TRAIL Thesis Series, the Netherlands

Liu, S., Modeling, Robust and Distributed Model Predictive Control for Freeway Networks, T2016/7, May 2016, TRAIL Thesis Series, the Netherlands

Calvert, S.C., Stochastic Macroscopic Analysis and Modelling for Traffic Management, T2016/6, May 2016, TRAIL Thesis Series, the Netherlands

Sparing, D., Reliable Timetable Design for Railways and Connecting Public Transport Services, T2016/5, May 2016, TRAIL Thesis Series, the Netherlands

Rasouli, S, Uncertainty in Modeling Activity-Travel Demand in Complex Urban Systems, T2016/4, March 2016, TRAIL Thesis Series, the Netherlands

Vries, J. de, Behavioral Operations in Logistics, T2016/3, February 2016, TRAIL Thesis Series, the Netherlands

Goñi-Ros, B., Traffic Flow at Sags: Theory, Modeling and Control, T2016/2, March 2016, TRAIL Thesis Series, the Netherlands

Khademi, E., Effects of Pricing Strategies on Dynamic Repertoires of Activity-Travel Behaviour, T2016/1, February 2016, TRAIL Thesis Series, the Netherlands

Cong, Z., Efficient Optimization Methods for Freeway Management and Control, T2015/17, November 2015, TRAIL Thesis Series, the Netherlands

Kersbergen, B., Modeling and Control of Switching Max-Plus-Linear Systems: Rescheduling of railway traffic and changing gaits in legged locomotion, T2015/16, October 2015, TRAIL Thesis Series, the Netherlands

Brands, T., Multi-Objective Optimisation of Multimodal Passenger Transportation Networks, T2015/15, October 2015, TRAIL Thesis Series, the Netherlands

Ardiç, Ö., Road Pricing Policy Process: The interplay between policy actors, the media and public, T2015/14, September 2015, TRAIL Thesis Series, the Netherlands

Xin, J., Control and Coordination for Automated Container Terminals, T2015/13, September 2015, TRAIL Thesis Series, the Netherlands

Anand, N., An Agent Based Modelling Approach for Multi-Stakeholder Analysis of City Logistics Solutions, T2015/12, September 2015, TRAIL Thesis Series, the Netherlands

Hurk, E. van der, Passengers, Information, and Disruptions, T2015/11, June 2015, TRAIL Thesis Series, the Netherlands